Metabonomic Profiling of Oesophageal Cancer

by

Danny Yakoub

Thesis submitted in part fulfillment of the requirements for the degree of

Doctor of Philosophy (Ph.D.) of Imperial College London

Division of Surgery, Oncology, Reproductive Biology and Anaesthetics

Department of Biosurgery and Surgical Technology

Imperial College London at St Mary's Hospital

November 2009

DECLARATION

I declare that this thesis

Metabonomic Profiling of Oesophageal Cancer

is entirely my own research under the supervision of Professor George Hanna and Dr Hector Keun. The research was carried out in the Division of Surgery, Oncology, Reproductive Biology and Anaesthetics, Department of Biosurgery and Surgical Technology and the Department of Biomolecular Medicine at Imperial College London. All published and unpublished material used in this thesis has been given full acknowledgement. None of this work has been previously submitted to this or any other academic institution for a degree or diploma, or any other qualification.

Danny Yakoub

Clinical Research Fellow/ PhD student

Department of Biosurgery and Surgical Technology

Imperial College London

ABSTRACT

Background and aims

Early detection of oesophageal cancer is the most effective strategy to improve its outcome. The thesis explores the metabolic characteristics of oesophageal tumours as compared to normal tissue from same patients as well as that from healthy individuals. The aim is to characterise the basic metabolic profile of oesophageal cancer, detect possible evidence of field cancerization and to characterise effect of chemotherapy on oesophageal cancer tissue. The clinical benefit is to develop a non-invasive early test to be translated to the bed side/laboratory practice for screening, diagnosis and prediction of response to chemotherapy for patients with oesophageal tumours.

Methods

Using ^{1}H Magic Angle Spinning – Nuclear Magnetic Resonance (MAS-NMR) spectroscopy of intact tissue, we generated metabolic profiles of tumour tissue, proximal histologically normal mucosa from cancer patients (PHINOM) and mucosa from a control group. Using multivariate regression and receiver-operator characteristic analysis we were able to identify a panel of metabolites discriminating malignant and histologically-normal tissues from cancer patients from that of controls.

Results

While 26% and 12% of the spectral profile regions were uniquely discriminating tumour or control tissue respectively, 5% of the profile exhibited a significant progressive change in signal intensity from controls to PHINOM to tumour. Regions identified were assigned to phosphocholine, glutamate, myo-inositol, adenosine-containing compounds, uridine-

containing compounds and inosine. In particular, the phosphocholine to glutamate metabolite ratio in histologically-normal tissue signified the presence of oesophageal cancer (n=123, AUC 0.84, $p<0.001$). Metabolites that were found to be significantly altered in correlation to response to chemotherapy are lysine, glutathione, creatine, taurine, uracil and tyrosine

Conclusion

The results of the study enable better understanding of the metabolic perturbations in oesophageal and cancer. The findings support the hypothesis that field effects are present in oesophageal cancer, even in the absence of Barrett's oesophagus. This indicates that metabolic profiling of tissue can potentially play a role in the surveillance of cancer especially in high risk groups. It also shows the potential of using this methodology to study the prediction of response to chemotherapy. This helps aiding the clinical decision making process and the implementation of personalized treatment protocols for different patients according to their disease extent and potential for response to chemotherapeutics.

DEDICATION

To the memory of my father

Ilia Yakoub

1943 - 2004

ACKNOWLEDGEMENTS

I would first like to express my sincerest gratitude to my PhD supervisor Professor George Hanna for offering me the opportunity to work with him. George has taught me how to do things the right way, not the easy way. I am very grateful for his continuous guidance, valuable advice and untiring support over the past four years.

I would also like to thank my co-supervisor Dr. Hector Keun for his support and fruitful discussions during the course of the study, relentlessly teaching me principles of NMR and pattern recognition techniques.

My appreciation also goes to Dr Robert Goldin at the Department of pathology, St Mary's Hospital, London for his help with establishment of the pathological backbone of this study. I also extend my gratitude to members of the Department of Biosurgery and Surgical Technology and The Department of Biomolecular Medicine in the Division of SORA, Imperial College London headed by Professor Lord Ara Darzi KBE, for their accommodation and continuous support. I especially thank Mr Akram George for providing some of the data on image analysis of pathological slides.

I would like also to thank my mother, Dr.-Ing. Mahassen Rizk for her continuous encouragement. Finally, and mostly I owe my dearest wife Irene and my children Laura and Anthony for their tolerance and enduring support. Without their unconditional love and help, I would have never completed this work. I will continue to make up for them the days I have been away physically or mentally.

CONTENTS

DECLARATION ---- 2

ABSTRACT ---- 3

DEDICATION ---- 5

ACKNOWLEDGEMENTS ---- 6

CONTENTS ---- 7

LIST OF TABLES ---- 11

LIST OF FIGURES ---- 12

ABBREVIATIONS ---- 15

1. CHAPTER 1. REVIEW OF LITERATURE ---- 16

1.1 Cancer cell metabolism ---- 17
1.1.1 Mitochondrial metabolism and cancer ---- 18
1.1.2 Carbohydrate metabolism ---- 20
1.1.2.1 Glycolysis ---- 20
1.1.2.2 The citric acid cycle ---- 21
1.1.2.3 Pentose phosphate pathway ---- 22
1.1.2.4 Glucose uptake in tumour cells ---- 24
1.1.2.5 Fluorodeoxyglucose and Positron Emission Tomography scanning ---- 25
1.1.3 Amino acid metabolism ---- 27
1.1.4 Lipid metabolism ---- 28
1.1.4.1 Magnetic Resonance Spectroscopy (MRS) imaging of tumour lipid metabolism ---- 31
1.1.4.2 Clinical applications ---- 33

1.2 Field cancerization ---- 33
1.2.1 Field cancerization in oesophageal and gastric cancers ---- 37

1.3 Demographics of gastric and oesophageal cancer ---- 39

1.4 Molecular basis of chemotherapeutic effect on cancer tissues ---- 39
1.4.1 Predictive biomarkers in oesophago-gastric cancer ---- 42
1.4.2 Chemotherapeutics used in gastric and oesophageal cancers ---- 43
1.4.2.1 5-Flourouracil metabolism pathway ---- 43
1.4.2.2 Platinum compounds ---- 46
1.4.2.3 Other chemotherapeutics used in gastric and oesophageal cancer treatment ---- 48
1.4.3 Factors affecting cancer cell death and response to chemotherapy ---- 48
1.4.3.1 Apoptosis ---- 48
1.4.3.2 Survivin ---- 48
1.4.3.3 Bax ---- 49
1.4.3.4 Cyclooxygenase-2 (COX-2) ---- 49
1.4.3.5 Transcription factors ---- 50
1.4.3.5.1 TP53 (p53) ---- 50
1.4.3.5.2 Nuclear factor kappa B ---- 50
1.4.3.5.3 Hypoxia-inducible transcription factor-1 (HIF-1) ---- 50
1.4.4 Gene expression profiling in oesophago-gastric cancer ---- 52

1.5 Pathology and staging of oesophageal cancer ---- 53

1.6 Diagnosis and multimodality management of gastro-oesophageal cancer ---- 54

1.7 Outcome of gastro-oesophageal tumours ---- 57

1.8 Barrett's disease ---- 58

1.9 Metabonomics ---- 60

1.9.1 Introduction ---- 60
1.9.2 Theoretical basis of NMR spectroscopy ---- 60
1.9.3 Magic angle spinning (MAS) ---- 62
1.9.4 NMR Pulse sequences ---- 65
1.9.4.1 1D experiments ---- 66
1.9.4.2 2D experiments ---- 67
1.9.5 Water presaturation ---- 67
1.9.6 Biological applications of NMR spectroscopy ---- 68
1.9.7 Data processing and analysis ---- 70
1.9.7.1 Chemometrics and pattern recognition (PR) ---- 70
1.9.7.2 Principal component analysis (PCA) ---- 71
1.9.7.3 Scores and loadings ---- 72
1.9.7.4 Soft Independent Modelling of Class Analogy (SIMCA) ---- 73

1.10 Study aims and objectives ---- 74

1.10.1 Overall aim ---- 74
1.10.2 Detailed objectives ---- 74
1.10.3 Thesis layout ---- 74

2. CHAPTER 2. METHODOLOGY ---- 76

2.1 Patients and Methods ---- 77

2.1.1 Patients ---- 77
2.1.2 Arrangements for sample storage ---- 78
2.1.2.1 Establishment of tissue bank ---- 78
2.1.2.2 Ethics approval for metabonomic studies ---- 78
2.1.2.3 Establishment of patient database ---- 79

2.2 Sample collection ---- 79

2.2.1 Tissue samples ---- 79
2.2.1.1 Surgical samples ---- 79
2.2.1.2 Endoscopic samples ---- 80
2.2.2 Blood samples ---- 80

2.3 Sample preparation for NMR ---- 81

2.3.1 Tissue samples ---- 81
2.3.2 Blood samples ---- 81
2.3.3 Tissue extraction ---- 82

2.4 Sample analysis by NMR Spectroscopy ---- 82

2.4.1 Tissue ^{1}H –MAS NMR Spectroscopy ---- 82
2.4.2 1D NMR spectroscopy for blood samples ---- 83

2.5 Data processing and analysis ---- 84

2.6 Pathological examination ---- 85

2.7 Validation studies: ---- 85

2.7.1 Validation of methods of tissue collection, storage and NMR processing ---- 85
2.7.2 Validation of statistical methods used during data processing ---- 87
2.7.3 Validation of metabolic profile results ---- 88

3. CHAPTER 3. METABONOMIC PROFILING STUDIES ---------- 97

3.1 Study I: Global metabonomic phenotyping of oesophageal and gastric cancer patients------98
3.1.1 Hypothesis ----------98
3.1.2 Objectives of the study ----------98
3.1.1 Patients and data analysis ----------98

3.2 Study II: Field effects in non-dysplastic tissue from oesophageal cancer patients ----------99
3.2.1 Hypothesis ----------99
3.2.2 Objectives of the study ----------99
3.2.3 Patients and data analysis ---------- 100

3.3 Study III: Profiling metabonomic response of oesophageal adenocarcinoma to chemotherapy 100
3.3.1 Hypothesis ---------- 101
3.3.2 Objectives of the study ---------- 101
3.3.3 Patients and data analysis ---------- 102
3.3.4 Response to chemotherapy ---------- 103

4. CHAPTER 4. RESULTS ---------- 105

4.1 Study I: Global metabonomic phenotyping of oesophageal and gastric cancer ---------- 106
4.1.1 Patients ---------- 106
4.1.2 Global phenotyping ---------- 107
4.1.3 Analysis of oesophageal tissue ---------- 114
4.1.4 Blood samples analysis ---------- 120
4.1.5 Summary of findings ---------- 121

4.2 Study II: Field effects in non-dysplastic tissue in oesophageal cancer patients ---------- 123
4.2.1 Patients ---------- 123
4.2.2 NMR and histopathological testing of tissue samples ---------- 124
4.2.3 Metabolic profile changes progressively from tumour tissue to PHINOM to tissue from controls 125
4.2.4 Surrogate biomarker metabolites identified by discriminant analysis ---------- 127
4.2.5 Comparison of other metabolites showing similar trend ---------- 131
4.2.6 Summary of findings ---------- 133

4.3 Study III: Profiling metabonomic response of oesophageal adenocarcinoma to chemotherapy 134
4.3.1 Patients ---------- 134
4.3.2 Demonstrating the generic effect of chemotherapy on tissues ---------- 135
4.3.3 Differential effect of chemotherapy on normal and tumour tissue ---------- 138
4.3.4 Differential effect of chemotherapy on blood samples ---------- 141
4.3.5 Examination of specific chemotherapy induced metabolic alterations in patients with matched samples 143
4.3.6 Metabolic profile components of differential response to chemotherapy ---------- 144
4.3.7 Summary of findings ---------- 147

5. CHAPTER 5. FINAL DISCUSSION ---------- 149

5.1 Study I: Global metabonomic phenotyping of oesophageal and gastric cancer ---------- 150
5.1.1 Component differences between cancer and normal tissues ---------- 150
5.1.2 Metabolic profiling of oesophageal tissue ---------- 152
5.1.2.1 Junctional Tumours ---------- 153
5.1.2.2 Oesophageal adenocarcinoma vs. squamous carcinoma ---------- 153
5.1.2.3 Barrett's oesophagus ---------- 154
5.1.2.4 Failure of staging correlation ---------- 155
5.1.3 Pattern recognition validity ---------- 155

5.2 Study II: Field effects in non-dysplastic tissue in oesophageal cancer patients ---------- 156
5.2.1 Concept of 'field cancerization' ---------- 156
5.2.2 Metabonomic evidence of field cancerization ---------- 157
5.2.3 Clinical implication of field cancerization findings ---------- 159
5.3 Study III: Profiling metabonomic response of oesophageal adenocarcinoma to chemotherapy 160
5.3.1 Metabonomic response to chemotherapy ---------- 160
5.3.2 Clinical implications of metabonomic biomarkers to chemotherapy effect ---------- 161
5.3.3 Limitations of the study ---------- 163
5.4 Conclusions ---------- 163
6. CHAPTER 6. FUTURE STUDIES ---------- 165
6.1 Relationship between metabolic profiles and stage of cancer ---------- 166
6.2 Characterization of pre-malignant tissues ---------- 166
6.3 Effect of therapeutic modalities on body fluids metabolic profiles ---------- 167
7. REFERENCES ---------- 168
8. APPENDIX 1. ---------- 188
9. APPENDIX 2. ---------- 199
10. APPENDIX 3. ---------- 215
11. APPENDIX 4. ---------- 217
12. APPENDIX 5. ---------- 219
13. APPENDIX 6. ---------- 223
14. APPENDIX 7. ---------- 226

LIST OF TABLES

Table 1. Examples of important ongoing chemotherapy Phase III clinical trials --- 42
Table 2. UICC TNM designations ---------- 56
Table 3. Disease stage with corresponding TNM designation ---------- 56
Table 4. Examples of studies using metabonomics in literature---------- 71
Table 5. Grading of tumor regression after neoadjuvant radiochemotherapy ----- 105
Table 6. General characteristics of patients included in tissue analysis ---------- 109
Table 7. Characteristics of patients included in the study---------- 117
Table 8. Patient and sample characteristics---------- 126
Table 9. Discriminatory spectral regions ---------- 130
Table 10. Patient characteristics involved in the study of the Profiling metabonomic response of oesophageal adenocarcinoma to chemotherapy ---------- 136
Table 11. Comparative content of some of the metabolites observed comparing pre and post chemotherapy malignant tissue ---------- 142
Table 12. Comparative content of some of the metabolites observed comparing pre versus Post chemotherapy PHINOM---------- 142
Table 13. Pathological properties (Mandard's grade of response and %fibrosis) and metabolites content (measured in average of relative integral values) of analyzed samples ---------- 147
Table 14. Spearman's correlation coefficients demonstrating metabolites that show significant change in relation to tissue responsiveness to chemotherapy 148
Table 15. Sample weights in sequence of analysis---------- 217
Table 16. All carcinoma tissue versus all normal oesophageal tissues ---------- 219
Table 17. All oesophageal versus junctional cancer tissues ---------- 220
Table 18. Intraobserver agreement on Mandard Regression Grading (MRG) after neoadjuvant therapy ---------- 227
Table 19. Interobserver reproducibility of Mandard Regression Grading (MRG) after neoadjuvant therapy---------- 227

LIST OF FIGURES

Figure 1. Glycolysis---------- 23
Figure 2. Glutamine metabolism---------- 28
Figure 3. Simplified overview of tumour lipid metabolism.---------- 29
Figure 4. The metabolic pathway of 5-fluorouracil (5-FU)---------- 45
Figure 5. Pathways involved in the repair of platinating agents and ionising radiation---------- 47
Figure 6. Genetic alterations involved in the progression of Barrett's metaplasia toward Barrett's adenocarcinoma---------- 59
Figure 7. Magic angle spinning involves rapid rotation of a sample inclined at the magic angle of 54.7° to the static field ---------- 64
Figure 8. Example of 1D spectrum acquired by the author during the course of the study (Chemical shifts 0.6 – 2.7) ---------- 66
Figure 9. Example of 2D spectra generated by the study via 2D spectral analysis - 67
Figure 10. Normal oesophagus of cancer patients taken under different anaesthetic conditions ---------- 86
Figure 11. Assignment of spectra generated by the study (Chemical shifts 0.6 – 2.7) ---------- 89
Figure 12. Assignment of spectra generated by the study (Chemical shifts 2.75 – 4.3) ---------- 90
Figure 13. Assignment of spectra generated by the study (Chemical shifts 5.3 – 9) 90
Figure 14. Assignment of spectra generated by the study via 2D spectral analysis to examine physical proximity of compound components confirming its identity---------- 91
Figure 15. Confirmation of assignments via examination of chemical structure---- 92
Figure 16. Confirmation of assignments via examination of chemical structure---- 93
Figure 17. Confirmation of assignments via examination of chemical structure---- 94
Figure 18. Showing similar NMR peaks and difference between tumour and normal tissue in intact tissue and extracted samples---------- 95
Figure 19. Overlaid average ^{1}H MAS-NMR CPMG spectra of malignant and proximal non-tumour oesophageal tissue. Spectra show some peaks are identical (e.g. most amino acids) while others which are different (higher or lower) between normal and malignant oesophageal tissue (e.g. lactate, lipids, glutamate) suggesting differential changes of various classes of metabolites involved in separate pathways are due to pathological effect rather than systematic error---------- 108
Figure 20. Differences in part of the median CPMG spectra between normal and malignant oesophageal tissues---------- 109
Figure 21. Overlaid 1H MAS-NMR CPMG spectra of oesophgeal and gastric tissue All tissues were obtained prior to chemotherapy. A portion of aliphatic region shows systematic increase of free choline, phosphocholine, glycerophosphocholine and taurine in tumour compared to normal tissue ---------- 110

Figure 22. Spectra of non chemotherapy-treated tissue (inclusive of oesophageal and gastric samples) showing systematic increase of uracil and phenylalanine in tumour compared to normal tissue ---------- 111
Figure 23. Scores plot of a PCA model differentiating between different types of tissue samples---------- 112
Figure 24. Loadings plot of PCA model differentiating between different types of tissue samples---------- 113
Figure 25. Choline resonances in oesophageal tissue extracts showing similar changes to that of intact tissues seen in Figure 21 ---------- 116
Figure 26. PCA scores plot of CPMG spectra of oesophageal tissues showing progressive separation along the same vector between normal mucosa, squamous carcinoma and adenocarcinoma with Barrett's dysplasia (R^2X 0.691, Q^2cum 0.541) ---------- 117
Figure 27. Scores plot showing clustering of squamous and adenocarcinoma and their normal counter parts---------- 117
Figure 28. Loadings line plot showing the contribution of different metabolites to differentiating normal and malignant clusters e.g. lactate, creatinine and intermediates of glucose metabolism---------- 118
Figure 29. Differential metabolite concentrations of glutamine, glutathione, scylloinositol and uracil between cancer tissue and normal tissue (n=34) ---------- 119
Figure 30. Differential metabolite concentrations of glutamine, glutathione, scylloinositol and uracil compared in an independent set of samples (n=18) ---------- 119
Figure 31. 1D median spectra of serum samples showing differences which seems to be due to malignancy regardless chemotherapy status ---------- 120
Figure 32. PCA model of serum samples from oesophageal cancer patients vs. normal controls ---------- 121
Figure 33. Metabolic profiling by ^{1}H-NMR MAS spectrometry with pattern recognition analysis reveals systematic metabolic differences in between malignant, PHINOM and control oesophageal tissue. A) oesophageal cancer; B) PHINOM;C) aliphatic and D) aromatic regions of a typical ^{1}H-MAS-NMR spectrum of normal oesophageal tissue; E) mean spectra of tissue groups indicating metabolites exhibiting systematic differences in a training set of 45 samples; F) Multivariate 'scores' from a PLS-DA model classifying the tissue groups in the training set; G) Validation of the PLS-DA model by comparison to the classification statistics of models generated after (100) random permutations of the class matrix (Y) ---- 126
Figure 34. 3D PLS-DA model comparing normal tissue from cancer patients with that from non-cancer patients (NN=normal oesophagus healthy controls, NM=PHINOM group) (R^2X 0.779, Q^2cum 0.584) ---------- 127
Figure 35. Identification of spectral features defining intermediate metabolic change in non-tumour tissue from cancer patients. (A) Proportion of spectra area significantly differentiating between tissue groups based on two PLS-discriminant analysis models calculated as described in methods, which classified tumour from PHINOM or control from PHINOM. (B) Heat

map and hierarchical clustering analysis (HCA) of metabolite resonances occupying spectral regions exhibiting intermediate change in PHINOM in the training set. Data are presented as z-scores (scaled to unit variance) and average linkage was used for the analysis. (C) Box plots of the phosphocholine / glutamate ratio across the full sample set, clustered by tissue of origin and route of sampling. Outlying values >2 S.D. (full circles) and >3 S.D. (star) from the mean are indicated ---------- 130
Figure 36. Prediction PLS-DA model constructed on healthy samples and normal oesophageal samples of cancer patients with no general anaesthetic, predicting in NM group. NM: PHINOM group---------- 131
Figure 37. Comparison of glutamine content in tissues showing progressive decrease from normal (NN) to PHINOM (NM) to tumour (MM) (p<0.001, Kruskal Wallis test) ---------- 132
Figure 38. Comparison of glutathione content in tissues showing progressive decrease from normal (NN) to PHINOM (NM) to tumour (MM) (p<0.001, Kruskal Wallis test) ---------- 132
Figure 39. Comparison of tyrosine content in tissues showing progressive increase from normal (NN) to PHINOM (NM) to tumour (MM) (p<0.001, Kruskal Wallis test) ---------- 133
Figure 40. Comparative changes in spectral segments occurring in both malignant and PHINOM after chemotherapy treatment suggesting generic effect of chemotherapy on both tumour and normal tissues---------- 135
Figure 41. Comparative changes in spectral segments occurring in both malignant and PHINOM after chemotherapy treatment suggesting generic effect of chemotherapy on both tumour and normal tissues---------- 136
Figure 42. Relative ratios of lactate/cholines and phosphocholine/cholines among tumour and normal tissues before and after chemotherapy ratios (p<0.05, Kruskal-wallis test)---------- 136
Figure 43. Lactate/glucose ratio after chemotherapy ---------- 137
Figure 44. PCA plot showing oesophageal tissues colour coded according to chemotherapy status and divided by a line according to histological diagnosis---------- 138
Figure 45. Differential phenyl alanine content in different tissue types (p=0.014, Kruskal-wallis test)---------- 139
Figure 46. Differential content of adenine containing compounds in different tissue types (p-value < 0.001, Kruskal Wallis test) ---------- 139
Figure 47. Lysine /creatine ratio trend after chemotherapy treatment ---------- 141
Figure 48. 1D median spectra of serum samples showing differences which may be attributed to isolated effect of chemotherapy ---------- 142
Figure 49. PCA plot showing both tumour and normal tissues from the same patients, pre and post chemotherapy, move towards a common metabolic phenotype ---------- 143
Figure 50. Metabolite differences according to response to chemotherapy when patients were divided into two groups Mandard 1-3 (left column for each metabolite) vs. Mandard 4, 5 (right column for each metabolite) ------- 147

ABBREVIATIONS

CPMG Carr-Purcell-Meiboom-Gill

COSY Correlation Spectroscopy

FID Free induction decay

FT Fourier transformation

MAS Magic angle spinning

NMR Nuclear magnetic resonance

PR Pattern recognition

ppm parts per million

RF Radiofrequency

TOCSY Total Correlation Spectroscopy

TSP sodium 3-trimethylsilyl-[2,2,3,3- $^{2}H_{4}$]-1-propionate

1. CHAPTER 1. REVIEW OF LITERATURE

1.1 Cancer cell metabolism

In spite of the significant advancements made in cell biology and the molecular biology of cancer over the past decades, cancer cell metabolism remains one of the least explored and forgotten areas of cancer biology and cancer therapy. Recently, increasing evidence has shown the potential role of cancer cell metabolism and its controlling factors for cancer development, progression and treatment. Objective evaluation of the data in this area is essential despite being in an early experimental and clinical stage. Attempts on this evaluation have been made possible by the introduction and extensive use of new methods and accurate techniques for the study of cell ultra structure, genomic, proteomic, transcriptomic and metabonomic cell mechanistics [1]. The study of metabolic, m-RNA (messenger RNA), lysosomes, cell surface receptors, mitochondrial DNA (mt-DNA) as well as mitochondrial metabolism significantly advanced knowledge of cancer cell metabolism. Various new methods were developed to look at these variables from different aspects have been devised, most prominently advances in genomics, proteomics and metabonomics [2-9]. Amongst those, metabonomics which is defined as "The quantitative measurement of the time-related multi-parametric metabolic response of living systems to patho-physiological stimuli or genetic modification"[10]. Metabonomics complements and enhances the information provided by genomics and proteomics [11] and has already shown promise in identifying metabolite-based biomarkers in ovarian, brain and liver cancers [12-14].

It has been shown that there is a strong relationship between cancer cell metabolism and cancer cell structure, thus, the early detection of metabolic, and genetic abnormalities will be of value in predicting the outcome of cancer therapies (hormone therapy,

chemotherapy, cell differentiation therapy, cytokine therapy, gene and antisense therapy). Electron and proton transport across cell membranes, ion, and proton pumps (H+, K+, ATP ase), Calcium Ca^{2+} channels, oxidative phosphorylation involving ATP synthesis and some enzymes of tricarboxylic acid (Krebs cycle), metabolic oxidative stress and, antioxidants were shown to have considerable potential for providing biomarker pathway pools where direct significance to novel therapy development can be explored [15,16]. Recent proteomic data have shown alterations of metabolic pathways in colonic cancer, these included glycolysis, gluconeogenesis, tricarboxylic acid cycle and purine / pyrimidine metabolism [17]. This was complemented by metabonomic data from ^{1}H NMR spectroscopy studies showing significant increases in taurine, choline-containing compounds and lipid resonances in malignant colonic mucosa [18]. These metabolic pathway changes subsequently change tissue metabolic profiles, which can potentially be detected and explored as potential biomarkers for cancer detection, staging, and can help tailoring treatment to patients according to their predicted prognosis [19].

1.1.1 Mitochondrial metabolism and cancer

Recent evidence strongly suggests that mitochondria, the power plants of cells producing energy needed for vital structural and functional maintenance, play an additional important role in cancer cell growth and proliferation. Under electron microscopy, mitochondria have two membranes, an outer smooth membrane and an inner membrane with multiple introflexions known as cristae. The inner compartment contains the matrix, a gel-like substance which is approximately 50% protein. The inner mitochondrial membrane contains the respiratory chain proteins which consist of electron transport,

succinate and NADH dehydrogenase activity, oxidative phosphorylation, or translocation phospholipid synthesis, and ATPase activity. The outer membrane and the protein-rich mitochondrial matrix contain the enzyme of the Krebs cycle fatty acid oxidation, elongation of fatty acids, and synthesis of phospholipids. The normal mitochondria membrane is impermeable to protons [20]. Mitochondria are under the control of two genomes, their own (mt-DNA), and that of nuclear DNA, (n- DNA). This symbiosis allows mammalian cells to produce energy more efficiently via catabolism of glucose by an electron-proton transfer, and oxidative-phosphorylation reactions taking place in the tricarboxylic acid cycle (*Krebs cycle*). This produces ATP, lactic and pyruvic acid, and is essential for cell growth and survival. Molecular studies showed that human mt-DNA is a 16,569-nucleotide pair, a closed circular molecule (compared to linear stranded double helix nuclear DNA), that codes for essential genes of oxidative phosphorylation plus the structural rRNA (ribosomal RNA) and tRNA (transfer RNA) necessary for their expression. Mt-DNA is maternally inherited, and thought to be of separate evolutionary origin, being derived from the circular genomes of the bacteria that were engulfed by the early ancestors of today's eukaryotic cells. Recent research has been centred on exploring the potential role of mitochondrial metabolism and mt-DNA in carcinogenesis, and in novel anticancer drugs development. For instance, it has been suggested that by reducing or suppressing the mitochondrial ATP production, which plays an important role in cell cycle progression, it would be possible to inhibit the cell cycle at the transition from G1 to S and G2 to M phase; both are important checkpoints of cell cycle progression and cell growth. Electron microscopic studies revealed that cancer cells contain fewer mitochondria than normal cells, which also exhibit several perturbances as damaged

cristae and disrupted inner membrane. Such abnormalities could explain the role of mitochondria in carcinogenesis when carcinogens interact with mt-DNA as well as protein synthesis leading to dysfunctions of the respiratory chain and oxidative phosphorylation. In addition, it could point to a potential role of mitochondria in acquired resistance to chemotherapeutics. Therefore, mitochondria can become a central target for new cancer therapeutics which can fight carcinogenesis as well as facilitate response to other chemotherapeutics; for example, Rhodacyanine MKT-077 was found to have a selective cytotoxic damage in the mitochondrial ultra structure of carcinoma cells but not in similarly treated normal epithelial cells [1].

1.1.2 Carbohydrate metabolism

1.1.2.1 Glycolysis

This is the process of metabolism of the glucose molecule and eventually converting it into two molecules of pyruvate. It is a set of reactions that occur in the cytosol. The most common type of glycolysis is the *Embden-Meyerhof pathway* (Figure 1.) [21]. Glycolysis has three control elements: The first reaction is a control element, the conversion of glucose to glucose 6-phosphate catalysed by the enzyme hexokinase. This enzyme binds to the outer membrane of the mitochondrion. Hexokinase reduces the ATP to ADP and produces glucose 6-phosphate. Meanwhile, ADP enters the mitochondrion again and becomes an acceptor for phosphoryl groups. The second important step is the conversion of fructose 6-phosphate to fructose 1,6-bisphosphate catalysed by phosphofructokinase, which is the most important control element in glycolysis. Unlike the other control

elements hexokinase and pyruvate kinase, this is the only unique irreversible step in glycolysis (i.e. it catalyses the reaction of molecules that are strictly glycolytic intermediates). The third irreversible step in glycolysis is the reaction phosphoenolpyruvate–pyruvate, catalysed by pyruvate kinase. At the end of glycolysis, pyruvate is subject to four different metabolic fates. Under anaerobic conditions, pyruvate is reversibly converted into lactate; a second fate is to be transaminated into the amino acids alanine, valine and leucine. A third fate is to be carboxylated inside mitochondria into oxaloacetate, an intermediate of the citric acid cycle. And last but not least, is its conversion into acetyl-CoA inside mitochondria. This molecule can be the supplier of two-carbon fragments needed for the synthesis of lipids or it can enter the citric acid cycle if there is a need for ATP [22].

1.1.2.2 The citric acid cycle

The citric acid cycle, also called the tricarboxylic acid cycle or *Krebs cycle*, occurring in the mitochondria, is the final common pathway for the oxidation of glucose and other fuel molecules. Some intermediates can also be transaminated into amino acids. The first step in the cycle is the condensing of acetyl-CoA with oxaloacetate, thus generating a six-carbon molecule: citrate. In the following steps citrate is again converted into oxaloacetate. The energy yield from the several steps is 3 NADH, 1 FADH and 1 GTP per molecule of pyruvate. The NADH and FADH molecules transfer their electrons to oxygen in the electron-transport chain to generate 3 ATP per NADH and 2 ATP per FADH. This is necessary for the continuity of the cycle, since a constant supply of the

electron acceptors NAD + and FAD+ is required for the cycle to proceed. Hence, the citric acid cycle is obligatorily aerobic [22].

1.1.2.3 Pentose phosphate pathway

This is a pathway that starts with some intermediates of glycolysis with the ability to produce NADPH, which serves as an electron donor in reductive biosynthesis. It takes place in the cytosol also, and is largely involved in the *de novo* synthesis of nucleic acids and therefore cell proliferation *in vitro* and *in vivo* [22].

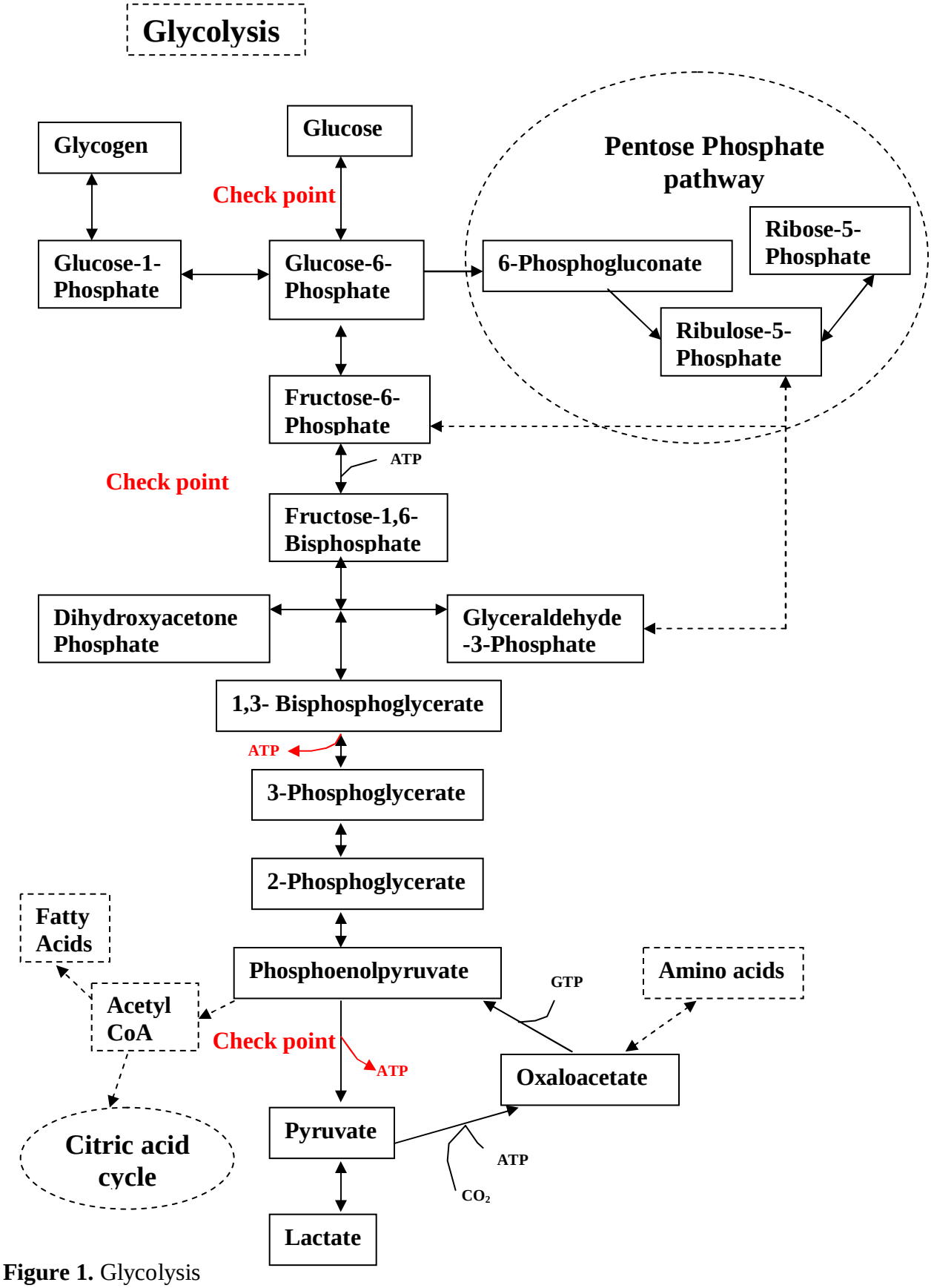


Figure 1. Glycolysis

1.1.2.4 Glucose uptake in tumour cells

'Aerobic glycolysis', uniquely observed in cancer, is the conversion of glucose to lactic acid in the presence of oxygen. This is known as the '*Warburg effect*' [23]. In 1926, *Otto Warburg* postulated that cancer cells originate due to a transition from aerobic energy metabolism of normal cells to an anaerobic metabolism with high anaerobic glycolysis and high lactic acid synthesis following injury to the cell respiratory system [24]. However, radioisotopic studies done subsequently, revealed that cancer cells have the same ability to convert glucose (and fatty acids) to CO2 as normal cells do; therefore, high glycolysis and lactic acid production alone, cannot explain the origin of cancer cells [25,26]. Although these studies defied the '*Warburg hypothesis*', the experimental and clinical observation of increased glycolysis in tumours even in the presence of oxygen have been repeatedly reported [27].

A normal cell derives most of its energy from oxidative phosphorylation, so the fact that, in a rapidly growing tumour cell, the citric acid cycle shows minor activity and the cell depends on glycolysis for more than half of its energy needs indicates a very important metabolic difference between a normal and a malignant cell [28]. Besides producing of energy, glycolytic intermediates are also involved in two other features of growing tumours: enhanced DNA/RNA synthesis by means of the pentose phosphate pathway and the synthesis of lipids (out of fructose 1,6-bisphosphate), essential for membrane synthesis. The glycolytic capacity of a given tumour is now generally assumed to be characteristic of its state of differentiation [22,29,30].

Singh et al. suggested that the promoting force for this increased glycolytic flux is the phosphorylation of glucose, the first reaction of the glycolytic pathway [31]. This step is

catalysed by hexokinase and it is this enzyme that shows an increased activity in tumour cells [32,33]. At least two factors contribute to this increased activity of hexokinase. One is the difference in binding to the outer membrane of the mitochondrion, the other is the overproduction of this enzyme in malignant cells compared to normal cells. That group also studied hexokinase in liver cells and found that the percentage of membrane-bound enzyme activity increases with the grade of malignancy, varying from about 30% of the total activity in normal liver cells to about 70% in dedifferentiated tumour cells [33]. Another variable is p53, in normal cells, p53 acts as a cell-cycle checkpoint protein, thus halting the cell in Gl phase in the event of DNA damage. In one of the published experiments [34], there appeared to be a positive regulatory effect of mutated p53 (two point mutations in its cDNA were demonstrated) on the hexokinase pro-motor. In the AS-30D hepatoma cells, p53 was highly abundant in its mutated form, with a longer half-life than wild-type p53 [35]. This could be the key to a possible link between loss of cell-cycle control in rapidly growing tumour cells and their propensity to catabolise glucose at high rates, one of the commonest biochemical signatures of cancer cells [22].

1.1.2.5 Fluorodeoxyglucose and Positron Emission Tomography scanning

The glucose analogue deoxyglucose, which has one oxygen atom less than the glucose molecule, is transported into the cell in the same way as glucose. Once it has reached the cytosol, it is phosphorylated to deoxyglucose 6-phosphate by the enzyme hexokinase, just like normal glucose. The next reaction in glycolysis, producing deoxyfructose 6-phosphate, in effect a rearrangement of the carbonyl group from the C-1 to the C-2 position in the ring structure, is not possible because this would require an oxygen atom

at the C-2 position. Thus, deoxyglucose 6-phosphate is trapped in the cell, as the reverse reaction to deoxyglucose does not take place because of the low concentration of glucose 6-phosphatase in tumour cells. When labelled with 18F, PET can reveal this molecule. Hence, a high uptake of ^{18F}fluorodeoxyglucose (FdGlc) reflects an increased glucose metabolism in, for example, tumour cells [22]. FdGlc PET is recognized to be an accurate, non-invasive tool for imaging, specific diagnosis and staging of a wide range of different tumours [37]. Furthermore, it is even thought to be useful in the evaluation of cancer prognosis and efficacy of anticancer therapy [38]; FdGlc PET measures the metabolic activity reflecting the inhibition of proliferative activity caused by anticancer therapy [39]. *Crippa et al*. demonstrated that standardised uptake value of FdGlc was correlated with prognostic factors such as histopathological grading and p53 expression [40].

Measuring metabolic activity in tumours has attracted special attention, especially since clinical studies on gliomas and lymphomas have shown that hypermetabolic tumours usually have a poorer prognosis than hypometabolic ones [41]. However, a number of factors in scintigraphic tumour metabolic activity measuring should be taken into account. First, tumour inhomogeneity hampers the assessment of the real metabolic status of the tumour as a combination of activities of tumour cells; normal cells, matrix and premalignant cells are measured rather than pure tumour activity. Second, *Kubota et al*. [42,43] reported on that both invading macrophages and granulation tissue formed by the inflammatory reaction induced by tumours, showed a higher uptake of FdGlc than did viable tumour cells. Third, there is hardly any literature on the time period needed to lapse before the start of the scintigraphic examination. FdG1c uptake with time is most likely dependent on local parameters, such as mitotic activity and growth rate. Also early

uptake by inflammatory cells may falsify a positive result. Despite the increasing clinical use of FdGlc PET that has proved to be of great value in solving individual clinical problems, the issue of quantification remains unresolved.[22].

1.1.3 Amino acid metabolism

Glutamine metabolism (Figure 2.) in cancer cells has long been reported to exceed the use of other nonessential amino acids [44,45]. Glutamine is the most abundant free amino acid in the body [46] and plays a key role in intermediary metabolism for rapidly dividing cells such as enterocytes and cells of the immune system. Glutamine has been shown to be an unusually good substrate for oxidation by tumour cell mitochondria; predictably, tumour glutaminase activity is relatively high. Phosphate-dependent glutaminase converts glutamine to glutamate and ammonia and is the first step in a series of reactions that generate the metabolic intermediates required for cell growth. Glutaminase activity increases proportionally with tumour glutamine consumption and growth rates, and the low intracellular glutamine concentrations have been attributed, in part, to an increase in the activities of glutamine-using nucleotide biosynthetic enzymes and glutaminase. Physiologic concentrations of circulating glutamine are essential for optimal growth of malignant cells in culture. The tumour acts as a "*glutamine trap*". Malignant cells transport glutamine across their plasma cell membrane at a faster rate than do their non-malignant counterparts. For example, human hepatoma cells consume glutamine at a rate five- to tenfold faster than do normal hepatocytes [47]. Because solid tumours are poorly vascularized, it has been suggested that they are endowed with efficient transport systems to compete with the host for glutamine [47]. After glutamine enters the cytoplasm, it must

be transported into the mitochondria before it is hydrolyzed by phosphate-dependent glutaminase. In the majority of patients with cancer, glutamine depletion develops with time, both from the disease process itself and from the catabolic effects of antineoplastic therapies.

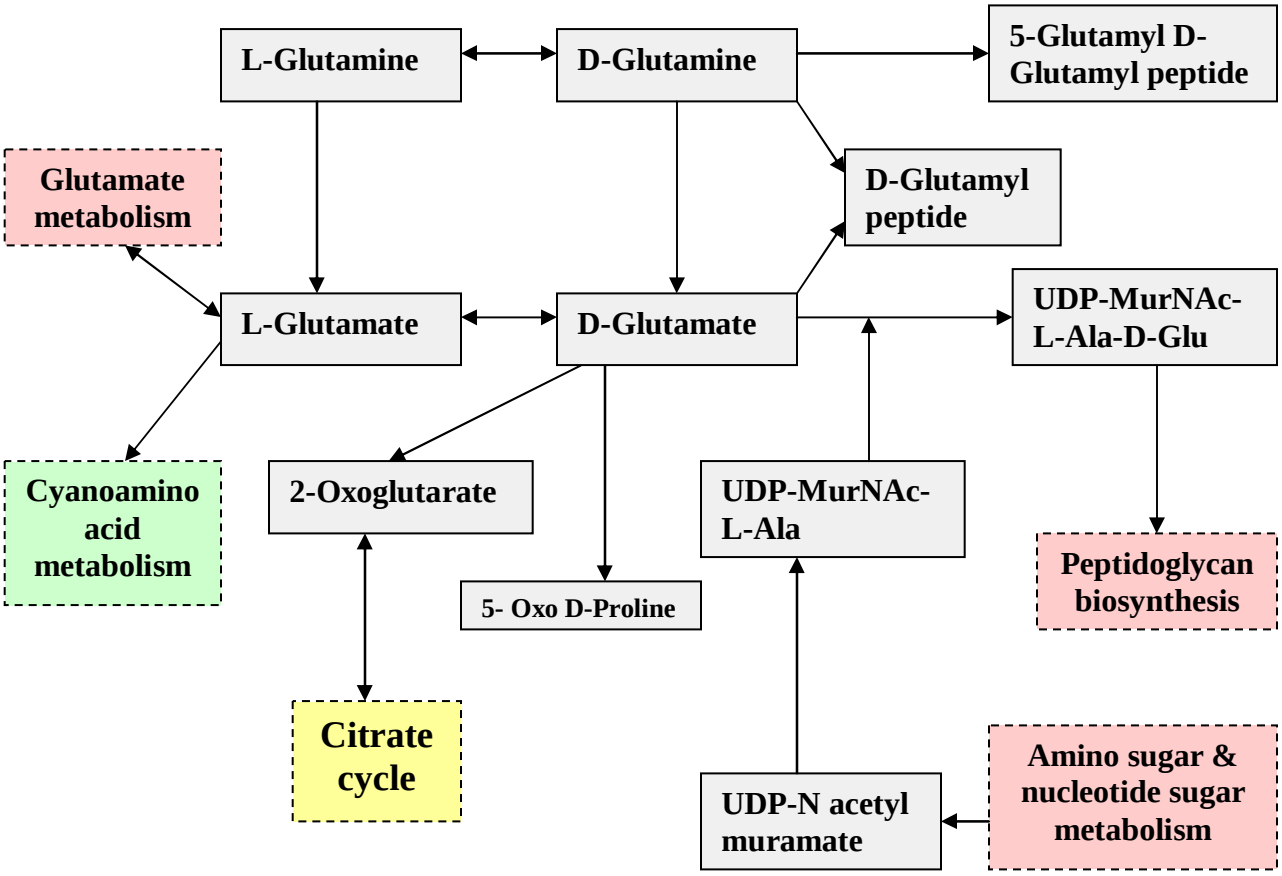


Figure 2. Glutamine metabolism

1.1.4 Lipid metabolism

In addition to increased glycolytic activity, several alterations of lipid metabolism are often found in cancer cells, including over expression of fatty acid synthase (FAS) and choline kinase (ChoK). FAS catalyzes the *de novo* synthesis of fatty acids from acetyl-

CoA, malonyl-CoA, and nicotinamide adenine dinucleotide phosphate (NADPH) [48]. In the liver and adipose tissue, FAS helps storage of energy derived from carbohydrate metabolism as triglycerides. In contrast, human cancer cells do not store significant amounts of triglycerides but esterify fatty acids to phospholipids, such as phophatidylcholine (Figure 3.) [48,49].

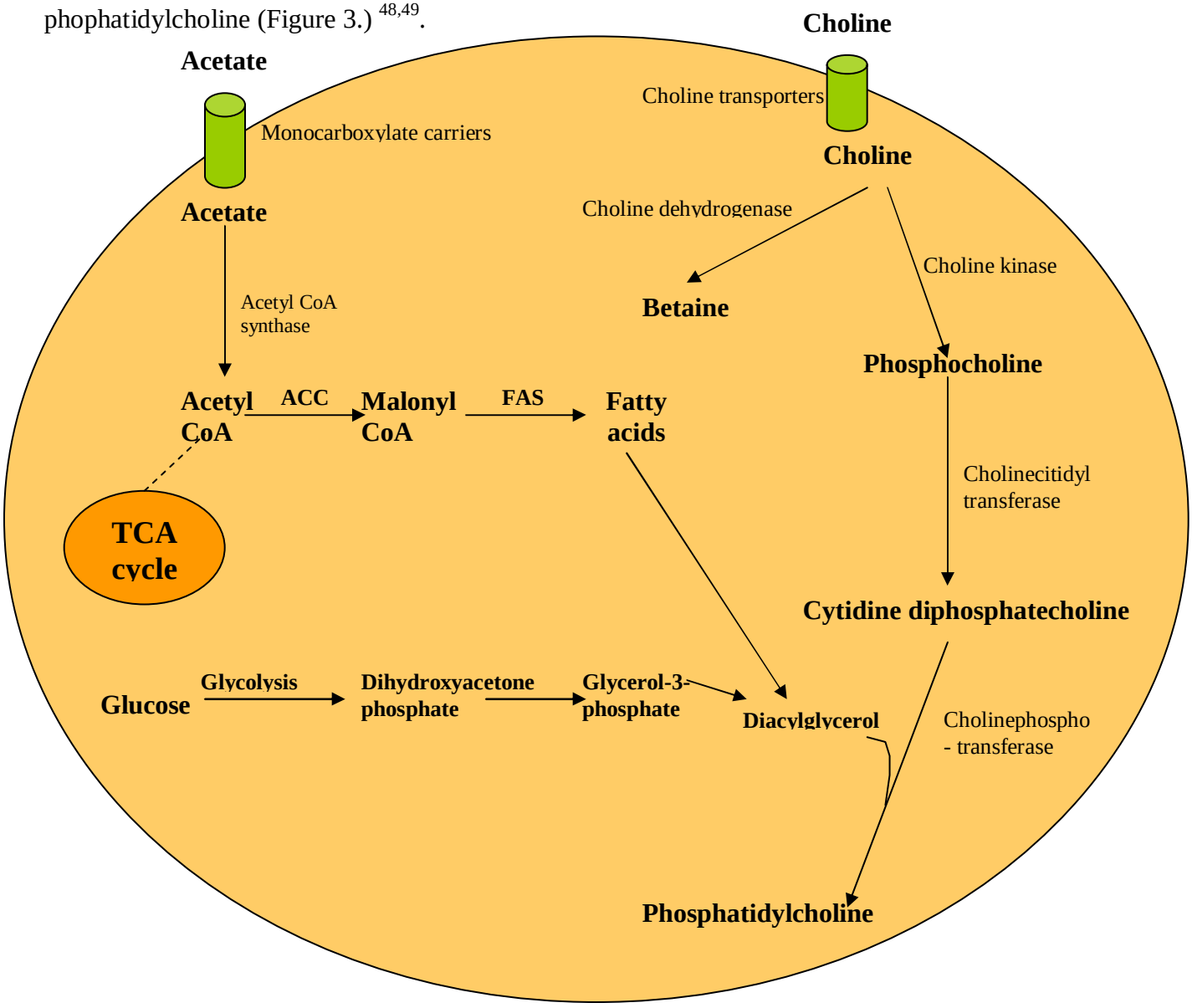


Figure 3. Simplified overview of tumour lipid metabolism. ACC = acetyl-CoA carboxylase; CDP = cytidine diphosphate; FAS = fatty acid synthase. Fatty acids are activated to acyl-CoA and in a 2-step reaction form diacylglycerides with glycerol 3-phosphate. These diacylglycerides then react with CDP-choline to form phosphatidylcholine [49].

Many malignant tumours, including lung, colon, breast, ovarian, and prostate cancer, have been shown to overexpress ChoK[50]. ChoK phosphorylates free choline to phosphocholine (PCho), which represents the first step of choline metabolism. Catalyzed by choline-cytidyltransferase (CCT), PCho can then react with CTP (cytosine triphosphate) to form cytosine diphosphate-choline (CDP-choline). The phosphorylcholine unit of CDP-choline is then transferred to a diacylglycerol (DAG) by cholinephosphotransferase (CPT) to form phosphatidylcholine (PC), a major constituent of the mammalian cell membrane [50,51]. PC can be metabolized by 3 phospholipases (phospholipases A2, C, and D). These phospholipases hydrolyze different bonds of PC. Phospholipase A2 splits PC into lyso-PC and a free fatty acid (FFA), metabolism by phospholipase C results in PCho and DAG, and phospholipase D generates choline and phosphatidic acid [51]. Thus, the intracellular choline levels are determined by both the rate of choline uptake as well as the rate of phosphatidylcholine synthesis and degradation [52]. Choline kinase expression has been shown to be associated with particular cell stresses as polycyclic aromatic hydrocarbon carcinogens or carbon tetrachloride intoxication [53,54]. These results indicate that choline kinase is a member of an acute responsive gene family, although the exact role of choline kinase induction as well as of newly generated PCho in various cell stresses are currently not fully revealed. PCho has also been shown to act as a second messenger in cell growth signaling [55]. Several oncogenes such as ras, src, raf, and mos increase choline kinase activity when expressed in mouse fibroblasts [53]. Likewise, transfection of human mammary epithelial cells with the erbB2 oncogene has been reported to cause a significant increase in P-Cho levels [56,57]. Choline kinase activity and phosphocholine levels were generally not well correlated with proliferation rates [56,58]

suggesting that activation of choline kinase cannot be explained alone with net PC synthesis by proliferating cells.

Other studies found that due to the increase in total cell mass of the proliferating cancer, cells need a net increase in lipid biosynthesis, especially to serve increased membranogenesis, i.e. proliferating tumour cells are prolific lipogenic cells [59]. Furthermore, biochemical alterations mainly detected in poorly differentiated and rapidly growing tumours, are related to modifications in lipid composition (e.g. decrease in polyunsaturated fatty acids and/or increase in cholesterol to phospholipid ratio) with subsequent alterations of membrane bi-layer fluidity and enzyme activities. Yet, little is known about the specific alterations at the level of mechanisms of intracellular compartmentalization responsible for biosynthesis, trafficking and turnover of the major phospholipid components (PL); thus at this time there is an established role of these molecules as both 'passive' structural building blocks of cell structure and 'active' regulators of cell function. Novel approaches such as metabonomics methods opened up new ways to investigate biochemical alterations occurring in tumours, notably at the level of phospholipid and lipid metabolism [60].

1.1.4.1 Magnetic Resonance Spectroscopy (MRS) imaging of tumour lipid metabolism

Earlier studies on significance of choline metabolites in human tumours used mostly ^{31}P-MRS. However, proton MRS was used with higher success due to its better sensitivity (owing to its very high abundance in tissues), consequently, improved spatial resolution (having much more distinct sharp peaks) compared with ^{31}P-MRS [61]. In proton (^{1}H)

MRS, the total choline (tCho) peak is a measure of the concentration of choline, phosphocholine, glycerophosphocholine, betaine, and taurine [51]. tCho has been shown to be increased in a variety of malignant tumours, including breast cancer prostate cancer and brain tumours [61]. Another significant metabolic abnormality observed with MRS in brain tumours is a reduction of the neuronal marker N-acetyl aspartate (NAA) and total creatine (tCr, creatine and phosphocreatine) and an increase of tCho [62]. The tCho concentration gradually increased from normal white matter to grade II astrocytomas and to grade III astrocytomas. However, the tCho signal falls in glioblastoma multiforme, which has been attributed to possible dilution of the signal by necrotic tissue [63]. Variations of the tCho signal caused by differences in cellular density can be corrected by normalizing tCho by tCr [63-65]. Compared with normal prostate tissue, prostate cancer demonstrates decreased levels of citrate and increased levels of tCho. Production and secretion of citrate is an important function of the human prostate [66]. Citrate is synthesized from oxaloacetate (OAA) and acetyl-CoA by citrate synthase. The next step of citrate metabolism in the *Krebs cycle* is the isomerization of citrate to isocitrate by the enzyme aconitase. However, in the prostate the activity of aconitase is low and consequently citrate accumulates and is eventually secreted [66]. Thus, the normal prostate gland is characterized by "aerobic glycoloysis" due to inhibition of *Krebs cycle* and consequently inhibition of oxidative phosphorylation [67]. Consequently, the choline-to-citrate ratio has been used to detect prostate cancer with MRSI and to differentiate prostate cancer from benign prostate hyperplasia [68].

1.1.4.2 Clinical applications

PET with radio-labeled choline has been used successfully in study of prostate cancer, as this tumour is frequently negative on ^{18F}-FDG PET [69]. Furthermore, urinary excretion of ^{11C}-choline is markedly lower than that of ^{18F}-FDG, which facilitates evaluation of primary and recurrent tumours in the pelvis [70]. Choline uptake of prostate cancer has not turned out to be closely correlated with grading and *Gleason score* [61,71-73]. However, antihormonal therapy has been shown to decrease choline uptake of newly diagnosed prostate cancer [73]. Choline was taken up by hyperplastic prostate tissue and by various inflammatory lesions, including chronic and acute prostatitis, which limited the specificity of choline PET for detection and correct localization of cancer foci within the prostate [74].

1.2 Field cancerization

For a long time, it has been postulated that cancer begins with multiple cumulative epigenetic and genetic alterations that sequentially transform a cell or a group of cells in a particular organ. One could extrapolate that the early genetic events might well lead to clonal expansion of pre-neoplastic daughter cells forming a particular tumour field, where subsequent genomic changes in some of these cells drive them towards the malignant phenotype. The fully transformed cells are readily identified histopathologically as cancers owing to changes in cell morphology. However, a population of cells with early genetic changes (without histopathology) remain in the organ, demonstrating the concept of field cancerization. Identification of molecular signatures in these genetically transformed but histologically normal cells have potentially excellent clinical utility;

namely in risk assessment, early cancer detection, monitoring of tumour progression and definition of tumour margins [75].

The idea of field cancerization was initially conceived by *Slaughter* almost a decade prior to introducing the term in 1953. In an earlier publication he stated that; "cancer does not arise as an isolated cellular phenomenon, but rather as an anaplastic tendency involving many cells at once" [76]. The term "lateral cancerization" was subsequently used to indicate that the lateral spread of tumours was due to progressive transformation of cells adjacent to a tumour, rather than the spread and destruction of the adjacent epithelium by pre-existing cancer cells [77]. In a more extensive study where histopathologic review of 783 oral cancer patients was done, *Slaughter* used the term “field cancerization” to describe the existence of generalized carcinogen induced early genetic changes in the epithelium from which multiple independent lesions occur, leading to the development of multifocal tumours [78].

At that time, the demonstration of the presence of histologically abnormal cells that are normal looking in close proximity to malignant cells was reported; these were considered part of the transformed cells in the tumour field, and consequently were suggested to be responsible for local tumour recurrences. These observations were made in the absence of modern molecular techniques, when the discovery of the genetic material was emerging. More assuring of the veracity of these observations, recent studies using various sophisticated genetic analyses have provided unequivocal evidence in support of the work of *Slaughter* [79].

However, field cancerization theories could not explain exactly how these cancer fields develop. Some authors suggested that a particular carcinogen could have induced

multiple distinct genetic alterations in different cells resulting in polyclonal pre-neoplastic lesions in adjacent tissue from which multiple tumours develop. Others believed that a single genetic event occurs in a cell that then clonally expands and laterally spreads to replace the normal epithelium, and therefore create a large area of pre-neoplastic field from which multiple tumours develop. Alternatively, an early genetic event occurring simultaneously in a group of cells such that subsequent genetic lesions drive some cells towards malignancy is another postulation. Is it also possible that some field changes are created during organogenesis when some altered cells proliferate to generate a vast area of preconditioned epithelial surface, such that subsequent genetic lesions in some cells result in multiple cancers? While all these theories of field cancerization are possible, molecular data accrued from studies of head and neck, oesophagus, and bladder cancers support the clonal expansion model [80-82]. This model is believed to possibly explain how multiple tumours develop in organs such as skin, colon, oesophagus, stomach, bladder, cervix, and vulva that have contiguous epithelium. In spite of its possibility, it is less likely that the spread of monoclonal cells can explain the development of multiple tumours in glandular tissues like the lung, breast, ovary, pancreas, and prostate as these have discontinuous glandular epithelial organization, even when exposed to the same carcinogen. Recent molecular techniques have enabled detection of alterations at all genomic levels. Epigenetic gene silencing, chromosomal anomalies, loss of heterozygosity (LOH), DNA sequence analysis for SNP and mutation detection, altered gene expression (transcripts and proteins), and mitochondrial genome changes have all been demonstrated in both precancerous lesions and normal appearing cells close to tumours [82-89].

Another issue to consider in explanation of field cancerization is mitochondrial genome mutations. The mitochondria produce almost all the energy required for cellular physiology, and an inevitable byproduct of this reaction is the generation of reactive oxygen species (ROS), which can damage nucleic acids, proteins and lipids. The mitochondrial genome is less protected and has an inefficient repair mechanism compared to the nuclear genome, and yet is bathed by ROS. Therefore, it has a high mutation rate, and this may signal the genesis of cancer [90]. It is thus likely that the modest mt-DNA molecule might sustain early genetic damage, and thus an even earlier biomarker indicative of field cancerization compared to nuclear genomic alterations that have been extensively studied.

Therefore, field cancerization can be viewed as a general phenomenon of epithelial tumours. An important physiologic function of epithelia is their protective role that inevitably exposes them to environmental substances, including carcinogens that can create a vast area of genetically altered cancer fields. Epithelial cells frequently self renew and can undergo abnormal proliferation. Hyperplastic epithelia could form the basis of neoplastic transformation leading to the formation of the most common types of cancers of the human body. Molecular signatures of field cancerization have been documented for several epithelial tumours including those of the head and neck [91], oesophagus [92], stomach [93], lungs [94], skin [95], cervix [96], vulva [97], bladder [98], colon [85], breast [87], ovary [99], pancreas [100], and recently the prostate [101]. It has even been conceptualized in brain and hematologic malignancies [102,103].

1.2.1 Field cancerization in oesophageal and gastric cancers

Development of oesophageal cancer in *Barrett's* oesophagus has repeatedly served as a model to study clonality and tumour progression in field cancerization. *Prevo et al*. used p53 mutation as a clonal marker to map 213 endoscopic biopsies from 58 patients; the study demonstrated that 50% were clonal and occupied cancer fields ranging from 1 cm to 9 cm [80]. Other genetic observations as LOH at 9p21 (p16 locus) and 17p13 (p53 locus) have also been used to map fields in the oesophagus [104]. In 61 patients with 404 samples, LOH was observed in 73% of cases. Clone sizes were heterogeneous and variable in terms of field perimeters; some even occupied the entire *Barrett's* segment [104]. Epigenetic gene silencing of APC, CDH1, ESR1 and p16 are examples of other studies on *Barrett's* oesophagus and its predisposition to cancer development. Hypermethylation in large contiguous fields were observed, further confirming molecular field cancerization in *Barrett's* metaplasia [105]. In a prospective study where 267 patients were followed, it was demonstrated that clone sizes (which is an index of clones multiplied by the length of *Barrett's* segment they occupied) with p53 LOH and ploidy, were a better predictor of progression towards adenocarcinoma [106]. Recently, a clonal cellular diversity theory attempted explanation of progression of *Barrett's* oesophagus towards adenocarcinoma; this was done by applying the principles of ecology and evolution, (mutation rate, population size of evolving clones, rate of natural selection or clonal expansion), clonal diversity was a strong predictor of disease progression, even after controlling for known risk factors such as p53 LOH and ploidy abnormalities [107,108]. This finding is an example of how a laboratory observation can be translated into a clinically relevant test in terms of disease surveillance. However, the sensitivity and specificity and more importantly the

economic efficiency of such a test are factors that could potentially slow development down that route.

On the other hand, genetic evidence has been provided for the multicentricity of synchronous multiple gastric cancers. Analysis of mutation pattern in genes as APC, MCC and p53 genes in multiple tumours concluded that there was discordance in mutation patterns in these tumours [109]. Therefore, pointing to the possibility that independent genetic events in a preconditioned epithelium may have caused these multiple lesions. In addition, epigenetic silencing via CpG island hypermethylation of LIMS1, a gene involved in cell dispersion has been demonstrated in 53% of gastric cancers [93]. Also, C-erb amplification was observed in a subset of tumours and the normal mucosa close to tumour margin [110], and aneuploidy was frequent in normal mucosa at about 3 cm distance from the tumour margin [111].

Therefore, field cancerization has become a well-documented process of malignant transformation in oesophago-gastric tumours. With technological advancement, the future should benefit from well designed studies aimed at identifying genetic markers and pathways useful in disease management. An obvious shortcoming in almost all the studies of field cancerization is the lack of extensive genome-wide scans that will enable early and important genetic changes in tumour evolution to be uncovered. Many studies have relied heavily on known markers associated with a particular tumour. Such selected tumour markers might be later acquisitions in the disease process, and will be missed in peri-tumoural samples or precancerous lesions. Comprehensive high-throughput analyses for the discovery of early and relevant genetic and functional genomic changes that extend across global networks and represent modular alterations of multiple targets (or

surrogates) of terminal histologically differentiated stages of cancer subtypes will be essential for early detection, risk assessment and primary chemoprevention [75].

1.3 Demographics of gastric and oesophageal cancer

The demographics of gastro-oesophageal cancer have been changing dramatically across the Western world over the past several decades. While incidence rates for oesophageal squamous cell carcinoma and distal gastric carcinoma have been declining, the trends for adenocarcinoma of the oesophagus and proximal stomach have been raising rapidly [112]. In spite of a decline in incidence of gastric cancer in developed countries, it remains the second most cause of cancer-related deaths in the world [2].

Approximately 876 000 persons are diagnosed with the disease and approximately 649 000 die from it every year [113]. Although surgery plays a central role in the overall management of operable disease, it is clear that additional therapy is required to improve patient outcomes. The United Kingdom Medical Research Council Adjuvant Gastric Infusional Chemotherapy (*MAGIC*) trial demonstrated a 25% reduction in the risk of death and a significant improvement in 5 year survival in patients given perioperative chemotherapy compared to those treated with surgery alone [114].

1.4 Molecular basis of chemotherapeutic effect on cancer tissues

Chemotherapy is an integral part of management protocols of oesophageal and gastric cancer. Accepted approaches include preoperative chemotherapy followed by surgery (oesophageal cancer), chemo-radiotherapy alone (oesophageal cancer) and perioperative chemotherapy (gastric and gastro-oesophageal adenocarcinomas). The underlying principles behind neoadjuvant therapy are to improve resectability by tumour

shrinkage/downstaging and to treat occult metastatic disease as early as possible. The response rate to cytotoxic therapy is about 40% in oesophago-gastric cancer. Available evidence suggests that a favourable histopathological response to cytotoxic therapy may be a useful positive predictive marker in oesophago-gastric cancer. However, the ability to predict tumour response in routine clinical practice is difficult and is an area of intense investigation.

Chemotherapeutics used to treat oesophageal cancer include 5-fluorouracil (5-FU), cisplatin, carboplatin, bleomycin, mitomycin, doxorubicin, methotrexate, paclitaxel, vinorelbine, topotecan, and irinotecan. In chemoradiotherapy, the most frequently used drugs are 5-FU and cisplatin given together [115]. Many trials are currently underway to assess efficacy of different treatment combinations for management of gastro-oesophageal cancer (Table 1.)

Name	**Design**	**Indication**
TOGA	XP or FP +/- trastuzumab	Advanced gastric cancer HER2-positive
AVAGAST	XP +/- bevacizumab	Metastatic gastric cancer
REAL-3	EOX +/- panitumumab	Advanced esophagogastric cancer
FFCD 03-07	ECX followed by FOLFIRI vs FOLFIRI followed by ECX	Advanced esophagogastric cancer
EXPAND	XP +/- Cetuximab	Advanced/Metastatic gastric cancer
MAGIC-B	Periperative ECX +/- bevacizumab	Neo-adjuvant gastric cancer
CLASSIC	XELOX vs observation	Adjuvant gastric cancer

Table 1. Examples of important ongoing Phase III clinical trials, including monoclonal antibodies and signal transduction/tyrosine kinase inhibitors

In the *MAGIC* trial (vide supra), surrogate markers of tumour response and downstaging, such as smaller primary tumours (3 cm vs 5 cm), early-stage tumours (T1 and T2 vs T3 and T4), and less advanced nodal status (N0 or N1 vs N2 or N3) were significantly more frequently recorded in the perioperative chemotherapy group compared to the primary surgery group [114]. Similar results have also been demonstrated in the *MRC OEO2* trial of surgical resection with or without preoperative chemotherapy (consisting of two cycles of cisplatin and 5- fluorouracil (5-FU) chemotherapy) in oesophageal cancer [116]. The seminal study by *Mandard et al* [117] reported on the predictive/prognostic significance of histopathological response to cytotoxic therapy in oesophageal cancer specimens following neoadjuvant chemo-radiotherapy. It is to be noted that specimens used in that study were predominantly squamous cell carcinomas. Tumour regression grade (TRG) analysis was used as a marker of treatment response and was undertaken and scored from complete regression (TRG1) to absent regression (TRG5). Of 93 patients, 42% were TRG1–2, 20% TRG3 and 33% were TRG4–5. Tumour size, pathological lymph node status, TRG and oesophageal wall involvement correlated highly with disease-free survival. On multivariate analysis, however, only TRG (TRG1–3 vs TRG4–5) remained a significant ($p=0.001$) predictor of disease-free survival [117]. Similar results for gastric cancer patients receiving neoadjuvant chemotherapy were demonstrated in another study where survival benefit was shown to be significantly improved in the group of patients where histopathological evidence of response to cytotoxic therapy was achieved [118].

One of the arguments against preoperative therapy has been the risk of delaying surgery in those patients who do not respond to chemotherapy, in spite of the fact that current evidence suggests that preoperative treatment does not negatively impact on surgical

outcomes [114]. Therefore, predictive markers of response would be of unequalled significance in individualizing patient treatment as it would preclassify those patients likely to respond to combination therapy from those likely to be non-responsive and may progress during therapy.

1.4.1 Predictive biomarkers in oesophago-gastric cancer

The role of predictive biomarkers has been well established in solid tumours such as in breast cancer (Her-2 overexpression predicts response to herceptin and oestrogen receptor positivity predicts tamoxifen response), chronic myeloid leukaemia (breakpoint cluster region–Abelson murine leukaemia oncogene (BCR–ABL) translocation predicts response to imatinib mesylate), lung cancer (epidermal growth factor receptor (EGFR) kinase domain mutations predict response to erlotinib or geftinib), brain tumours (EGFR mutations in the extracellular domain and response EGFR inhibitors) and colonic cancer (mutations in KRAS predict response to EGFR specific antibody therapy) [115].

Conventional protocols are being used to treat gastro-oesophageal tumours based on their site of origin rather than taking into account their biological characteristics. Current clinical parameters such as TNM staging, tumour location, sex and histological subtype are unable to help predict non-responders to chemotherapy. Recent molecular biology research has confirmed that the cancerous phenotype is a sum total of genetic and epigenetic changes that confer selective survival advantage to clones of cells we define as cancer. Similarly, the ultimate response to chemotherapy is also likely to be dictated by a sum of the genetic make-up of tumours and the various cellular metabolic pathways they may initiate. Search for an ideal biomarker for prediction of response to chemotherapy

has been the daunting task of many research groups working on various cellular genomic and functional genomic levels. An ideal predictive marker should be reliable, readily available, and detectable by reasonably acceptable laboratory techniques.

1.4.2 Chemotherapeutics used in gastric and oesophageal cancers

Alkylating agents (cisplatin and oxaliplatin), 5-FU, capecitabine, anthracyclins and ionising radiation are the predominant cytotoxic agents used in the treatment of oesophago-gastric cancer. Induction of DNA damage in cancer cells is the main cytotoxic effect of systemic chemotherapy and radiotherapy. The cellular responses involved in mediating the cytotoxicity of these agents are complex. Predictive biomarkers have been investigated at a genetic level (eg, polymorphisms), transcriptional level (mRNA expression) or at the protein level. Cells respond to the cytotoxic effect of chemotherapeutics in variable ways.

1.4.2.1 5-Flourouracil metabolism pathway

5-FU belongs to the family of drugs known as antimetabolites and principally acts via inhibition of DNA and RNA synthesis [119,120]. The predominant mechanism for the cytotoxicity of 5-FU is via ‘‘thymineless death’’. Upon entering cells, 5-FU is converted to 5-fluorodeoxyuridine (5- FUDR) by the enzyme thymidine phosphorylase (TP). 5-FUDR is converted to 5-fluorodeoxyuridine monophosphate (5-FdUMP) by thymidine kinase (TK). 5-FdUMP competes with endogenous deoxyuridine monophosphate (dUMP) for binding to thymidylate synthase (TS) in a complex that is stabilised by 5,10-methylenetetrahydrofolate (CH2THF) (the enzyme methylenetetrahydrofolate reductase

(MTHFR) converts CH2THF to 5-methyltetrahydrofolate) (Figure 4.). Binding of 5-FdUMP to TS depletes the thymidine nucleotide pool and hence DNA synthesis. Though the exact molecular mechanisms are unclear, recent studies suggest that depletion of dTMP leads to imbalances in the deoxynucleotide pool and accumulation of dUMP and dUTP which may be incorporated into the DNA [121]. In addition, 5-FU is also converted to 5- fluorouridine monophosphate (5-FUMP), by the action of orotate phosphoribosyltransferase (OPRT). 5-FUMP is converted to 5-fluorouridine diphosphate (5-FUDP) and then to 5-fluorouridine triphosphate (5-FUTP), which inhibits RNA synthesis.

Capecitabine is also an anti-metabolite belonging to the fluoropyrimidine carbonate class. It is an orally administered precursor of 5-FU and is converted to 5-FU by carboxyesterase (CE), cytidine deaminase (CD) and TP (Figure 4.). The daily oral administration of capecitabine parallels the intravenous infusion of 5-FU in efficacy, yet with more patient and health care system convenience [122]. S-1 is another orally available 5-FU derivative; it combines three pharmacological agents: tegafur, a pro-drug of 5-FU; gimeracil, which reversibly inhibits DPD (the enzyme involved in inactivation of 5- FU); and potassium oxonate, which reversibly inhibits the enzyme responsible for phosphorylation of 5-FU (orotate phosphoribosyltransferase) thereby reducing the gastrointestinal side effects of 5-FU [123].

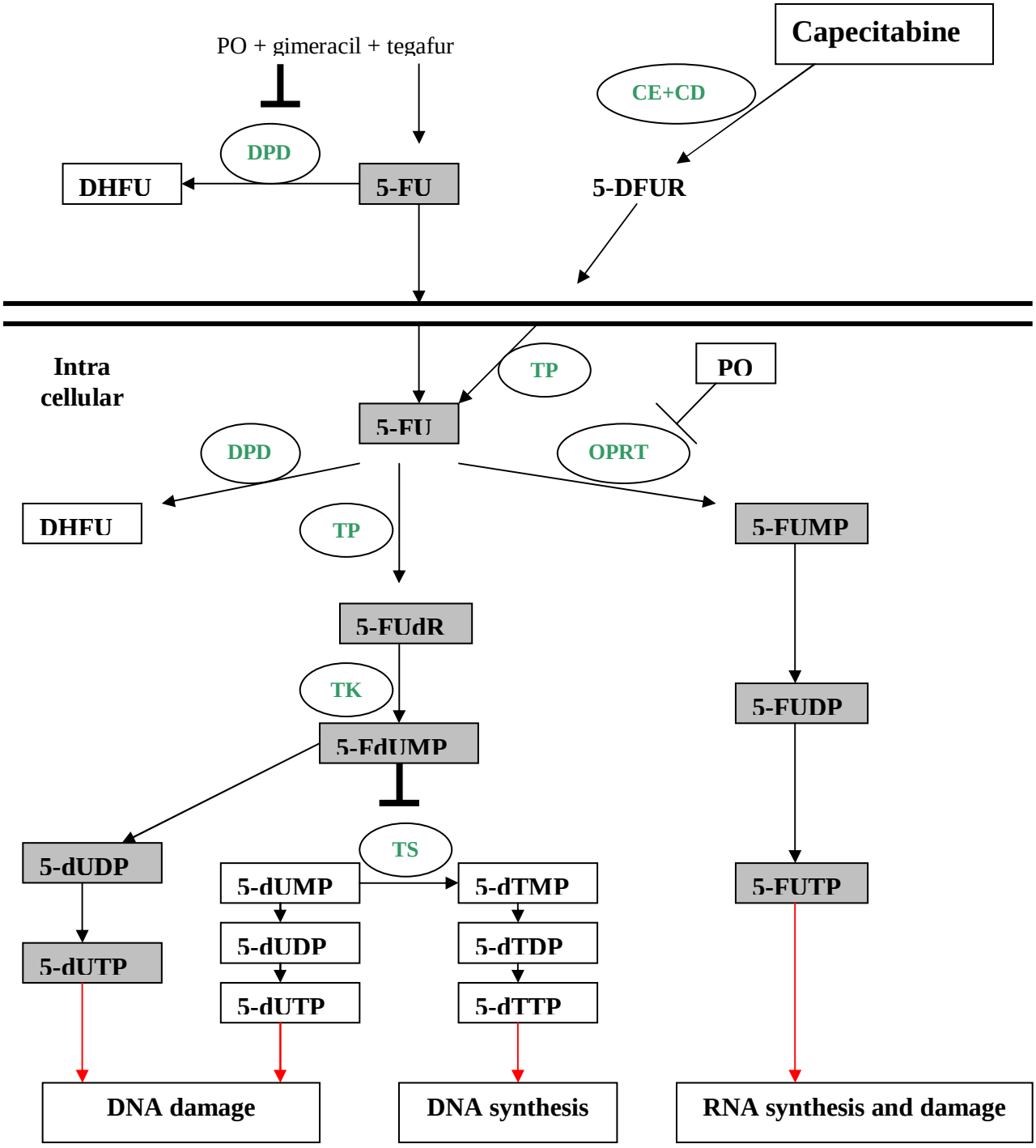


Figure 4. The metabolic pathway of 5-fluorouracil (5-FU). Possible predictive factors of response within this pathway are shown in green. CD, cytidine deaminase; CE, carboxyesterase; 5-DFUR, 59-deoxy-5-fluorouridine; DPD, dihydropyrimidine dehydrogenase; DHFU, dihydrofluorouracil; 5-FU, 5-fluorouracil; OPRT, orotate phosphoribosyltransferase; PO, potassium oxonate; TK, thymidine kinase; TP, thymidine phosphorylase; TS, thymidylate synthase.

1.4.2.2 Platinum compounds

Cisplatin and oxaliplatin are the main platinating agents used in the treatment of oesophageal and gastric cancer. Cytotoxicity is predominantly due to their ability to generate free radicals and bind to DNA and produce cross-links leading to DNA damage. Therefore, DNA repair capacity represents the major factor affecting the therapeutic efficacy in cancer cells (Figure 5). The nucleotide excision repair (NER) pathway is the predominant DNA repair pathway that is involved in the repair of bulky DNA-damaging lesions induced by platinating agents. NER is a highly conserved, versatile and robust DNA repair pathway that deals with a wide range of DNA lesions such as those that distort the DNA double helix, DNA base pairing and interfere with DNA replication and transcription. Two sub-pathways of NER have been described in literature: (1) the transcription-coupled nucleotide excision repair (TCR) pathway which targets lesions specifically in the transcribed strand of expressed genes; and (2) the global genome nucleotide excision repair (GGR) pathway which deals with lesions in the rest of the genome. Free radicals generated either by radiation or platinating agents may also induce oxidative DNA base damage that is predominantly repaired in base excision repair (BER) machinery. Glutathione S-transferases (GSTs) have been shown to be crucial enzymes involved in detoxification of platinating agents. Among the various isoforms of GSTs, GST pi has been shown to bind to platinum and also allows its export from the cytosol using an MDR energy-dependent efflux pump mechanism [115].

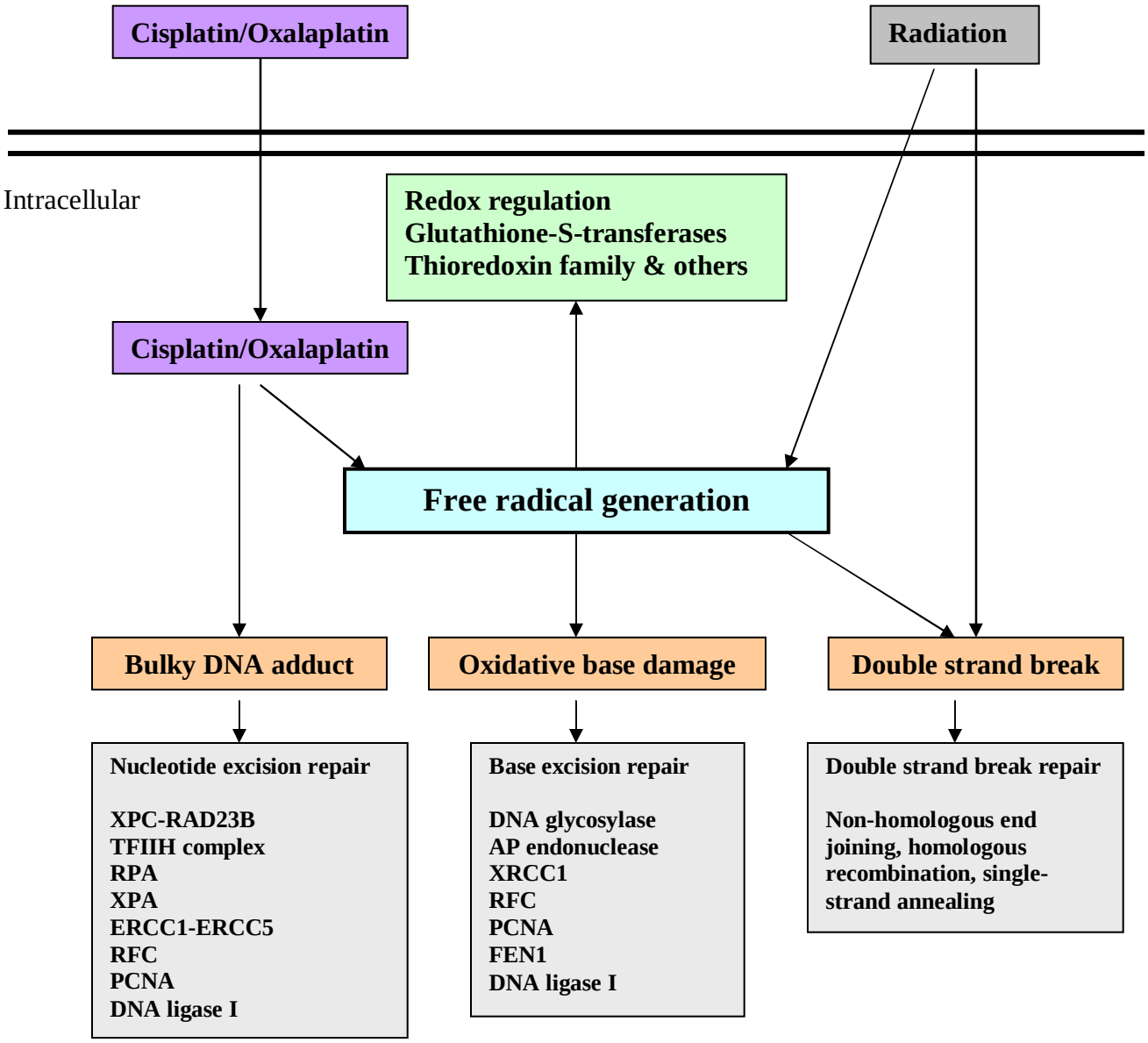


Figure 5. Pathways involved in the repair of platinating agents and ionising radiation are summarised here. Predictive markers within the pathways are shown in bold. AP, apurinic/apyrimidinic; ERCC, excision repair cross-complementing group; FEN-1, flap structure specific endonuclease 1; PCNA, proliferating cell nuclear antigen; RAD23B, RAD23 homolog B; RPA, replication protein A; RFC, replication factor C; XPA and XPC, xeroderma pigmentosum complementation groups A and C; XRCC1, x ray cross-complementation group 1. The TFIIH complex is cdk7, cyclin H, maturationassociated protein 1 (MAT1), xeroderma pigmentosum complementation groups B and D (XPB and XPD), p34, p44, p52 and p62.

1.4.2.3 Other chemotherapeutics used in gastric and oesophageal cancer treatment

Other chemotherapeutic agents used in the treatment of oesophago-gastric cancer include docetaxel which is a taxane analogue that inhibits microtubule disassembly [124] and irinotecan which is a topoisomerase I inhibitor [125].

1.4.3 Factors affecting cancer cell death and response to chemotherapy

1.4.3.1 Apoptosis

The mechanism by which cancer cells die is complex and may include necrosis, mitotic catastrophe and apoptosis (programmed cell death). It has been well documented that chemotherapy and irradiation initiate cell death mainly through apoptosis. There are at least two known pathways of apoptosis in cells: (1) the extrinsic pathway that is activated by interaction with death receptors on the cell surface; and (2) the intrinsic pathway largely mediated by the mitochondria. Chemotherapy and irradiation initiate apoptosis through the mitochondrial (intrinsic) pathway. However, this is tightly controlled by pro-apoptotic and antiapoptotic factors. These factors have been considered potentially important predictive markers in oesophago- gastric cancer [115].

1.4.3.2 Survivin

Is a prominent member of the inhibitor of apoptosis (IAP) family that halts the activation of downstream checkpoints of apoptosis such as the caspases[126]. Survivin expression may be the reason behind resistance to cisplatin-induced apoptopsis during chemotherapy. In a study of 42 patients with gastric cancer the mRNA expression of surviving and its

relationship between expression and sensitivity of cisplatin (CDDP) was examined. Survivin was frequently upregulated in gastric cancer tissue and was negatively associated with overall survival in patients in that study [127]. Another study of 51 patients with oesophageal squamous cell cancer receiving cisplatin and 5-FU neoadjuvant chemotherapy showed that survivin expression in the cancer tissue in patients who achieved a partial response was significantly lower than that in patients with no response or those with progressive disease [128].

1.4.3.3 Bax

A study by *Kang et al*. in 63 patients treated by definitive chemo-radiotherapy for locally advanced oesophageal cancer, examined protein expression of Bax, p53, Bcl-2 and galectin-3 in pre treatment biopsy specimens. Low expression of Bax was significantly correlated with a lack of clinical complete response. In addition the low expression of Bax was associated with a poor overall median survival of 8 months vs. 16 months in the other group [129].

1.4.3.4 Cyclooxygenase-2 (COX-2)

Although the molecular mechanism is not clear, COX-2 may be involved in the upregulation of factors that promote cell survival. High levels of COX-2 have been reported in oesophageal [130] and gastric cancers [131]. Over-expression of COX-2 has been found to be associated with resistance to apoptosis. In a study of 52 patients with resectable oesophageal cancer following neoadjuvant chemo-radiotherapy, high COX-2 protein expression levels seem to be significantly associated with poor prognosis and a poor histopathological response to chemotherapy [132].

1.4.3.5 Transcription factors

1.4.3.5.1 TP53 (p53)

TP53 (p53) is widely accepted to be an important transcription factor involved in key cellular activities as cell cycle regulation, apoptosis and DNA repair. Mutation of p53 is a hallmark of many cancers. Mutant p53 tends to be resistant to degradation and hence p53 protein expression in tumours is considered a surrogate marker of p53 mutation and therefore may correlate with tumour resistance. p53 negativity has been correlated with good tumour response in gastric cancer [133]. On the other hand, the results have been conflicting in oesophageal cancer. While one study suggests that p53 negativity may correlate positively to tumour response [134], other studies did not find any correlation between p53 protein expression and response to cytotoxic therapy [135,136]. Also, another study suggests that p53 mutations may correlate with complete pathological response and improved survival [137].

1.4.3.5.2 Nuclear factor kappa B

Nuclear factor kappa B (NF-kB) protein expression was studied in 43 patients with oesophageal cancer (both squamous cell and adenocarcinomas) who underwent neoadjuvant chemo-radiotherapy. NFkB positivity correlated with lack of tumour response and poor overall survival [138].

1.4.3.5.3 Hypoxia-inducible transcription factor-1 (HIF-1)

The hypoxic microenvironment is being believed to selects cells that are capable of evading apoptosis and survive in the absence of normal oxygen availability. Tumour hypoxia is an important factor in induction of angiogenesis within tumours. Therefore, it

is accepted that the hypoxia-inducible transcription factor-1 (HIF-1) mediated pathway is critical for tumour angiogenesis [139]. HIF-1 transcription factors cause the overexpression of several genes that control various biological processes necessary for tumourigenesis such as cell proliferation, apoptosis, immortalisation, migration and angiogenesis (VEGF expression) [139]. In a recent study in gastric cancer, patients with VEGF negative tumours had response rates very similar to VEGF positive tumours. However, median survival in VEGF negative tumours was significantly longer than in VEGF positive tumours. This points out the prognostic significance of VEGF in gastric cancer [140]. Multiple other pathways have also been identified as being strong effectors of the mechanism of cellular resistance to chemotherapeutics, these include but not exhaustive of Multi-drug resistance related protein-1 (MRP-1) and multidrug resistance related gene-1, tyrosine kinases, messenger RNA expression levels of c-erb-B1 and c-erb-B2, EGFR protein expression, Caldesmon and also polymorphisms of glutathione S-transferases.

The studies described above have focused on a single marker or a set of markers targeting a specific pathway or a set of pathways that may be involved in cellular response to cytotoxic agents. However, as emphasized before that the cancer phenotype is a sum total of genetic and epigenetic alterations and, therefore, the ultimate response to cytotoxic therapy in cancer is also likely to be dictated by these genetic and epigenetic changes involving perhaps several thousands of genes within the cancer genome. Recent advances in genomics, proteomics and metabolomics have for the first time provided tools of global profiling of a biological set in order to make it possible to explore these genome/proteome/metabolome wide marker patterns [141].

1.4.4 Gene expression profiling in oesophago-gastric cancer

Gene expression profiling has been less well researched in gastric and oesophageal cancer as compared to other tumours as breast cancer [142]. However, valuable insights have been given in a few recent studies in patients with oesophageal cancer treated with neoadjuvant chemo-radiotherapy. In one study of nineteen patients [143], approximately 400 genes were differentially expressed between the two groups; the molecular profile generated by gene expression analyses of pre-treatment endoscopic biopsies was correlated with pathological response. Unsupervised hierarchical cluster analyses separated tumours into two molecular subtypes. Pathological complete response was seen in six of the nineteen patients (32%); five of the six patients clustered into subtype I suggesting that gene signatures may predict response. In addition, survival rate was less in molecular subtype II. Genes involved in apoptosis, calcium homeostasis, stress response and proliferation was differentially expressed in both groups [143]; down regulation of epidermal differentiation complex (EDC) genes (S100A2 and SPRR3) at chromosome 1q21 was associated with resistance to chemotherapy. A subsequent study by the same group has provided further evidence that expression levels of genes mapping within and close to the EDC may determine sensitivity to chemo-radiotherapy [144]. Another study in 33 oesophageal squamous cell carcinomas treated with chemo-radiotherapy identified 57 genes that correlated with short-term survival, and 120 genes with long-term survival. Genes up regulated in long-term survivors were largely those involved in immune response, additionally, immunohistochemical staining suggested that the effects of chemo-radiotherapy were correlated with CD8 positive staining in long-term survivors [145]. *Duong et al.* were able to identify a 32-gene mathematical model that

could predict response to neoadjuvant chemo-radiotherapy in squamous cell carcinomas [146]. The most interesting gene from this study was the gene Siah2, which is known to induce expression of hypoxia-inducible transcription factors. Decreased expression of that gene was seen in patients with squamous cell carcinoma who had CT, endoscopy/biopsy and FDG-PET proven complete response to chemoradiotherapy [146]. The aforementioned studies may provide preliminary data on the role of potential biomarkers in oesophago-gastric cancer. However, published studies are limited and patient numbers are too small to provide convincing evidence that this approach is feasible in routine clinical practice. Therefore, whether predictive markers will be routinely incorporated in clinical practice remains to be seen. Biomarker research is expensive and the data generated from these investigations are complex. It is clear that a concerted international effort between academia and industry is critical if practice of personalised medicine for our cancer patients is to be realised.

1.5 Pathology and staging of oesophageal cancer

Once diagnosis of gastric and oesophageal caner is made, the subsequent question is the staging of these tumours as this will dictate subsequent management protocols. The staging system proposed by the *Union Internationale Contre le Cancre* (UICC). This is the most widely used system for dictating management policies in oesophageal cancer patients (Table 2, 3.) [147].

T PRIMARY TUMOUR	
Tis	Carcinoma *in situ*
T1	Invades lamina propria or submucosa
T2	Invades muscularis propria
T3	Invades periesphageal tissue
T4	Invades adjacent structures
N REGIONAL LYMPH NODES	
N0	No regional node involvement
N1	Regional node involvement
N1-4	More distant node involvement
M DISTANT METASTASIS	
M0	No distant metastasis
M1	Distant metastasis

Table 2. UICC TNM designations

STAGE	**TNM DESIGNATION**
0	Tis N0 M0
I	T1 N0 M0
IIA	T2-3 N0 M0
IIB	T1-2 N1 M0
III	T3 N1 M0, T4 any N M0
IV	Any T Any N M1

Table 3. Disease stage with corresponding TNM designation

1.6 Diagnosis and multimodality management of gastro-oesophageal cancer

The multidisciplinary management of gastric and gastro-oesophageal cancers, in diagnosis as well as in treatment strategies has become the standard of care now after results of recent randomised studies became available. The time has come for the launch of multimodal treatments to increase the chance of better outcome, longer survival or even cure. By using this team approach, all diagnostic and therapeutic disciplines, such as

the gastroenterologist, surgeon, oncologist, radiologist and radiotherapist, will be instrumental in planning the effective administration of their treatment modalities. The diagnostic arsenal, i.e. CT scan, endoscopic ultrasound (EUS), mini-laparoscopy, MRI and PET, allows improved pre- or postoperative staging [148]. For endoscopically large tumours and tumours of the gastro-oesophageal junction in particular, CT scan of the abdomen/thorax and EUS are mandatory for an exact preoperative tumour and node metastases staging. EUS allows the differentiation between small and large tumours as well as staging or biopsies of mediastinal and celiac lymph nodes. In addition, mini-laparoscopy is a valuable tool, as peritoneal carcinosis is found in about 20% to 30% of all gastric cancer patients at first diagnosis [149]. As PET scan has also been shown to effectively predict clinical response in oesophageal and gastric cancer, it might potentially allow better allocations and adjustments for further individualized and optimized treatment strategies. Staging with PET may best be used either in patients with locally advanced disease who may benefit from curative resection, if distant metastases are not found, or in patients with high-grade stenosis, where EUS is not applicable [148].

The accuracy of EUS for assessing T and N status has been reported to be 85% and 75%, respectively, while the sensitivity of CT for staging T and N disease has been reported to be about 50% and 60–87%, respectively. Thus, the combined use of all three modalities (CT, EUS, PET) is often needed for initial staging of oesophageal cancer [150]. Most centres in the UK offer endoscopic surveillance for predisposing conditions as Barrett's oesophagus with the aim to detect early, curable lesions. Surveillance in its current form is cumbersome and expensive [151].

Depending on tumour stage, current treatment options for oesophageal and gastric cancer range from endoscopic mucosal resection to preoperative chemo- radiotherapy followed by oesophagectomy or gastrectomy and associated radical lymphadenectomy (D2 Gastrectomy) with a curative intent is done to remove the tumour and all draining lymph node groups, thus achieving an R0 resection margin; this has now become the standard of care. This is further augmented with post operative chemotherapy and/or radiotherapy according to number and position of lymph nodes involved. Most of these therapeutic approaches are associated with substantial morbidity and mortality, as well as a long-term compromise in quality of life. Accurate pre-therapeutic staging by imaging techniques is therefore crucial in order to select the appropriate form of therapy [152]. Although surgery remains the standard treatment for non-disseminated gastric and oesophageal cancer, a variety of combined modality treatments have been investigated in order to induce downstaging of the tumour, improve local control, treat micro-metastases, and ultimately improve long term survival. For example, induction chemotherapy given before surgery has been shown to improve outcome in subgroups of patients as reported in recent large prospective randomized trials such as the UK Medical Research Council (MRC) trial for oesophageal cancer [116] and the presentation of the first survival results of the MRC Adjuvant Gastric Infusional Chemotherapy (*MAGIC*) trial [114].

However, no indicators exist which can reliably predict response to chemotherapy. Histological grading of oesophageal tumours has been used as a prognostic indicator in patients treated with combined neoadjuvant therapy and surgery. It is important to identify non-responders so that unnecessary, potentially harmful treatment is not given to those who will not benefit [153,154]. Many molecular markers have been proposed as

predictors of response e.g. P53, Ki-67, yet none with reliable significance. PET, as a complementary investigation to cross-sectional imaging studies has been shown, in two studies, to differentiate responding from non-responding tumours early in the course of neoadjuvant systemic chemotherapy [155,156]. This is based on the fact that it is considered as a "metabolic" imaging study that relies on differences between tumour cell glucose metabolism and that of normal cells. In follow up of patients, the changes in tumour metabolic activity may be employed to individualize the use of chemotherapy in patients with oesophageal and gastric cancer[10,157].

1.7 Outcome of gastro-oesophageal tumours

Gastro-oesophageal cancer is a highly lethal disease with a 5-year mortality >80%. Even after intended curative surgery, overall survival remains poor. In approximately two-thirds of the patients local recurrences and/or distant metastases are detected within five years of follow-up [160]. In approximately 30% of patients undergoing surgery, who were clinically considered to have resectable disease, radical excision with curative intent could not completely eliminate microscopic residuals of the disease as noted on pathological examination of surgical specimens [161]. The shortcomings in current diagnosis and staging tools for gastric and oesophageal cancer indicate that the actual patient selection for multimodality treatment and the assessment of their outcome remains unreliable [162]. Hence, the need for a non-invasive diagnostic test that assesses tumour type, behaviour, stage or even predicts histopathological response to preoperative therapy has been emphasized by many investigators [152].

1.8 Barrett's disease

It is defined as columnar metaplasia of normal oesophageal squamous epithelium of lower oesophagus due to chronic gastro-oesophageal acid reflux. It is thought to be a precursor to adenocarcinoma of the oesophagus. It increases risk of developing malignancy to 40-50 times that of normal epithelium [163]. Histopathological examination can accurately distinguish between normal and malignant epithelium, nevertheless, it cannot predict the potential for malignant transformation in *Barrett's* epithelium [164]. Immuno-histochemical studies searching for detectable markers have been recently focusing on predicting progression from intestinal metaplasia to dysplasia and low-grade to high-grade dysplasia/ adenocarcinoma. Many groups have been working on projects to qualify tumour suppressor genes, cell adhesion molecules and apoptosis-related genes as potential tumour markers (Figure 6.). Current data describe high-grade dysplasia and adenocarcinoma as a direct outcome of continuous progression of *Barrett's* oesophagus. However, no single marker reliably discriminates lesions that will progress from those that will not [157]. Recent advancement in molecular profiling analysis provides new tools for assessing hundreds to thousands of genes, RNA, proteins or metabolites in a single experiment. This has led to the emergence of new sciences according to target structure e.g. genetics, genomic-scale mRNA expression (Transcriptomics), cell and tissue-wide protein expression (Proteomics), and last but not least, metabolite profiling using NMR spectroscopy followed by analysis using bioinformatics and pattern recognition techniques (Metabonomics). These new sciences individually, or rather in integration, enable mining for new diagnostic and therapeutic targets that can give the answer for many problems in the management of cancer [165].

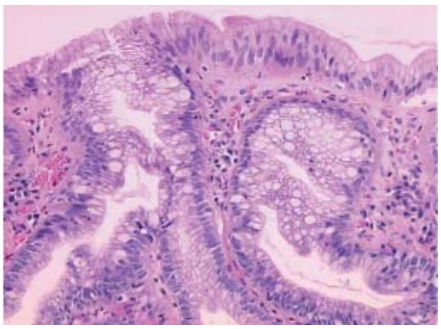
Squamous cell epithelium

Gastro-oesophageal reflux

Barrett's metaplasia

Molecular events:

- **Cyclin D1**
- **Proliferation**
- **p53 + 17p LOH**
- **G1 & G2**
- **bcl-2**
- **src**
- **COX-2**
- **p16 LOH+methylation**

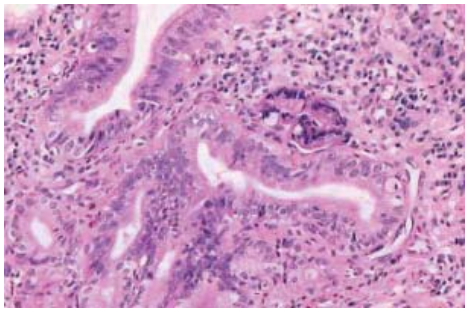


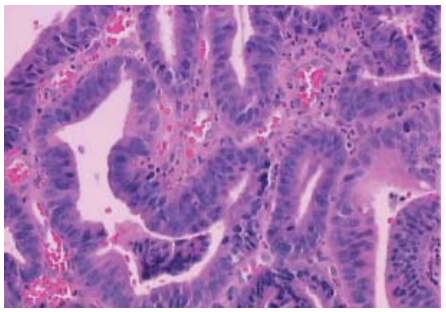
Intestinalised epithelium in Barrett's oesophagus (BO) with mild regenerative changes. Note that a mild degree of crypt distortion, budding and crowding is a normal component of metaplastic epithelium in BO.

Barrett's dysplasia

Molecular events:

- **Growth factors and receptors**
- **S phase**
- **p53 + 17p LOH**
- **p27**
- **telomerase**
- **aneuploidy**
- **5q LOH**
- **CD44s**
- **Apoptosis**
- **E-cadherin-catenin**
- **CD44v**





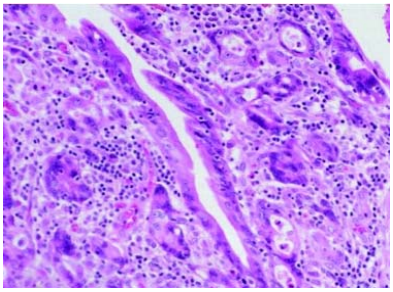
Low grade dysplasia (LGD): The nuclei are pencil shaped, hyperchromatic and stratified, but limited to the basal half of the cell cytoplasm, except focally in the surface epithelium. There are minimal architecture abnormalities.

High grade dysplasia (HGD): Crowded crypts with more severe nuclear stratification. There is mild architectural distortion. The nuclear/cytoplasmic ratio of HGD is markedly increased compared with LGD.

Barrett's adenocarcinoma

Molecular events:

- **p21**
- **c-erbB2**
- **Cathepsin B**
- **G2/M**
- **uPA**
- **p16+methylation+mutations**
- **Fas/APO-1**



High power view of HGD with intramucosal adenocarcinoma: The intramucosal adenocarcinoma is characterised by a proliferation of small irregular glands with markedly atypical nuclei infiltrating the lamina propria in a haphazard fashion that cannot be explained on the basis of involvement of preexisting crypts

Figure 6. Genetic alterations involved in the progression of Barrett's metaplasia toward Barrett's adenocarcinoma. (Alterations that occur in the early stages are usually also present in the advanced histologic stages. In each histologic category, the alterations are placed randomly; there is no hierarchical order. Slides are part of St Mary's Hospital, London histopathology slides database)

1.9 Metabonomics

1.9.1 Introduction

Metabonomics is defined as “The quantitative measurement of the time-related multi-parametric metabolic response of living systems to patho-physiological stimuli or genetic modification” [10]. Metabonomics studies provide a quantitative description of the low-molecular mass endogenous metabolites present in a biological sample such as urine, plasma or tissue. In such studies analysis is usually performed using high field ^{1}H nuclear magnetic resonance (NMR) spectroscopy, which gives a "metabolite fingerprint" [166]. This rapidly advancing science has been mostly employed in toxicology and drug development research in addition to cancer research in studies as early as the eighties[167], but recently with the advent of robust mathematical models and sophisticated statistical techniques, various new studies employed it further in cancer investigation, especially early detection of cancer studies. One study on detection of early ovarian cancer indicated that the sera from patients with EOC and healthy postmenopausal women could be identified with 100% sensitivity and specificity. Results as these are yet to be augmented by further thorough studies applying the technique on various cancers [168].

1.9.2 Theoretical basis of NMR spectroscopy

The theoretical basis for nuclear magnetic resonance (NMR) was proposed by Pauli in 1924 and demonstrated and further developed by Bloch and Purcell in 1946 [169]. The theory states that atomic nuclei possessing the spin property would exhibit split energy levels when exposed to a magnetic field and either align or oppose with this external field. Electromagnetic pulses in the radiofrequency range induce transitions across these

energy levels. The signal emitted by return of nuclei to their ground state energy levels on stopping the magnetic field energy decays in the interval between pulses (Free induction decay (FID)). This time domain signal is then converted to frequency domain by Fourier transformation that finally provides an NMR spectrum. Molecular characteristics that can be deduced from this spectrum include:

a) Chemical shift: indicates nuclei's chemical environment resulting from differences in electron density. The chemical shift, δ, is a relative scale in the order of 10^{-6}, thus the units are in parts per million (ppm) which reflects the relative frequency of each detected signal

b) Spin or scalar coupling: where electron-electron interaction between adjacent nuclei affect their energy states resulting in a spin state that reflects as line splitting on the NMR spectrum

c) Signal intensity: is proportional to the number of nuclei present in each of the chemical environments within the molecules. Relative concentration of a compound (signal) can be calculated by comparisons to signal intensity of an internal standard of known concentration

However, line width may compromise NMR spectral resolution. This may be contributed to by intrinsic factors in the sample or by factors related to NMR instrumentation. Examples of sample intrinsic factors are chemical anisotropy and dipolar coupling. The asymmetrical distribution of electron density within chemical bonds may sustain chemical anisotropic effects on chemical shifts in the spectrum; and this effect is exaggerated in unsaturated bonds, where the position of electrons, circulating under the

effect of external magnetic field, determines shielding of the nucleus to that field. Dipolar coupling is defined as the direct influence of the magnetic environment of one nucleus on another. In two adjacent nuclei, continually fluctuating static fields are experienced by both, and will have direct influences on each other. Chemical anisotropy and dipolar coupling produces no splitting in spectra of liquids, as they are in continual motion so that the net effect of the two states on a neighbouring nucleus averages to zero. On the other hand, in tissues, the limited rotational motion of molecules these processes result in low spectral resolution.

1.9.3 Magic angle spinning (MAS)

Over the last three decades NMR various analytic and experimental methods have been used, yet have only relatively recently MAS has come into use in mainstream high-resolution NMR. This transition has been prompted by technical developments in instrumentation, more specifically in probe head design. Magic-angle spinning of (partially) fluid heterogeneous samples, a technique that has been used extensively over the years for solid-state materials and which demands very fast sample rotation, typically at 1 to 70 kilohertz. In any condensed phase, a nuclear spin experiences a great number of interactions. The main three interactions (dipolar, chemical shift anisotropy, quadrupolar) often lead to very broad and featureless lines. However, these three interactions in solids are time-dependent and can be averaged by MAS. The nuclear dipole-dipole interaction, between magnetic moments of nuclei averages to zero only at the magic angle, θ=54.7. The chemical shift anisotropy, a nuclear-electron interaction, averages to a non-zero value. The quadrupolar interaction is only partially averaged by MAS leaving a residual

secondary quadrupolar interaction. In liquids, e.g. a solution of an organic compound, most of these interactions will average out because of the rapid time-averaged molecular motion that occurs. This orientation averaging in solution is mimicked by MAS of a solid. This causes the signal to become much narrower, giving rise to the isotropic value (which is of interest for structural determination of solid materials and compounds) and spinning sidebands which occur at multiples of the spinning speed and can be used to determine the chemical shift anisotropy of the nuclei. Direct NMR analysis of tissue samples, even when solvated, is complicated by two principal factors which can significantly degrade spectrum resolution [170]:

• Restricted motion of the analytes

• Physical heterogeneity within the sample

In a tissue sample, the restricted motion of the analytes relative to that of free molecules in solution may mean that dipolar couplings, D, are not fully averaged to zero. These have a time-averaged angular dependence:

$$D \alpha r^{-3}(3 \cos^2 \theta - 1)$$

where r is the internuclear separation and θ the angle between the static field and the internuclear vector. For isotropically tumbling molecules in low-viscosity solutions, the angular term is averaged to zero as the molecule freely rotates so dipolar couplings are not observed. When motion is sufficiently restricted, some residual dipolar coupling may be reintroduced, which will contribute to broadening of the NMR resonances. The use of long linker chains allows greater motion of the terminal analyte in solution and can

therefore reduce this effect. A potentially greater problem lies in the sample heterogeneity. Tissue samples suffer from local field inhomogeneity at the tissue solvent interfaces due to magnetic susceptibility differences and this leads to severe line broadening. Magnetic susceptibility has a similar angular dependence to that above, and line-broadening from both dipolar couplings and susceptibility discontinuities can be eliminated by rapid rotation of the sample about the so-called `magic angle' $\theta = 54.7°$ (Figure 7.), such that the above angular term becomes zero and the overall molecular motion emulates that in solution [170].

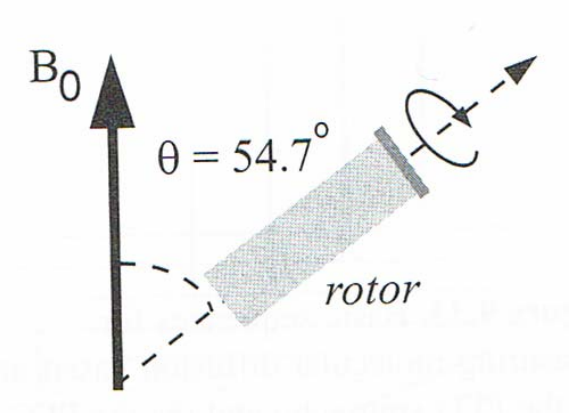


Figure 7. Magic angle spinning involves rapid rotation of a sample inclined at the magic angle of 54.7° to the static field [170].

The MAS spectrum shows up to three-fold signal-to-noise gain yet uses one tenth of the sample relative to the conventional solution spectrum, and has considerably greater information content. To achieve such results, samples are typically spun at rates of 1-70 kHz, in purpose-built rotors. The rotors are made from a number of different materials such as ceramics e.g. zirconia, silicon nitride or polymers such as poly-methyl-

methacrylate (PMMA), polyoxymethylene (POM). The cylindrical rotors are axially symmetric about the axis of rotation. Samples are packed into the rotors and these are then sealed with a single or double end cap. These caps are made from number of different materials e.g. Kel-F, Vespel, zirconia or boron nitride depending on the application required. The physical spinning of the sample is achieved via an air turbine mechanism. These turbines (or rotors) come in a variety of diameters (outside diameter), from 2.0-15.0 mm, and are usually spun on air or nitrogen gas. MAS needs no sample pre-treatment and can be done using only about 6 mg of material. The full range of high-resolution one- and two-dimensional techniques can now be applied to tissue samples under MAS conditions for the complete, non-destructive identification of metabolite profile. This helps preserve the samples for subsequent genomic/proteomic and transcriptomic analysis of the samples allowing direct integration of acquired metabonomic data with data from these methodologies.

1.9.4 NMR Pulse sequences

NMR pulse programs control the number, duration and intensity of pulses and as well delay times between pulses. The simplest pulse sequence can therefore be referred to as ‘pulse and acquire’; a single radiofrequency pulse followed by FID recording. If this sequence is repeated with enough time to allow relaxation and avoid saturation, the larger the number of repetitions, there is improvement of signal to noise upon summation of acquired FIDs. Various pulse sequences have been described.

1.9.4.1 1D experiments

NOESYpr1D is a sequence where presaturation of the water peak allows detection of the rest of peaks with fairly better quality. CPMG is another sequence where signals from high molecular weight species such as proteins are selectively filtered out of the resulting spectrum by exploiting differences in relaxation times (Figure 8.).

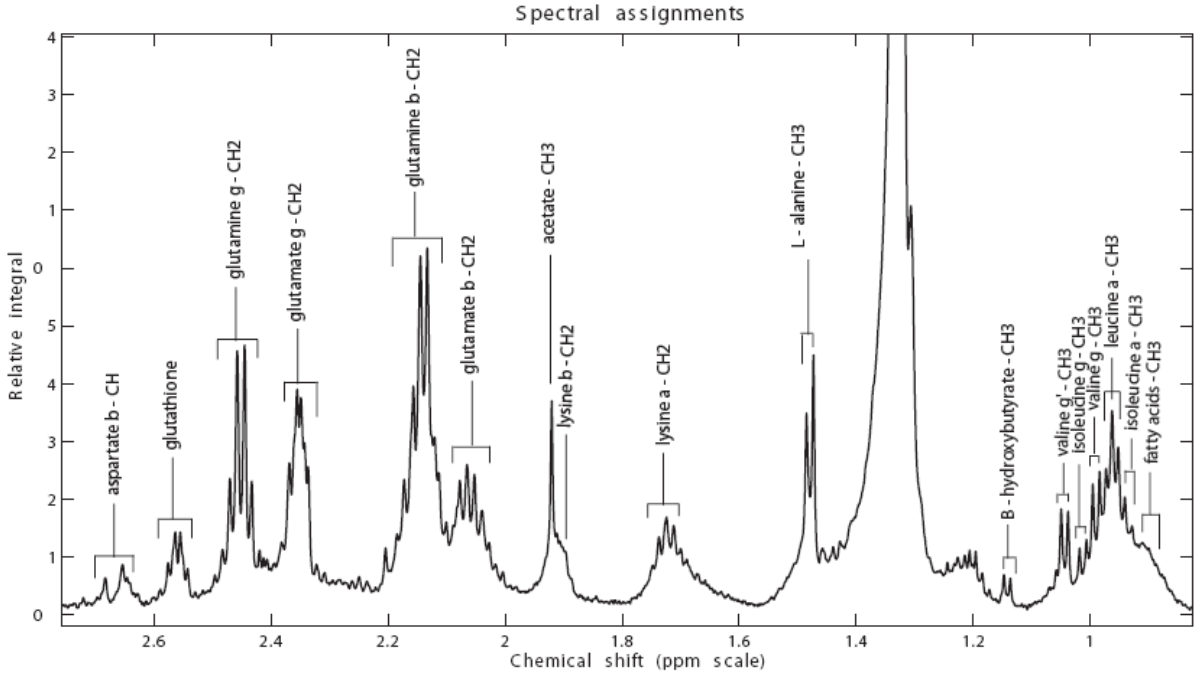


Figure 8. Example of 1D spectrum acquired by the author during the course of the study (Chemical shifts 0.6 – 2.7)

1.9.4.2 2D experiments

These include J-Resolved, Correlation spectroscopy (COSY) (Figure 9.) and Total correlation spectroscopy (TOCSY) experiments and were done to allow detection of intermolecular relationships in the spectrum.

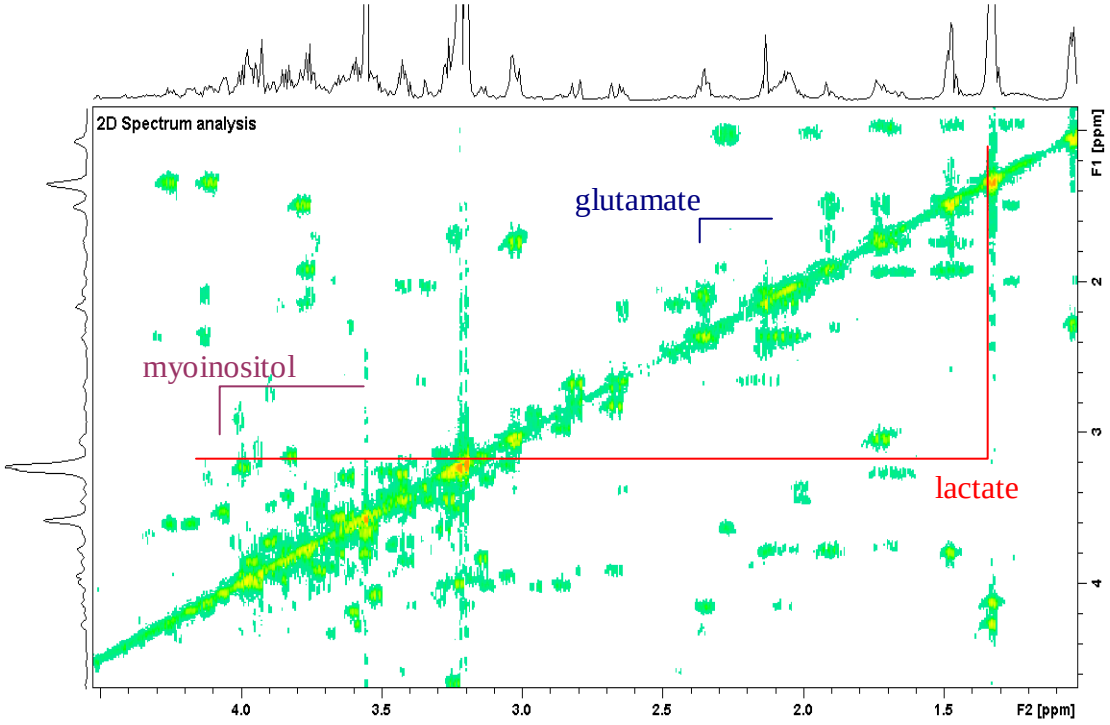


Figure 9. Example of 2D spectra generated by the study via 2D spectral analysis

1.9.5 Water presaturation

As water forms the greater proportion of any biological sample, with abundance of ^{1}H, peaks acquired has the highest intensity and may distort the signals received from other compounds of less concentration. Therefore, the application of low energy pulse (typically ~ 50Hz) before the main pulse will lead to acquisition of a signal that is

reduced in intensity in a discrete region of the spectrum. This 'presaturation' pulse, when applied at a frequency at which protons from water precess, can discriminately saturate the intensity around the water peak, thus allowing for other signals to be observed more easily after the main pulse.

1.9.6 Biological applications of NMR spectroscopy

To date, various studies used NMR spectroscopy for investigation of clinical problems using various human biological samples using both conventional and MAS NMR spectroscopy. Examples are summarized in table 4.

Study	**Year**	**Samples used**		**Field of study**
		Biofuids	**Tissue**	
Martino et al. [171]	1987	Bile	--	Drug metabolism
Nicholson et al. [172]	1989	Urine	--	Toxicology
Ellul et al. [173]	1992	Bile	--	Biochemical composition
Anthony et al.[174]	1992	Plasma	--	Toxicology
Koschorek et al.[175]	1993	CSF	--	Neuropathology
Husted et al.[176]	1993	--	Myelin	Biochemical composition
Nicholson et al.[177]	1995	Urine	--	Drug metabolism
Cheng et al.[178]	1996	--	Lymph nodes	Oncology
Holmes et al.[179]	1997	Urine	--	Inborn errors of metabolism
Liu et al.[180]	1997	Plasma	--	Biochemical composition
Nicolls et al.[181]	1997	Urine	--	Drug metabolism
Traikia et al.[182]	1997	--	Liposomes	Membrane composition
Humpfer et al.[183]	1997	--	Erythrocytes	Biochemical composition
Moka et al.[184]	1997	--	Renal tissue	Oncology
Cheng et al.[185]	1997	--	Brain tissue	Oncology
Beckwith-Hall et al.[186]	1998	Urine	--	Toxicology
Tomlins et al.[187]	1998	Semen	--	Biochemical composition

Guo et al.[188]	1998	--	Atheromas	Biochemical composition
Tomlins et al.[189]	1998	--	Prostate tissue	Oncology
Cheng et al.[190]	1998	--	Breast tissue	Oncology
Meshitsuka et al.[191]	1999	Synovial fluid	--	Arthritis
Tkadlecova et al.[192]	1999	Aqueous humour	--	Biochemical composition
Millis et al.[193]	1999	--	Adipocyte tissue	Oncology
Garrod et al.[194]	1999	--	Renal tissue	Biochemical composition
Griffin et al.[195]	2000	--	Renal tissue	Toxicology
Brindle et al.[168]	2002	Plasma	--	Coronary disease
Doran et al.[163]	2003	--	Oesophageal tissue	Oncology
Dave et al.[2]	2004	--	Barrett's mucosa	Oncology
Sitter et al.[196]	2004	--	Uterine cervix	Oncology
Odunsi et al.[168]	2004	Plasma	--	Oncology
Mun et al.[197]	2004	--	Gastric tissue	Oncology
Bourne et al.[198]	2005	--	Melanoma	Oncology
Holmes et al.[199]	2006	CSF	--	Schizophrenia
Bala et al.[200]	2006	Gut aspirate	--	Biochemical composition
Fang et al.[201]	2007	--	Pancreatic tissue	Oncology
Tessem et al.[202]	2008	--	Prostate tissue	Oncology
Jordan et al.[203]	2009	--	Colon tissue	Oncology
Bollard et al.[204]	2009	Urine, Serum	Liver	Liver regeneration
Smith et al.[205]	2009	Urine	--	Toxicology

Table 4. Examples of studies using metabonomics in literature

Recently, the development of high resolution ^{1}H magic-angle spinning (MAS) NMR spectroscopy has had a substantial impact on the ability to analyse intact tissue specimens [206]. It the most widely used technique as it has the highest sensitivity considering abundance of ^{1}H in biological samples; nevertheless, NMR can be employed to detect other biologically relevant nuclei such as ^{31}P, ^{15}N or ^{13}C.

Progress in magnetic resonance spectroscopy techniques and data analysis have improved its capability to determinate the pathology of human tissues based only on their metabolic profiles, and this approach has been applied on many cancer tissues as shown in table 4 above. It could even identify some stages in pathological processes before they are morphologically apparent e.g. be visualized by light microscopy e.g. thyroid follicular tumours [207,208].

1.9.7 Data processing and analysis

1.9.7.1 Chemometrics and pattern recognition (PR)

Chemometrics is the term generally applied to describe the use of PR and related multivariate statistical approaches to analyse chemical numerical data [209]. One of the problems of interpreting the data in metabonomics studies is the determination of significant changes in a large set of NMR spectra of a biofluid or tissue from a cohort of animals or humans demonstrating a variety of effects such as normal physiological variation that might obscure the disease process effect. This can be achieved by the use of PR methods. Multiparametric data can be modelled so that the class of a separate sample can be predicted based on a series of mathematical models derived from the original data or 'training set' [210]. PR is invaluable in reducing the dimensionality of complex data sets, for example by 2-D or 3-D mapping procedures, thereby facilitating the visualization of inherent patterns in the data set.

PR methods can be divided into two categories: 'unsupervised' and 'supervised' methods. Unsupervised multivariate techniques are used to establish whether any intrinsic clustering exists within a data set and include methods that map samples

according to their properties without a priori knowledge of sample class. Examples of unsupervised methods include principal components analysis (PCA) and clustering methods such as hierarchical cluster analysis. On the other hand, supervised methods of analysis use the class information given for a training set of sample data to optimize the separation between two or more sample classes. These techniques include soft independent modelling of class analogy (SIMCA), K-nearest neighbour analysis and neural networks. Supervised methods require a second independent data set to test or validate any class predictions made using the training set [210]. Subtle biochemical changes in ^{1}H NMR spectroscopic profiles of bio-fluids can be obscured in NMR PR analysis by interfering factors such as variations in pH, which can cause changes in NMR chemical shifts because of differences in the ionization state of some molecules. Minimizing effect of these factors have been studied and accomplished by techniques, for example, by adding a standard amount of buffer to the sample prior to NMR spectroscopic analysis [211]. In addition, other methods are used as automatic data reduction techniques and exclusion of areas of the spectrum prior to PR analysis, as those containing water or urea, where the signal intensity is very variable due to water NMR peak suppression effects [212]. In addition, after identification of regions of interest it is prudent to return to the raw NMR spectra for peak assignment and metabolite identification.

1.9.7.2 Principal component analysis (PCA)

PCA is a technique for finding a set of weighted linear composites of original variables such that each composite (a principal component) is uncorrelated with the others. It was originally devised by *Pearson* in 1901 [213], though it is more often attributed to *Hotelling*

(1933) who proposed it independently [214]. The first principal component is such a weighted linear composite of the original variables with weights chosen so that the composite accounts for the maximum variation in the original data. The second component accounts for the maximum variation that is not accounted for the first. The third component likewise accounts for the maximum given the first two components and so on. Each PC is orthogonal and therefore independent of the other PCs. These weights are found by matrix analysis that gives the weights for the original variables. This statistical technique has been used extensively in metabonomics. The output of the method results in two matrices known as scores and loadings.

1.9.7.3 Scores and loadings

Scores are the co-ordinates for the samples in the established model and may be regarded as the new variables. Each point represents a single NMR spectrum. The PC loadings define the way in which the old variables are linearly combined to form the new variables. The loadings define the orientation of the computed PC plane with respect to the original variables and indicate which variables carry the greatest weight in transforming the position of the original samples from the data matrix into their new position in the scores matrix [215]. In the loadings plot, each point represents a different NMR spectral region. Unsupervised methods such as PCA are useful for comparing pathological samples with control samples, but supervised analyses that model each class individually are preferred where the number of classes is large. Two common supervised methods are SIMCA and partial least squares (PLS) [215].

1.9.7.4 Soft Independent Modelling of Class Analogy (SIMCA)

SIMCA operates by establishing the multivariate boundaries for each class in a data set. Based on a defined set of samples with known class identity referred to as a 'training set', statistical models are formed. A separate PCA is performed for each class of data within the training set, and an independent or 'test' set of samples is then used to examine the predictive ability of the models. Each sample in the test set is fitted to every class model and predictions are made on the quality of fit. SIMCA models are superior to some other supervised techniques in that a sample may be assigned to a single category, to more than one category or to no category at all. Therefore, it avoids forcing the sample into a given category. PLS is a method that relates a data matrix containing independent variables from a set of samples to a matrix containing dependent variables (or measurements of response). PLS can be used to examine the effect of time on a data set; a feature that is particularly useful for NMR data collected from samples taken over the course of a disease, therapy or toxic effect. PLS can be combined with discriminant analysis (DA) to establish a discriminant surface where the optimal position to place best separates different classes [215].

1.10 Study aims and objectives

1.10.1 Overall aim

Characterization of the metabolic profile of oesophageal cancer and investigation of its potential use in diagnosis and follow up.

1.10.2 Detailed objectives

1- Characterize the metabonomic profile differences in cancer tissues, especially those pertinent to glycolysis, glutaminolysis and choline metabolism intermediates.

2- Investigate the field cancerization concept and test whether differences in metabonomic profile specific for cancer is seen even to a lesser extent in the cancer field.

3- Qualify tissue metabolic response to chemotherapeutics based on the previous mentioned metabolic pathways and possible new biomarker pathways/compounds.

1.10.3 Thesis layout

- Chapter 2: will display the methodology used in samples collection, storage, NMR analysis, spectral data acquisition and mathematical analysis of these data using pattern recognition techniques and regression analysis.
- Chapter 3: will display the design and characteristics of participants of the three main studies, together with the driving hypotheses and summary of observations.
- Chapter 4: displays the actual results; it is subdivided into three sections corresponding to those in chapter 3. Each section will discuss the observations recorded in each study followed by analysis and interpretation of these results.

- Chapter 5: is a discussion of overall results of the three studies, putting the metabolic profile analysis findings in context with the corresponding clinical management perspectives of oesophageal cancer.
- Chapter 6: is compilations of ideas for future research based on the findings of this study. Finally, the bibliography and appendices containing detailed data sheets.

2. CHAPTER 2. METHODOLOGY

Author statement

This is to state that I carried out, personally, all the stages of this study including preparation of study protocols, ethical approval application, sample collection, coding and storage, sample analysis in NMR MAS spectroscopy (i.e. sample preparation, operating the spectroscope and optimisation of all spectral acquisition parameters), spectral analysis and processing, application of pattern recognition techniques and multivariate analysis of data, statistical analysis of results and interpretation of data and finally to writing up the results in this manuscript and in all the papers submitted for publication based on these results and data.

2.1 Patients and Methods

2.1.1 Patients

Subjects were recruited from five hospitals across London and the surrounding boroughs: St Mary's Hospital and Harley Street Clinic, London; Harefield Hospital in Middlesex, Watford Hospital in West Hertfordshire; Lister Hospital in East Hertfordshire. These were a combination of oesophageal cancer patients, gastric cancer patients, Barrett's dysplasia patients and healthy control subjects. Out of this pool of patients different samples were employed for analysis in each study based on the suitability of the patient clinical and pathological criteria to each study design. In addition, sample and subsequently NMR spectral quality largely dictated inclusion and exclusion of patient subgroups in each study.

2.1.2 Arrangements for sample storage

2.1.2.1 Establishment of tissue bank

The author under supervision of Mr Hanna has established an upper GI Cancer Tissue bank at St Mary's Hospital. The tissue bank is sponsored by Imperial College London, based at the Department of Biosurgery and Surgical Technology at St Mary's Campus. Ethical approval has been granted by St Mary's Hospital local Research Ethics Committee on 31/03/2005, REC Ref: 04/Q0403/119. The project was approved by St Mary's Hospital Research and Development department on 03/08/2005 RE: 04/BH/0014E (Ethical approval letter and relevant forms used is included in appendix 1). Samples are collected and stored according to protocols recommended by the National Cancer Research institute report (2004). Informed consent was obtained from all patients. The tissue bank followed the provisions of the Data Protection Act 1998, and the Human Tissue Act 2000. Samples were backed up with a database of the enrolled patients. The named custodian of all samples and data was registered in the data controllers register at the information commissioner's office and at Imperial College London.

2.1.2.2 Ethics approval for metabonomic studies

Ethical approval for metabonomic analysis of the samples was obtained from the Royal Brompton and Harefield REC on 17/08/2005. REC Ref: 05/Q0404/73; extended to St Mary's REC on 06/10/2005 REC Ref: 05/Q0403/165. Copy of the approval letter was kept with the tissue bank documents. Ethical approval letter and relevant forms used is included in appendix 2.

2.1.2.3 Establishment of patient database

The following data was collected and stored for all patients:

- Demographic data: age, sex, ethnic origin, weight, height, BMI, smoking and alcohol intake history (all to subsequently study possible isolated or confounding effect of these factors on metabonomic profiles of samples).
- Medical status data: co-morbidities e.g., drug history including medications taken on the day of sampling in details, past medical history, ASA class
- Chemotherapy history including type, number of cycles and date of last cycle
- Clinical staging data, PET results and variables
- Pathological data: pathological site, size, type, subtype, macroscopic picture, TNM stage, vascular, perineural or lymphatic invasion, *Helicobacter pylori* infection, Barrett's metaplasia, regression after chemotherapy according to Mandard's classification, nodes harvested/nodes with metastasis (operative samples). Example page of the data extraction spread sheet used is included in appendix 3.

2.2 Sample collection

2.2.1 Tissue samples

2.2.1.1 Surgical samples

The patient was approached in the night before the procedure, the project was discussed and a full informed consent obtained. On procedure day, once the main specimen was removed, pathology team was informed, specimen put in a dry bucket and was taken to pathology suite where one of the pathology consultants would be ready to cut out the

sample; this was to ensure blocking of the immediate adjacent mucosa/tumour to set the gold standard for sample identification and diagnosis. Cut pieces of 30-50 mg are obtained from the mucosa of the following sites: normal oesophageal mucosa, normal proximal gastric mucosa, normal distal gastric mucosa and tumour sample. Cut pieces are split for the study and the other half goes to pathological confirmation. Samples are wrapped in an aluminium foil without washing, to prevent leakage of metabolites, and then stored in labelled cryo-tubes in -80^0c freezers.

2.2.1.2 Endoscopic samples

The night before the procedure, patient was approached, project discussed and a full informed consent obtained. During endoscopy, three bites out of each area as above are taken to collect an adequate sized sample. Care was taken to wash the biopsy forceps with saline rather than alcohol or formalin. Samples are wrapped and transported for storage. Time from sample excision in surgery / endoscopy to freezing was less than 20 minutes for all samples. All samples are strictly mucosal with minimal submucosa. Normal samples were taken at least 5 centimeters away from any visible suspicious or malignant mucosa. Time to freezing for all surgical and endoscopic tissue samples ranged between three to twelve minutes with an average of six minutes.

2.2.2 Blood samples

An informed consent was obtained the night before sampling. All samples are taken at 8 am; all patients were fasted more than 8 hours. Tubes used were red topped (plain), Blue topped (Na Citrate) and light Green topped (Lithium heparin) were used to collect blood

in an aseptic technique. All containers are put on ice for 20-30 minutes then centrifuged at 1500 G. Aliquots of separated serum/plasma and urine are stored -80^{0}c.

2.3 Sample preparation for NMR

2.3.1 Tissue samples

Sample transported to NMR suite was done in liquid nitrogen/dry ice. Tissue was thawed in room temperature for a maximum of two minutes, which was usually enough for thawing the sample owing to its small mass. The sample was then washed with 200 µL of 95% D_2O for 10 seconds maximum to prevent leakage of any solutes. The weight of the wet sample was recorded (Sample weights are displayed in appendix 4.), then the sample was loaded in a zirconium rotor, ready for NMR spectroscopy. All samples were preserved after NMR spectroscopy for further histological/subsequent molecular analysis.

2.3.2 Blood samples

The procedure was performed in the class II suite. Samples prepared by adding 200µL serum/plasma to 400µL Phosphate buffer (Na_2HPO_4+ $NaHPO_4$+ 0.02%TSP+0.2% Na Azide in 95% D_2O +5% H_2O). Mixture was centrifuged at 15000 G for 5 mins. 550µL of this solution was pipetted into a labelled standard 5mm NMR tube, and frozen before use. At all times during the preparation the sample was kept on ice to avoid degradation. Only one freeze-thaw cycle was allowed for each aliquot and subsequent prepared NMR sample, again to avoid degradation of the sample.

2.3.3 Tissue extraction

Tissue samples were extracted by adding 300 µL of a solvent mixture of freshly prepared 1:2 mixture of duterated methanol:duterated chloroform in an Eppendorf tube; tissues were then crushed by a special plastic piston and homogenized by vortexing for one minute; then centrifuged at 1500 G for 5 minutes. After vortexing, 300 µL of D2O was added to each tube and tubes were again vortexed. Tubes were then centrifuged at maximum speed for 5 min. On removal from the centrifuge two layers could clearly be distinguished in each tube – one corresponding to the aqueous phase (the upper layer), with the organic phase on the bottom. Note that most of the methanol added to these tubes ends up in the aqueous phase. Thus the volumes of each layer are approximately 400 µL and 200 µL in the aqueous and organic phases, respectively. Approximately 350 µL was aspired directly from the upper layer (aqueous phase) using a Gilson p200 pipette and added to an NMR tube (507-HP, GOSS Scientific Instruments Ltd, Cheshire, U.K.). 200 µL of D2O was then added to each tube so that the sample volume was sufficiently large for detection by receiver coils in the NMR probe. 150 µL was then withdrawn from the lower layer (organic phase) and added to an Eppendorf tube. This was lyophilised overnight. The following day some of the lyophilised organic phase extracts were redissolved in 550 µL of CDCl3.

2.4 Sample analysis by NMR Spectroscopy

2.4.1 Tissue ^{1}H –MAS NMR Spectroscopy

Metabolic profiles were generated using ^{1}H MAS-NMR spectroscopy of intact oesophageal tumour tissue (‘tumour’) and of proximal histologically-normal mucosa

('PHINOM') from cancer patients together with normal mucosa from an age-matched control group ('control'), therefore, these will hereby be the names of these groups throughout the text. NMR spectra were acquired on a Bruker DRX600 spectrometer (Bruker Biospin, Rheinstetten, Germany) operating at 600. 13-MHz ^{1}H NMR frequency and 283 K. Shimming was done manually for each sample. ^{1}H NMR spectra of the samples were acquired using a 1D *Carr-Purcell-Meiboom-Gill (CPMG)* pulse sequence (RD-90°-(τ -180°- τ)$_n$-acquire). The CPMG sequence generates spectra edited by T_2 relaxation times, i.e., with reduced signals from high molecular weight species or systems in intermediate chemical exchange. In the experiments n = 300 and τ =400 μs, for a total T2 relaxation time of 240 ms. For all spectra, 256 free induction decays (FIDs) were collected into 32K complex data points; using a spectral width of 12 019 Hz (20 ppm), with a 2-s relaxation delay between pulses. A water pre-saturation pulse was applied throughout the relaxation delay.

2.4.2 1D NMR spectroscopy for blood samples

Prepared blood and urine samples in NMR tubes were loaded in automated sample holder and analysed at 298 Kelvin in a 600MHz NMR Spectrometer (Bruker, Karlsruhe, Germany). The pulse sequences used to profile the samples were NOESYpr1D, CPMG. The spectrometer was tuned and matched; Ninety degree pulse duration was calculated for each sample run. Shimming was optimized by gradient shimming for each sample.

2.5 Data processing and analysis

Data were zero-filled by a factor of 2, and the FIDs were multiplied by an exponential weighting function equivalent to a line broadening of 1 Hz prior to Fourier transformation using XWINNMR software (Bruker Biospin, Rheinstetten, Germany). The acquired NMR spectra were calibrated to the lactate-CH_3 resonance at 1.33 ppm and corrected for phase and baseline distortions. All subsequent data processing and analysis, unless specifically stated otherwise, was conducted using in-house software written and compiled in MATLAB (Mathworks) by *O. Cloarec, T.M.D Ebbels and H. C. Keun*. Spectra were interpolated from 32K to 42K data points using a cubic spline function to regularize the abscissa and improve calibration accuracy (final resolution 0.29 Hz/pt) prior to pattern recognition analysis.

For pattern recognition analysis, spectra were divided and signal integral was computed in δ 0.01 intervals across the chemical shift range δ 0.24-9.96. The region δ 4.7-5.2 was excluded to remove variation in the presaturation of the water resonance, also regions $\delta<0.8$ and $\delta>0.95$, were excluded to avoid the effect of baseline noise. Signals from local anaesthetic used during endoscopy were identified by separate anaesthetic NMR analysis, anaesthetic peaks did not correlate or affect the rest of the spectral regions as confirmed by correlation analysis; yet these peaks were excluded from the analysis so they do not confound the mathematical model development or the final statistical analysis. Therefore, 699 variables were left to be analysed in the following spectral regions: δ1.075-1.255, 1.355-1.405, 2.185-2.245, 2.265-2.275, 3.335-3.395, 3.625-3.775, 4.295-4.325 and 7.185-7.305. Each integrated NMR spectral region was then divided by sum of the total remaining intensity for each spectrum in order to normalize values. The reduced and

normalized NMR spectral data were imported into SIMCA-P (version 11, Umetrics AB, Umeå, Sweden) and each variable was mean-centred and Pareto scaled (divided by √standard deviation) prior to Partial Least Squares (PLS) regression.

2.6 Pathological examination

Samples matched to those undergoing NMR spectroscopy were subjected to staining with hematoxylin and eosin to ensure the benign or malignant nature of tissues. Normal oesophagus slides from 34 cancer patients and 50 noncancer patients underwent additional immuno-histochemical staining for the following markers Ki-67, P-53, terminal deoxynucleotidyl transferase-dUTP nick end labeling (TUNEL) and mucin where percentage of areas stained was accurately calculated by computational image analysis techniques. Two consultant pathologists (Dr Robert Goldin and Dr Josephine Lloyd, Department of Histopathology, St Mary's Hospital, London), both with special interest in oesophageal cancer examined the slides independently. In addition, they examined ten slides of each of the normal tissue from cancer and non-cancer groups blinded to the origin of the tissues.

2.7 Validation studies:

2.7.1 Validation of methods of tissue collection, storage and NMR processing

Studies to verify the quality of tissue collection and analysis were done to ensure the resulting spectra were not affected by the mode of collection, storage or the NMR operator.

a. Samples analysed at the beginning of the study were compared to those analysed near the end of the study, which makes a period of about 14 months, where the tissue was stored in -80^{0}C. Subtle differences were found, mostly in the aromatic part of the spectrum, in the form of poorer quality peaks and mild elevation of the noise signals. None was statistically significant.

b. Up to 10 samples were collected by a different research fellow, and analysed by a third one. When compared to the rest of the spectra, no apparent differences were found by visual examination of the spectra.

c. Surgical specimen samples were analysed against those collected by endoscopy and a PCA plot was constructed and showed absence of significant clustering of these groups (Figure 10). However, surgical samples were found to different than endoscopic samples in some of the metabolites measured, this difference was found to be nonsignificant when examined as an independent factor in separation of groups.

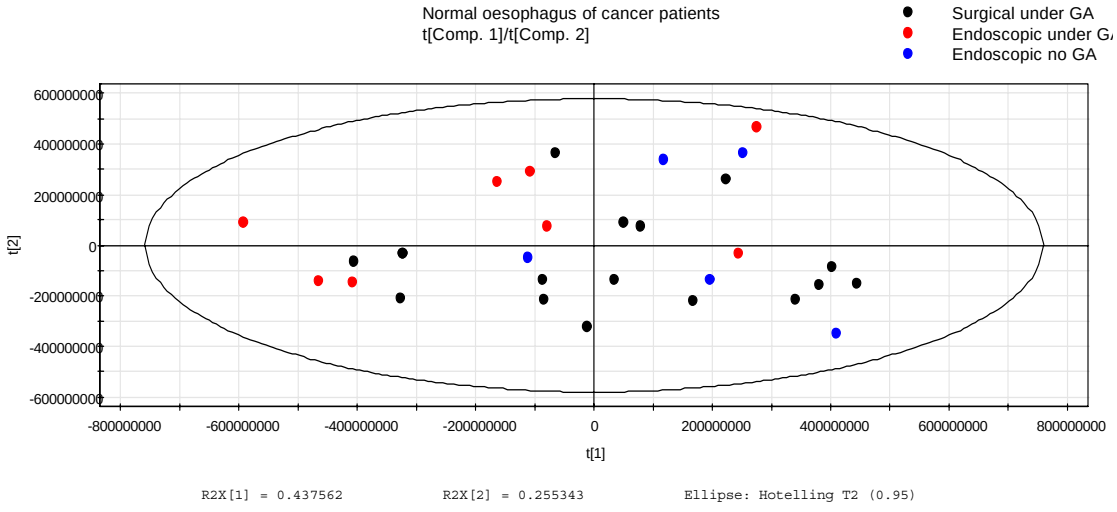


Figure 10. Normal oesophagus of cancer patients taken under different anaesthetic conditions

d. Local anaesthetic used during endoscopy was found to appear as a group of distinct peaks on the spectrum due to the fact it coated the oesophagus during endoscopy and was collected with the sample. Repeat of endoscopic sample collection was done to get samples from patients who approved only sedation during their endoscopy. Comparison and OPLS models showed lack of effect of those peaks on the rest of the spectrum; therefore these peaks were excluded from the analysis and the samples were used as regular.

2.7.2 Validation of statistical methods used during data processing

Statistical advisory service at Imperial College London was consulted as for different statistical tests used to validate the data distribution as well as those methods used in the final data analysis.

a. Normalisation methods: the data were processed by hand, by me, for: calibration, base line correction and normalisation of the spectra. This was done to assure consistency of processing, at the same time Dr Keun, the second supervisor would overlook processed data at regular intervals to ensure absence of systematic errors in processing. To ensure veracity of the mathematical processing, spectra were normalised to:

- median fold changes [216]
- constant = the value 1
- creatine peak average value
- average of healthy oesophageal mucosa spectra.

All normalisation methods were compared and yielded similar results in terms of group clustering on PCA analyses and on visual inspection of all spectral regions in all patient subgroups.

b. Data set variable value transformation: upon analysis of the data sets by SIMCA, alternative methods of data transformation was attempted e.g. log transformation, where the residuals get bigger for bigger values of the dependent variable maximizing display of differences between groups

c. Scaling methods: different scaling methods were tried to show maximal difference between data
    - Mean centering: showing actual raw changes of the data
    - Unit Variance scaling: the base weight is computed as 1/sdj, with sdj is the standard deviation of variable j computed around the mean.
    - Pareto Variance scaling: the base weight was computed as 1/sqrt (sd_j), Pareto scaling was in between no scaling and UV scaling and gives the variable a variance equal to its standard deviation instead of unit variance. Different transformation and scaling methods did not change the observation of results significantly confirming its validity.
    -

2.7.3 Validation of metabolic profile results

a. Peak assignment was done by:

i. Hand searching of electronic metabonomic databases online in addition to confirmation of assignment by at least 2 published studies in peer reviewed journals (Figures 11-13).

ii. Acquisition of 2 dimensional NMR experiments confirming spatial relations between components of the same structure (Figure 14.).

iii. Examining the spectra against the physico-chemical structure of the compound in question with exclusion of assignments that defy well established NMR rules of spectral assignment (Figures 15-17).

iv. A few spiking experiments were done to emphasize the identification of some of the compounds where the peaks in question are seen to magnify upon addition of the pure compound material to the tissue samples.

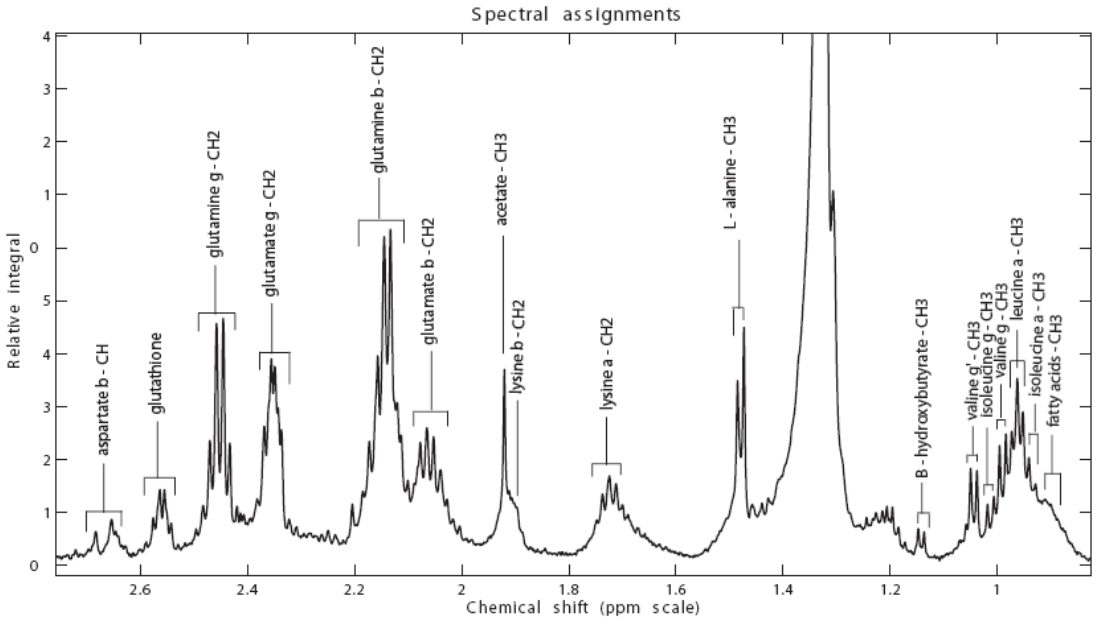


Figure 11. Assignment of spectra generated by the study (Chemical shifts 0.6 – 2.7)

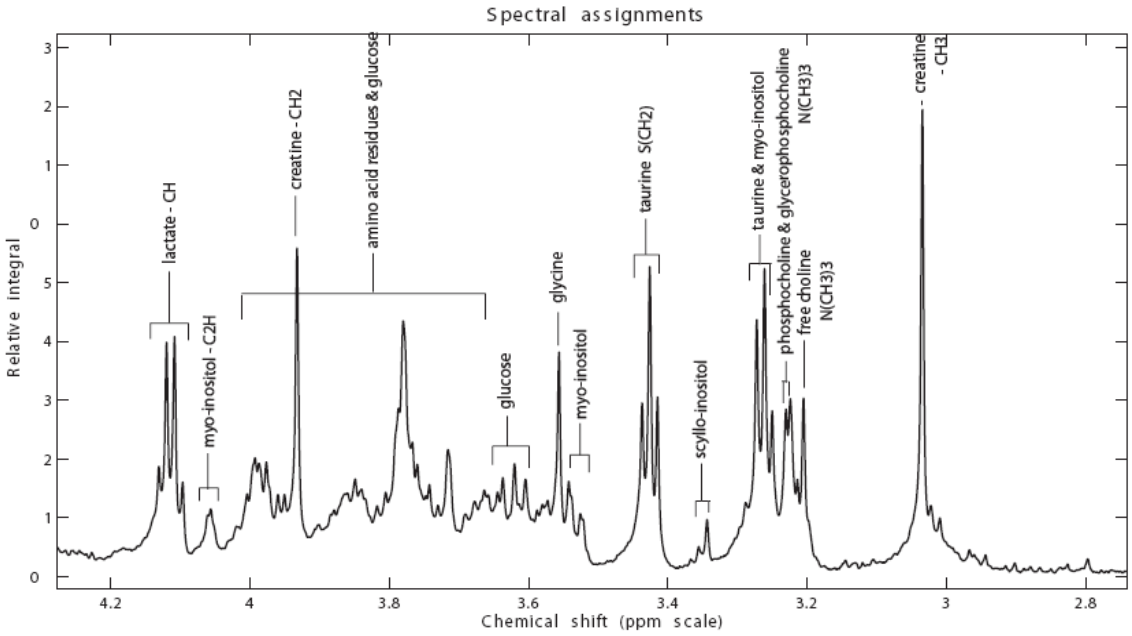


Figure 12. Assignment of spectra generated by the study (Chemical shifts 2.75 – 4.3)

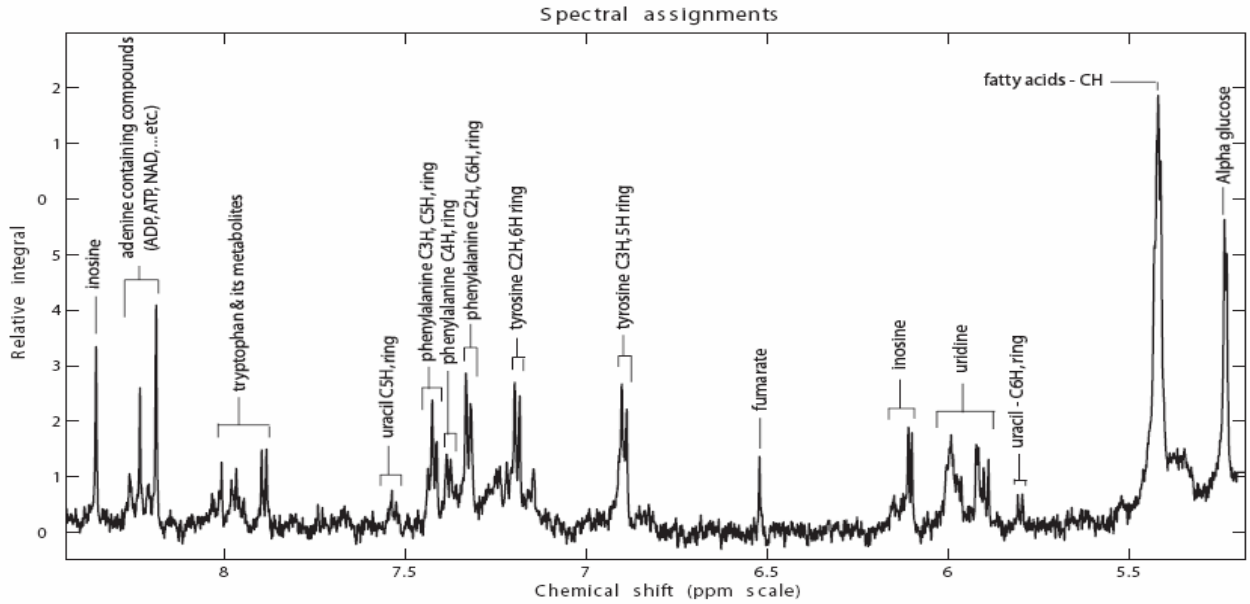


Figure 13. Assignment of spectra generated by the study (Chemical shifts 5.3 – 9)

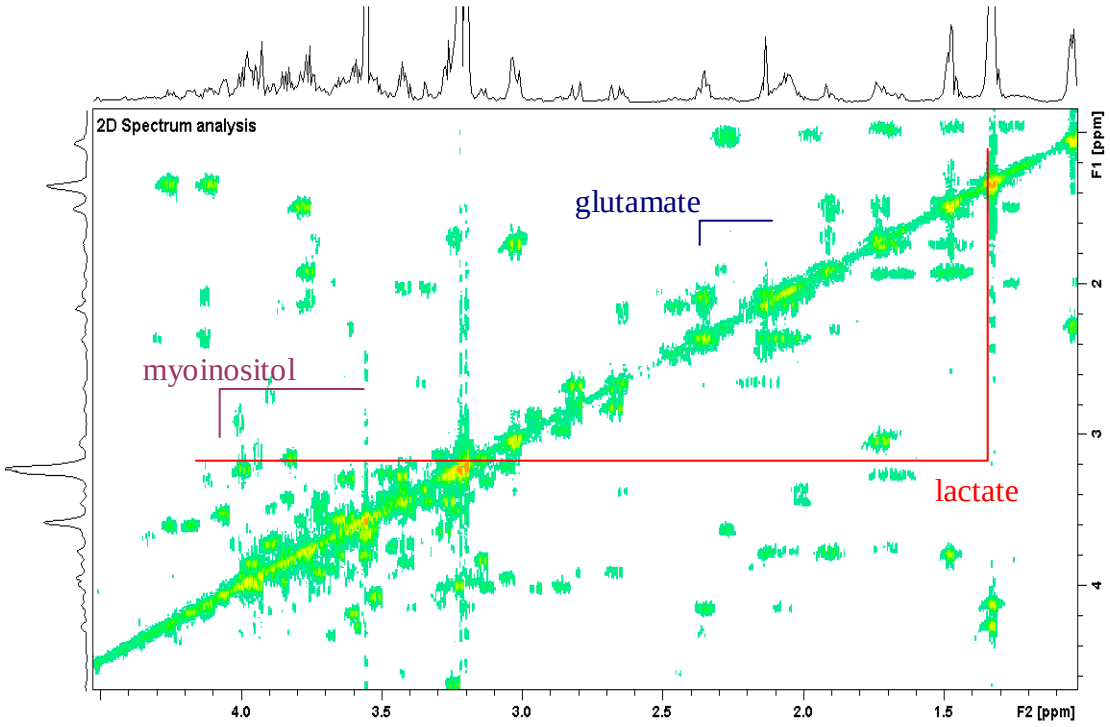


Figure 14. Assignment of spectra generated by the study via 2D spectral analysis to examine physical proximity of compound components confirming its identity

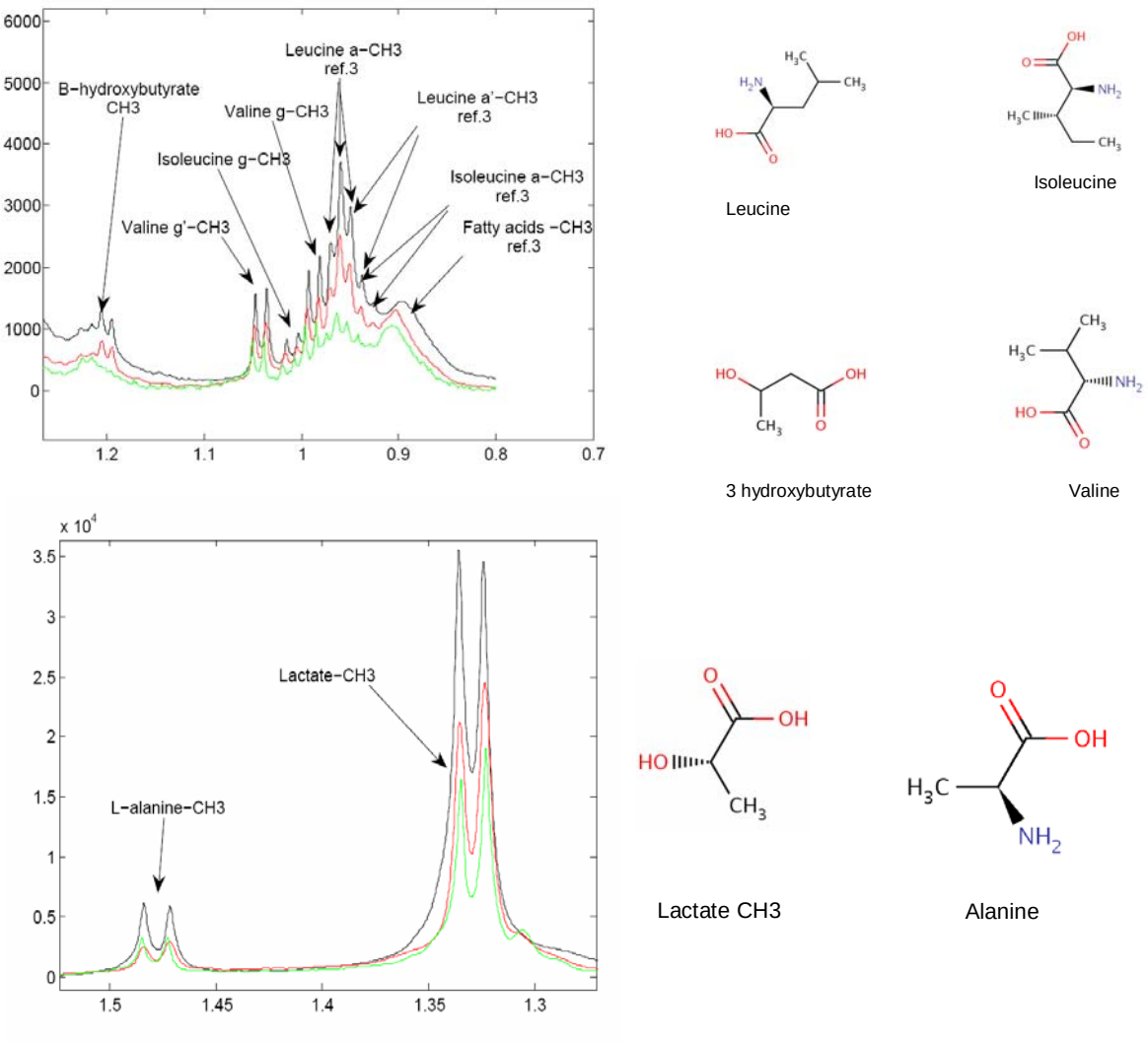


Figure 15. Confirmation of assignments via examination of chemical structure

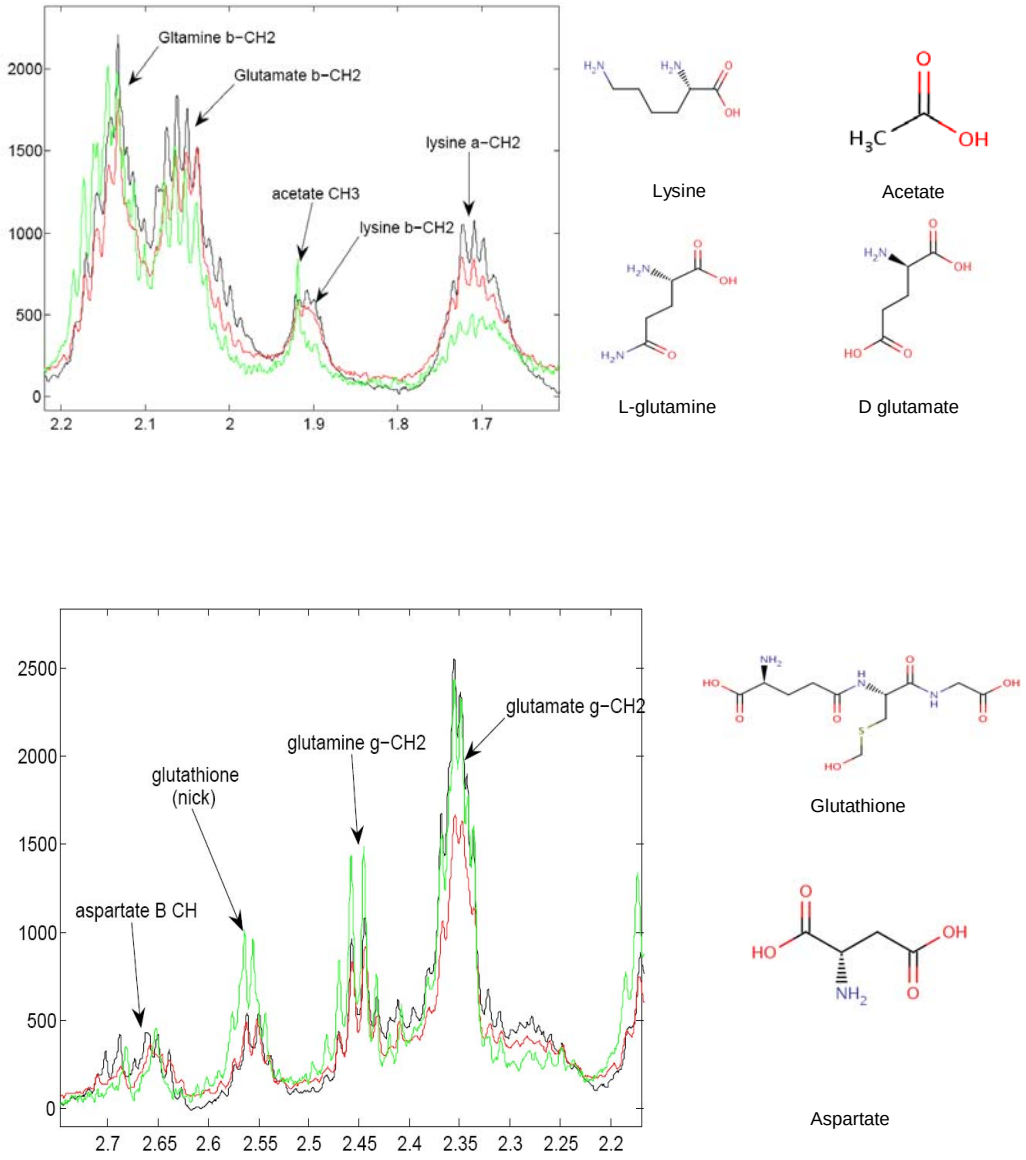


Figure 16. Confirmation of assignments via examination of chemical structure

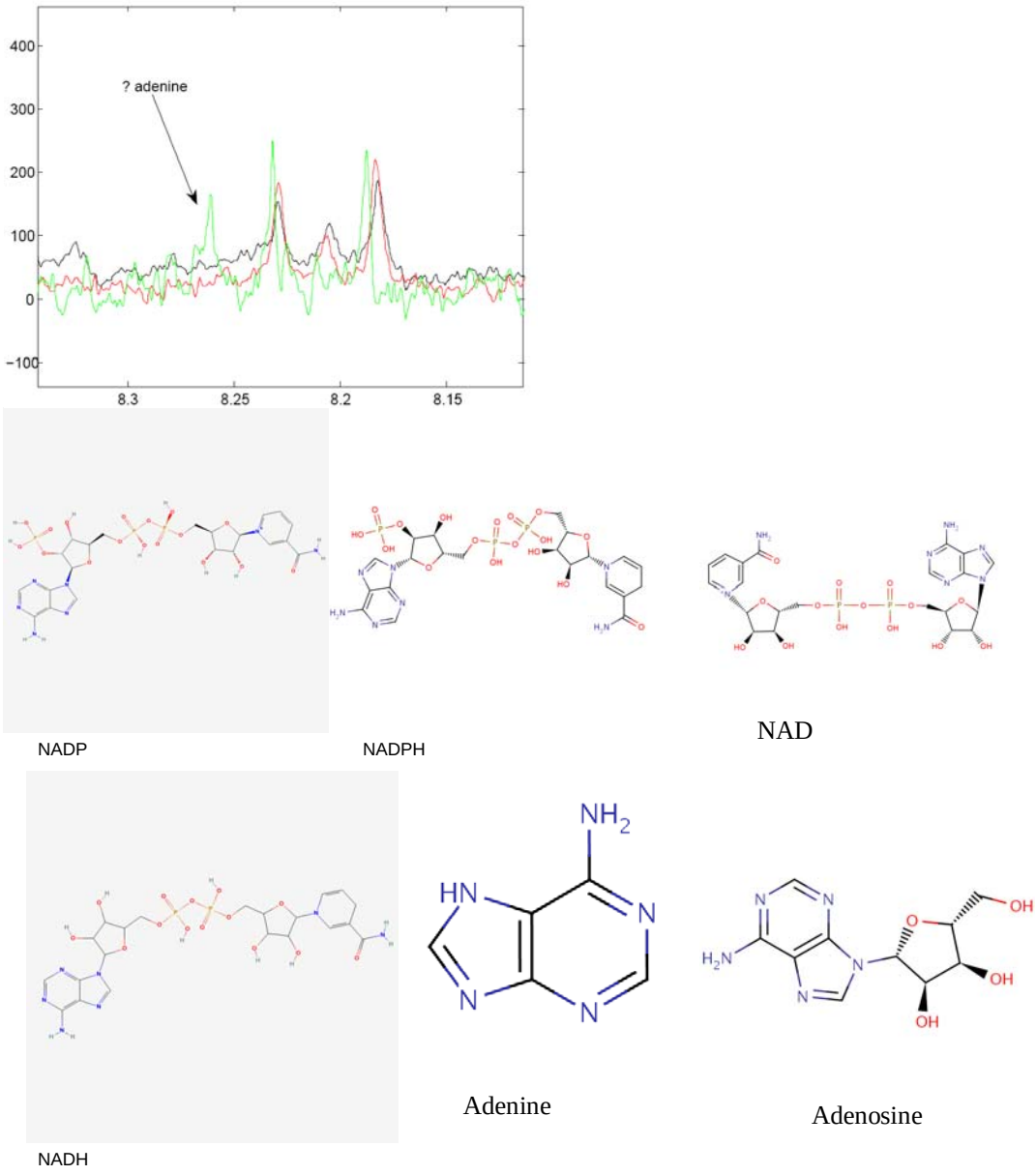


Figure 17. Confirmation of assignments via examination of chemical structure

b. Tissue extraction was done to ensure findings of the intact tissue running were not due to compartmentalization of certain compounds that might not have been visible to NMR due to tissue density. Findings were almost exactly the same in most of the compounds studied (Figure 18.). Only the broad lipid peaks were lost upon extraction of the tissue.

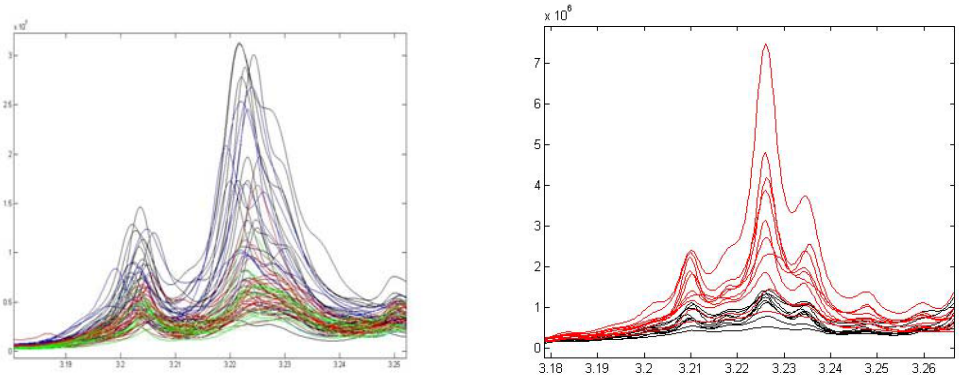


Figure 18. Showing similar NMR peaks and difference between tumour and normal tissue in intact tissue and extracted samples

c. Statistical methods used to examine the data were based on optimization of choice of appropriate statistical tests to produce the most reliable result and confirm significance when present. The following are examples:

i. The Lilliefors test was used to evaluate the hypothesis that the dataset has a normal distribution with unspecified mean and variance, against the alternative that it does not have a normal distribution.

ii. A two-sample Kolmogorov-Smirnov test was used to compare the distributions of values in the two data vectors when two data sets were compared. The null hypothesis for this test is that X1 and X2 have the same

continuous distribution. The alternative hypothesis is that they have different continuous distributions.

iii. Kruskal-Wallis and Wilcoxon ranksum tests are the nonparametric one-way Analysis of Variance (ANOVA), these were used to compare samples from two or more groups. The choice of a critical p-value to determine whether the result is judged "statistically significant" is left to the researcher. It is common to declare a result significant if the p-value is less than 0.05 or 0.01.

3. CHAPTER 3. METABONOMIC PROFILING STUDIES

3.1 Study I: Global metabonomic phenotyping of oesophageal and gastric cancer patients

Metabonomics investigations provide a quantitative description of the low-molecular mass endogenous metabolites present in a biological sample giving a "metabolite fingerprint" of cancer and normal tissues.

3.1.1 Hypothesis

Oesophageal cancer tissue has metabolic markers of increased rates of glycolysis and glutaminolysis as compared to normal tissue.

3.1.2 Objectives of the study

- Characterize the metabonomic profile of malignant and normal tissue samples from both oesophageal and gastric cancer patients with focus on glycolytic intermediary compounds and glutamine metabolism intermediates.
- Compare adenocarcinoma and squamous oesophageal cancer to normal tissue.

3.1.1 Patients and data analysis

Fifty seven patients were recruited in the study. Twenty seven patients had oesophageal cancer, 11 with oesophago-gastric junctional cancer and 15 had gastric cancer. Three patients had high grade dysplasia of the lower oesophagus with no evidence of carcinoma. Sample collection, preparation and NMR analysis with subsequent data processing and statistical analysis followed the same protocol described in section 2.5., 2.6. and 2.7). Principal component analysis (PCA) and Partial Least Squares Discriminate analysis (PLS-DA) was performed constructing various models. Outliers during model development were recorded for re-analysis and scrutiny.

3.2 Study II: Field effects in non-dysplastic tissue from oesophageal cancer patients

The concept of 'field cancerization' was introduced by *Slaughter* in 1953 stating that tumours arise within a transformed field with an altered biochemical phenotype [78]. It meant to describe the existence of generalized carcinogen induced early genetic changes in the epithelium from which multiple independent lesions occur, leading to the development of multifocal tumours[78]. In one of his earlier publications he stated: "cancer does not arise as an isolated cellular phenomenon, but rather as an anaplastic tendency involving many cells at once"[76]. This formed a belief that the lateral spread of tumours was due to progressive transformation of cells adjacent to a tumour, rather than the spread and destruction of the adjacent epithelium by pre-existing cancer cells[77]. Ever since, many studies were conducted to test this hypothesis in various cancers[85,87,94-101] by investigating the genetic and epigenetic mutations, transcriptional effects and proteomic profiling aspects of tumours. With present technological advancement, including laser capture micro-dissection and high-throughput genomic technologies, carefully designed studies using appropriate control tissue will enable identification of important molecular signatures in these genetically transformed but histologically normal cells[75].

3.2.1 Hypothesis

Histologically-normal mucosa from oesophageal cancer patients' tissue has metabolic properties of cancer but with less scale.

3.2.2 Objectives of the study

- Compare the metabonomic profile of histologically-normal mucosa from oesophageal cancer patients tissue with that from non-diseased controls
- Identify putative biomarkers of potential value in clinical diagnostic applications.

3.2.3 Patients and data analysis

Eighty seven patients were recruited; 35 with oesophageal adenocarcinoma and 52, age-matched, non cancer controls. Seventeen patients from the cancer group had chemotherapy during the course of the study, typically 3-6 courses of Cisplatin+5-fluorouracil or Epirubicin+Capecitabin. Control samples were taken from non-cancer patients during endoscopy for indications other than suspicion of malignancy. All but 21 of these patients received local anaesthetic during their endoscopy. Another set of matched samples from all sampled areas were fixed in paraffin for pathological examination. All samples were collected after an overnight fasting. Samples were annotated with full clinical details including demographic data, co-morbidities and drug intake.

Sample collection, preparation and NMR analysis with subsequent data processing and statistical analysis followed the same protocol described in sections 2.5, 2.6 and 2.7. Pathological assessment was conducted as section 2.8. Final analysis of the data in this study has been done in conjunction with Dr Hector Keun; where he kindly helped to perfect the statistical modelling and the final descriptive figure of the results.

3.3 Study III: Profiling metabonomic response of oesophageal adenocarcinoma to chemotherapy

Collectively, data from European and American studies suggest that administering systemic chemotherapy prior to surgery for oesophago-gastric cancer improves survival compared to surgery alone [114,116,217]. The response rate to cytotoxic therapy is about 40% in oesophago-gastric cancer. Available evidence suggests that a favourable

histopathological response to cytotoxic therapy may be a useful positive predictive marker in oesophago-gastric cancer. However, the ability to predict tumour response in routine clinical practice is difficult and is an area of intense investigation. The predictive/prognostic significance of histopathological response to cytotoxic therapy was reported by *Mandard et al* [117] in oesophageal cancer specimens (predominantly squamous cell carcinomas) following neoadjuvant chemo-radiotherapy. Tumour regression grade (TRG) analysis, as a marker of treatment response was undertaken in that study and scored from complete regression (TRG1) to absent regression (TRG5). Of the 93 patients in that study, 42% were TRG1–2, 20% TRG3 and 33% were TRG4–5. Tumour size, pathological lymph node status, TRG and oesophageal wall involvement correlated highly with disease-free survival. On multivariate analysis, however, only TRG (TRG1–3 vs TRG4–5) remained a significant (p=0.001) predictor of disease-free survival [117].

3.3.1 Hypothesis

Metabolic profile of oesophageal tissues vary with chemo-responsiveness in pathways described above as related to carcinogenesis and invasiveness.

3.3.2 Objectives of the study

- To observe the differences in metabolite content of tumour and normal tissue after chemotherapy.
- To correlate the histo-pathological response to neo-adjuvant chemotherapy with metabolic tissue profiling.

3.3.3 Patients and data analysis

Ninety nine patients were recruited; 47 with oesophageal adenocarcinoma and 52, age and sex matched, non- cancer controls. Twenty seven patients from the cancer group had chemotherapy in the form of 3 cycles of Cisplatin + 5-fluorouracil or Epirubicin + Capecitabin. The last chemotherapy dose was administered at least three weeks prior to sample collection. In cancer patients group, seven had complete response to chemotherapy; therefore tumour tissue could not be harvested. Tissues from non-cancer patients were used in this study as negative controls. In the non-cancer group, only 31 patients had local anaesthetic during their endoscopy. In six of the patients, tumour and PHINOM samples were collected before chemotherapy, and from the same areas of mucosa three weeks after chemotherapy have been completed. Samples from 18 post chemotherapy patients were collected and graded according to their response to chemotherapy by *Mandard's* grading system via visual histopathological as well as image analysis examination. All samples were collected after an overnight fasting. Samples were annotated with full clinical details including demographic data, co-morbidities and drug intake.

Sample collection, preparation and NMR analysis with subsequent data processing and statistical analysis followed the same protocol described in 2.5, 2.6 and 2.7. Samples matched to those undergoing NMR spectroscopy underwent pathological examination as per the protocol described in section 2.8.

3.3.4 Response to chemotherapy

The response to chemotherapy was determined by histopathological assessment where reporting was agreed upon by two expert pathologists independently examining the slides. Table 5 shows *Mandard* grading.

Tumour regression grade	Histological characteristics
1	Complete regression: no histologically identifiable residual cancer, only fibrosis
2	Rare residual cancer cells scattered through fibrosis
3	Increase in the number of cancer cells, but fibrosis still predominant
4	Residual cancer outgrowing fibrosis
5	Absence of regressive changes

Table 5. Grading of tumor regression after neoadjuvant radiochemotherapy according to Mandard [117]

In addition, stained areas and percentage of fibrosis areas reflecting extent of healing response to chemotherapy was accurately calculated by computational image analysis techniques. Using the *Sirius Red* stained sections, the percentage fibrosis for each specimen was calculated using an image analysis system consisting of a light microscope (Olympus) with attached digital camera (Nikon BX40; Nikon, Japan) and a frame-grabber board installed in an Intel Core based PC (Hewlett Packard) and NIS elements version 2.3 image analysis software (Nikon, Japan). Images of Sirius Red stained sections were captured at 10X magnification, digitized following interactive light intensity equilibration and analyzed as RGB 24-bit images. The images were captured at 2048 X 1536 resolution at 24-bit colour depth and 300 dpi. The 2-dimensional patterns were

measured by direct pixel counting on the binary images. Five representative fields from each slide were assessed and an average taken. Prior to proceeding with the use of x10 magnification for digitizing the specimens, fibrosis percentage measurements for 10 liver biopsies were compared using both x20 and x40 objective was chosen for scanning and subsequent fibrosis percentage measurement.

4. CHAPTER 4. RESULTS

During the course of the thesis, 282 samples were collected from 144 patients recruited from five hospitals across London and the surrounding boroughs: St Mary's Hospital and Harley Street Clinic, London; Harefield Hospital in Middlesex and Watford Hospital in West Hertfordshire and Lister Hospital in East Hertfordshire. These were oesophageal cancer patients, gastric cancer patients, Barrett's dysplasia patients and healthy control subjects. Out of this pool of patients different samples were employed for analysis in each study based on the suitability of the patient clinical and pathological criteria to study design. In addition, sample and subsequently NMR spectral quality largely dictated inclusion and exclusion of patient subgroups in each study. Hence, throughout the results section, the demographic data and sample characteristics are displayed in the patients and methods section of each study separately.

4.1 Study I: Global metabonomic phenotyping of oesophageal and gastric cancer

4.1.1 Patients

One hundred and thirteen samples from 56 patients were analyzed. Twenty seven patients had oesophageal cancer, 11 had junctional cancer and 15 had gastric cancer. Three patients had high grade dysplasia of the lower oesophagus with no evidence of carcinoma. Patient characteristics are displayed in table 6.

Tissue sample		Pilot study	Main study		Chemo-therapy Yes/No	Sex M/F	Total
			Cancer	Control			
Oesophageal cancer	**Adenocarcinoma**	2	19	--	10/11	18/3	27
	Squamous	--	6	--	1/5	4/2	
Barrett's oesophagus		--	3	--	2/1	3/0	3
Junctional tumours		1	10	--	7/4	10/1	11
Proximal gastric cancer		2	7	--	3/6	3/6	9
Distal gastric cancer		--	6	--	0/6	4/2	6
Normal oesophageal mucosa		2	28	4	14/20	23/11	34
Normal proximal gastric mucosa		2	12	3	4/13	8/9	17
Normal distal gastric mucosa		--	4	2	1/5	3/3	6
Totals		9	95	9			113

Table 6. General characteristics of patients included in tissue analysis

4.1.2 Global phenotyping

Median CPMG spectra showed that the larger part of the spectrum to be at apparently consistent amplitudes among normal and cancer tissue reflecting similar structural qualities of mucosal tissues. This in turn emphasizes the view that different resonances among pathologic groups essentially reflect the disease process. Visual inspection of the spectra detected obvious differences between normal and malignant tissues in gastric,

junctional and oesophageal samples. Examples from comparison of tissue spectra are shown (Figures 19-22).

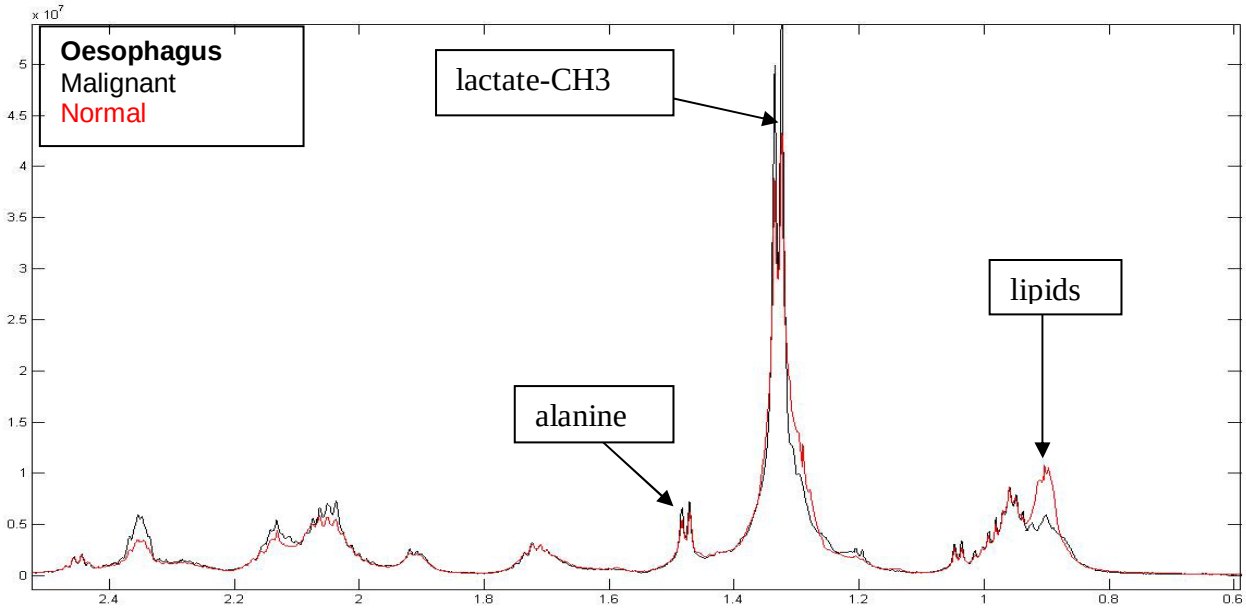


Figure 19. Overlaid average ^{1}H MAS-NMR CPMG spectra of malignant and proximal non-tumour oesophageal tissue. Spectra show some peaks are identical (e.g. most amino acids) while others which are different (higher or lower) between normal and malignant oesophageal tissue (e.g. lactate, lipids, glutamate) suggesting differential changes of various classes of metabolites involved in separate pathways are due to pathological effect rather than systematic error

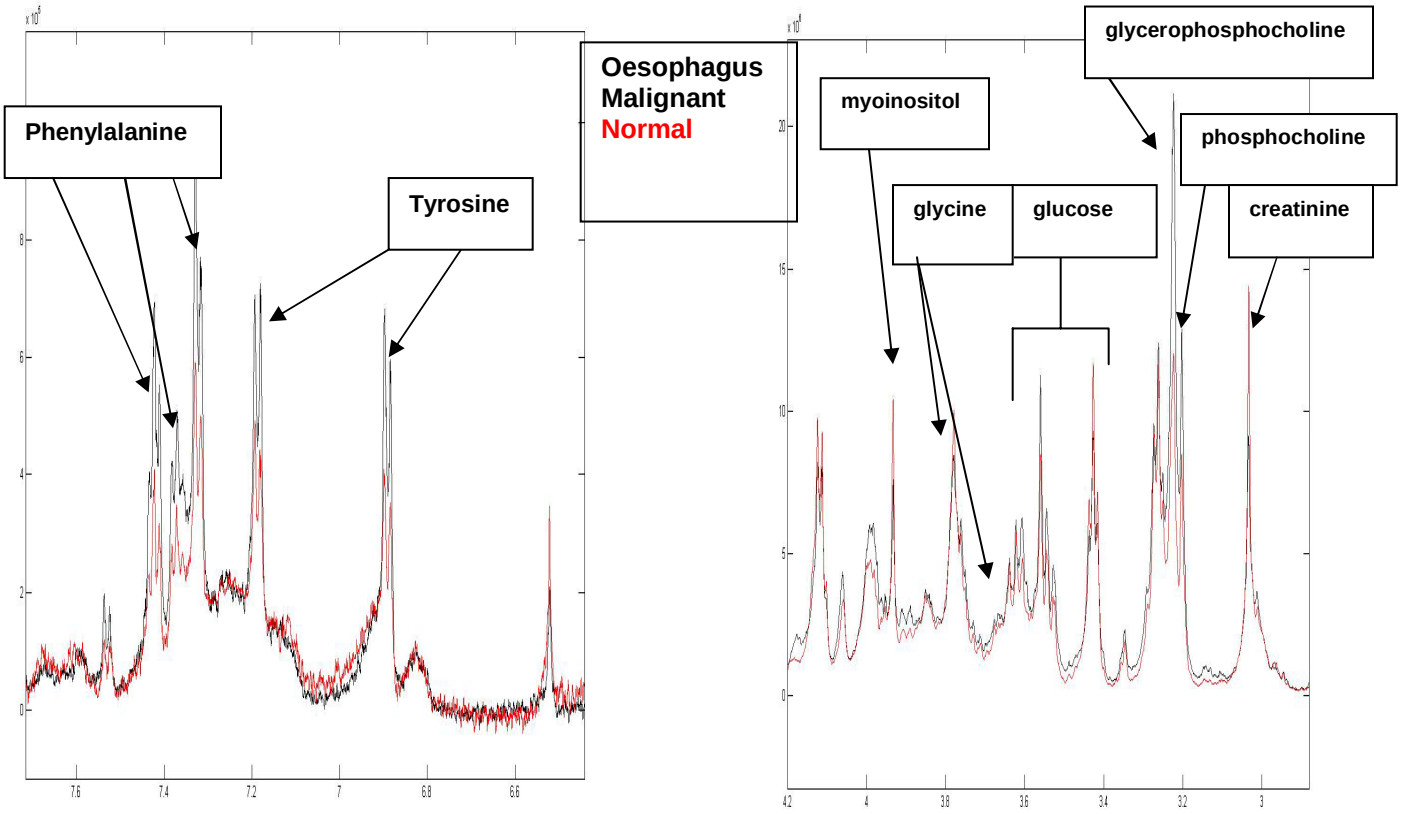


Figure 20. Differences in part of the median CPMG spectra between normal and malignant oesophageal tissues

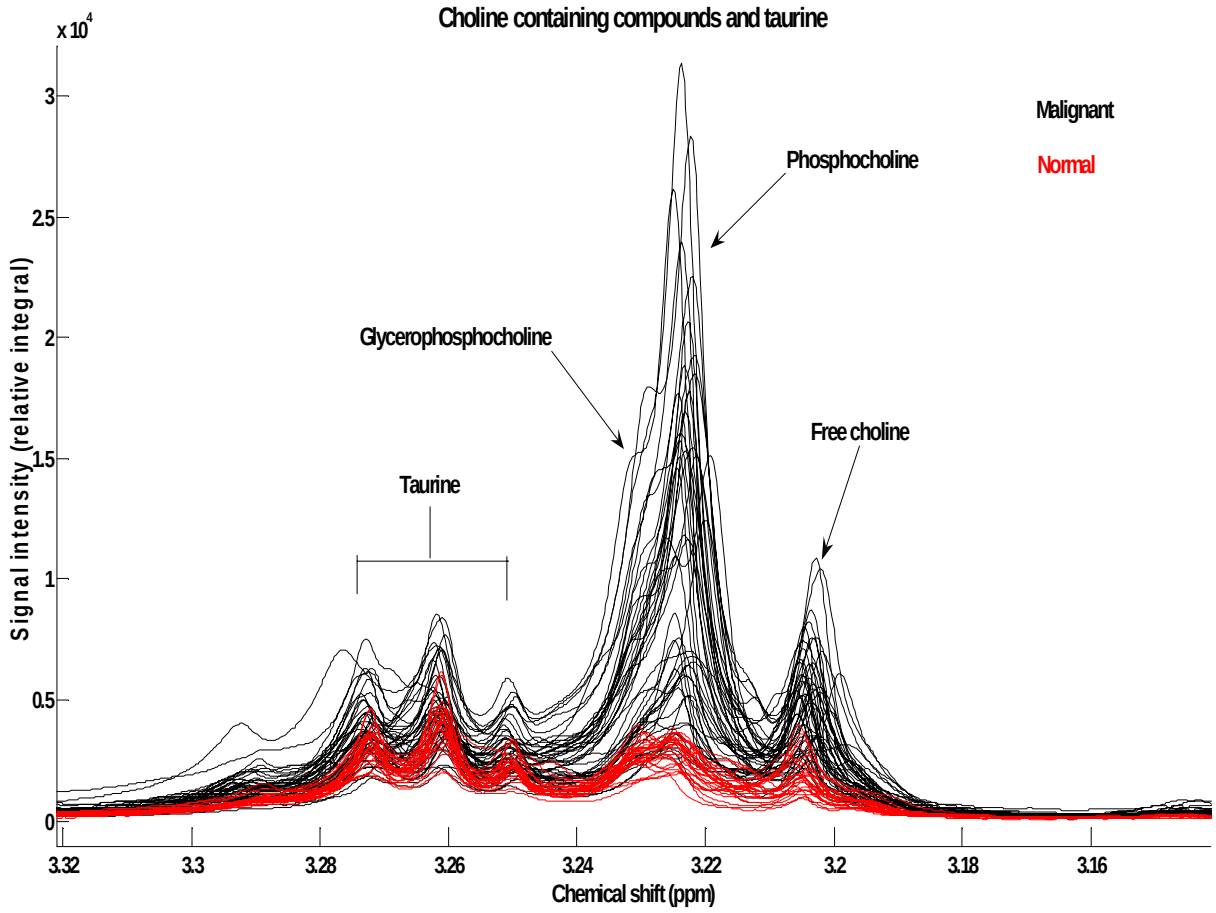


Figure 21. Overlaid ^{1}H MAS-NMR CPMG spectra of oesophgeal and gastric tissue. All tissues were obtained prior to chemotherapy. A portion of aliphatic region shows systematic increase of free choline, phosphocholine, glycerophosphocholine and taurine in tumour compared to normal tissue

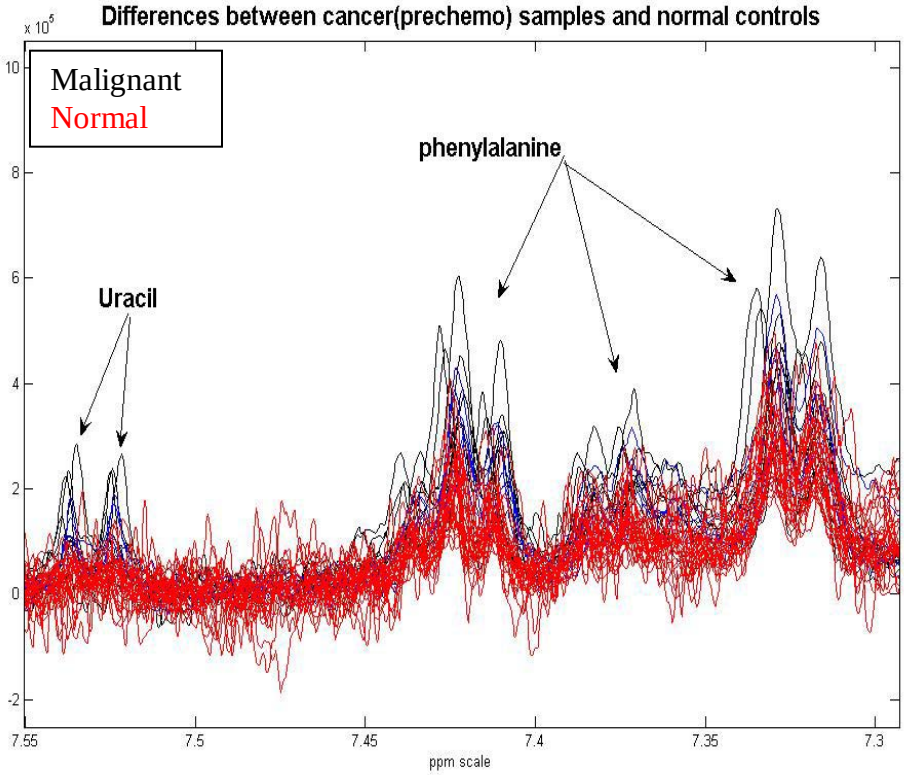


Figure 22. Spectra of non chemotherapy-treated tissue (inclusive of oesophageal and gastric samples) showing systematic increase of uracil and phenylalanine in tumour compared to normal tissue

Pattern recognition techniques were applied to investigate these differences and determine the main features discriminating between groups in the dataset. All tissue samples were included in the model as follows: oesophageal tumour tissue (squamous and adenocarcinoma), Barrett's epithelium, junctional tumours, proximal and distal gastric tumours, together with proximal and distal normal gastric mucosa. Proximal and distal gastric tissues were put in the same class to test for general discrimination of gastric from oesophageal tissue. After exclusion of outliers, analysis of the first two principal components of an unsupervised PCA model showed remarkable discrimination

between different tissues (Figure 23.). In general, oesophageal tissue could be seen clustered separately from gastric tissue. Normal oesophageal tissue could be seen to clearly separate from its malignant counterpart. Junctional tumours were scattered between both gastric and oesophageal tissue. Discrimination between normal and malignant gastric tissue could also be noted, although less clearly than in oesophageal samples.

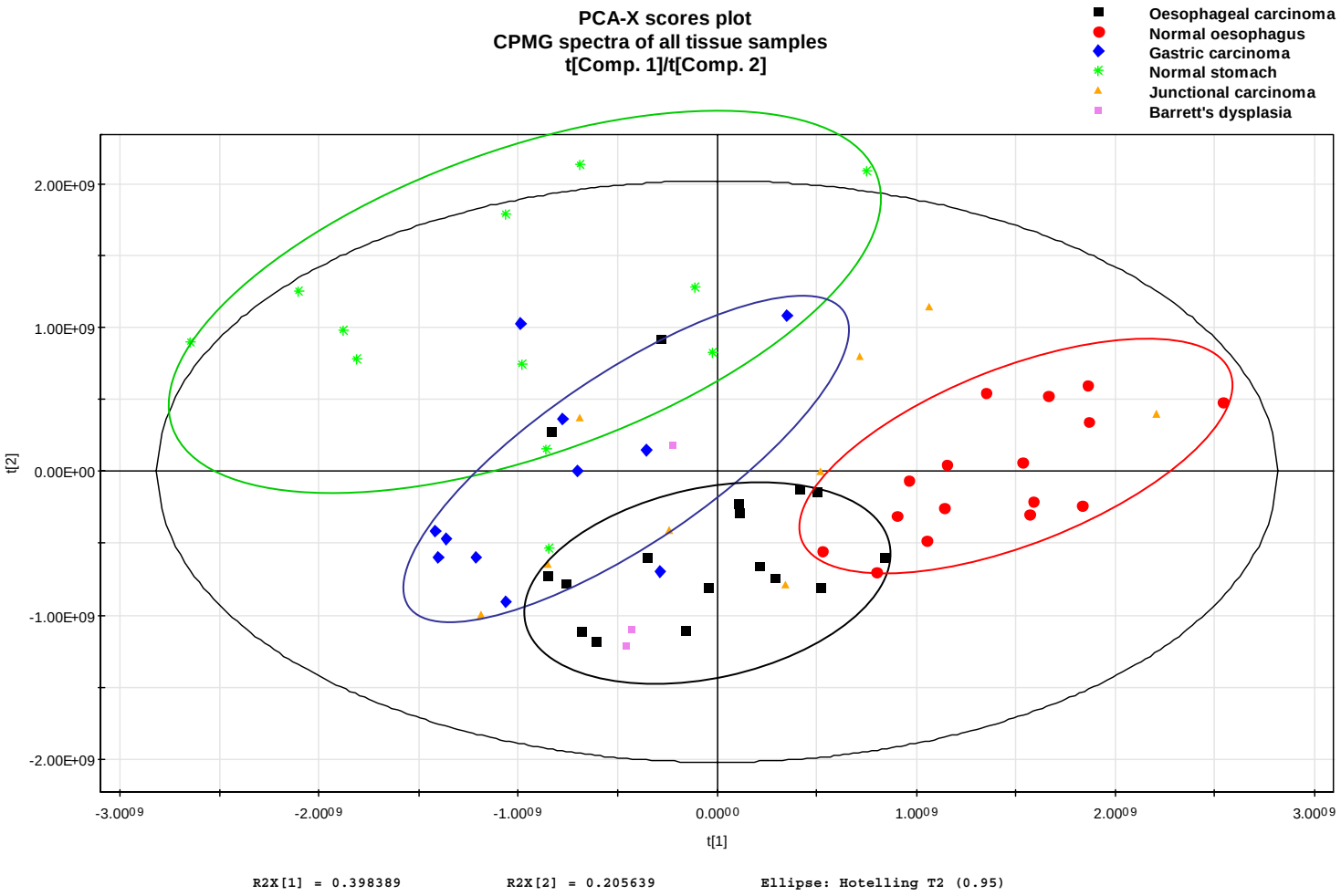


Figure 23. Scores plot of a PCA model differentiating between different types of tissue samples

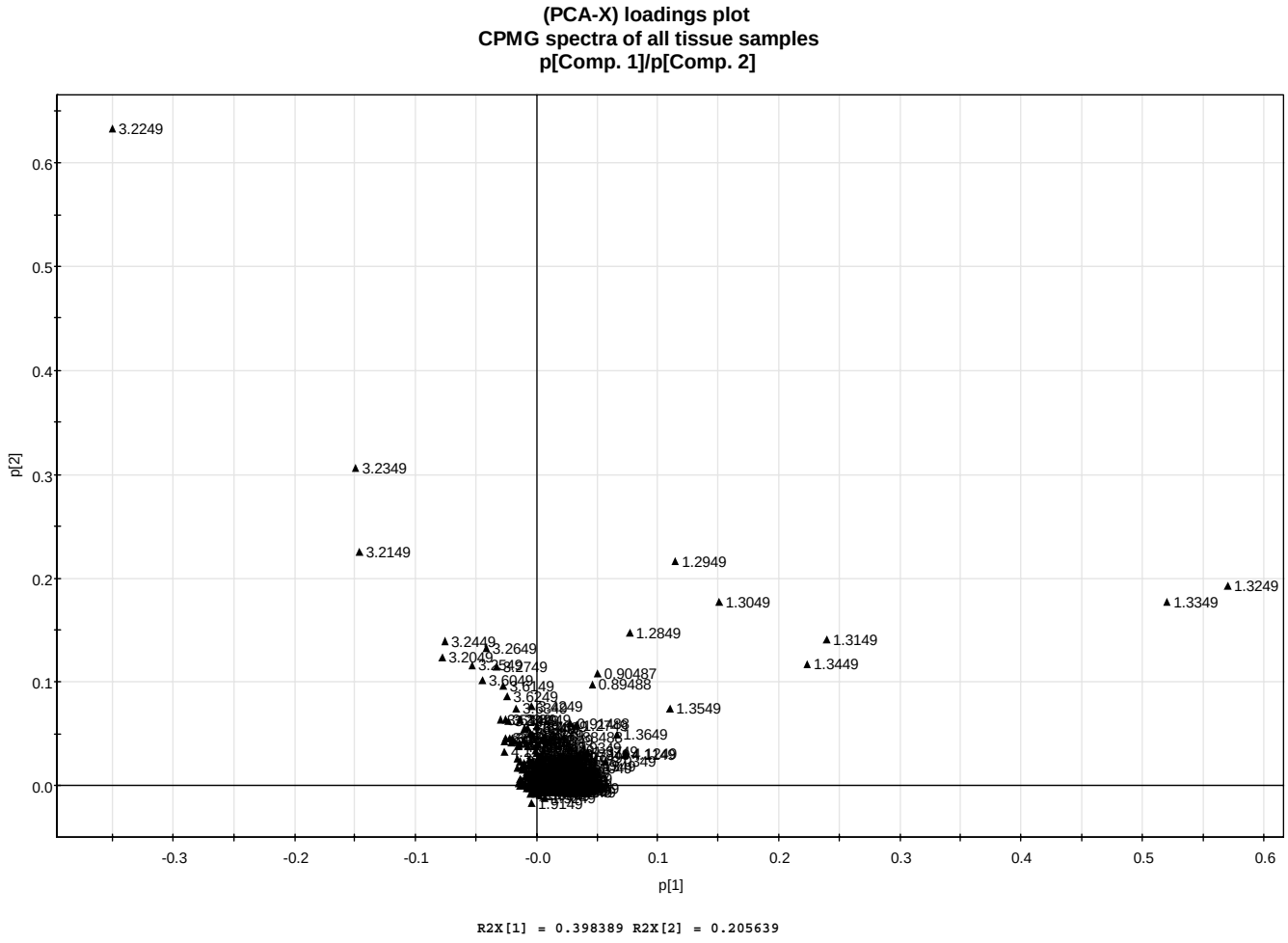


Figure 24. Loadings plot of PCA model differentiating between different types of tissue samples

Loadings of the PCA model shows that the model clustered the groups based mainly on lactate and choline containing compounds' resonances (Figure 24), where more cholines and lactate separated the malignant from the normal groups. A model of proximal and distal gastric cancers and normal tissues did show clustering of distal normal tissue from cancer but discrimination was less consistent for proximal tissue. Clustering was not

noted for any of age, sex, chemotherapy status, pathological type, subtype, grade, T or N stages. A separate PCA model built for proximal gastric tissue data alone failed to cluster malignant from normal. A supervised PLS DA model could separate the classes (data not shown), but with low sample numbers the reliability of these results are limited. With further sample collections it will be possible to test predictive ability with greater accuracy. A PCA model for distal gastric tissues showed separation of normal from malignant, but again because of small sample numbers, these results couldn't be interpreted with certainty. When a PCA model including all abnormal tissues only was constructed, there was no apparent differentiation between malignant samples from different tissues.

4.1.3 Analysis of oesophageal tissue

Oesophageal tissue was analyzed separately. Histopathological examination after H&E staining and immuno-histochemistry confirmed presence of adenocarcinoma in all tumour tissue samples. Neither of the normal tissues from cancer nor non-cancer patients showed evidence of malignant glands.

All junctional adenocarcinoma samples have been classified as Seiwert type I by pathological examination. NMR analysis proved very subtle differences from oesophageal tissues; semi-quantitative comparison based on averaging relative integrals of NMR spectra showed no significant difference in any of the resonances in the spectrum in either the tumour of the normal tissues respectively. Thus, for the purpose of this study, junctional tumours were reclassified as oesophageal tumours. Patient characteristics are displayed in table 7.

Sample	Histology	No. Of patients	Age range	Sex M/F	Chemotherapy status		T stage	N stage	Pathological grade
					Pre	Post	1/2/3/4	0/1/2	W/M/P/U
Oesophageal cancer tissues	Adeno	18	43-80	14/4	6	12	1/3/14/0	6/11/1	3/5/10/0
	Squamous	6	50-76	4/2	5	1	1/2/3/0	3/3/0	1/3/2/0
Junctional cancer tissues	Adeno	12	33-78	10/2	5	7	1/1/8/2	1/7/4	0/2/9/1
Cancer patient blood samples	Adeno	19	43-80	12/7	6	13	2/2/15/0	13/6/0	3/5/11/0
	Squamous	2	65-71	1/1	2	0	1/1/0/0	2/0/0	0/2/0/0
Healthy control blood samples	Normal	13	32-85	7/6	13	N/A	N/A	N/A	N/A

Table 7. Characteristics of patients included in the study. W: well differentiated, M: moderately differentiated, P: poorly differentiated and U: undifferentiated

Comparison between spectra of oesophageal tissue, an increased abundance of compounds as lactate, choline, phosphocholine and glycerophosphocholine, tyrosine, phenylalanine and myoinositol was noted in malignant tissue as compared to normal oesophageal epithelium (Detailed comparison of all assigned metabolites between different groups of tissues can be found in appendix 5). Glucose and lipid concentrations were relatively higher in normal tissue, while alanine concentration did not appear to vary significantly across the dataset (Figures 19 and 20). Examination of extracted oesophageal tissue was done to avoid effect of tissue compartmentalisation on metabolite profile; spectra showed similar changes to intact tissue analysis further validating the findings reported. An example is shown in Figure 25.

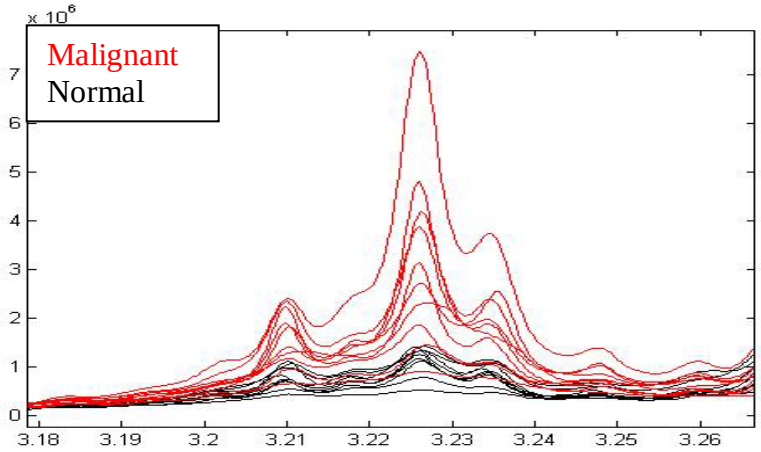


Figure 25. Choline resonances in oesophageal tissue extracts showing similar changes to that of intact tissues seen in Figure 21

On PCA of oesophageal tissue separately (Patient details are shown in table 7), PC1 could discriminate between generally normal and abnormal oesophageal tissue. It could also discriminate between squamous and adenocarcinoma. Squamous carcinoma appeared between normal and adenocarcinoma samples, which might be an expected consequence of metabolic drift from normal oesophageal mucosal tissue composition. Barrett's oesophagus appeared within adenocarcinoma samples (Figure 26); of note, these samples came from patients with adenocarcinoma of the oesophagus on a Barrett's background. Further sub analysis of squamous versus adenocarcinoma and their normal counterparts is shown in Figure 27. There was no significant difference/clustering according to age, sex, BMI, T, or N stage. The number of samples used was not enough to study subgroups of N stage difference for the same T stage or other more detailed categorisation.

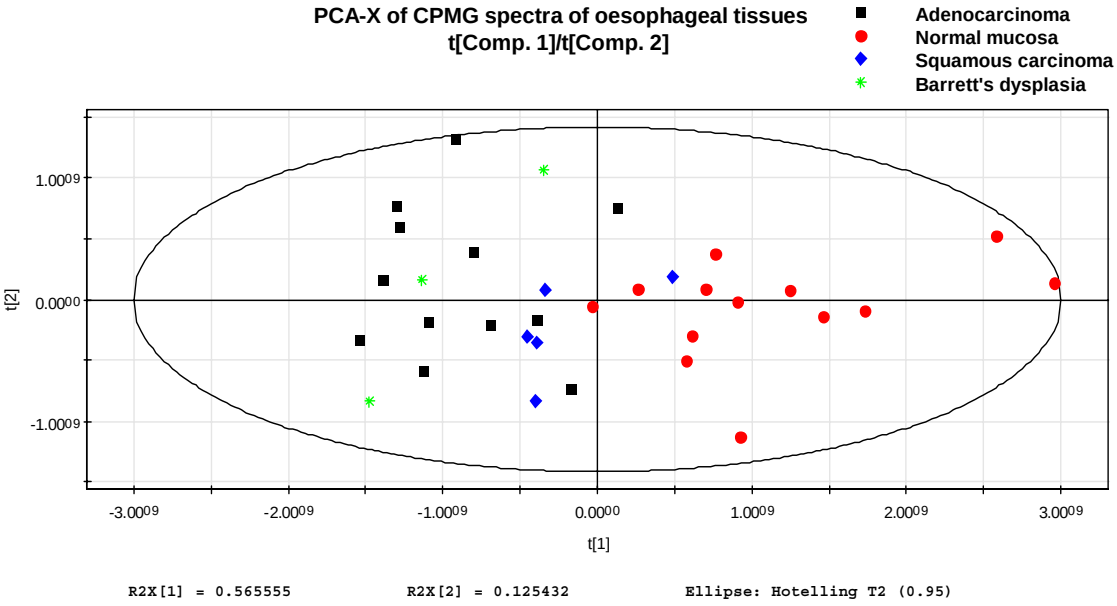


Figure 26. PCA scores plot of CPMG spectra of oesophageal tissues showing progressive separation along the same vector between normal mucosa, squamous carcinoma and adenocarcinoma with Barrett's dysplasia (R^2X 0.691, Q^2cum 0.541)

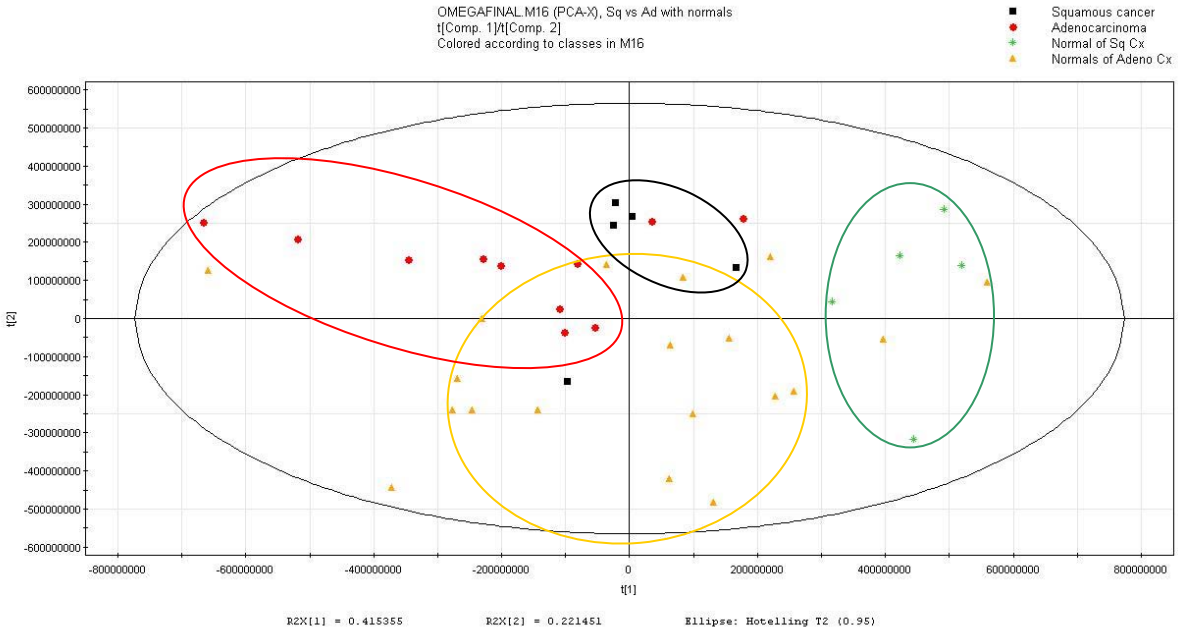


Figure 27. Scores plot showing clustering of squamous and adenocarcinoma and their normal counter parts

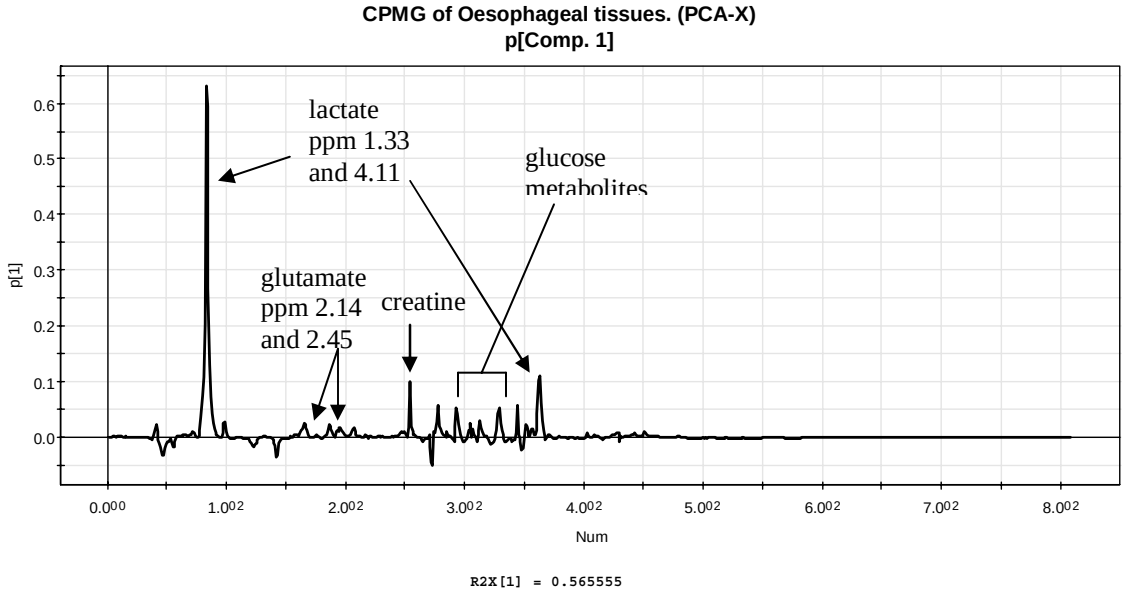


Figure 28. Loadings line plot showing the contribution of different metabolites to differentiating normal and malignant clusters e.g. lactate, creatinine and intermediates of glucose metabolism

Line loading plots identified the variable metabolites contributing to this separation (Figure 28); resonances from these metabolites were integrated in the raw spectra to allow quantitative analysis and assessment of statistical significance. Choline, phosphocholine and glycerophosphocholine, taurine, tyrosine, lactate, phenylalanine, uracil, scylloinositol and myoinositol metabolites were found to be more abundant in cancer tissue samples (n=24). Whereas normal tissue controls (n=38), had higher content of glucose, glutamine, glutathione and adenine containing compounds. All differences were statistically significant (*Wilcoxon* ranksum test $P<0.05$) (Figure 29 displays some of the relevant results). Findings were reproduced on analyzing an independent set of samples (n=12) validating the results (Figure 30).

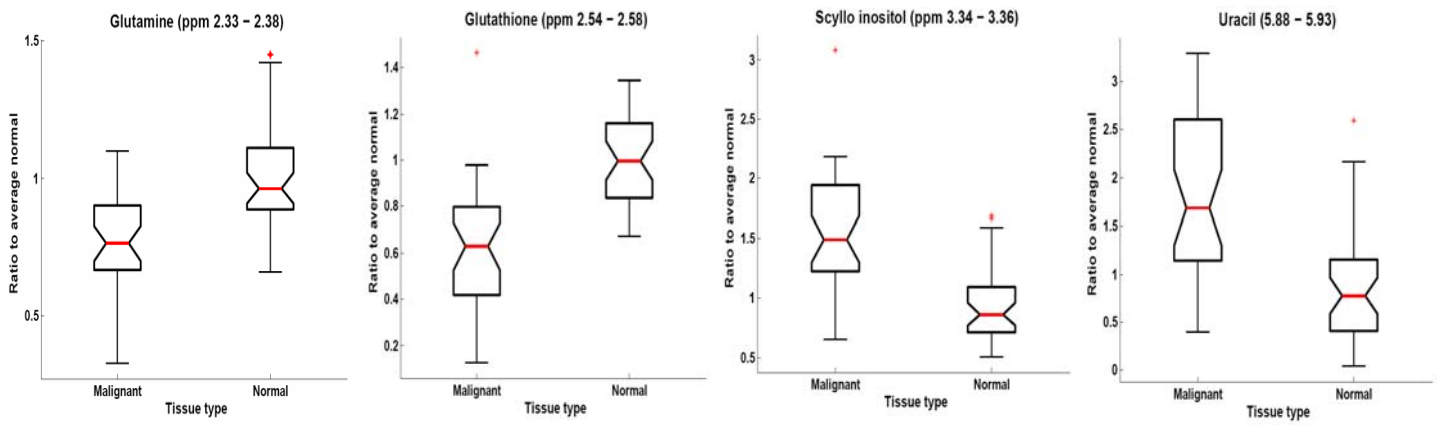


Figure 29. Differential metabolite concentrations of glutamine, glutathione, scylloinositol and uracil between cancer tissue and normal tissue (n=34)

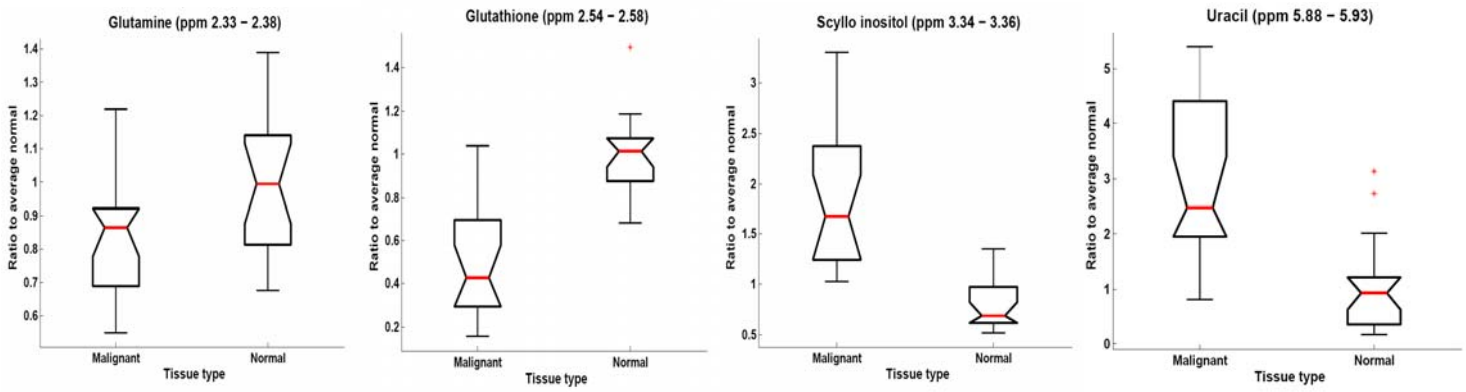


Figure 30. Differential metabolite concentrations of glutamine, glutathione, scylloinositol and uracil compared in an independent set of samples (n=18)

4.1.4 Blood samples analysis

Visual inspection of serum samples NMR analysis observed similar findings to tissue analysis data (Figure 31).

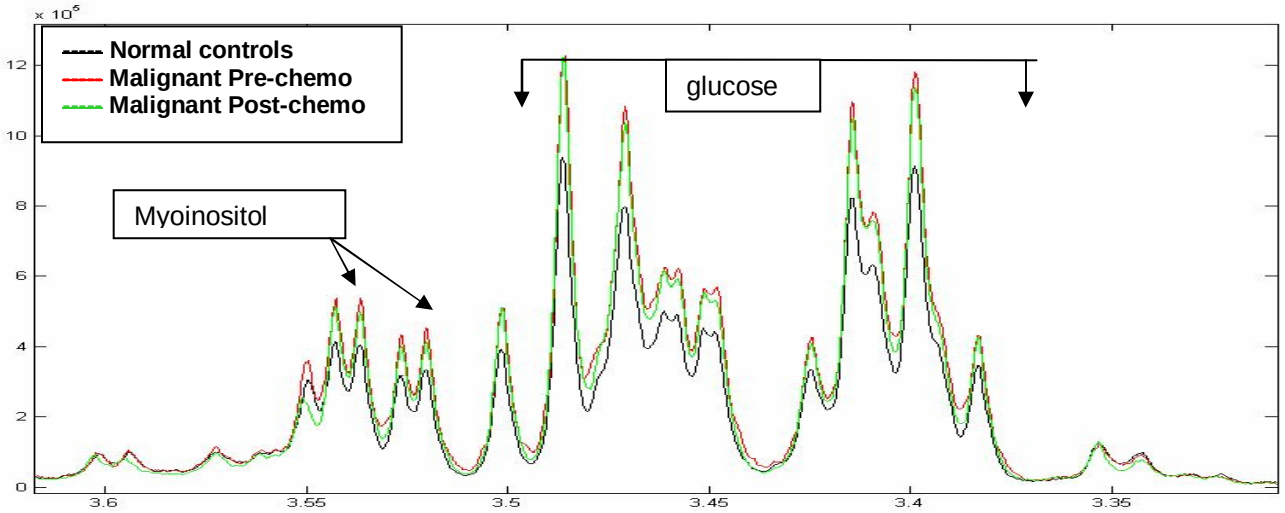


Figure 31. 1D median spectra of serum samples showing differences which seems to be due to malignancy regardless chemotherapy status

From a PCA model of blood samples spectral data; PC1 could moderately discriminate between normal and malignant samples. Within the malignant sample group further differentiation between pre-chemo and post-chemo samples can be seen. The results from PCA analysis support the observed group differences identified by visual inspection of the data (Figure 32). Patterns could not at this stage be correlated to variables as sex, age, BMI, type of tumour, pathological grade and TNM staging. This may be due to the number of samples used being insufficient for sub grouping.

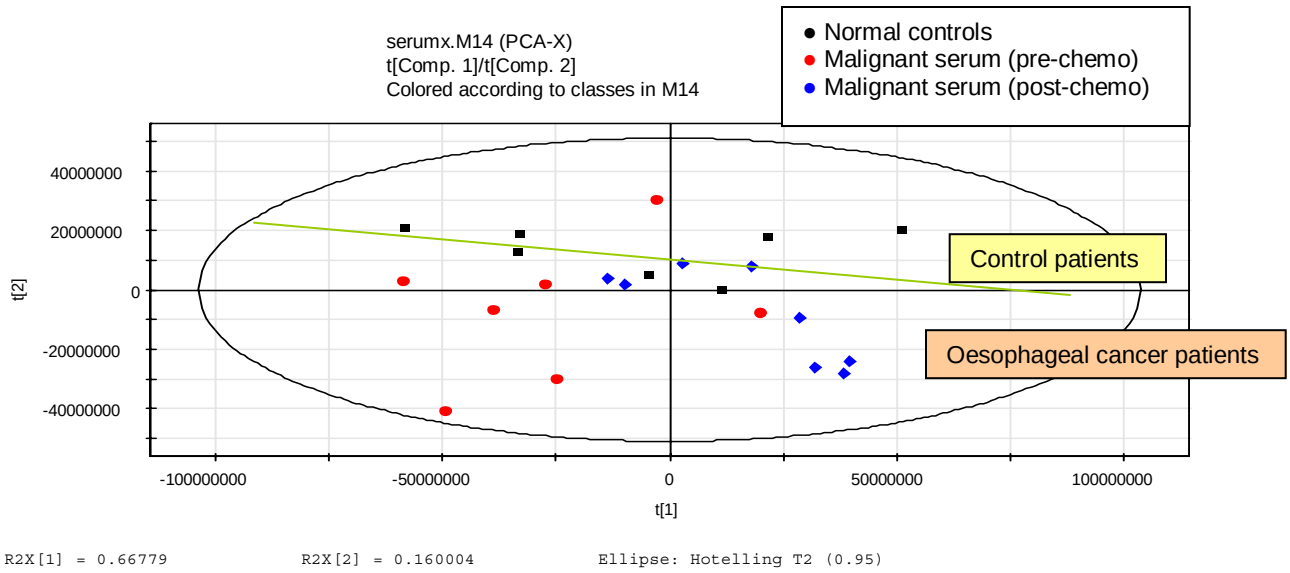


Figure 32. PCA model of serum samples from oesophageal cancer patients vs. normal controls

It is to be noted that analysis of serum samples was out of the scope of this study, as the author believe analysis of serum will have to be done in a more detailed and exhaustive way as it is hypothetically influenced by the health status of almost every other organ in the body. The small number of patients included cannot account for a statistically meaningful data. The analysis done hereby was executed to explore the potential of use of blood samples to reflect findings of the tissue analysis, thus suggesting a non-invasive alternative to cancer detection in these patients.

4.1.5 Summary of findings

The results of tissue analysis demonstrated differences between normal gastric and oesophageal tissue samples and their malignant counterpart. Principal component analysis showed that normal oesophageal and normal gastric samples appeared

considerably apart, while malignant oesophageal and gastric samples were closer and even overlapping together. Junctional tumour samples were distributed between both cancer groups reflecting the reported clinical and pathological dilemma whether these tumour arise from uppermost gastric or lowermost oesophageal mucosa.

On PCA of oesophageal tissue separately, there is distinct difference between normal and cancer oesophageal tissue. It also discriminates between squamous and adenocarcinoma. Squamous carcinoma appeared between normal and adenocarcinoma samples. Barrett's oesophagus appeared within adenocarcinoma samples. Loading plots identified the variable metabolites contributing to the separation between normal and cancer oesophageal tissues. Choline, phosphocholine and glycerophosphocholine, taurine, tyrosine, lactate, phenylalanine, uracil, scylloinositol and myoinositol metabolites were found to be significantly higher in cancer tissue samples. Whereas normal tissue controls, had significantly higher content of glucose, glutamine, glutathione and adenine containing compounds.

The TNM stage, grade of differentiation, age, sex, BMI, comorbidity had no apparent effect within the sample size of this study. The sample numbers used were also not enough to sub-classify Barrett's samples according to grade of dysplasia or test qualitative differences in their metabolic profiles. The Barrett's tissue used, all originated from cancer bearing patients, and so the apparent similarity to the adenocarcinoma samples may be due to the effect of the nearby cancer and not just the local dysplasia.

4.2 Study II: Field effects in non-dysplastic tissue in oesophageal cancer patients

4.2.1 Patients

Eighty seven patients were recruited; 35 with oesophageal adenocarcinoma and 52, age-matched non cancer controls. Seventeen patients from the cancer group had chemotherapy during the course of the study, typically 3 courses of Cisplatin+5-fluorouracil or Epirubicin+Capecitabin. Control samples were taken from non-cancer patients during endoscopy for indications other than suspicion of malignancy. All but 21 of these patients received local anaesthetic during their endoscopy. Another set of matched samples from all sampled areas were fixed in paraffin for pathological examination. All samples were collected after an overnight fasting. Samples were annotated with full clinical details including demographic data, co-morbidities and drug intake. Patient and sample characteristics are summarized in Table 8.

Patient Group		Control	Cancer	
N (total patients)		52	35	
Age (median yrs)		56.5	63	
Gender	Male	18	30	
	Female	34	5	
Grade	well differentiated	-	6	
	moderate	-	11	
	poor	-	18	
T Stage	1	-	3	
	2	-	4	
	3	-	27	
	4	-	1	
N stage	0	-	19	
	1	-	15	
	2	-	1	
	3	-	0	
Sample group		**Control**	**PHINOM**	**Tumor**
N (total samples)		53	38	32
Sampling	Endoscopic	53	17	15
	Surgical	-	21	17
Chemotherapy	Pre-	-	24	16
	Post-	-	14	16
N (training set)		19	14	12

All bar 14 samples were patient-matched between PHINOM and tumor

Table 8. Patient and sample characteristics

4.2.2 NMR and histopathological testing of tissue samples

Using ^{1}H MAS-NMR spectroscopy of intact tissue we generated metabolic profiles of oesophageal tumour tissue ('tumour') and of proximal histologically-normal mucosa ('PHINOM') from cancer patients together with normal mucosa from an age-matched control group ('control') (n=123; Table 8; Figure 33). Histopathological examination after haematoxylin and eosin staining and immuno-histochemistry confirmed presence of adenocarcinoma in all tumour tissue samples. Neither of the normal tissues from cancer nor non-cancer patients showed evidence of malignancy or dysplasia and the PHINOM group could not be separated from control group on blinded examination. No significant

differences were observed in proliferation (Ki67) or apoptosis (TUNEL) (data can be seen in appendix 6).

4.2.3 Metabolic profile changes progressively from tumour tissue to PHINOM to tissue from controls

In order to avoid confounding variation from chemotherapy, gender and the route of sampling, a training set was established that contained data from samples obtained only from male individuals that were not receiving neoadjuvant chemotherapy, and that were collected by endoscopy during routine diagnostic testing or staging laparoscopy (n=45). From visual inspection of the profiles from the training set, several metabolites appeared to exhibit a progressive change in intensity from tumour tissue to PHINOM to tissue from controls, consistent with the hypothesis that tumours arise within a biochemically altered tissue field (Figure 33E). Using partial least squares discriminant analysis (PLS-DA), a robust model was generated that could discriminate profiles based on the origin of the tissue, confirming that the metabolic profile of PHINOM is systematically different from that of both control and tumour tissue. (Figure 33 F-G; LV 2, Q^2Y 0.46, $p<0.01$ by permutation) and (Figure 34).

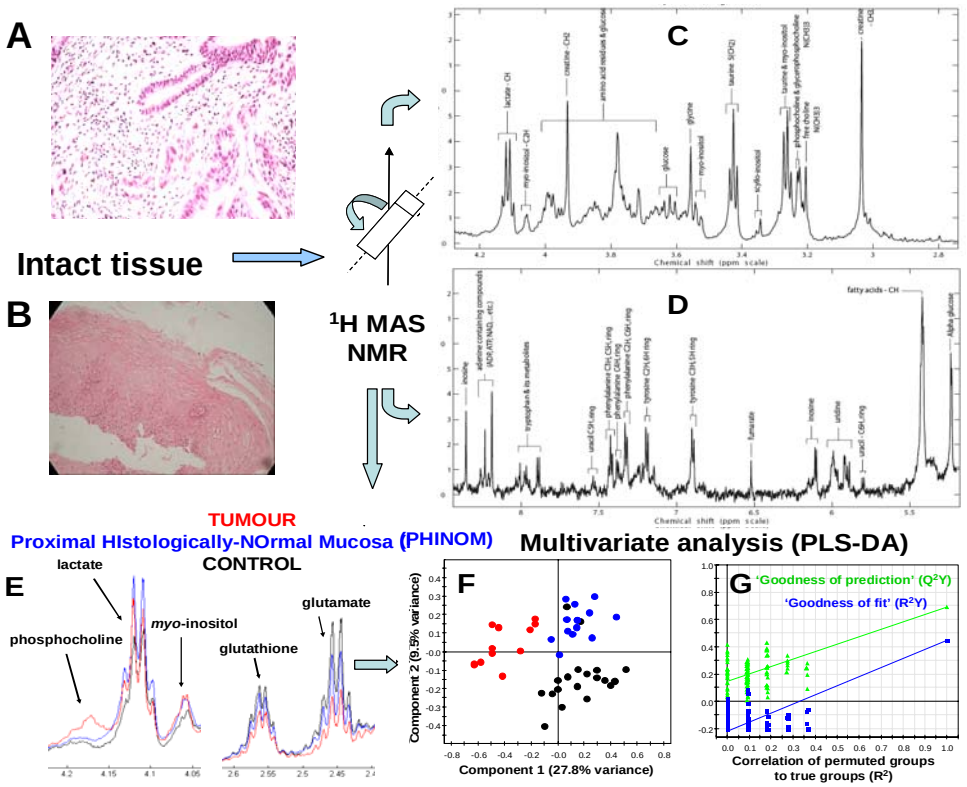


Figure 33. Metabolic profiling by ^{1}H-NMR MAS spectrometry with pattern recognition analysis reveals systematic metabolic differences in between malignant, PHINOM and control oesophageal tissue. A) oesophageal cancer; B) PHINOM;C) aliphatic and D) aromatic regions of a typical ^{1}H-MAS-NMR spectrum of normal oesophageal tissue; E) mean spectra of tissue groups indicating metabolites exhibiting systematic differences in a training set of 45 samples; F) Multivariate 'scores' from a PLS-DA model classifying the tissue groups in the training set; G) Validation of the PLS-DA model by comparison to the classification statistics of models generated after (100) random permutations of the class matrix (Y)

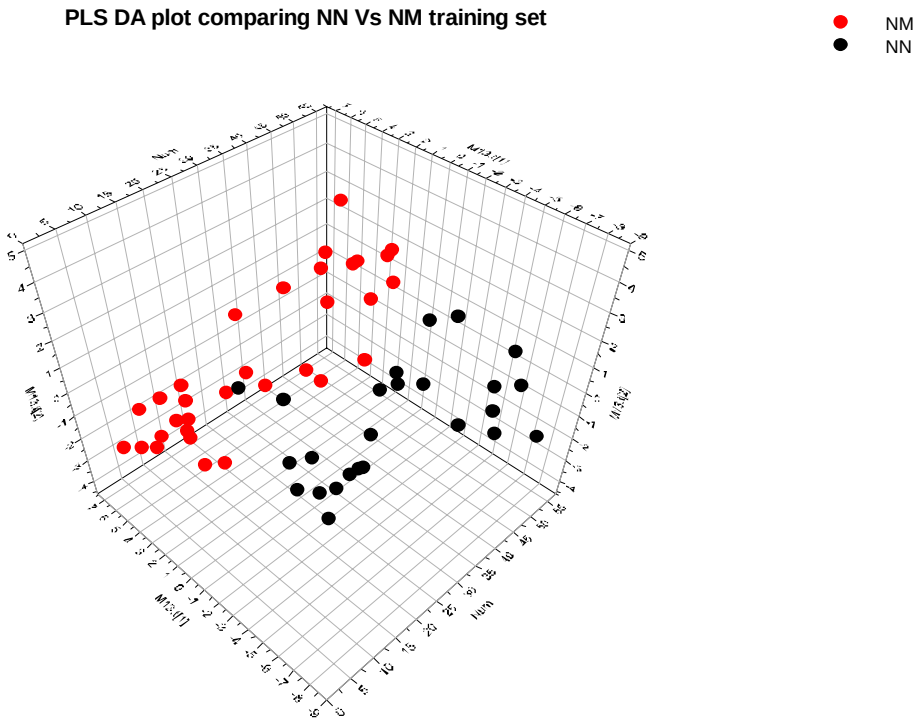


Figure 34. 3D PLS-DA model comparing normal tissue from cancer patients with that from non-cancer patients (NN=normal oesophagus healthy controls, NM=PHINOM group) (R^2X 0.779, Q^2cum 0.584)

4.2.4 Surrogate biomarker metabolites identified by discriminant analysis

To test the hypothesis further we derived two more discriminant analysis models trained to classify either controls from PHINOM or PHINOM from tumour. The variances in the regression coefficients were estimated by cross validation (7-fold) and spectral regions that were significantly correlated to the presence of cancer in each model were identified (by T test, $p<0.1$). While 26% and 12% of the spectral profile regions were uniquely discriminating tumour or control tissue respectively, 5% of the profile exhibited a significant and progressive change in signal intensity from controls to PHINOM to

tumour, significantly higher than expected by chance ($p \sim 10^{-26}$ assuming a binomial distribution, expected value 0.005%, Figure 35A). Regions identified as showing progressive change were interpreted as indicating the presence of putative biomarkers for a field effect, and resonances indicated by these regions were integrated for further analysis. Several of these resonances could be assigned to specific metabolites, namely: phosphocholine, glutamate, myo-inositol, adenosine-containing compounds, uracil and inosine by reference to literature data (Table 9).

Marker Region	Upper ppm	Lower ppm	Metabolite
A	2.18	2.1	glutamate
B	2.51	2.4	glutamate
C	3.16	3.09	unassigned
D	3.21	3.2	free choline
E	3.3	3.28	unassigned
F	3.53	3.5	myoinositol
G	3.57	3.55	glycine
H	4.08	4.04	myoinositol
I	4.22	4.15	phophocholine
J	6.02	5.95	uridine
K	6.13	6.17	inosine
L	7.51	7.55	uracil
M	7.91	7.87	tryptophan
N	8.2	8.17	adenines
O	8.22	8.2	adenines
P	8.25	8.29	adenines
Q	8.52	8.6	unassigned

Table 9. Discriminatory spectral regions

Hierarchical clustering of these metabolites indicated that they fell into two main groups, those increasing or decreasing with the presence of cancer, and clustering of the samples showed that this panel could distinguish most control tissue from PHINOM or tumour tissue, in a progressive fashion (Figure 35B). In principle each metabolite cluster could provide complementary information for sample classification, leading to better discrimination. To test if this was the case, phosphocholine/glutamate (PC/Glu) ratio was examined, as these metabolites were members of different clusters and both are part of distinct metabolic pathways that are well documented as being altered in the presence of malignancy. Receiver-Operator Characteristic (ROC) analysis for the detection of cancer in histologically normal samples from the training set using PC/Glu gave an AUC of 0.857 ($p=0.001$, std err 0.069 under non-parametric assumption) compared to AUC values of 0.752 ($p=0.015$) and 0.637 ($p=0.184$) for PC and Glu respectively. The distribution of the PC/Glu ratio in the full sample set was examined, which included data from female patients and surgical excision specimens that were independent from the analysis thus far ($n=123$; Figure 35C). PC/Glu showed a clear progression to higher values from control to PHINOM to tumour tissue and that the difference between PHINOM and tumour tissue is retained in samples obtained from surgery, despite a systematic difference in the PC/Glu ratio between endoscopic and surgical PHINOM samples (Figure 35C). ROC analysis produced AUC values of 0.84 for control vs. PHINOM samples and 0.98 and 0.91 respectively for endoscopic and surgical tumour vs. PHINOM, demonstrating both that discriminatory ability was retained in the full sample set and that the PC/Glu ratio is also marker for tumourigenic progression. The metabolic effect of surgical collection, presumably as a result of tissue ischemia was the only

apparent confounding factor of significance in our analysis. PLS DA plot showing predicted PHINOM samples in the training set model is shown in (Figure 36).

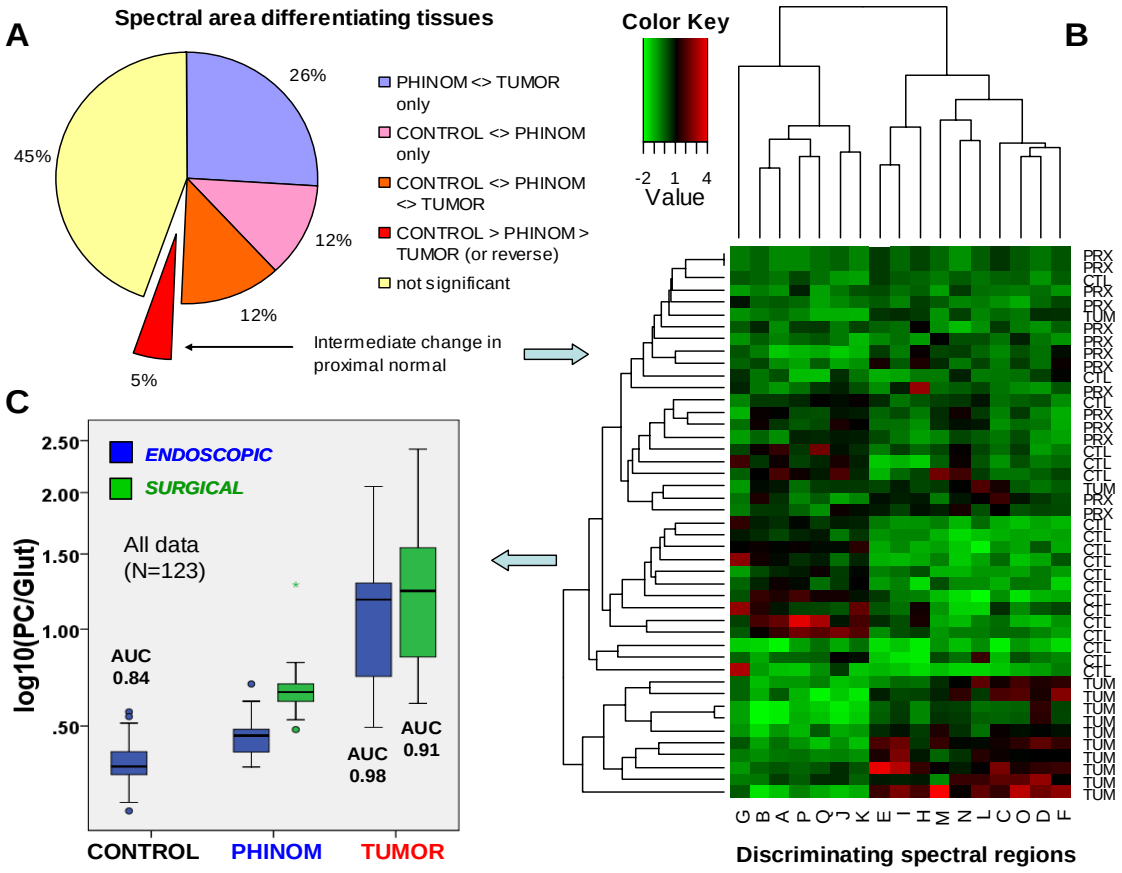


Figure 35. Identification of spectral features defining intermediate metabolic change in non-tumour tissue from cancer patients. (A) Proportion of spectra area significantly differentiating between tissue groups based on two PLS-discriminant analysis models calculated as described in methods, which classified tumour from PHINOM or control from PHINOM. (B) Heat map and hierarchical clustering analysis (HCA) of metabolite resonances occupying spectral regions exhibiting intermediate change in PHINOM in the training set. Data are presented as z-scores (scaled to unit variance) and average linkage was used for the analysis. (C) Box plots of the phosphocholine / glutamate ratio across the full sample set, clustered by tissue of origin and route of sampling. Outlying values >2 S.D. (full circles) and >3 S.D. (star) from the mean are indicated. ROC AUC values are indicated for the classification of each group relative to the sampling route match PHINOM group

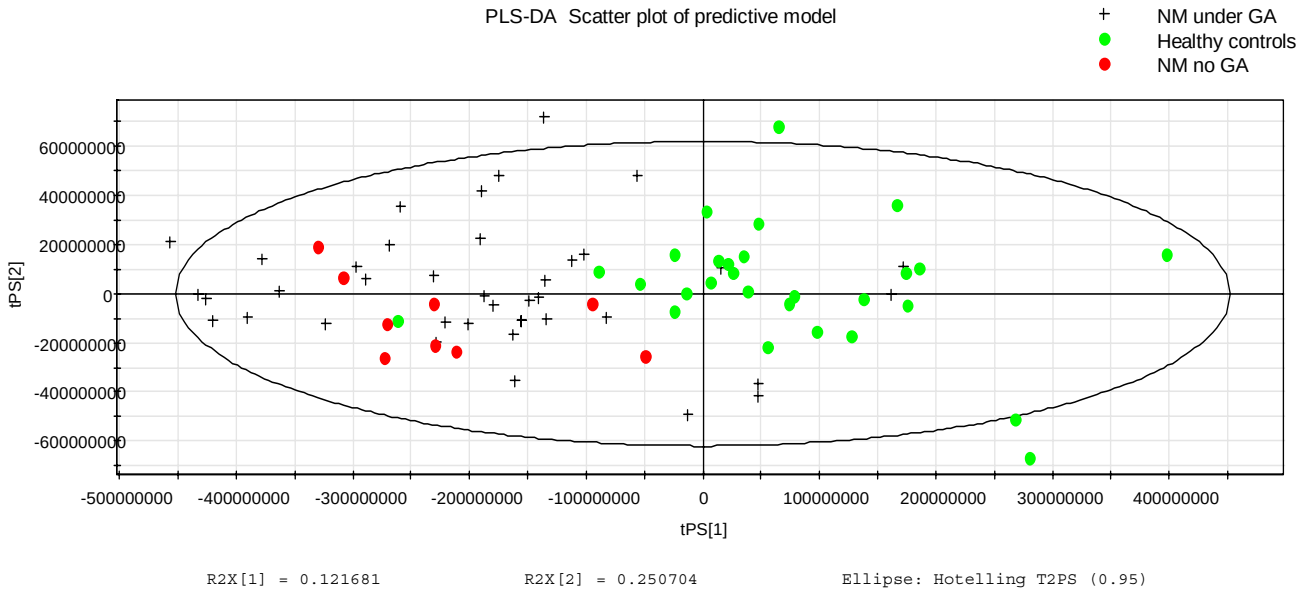


Figure 36. Prediction PLS-DA model constructed on healthy samples and normal oesophageal samples of cancer patients with no general anaesthetic, predicting in NM group. NM: PHINOM group

4.2.5 Comparison of other metabolites showing similar trend

Other metabolites as glutamine, tyrosine and glutathione showed similar progression between normal, PHINOM and malignant tissue samples (Figures 37, 38 and 39). These metabolites were compared as they belong to different metabolic pathways, also observation from tissue extracts are shown; where observation of differential increase or decrease in the compounds point out to the fact the previously observed variable values were not due to systematic error, processing/analysis miscalculations or compartmental effect on these metabolite contents as evidenced by data from tissue extracts.

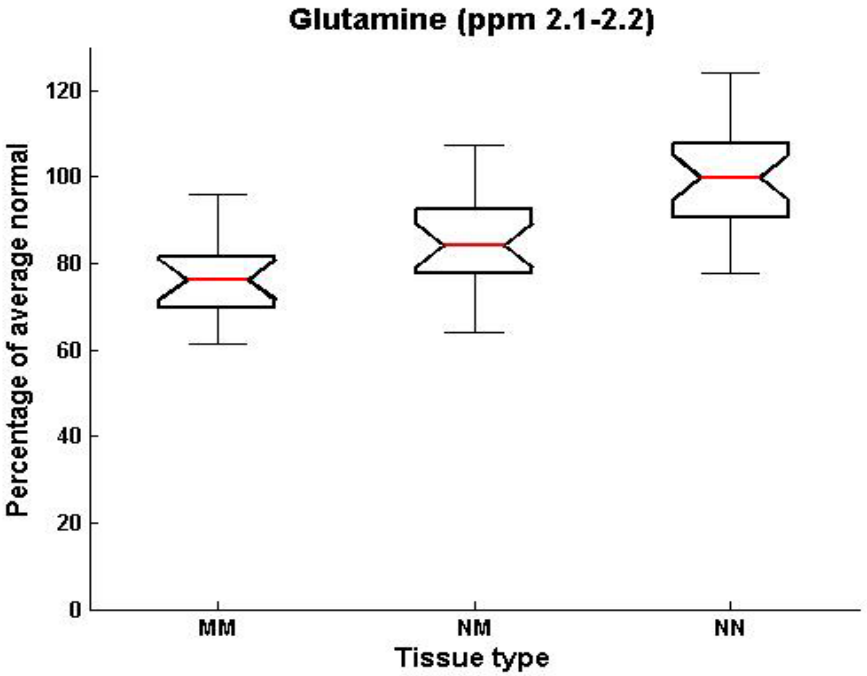


Figure 37. Comparison of glutamine content in tissues showing progressive decrease from normal (NN) to PHINOM (NM) to tumour (MM) ($p<0.001$, Kruskal Wallis test)

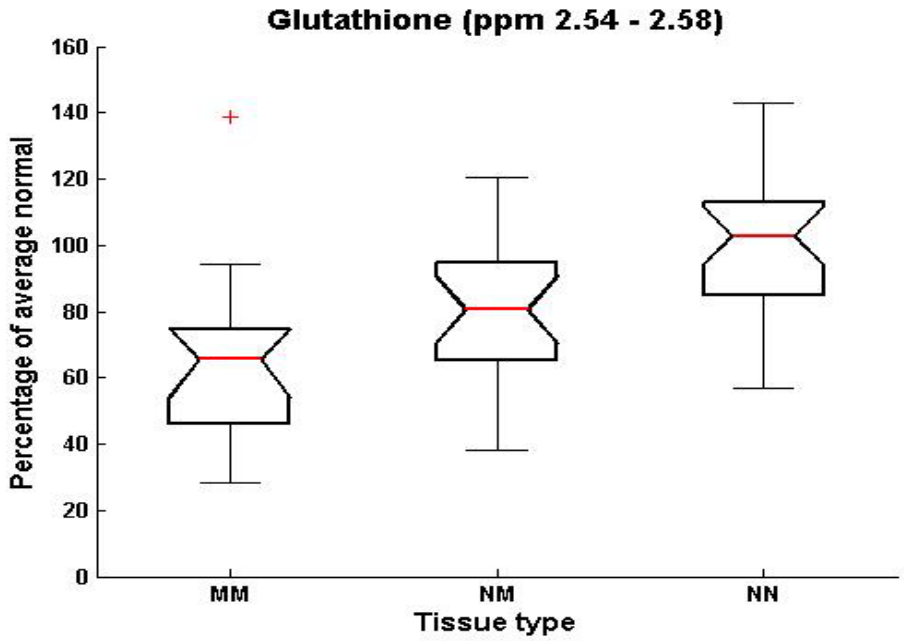


Figure 38. Comparison of glutathione content in tissues showing progressive decrease from normal (NN) to PHINOM (NM) to tumour (MM) ($p<0.001$, Kruskal Wallis test)

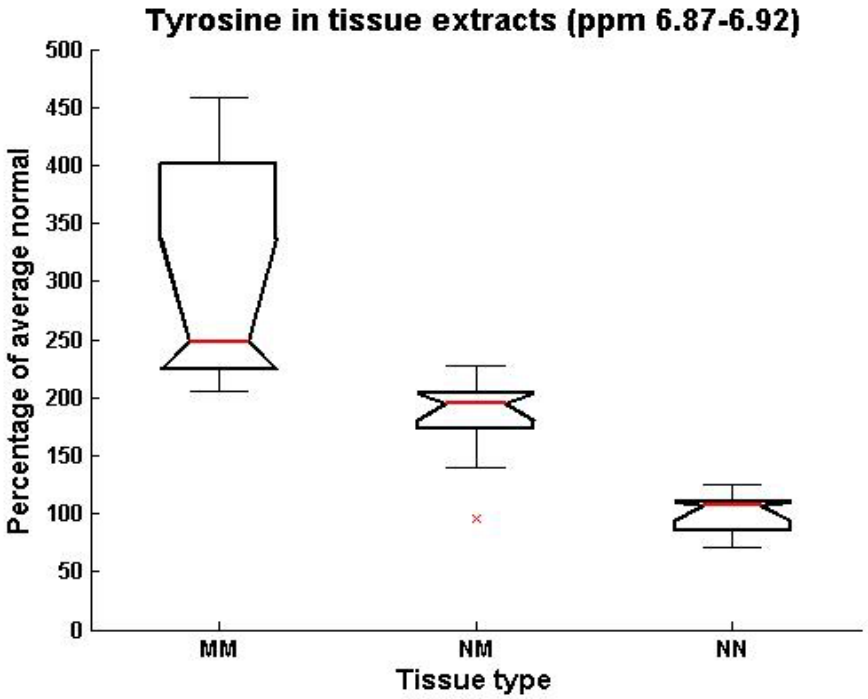


Figure 39. Comparison of tyrosine content in tissues showing progressive increase from normal (NN) to PHINOM (NM) to tumour (MM) ($p<0.001$, Kruskal Wallis test)

4.2.6 Summary of findings

By comparing histologically normal mucosa proximal to a tumour (PHINOM) with normal mucosa from non-diseased controls and tumour tissue, this study provides new evidence that field cancerization in oesophageal cancer manifests a metabolic phenotype and that metabolic profiling via ^{1}H MAS-NMR is sensitive to this phenomenon. Moreover, metabolites were identified that show a progression in detectable levels from normal to PHINOM to tumour tissue. Some of these metabolites, such as phosphocholine (PC), are well established metabolic biomarkers for malignant potential.

4.3 Study III: Profiling metabonomic response of oesophageal adenocarcinoma to chemotherapy

4.3.1 Patients

Ninety nine tissue samples from 47 patients were analysed; 47 patients had lower oesophageal/junctional adenocarcinoma and 52, age and sex matched, non- cancer controls. Twenty seven patients from the cancer group had 3 cycles of Cisplatin + 5-fluorouracil or Epirubicin + Capecitabin. Patient characteristics are displayed in table 10.

Patient group		**Cancer**	**Control**
Number		47	52
Age (Median yrs)		62.5	56.5
Gender	**Male**	30	18
	Female	17	34
Grade of differentiation	**Well**	8	-
	Moderate	21	-
	Poor	18	-
T stage	**1**	7	-
	2	12	-
	3	26	-
	4	2	-
N stage	**0**	22	-
	1	18	-
	2	7	-
	3	0	-

Sample group		**Tumour**	**PHINOM**	**Control**
Number		49	51	52
Sampling	**Surgical**	29	33	-
	Endoscopic	20	18	52
Anaesthesia	**General**	42	43	-
	Local	5	6	31
	None	2	2	21
Chemotherapy	**Pre**	22	20	-
	Post	27	31	-
Mandard grade	**1**	1	1	-
	2	2	2	-
	3	8	12	-
	4	8	9	-
	5	5	3	-
	unspecified	3	4	-

Table 10. Patient characteristics involved in the study of the Profiling metabonomic response of oesophageal adenocarcinoma to chemotherapy

4.3.2 Demonstrating the generic effect of chemotherapy on tissues

The NMR spectra were examined visually as well as compared mathematically by calculating differences in compound average values. Many non statistically significant differences were identified between individual metabolites among pre and post chemotherapy tissues. Areas where changes were noted to be similar in both normal and tumour tissues are suggested to be due to generic effect of chemotherapeutics on tissues. Examples include relative decrease in content of choline containing compounds (phosphocholine, glycerophosphocholine), their relation to each other and to lactate and also a decrease in content of other compounds such as adenine containing compounds, creatine and ethanolamine as shown in Figures 40, 41 and 42.

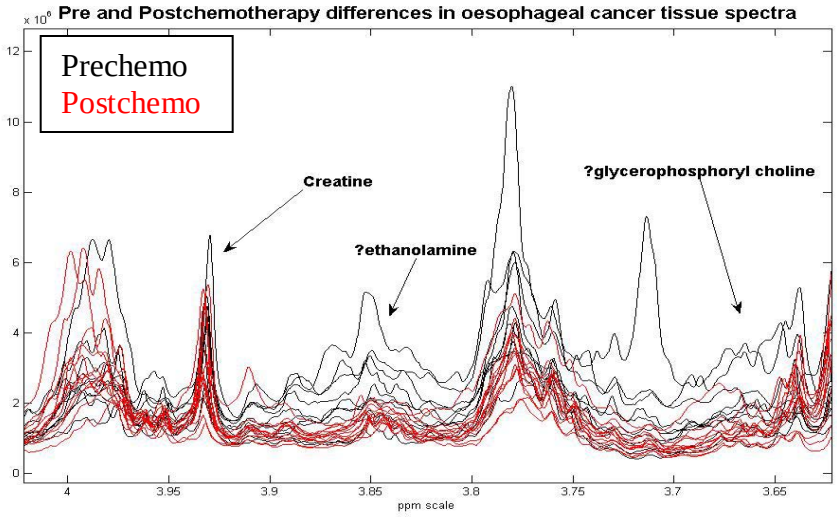


Figure 40. Comparative changes in spectral segments occurring in both malignant and PHINOM after chemotherapy treatment suggesting generic effect of chemotherapy on both tumour and normal tissues

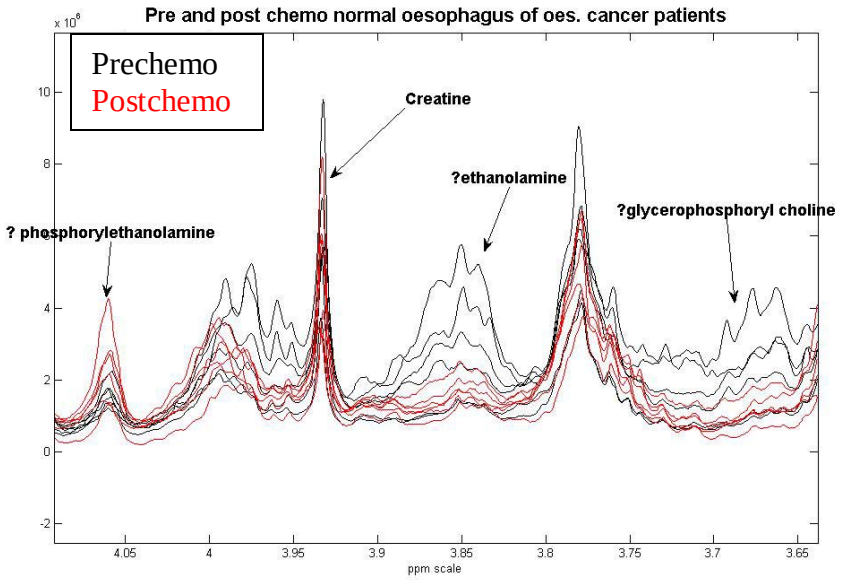


Figure 41. Comparative changes in spectral segments occurring in both malignant and PHINOM after chemotherapy treatment suggesting generic effect of chemotherapy on both tumour and normal tissues

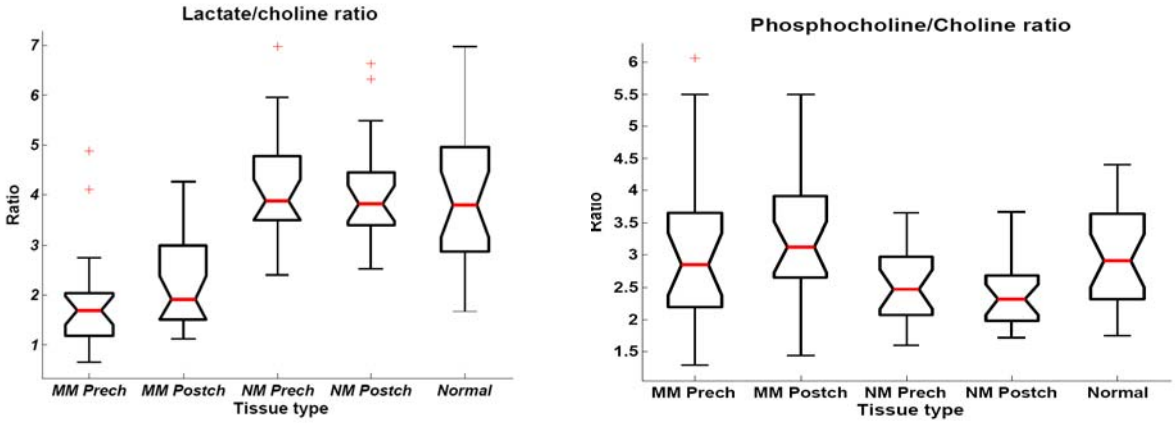


Figure 42. Relative ratios of lactate/cholines and phosphocholine/cholines among tumour and normal tissues before and after chemotherapy ratios ($p<0.05$, Kruskal-wallis test)

Lactate/glucose ratio which has been previously used in the literature to reflect glycolytic activity, showed the usual hallmark of increased glycolysis among malignant tissues as compared to PHINOM; however, it was not affected by chemotherapy (Figure 43).

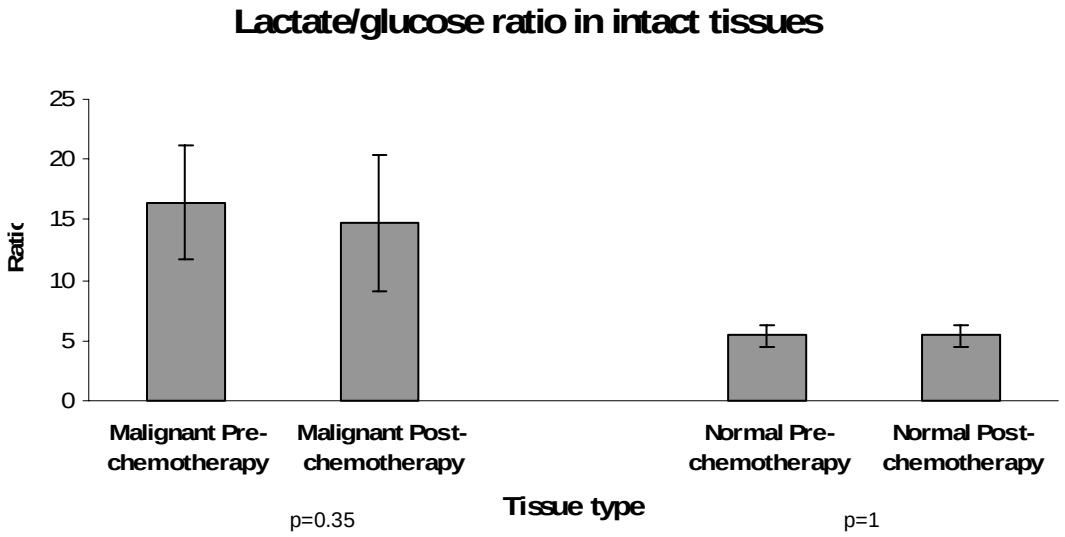


Figure 43. Lactate/glucose ratio after chemotherapy

Principal Component Analysis of the generated spectra confirmed what was observed by visual examination of spectra. The first component allowed obvious clustering of tissues treated with chemotherapy from pre-chemotherapy tissues in addition to baseline separation of histological types. The vector of difference between normal and tumour tissue was preserved both before and after chemotherapy (Figure 44).

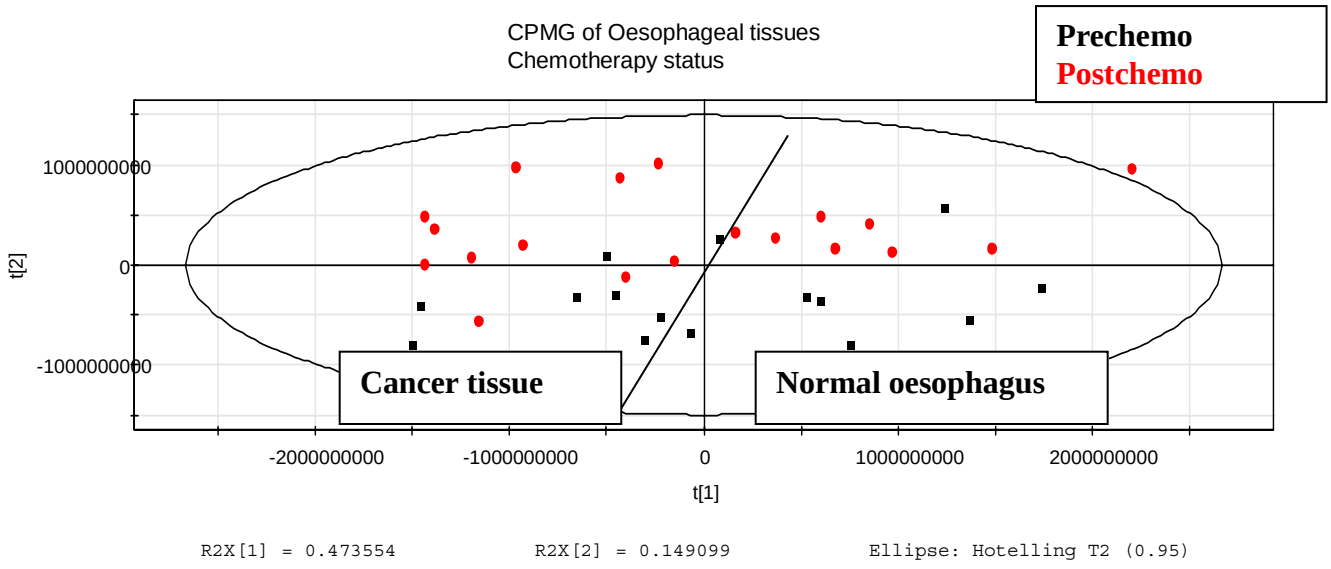


Figure 44. PCA plot showing oesophageal tissues colour coded according to chemotherapy status and divided by a line according to histological diagnosis

4.3.3 Differential effect of chemotherapy on normal and tumour tissue

Analysis of the content of other metabolites such as phenyl-alanine showed increase in amount in both normal and malignant tissue with chemotherapy, yet only the increase in malignant tissue was statistically significant (p=0.014, Student t-test) (Figure 45). Comparison of adenine containing compounds content showed similar trend with significant increase after chemotherapy in tumour tissue (p-value=0.003, Student t-test), a finding not observed in comparable PHINOM tissue (Figure 46).

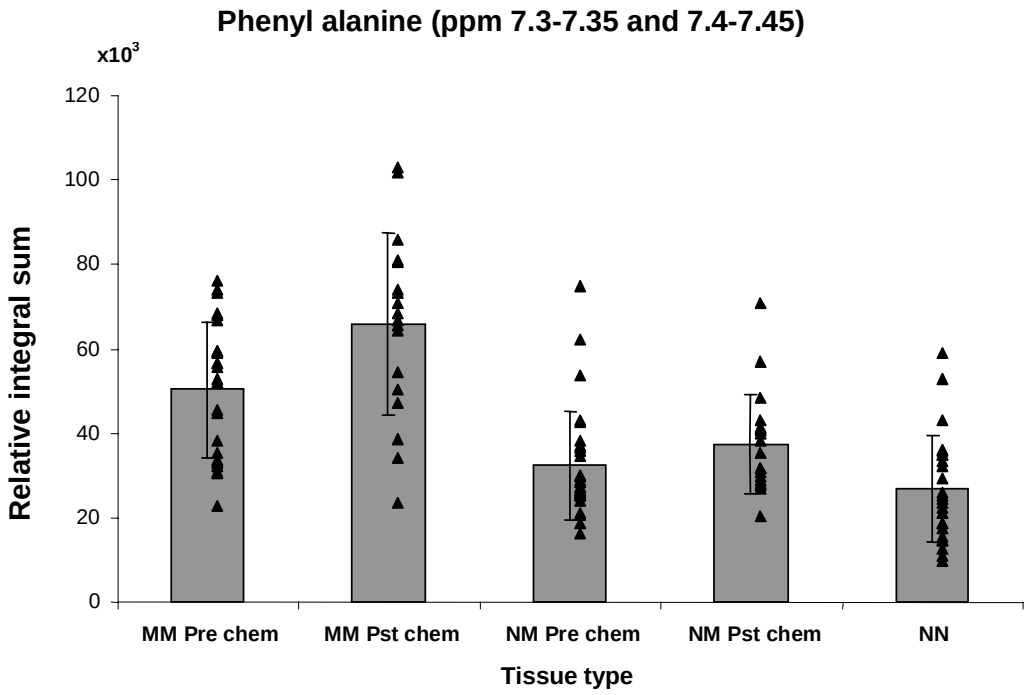


Figure 45. Differential phenyl alanine content in different tissue types (p=0.014, Kruskal-Wallis test)

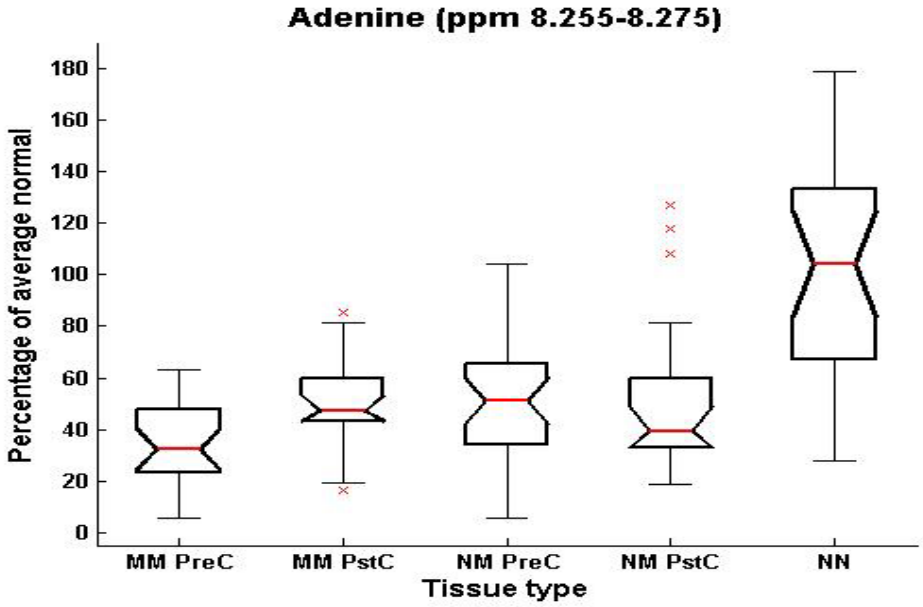


Figure 46. Differential content of adenine containing compounds in different tissue types (p-value < 0.001, Kruskal Wallis test)

Tables 11 and 12 show some of comparative content of some of the metabolites observed comparing pre and post chemotherapy tissue; it is obvious that the differential compounds are not exactly the same in PHINOM as compared to tumour tissue signifying a different metabolic phenotype for cancer tissue that results in a different metabolic response to chemotherapy than normal tissue.

Compound	**PPM range**	**Trend**	**p-value**
glutathione	2.54-2.58	Pre<Post	0.07
lysine	2.99-3.025	Pre > Post	0.02
phophocholine	3.214-2.224	Pre < Post	0.05
glycine/ α-Glucose/α-CH	3.7-3.81	Pre > Post	0.03
adenines	8.22-8.24	Pre < Post	0.003

Table 11. Comparative content of some of the metabolites observed comparing pre and post chemotherapy malignant tissue

Compound	**PPM range**	**Trend**	**p-value**
lactate	1.314-1.343	Post>Pre	0.04
acetate	1.88-1.95	Pre > Post	0.04
scyllo-inositol	3.34-3.36	Post>Pre	0.04
phophoryl-ethanolamine	3.965-4.005	Pre > Post	0.05
myoinositol	4.045-4.08	Post>Pre	0.03
lactate	4.09-4.14	Post>Pre	0.05
uroconate	7.86-7.9	Pre > Post	0.02

Table 12. Comparative content of some of the metabolites observed comparing pre versus Post chemotherapy PHINOM

Relative decrease in lysine/creatine ratio was seen in malignant tissue as compared to no change in normal tissue was seen; yet statistical significance could not be achieved. It is to be noted that part of the lysine resonance is overriding a lipid resonance; this is a factor that could suggest studying the lipid resonances as a possible cause for changes seen in the lysine/ creatine ratio (Figure 47).

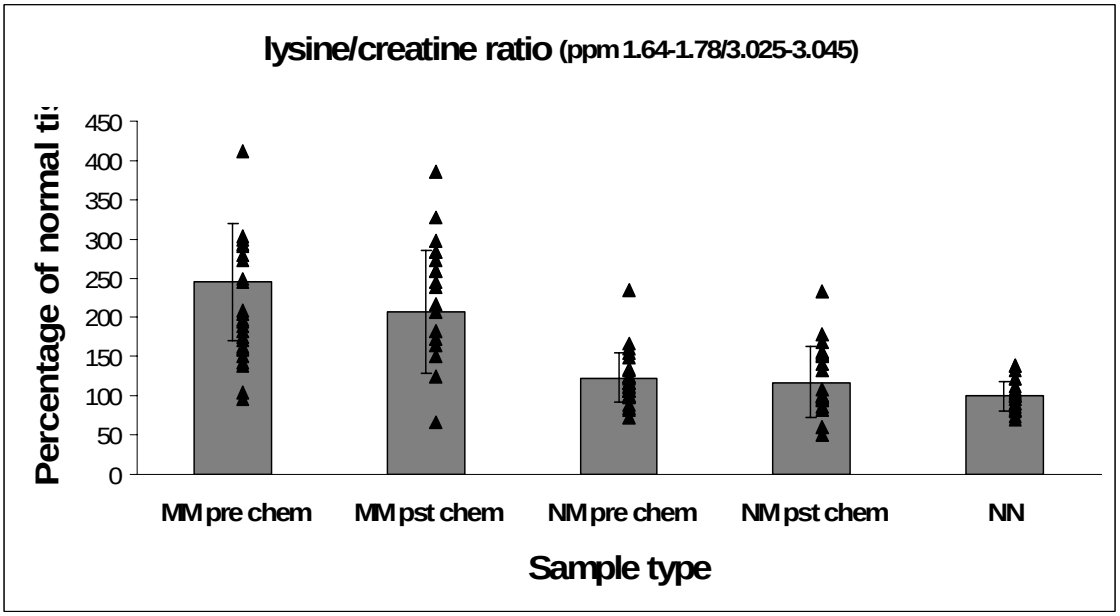


Figure 47. Lysine /creatine ratio trend after chemotherapy treatment

4.3.4 Differential effect of chemotherapy on blood samples

The 1D NMR spectroscopy of serum samples from oesophageal cancer patients and normal controls showed visible differences relating to disease status. Median spectra of all patient groups showed a greater abundance of several compounds in malignant serum samples irrespective of chemotherapy status as shown in study 1. Signals of lipoproteins, (LDL & VLDL CH_2 & CH_3 groups) and cholesterol appeared to be higher in samples taken after chemotherapy (Figure 48). This was a noted peak difference in chemotherapy

treated samples irrespective of whether they were normal or malignant tissues denoting the possibility that this is an isolated effect of chemotherapy.

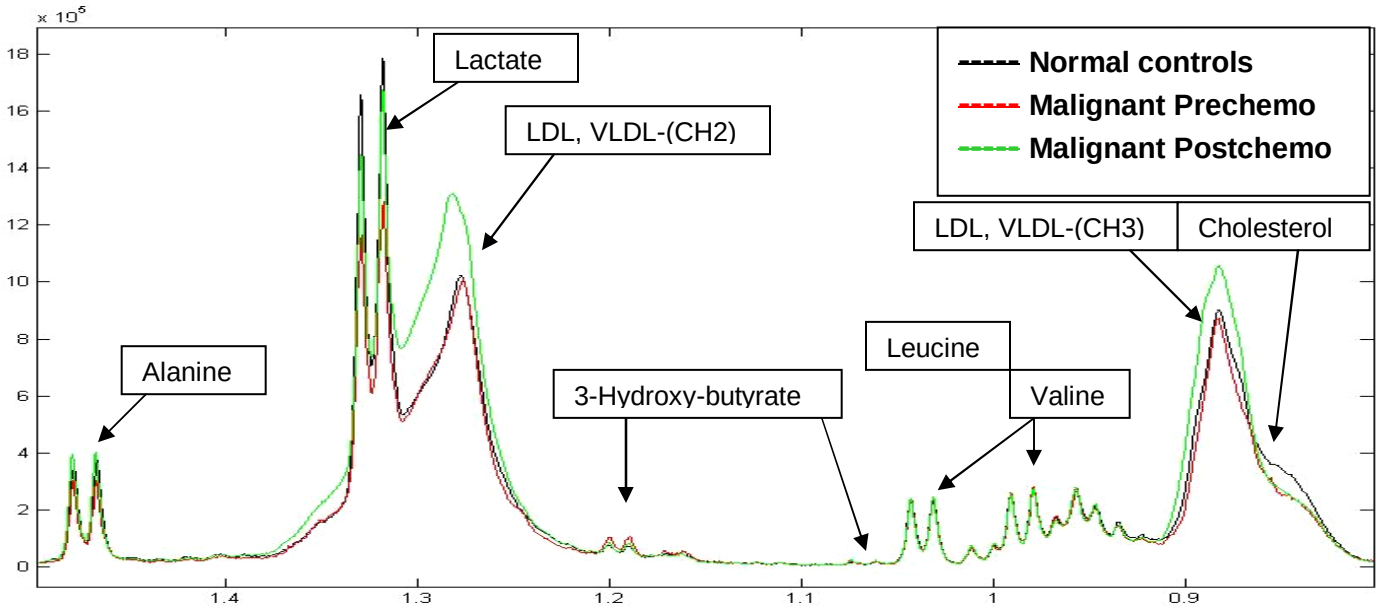


Figure 48. 1D median spectra of serum samples showing differences which may be attributed to isolated effect of chemotherapy

From a PCA model of these data; PC1 could moderately discriminate between normal and malignant samples. Within the malignant sample group further differentiation between pre-chemo and post-chemo samples can be seen. The results from PCA analysis support the observed group differences identified by visual inspection of the data. Patterns could not at this stage be correlated to variables as sex, age, BMI, type of tumour, pathological grade and TNM staging. This may be due to the number of samples used being insufficient for sub grouping.

4.3.5 Examination of specific chemotherapy induced metabolic alterations in patients with matched samples

In 6 patients where pre and post chemo samples were collected from each, a principal component analysis plot based on the previously described metabolite observations showed that both malignant and normal tissues move towards a middle metabolic phenotype after chemotherapy (Figure 49).

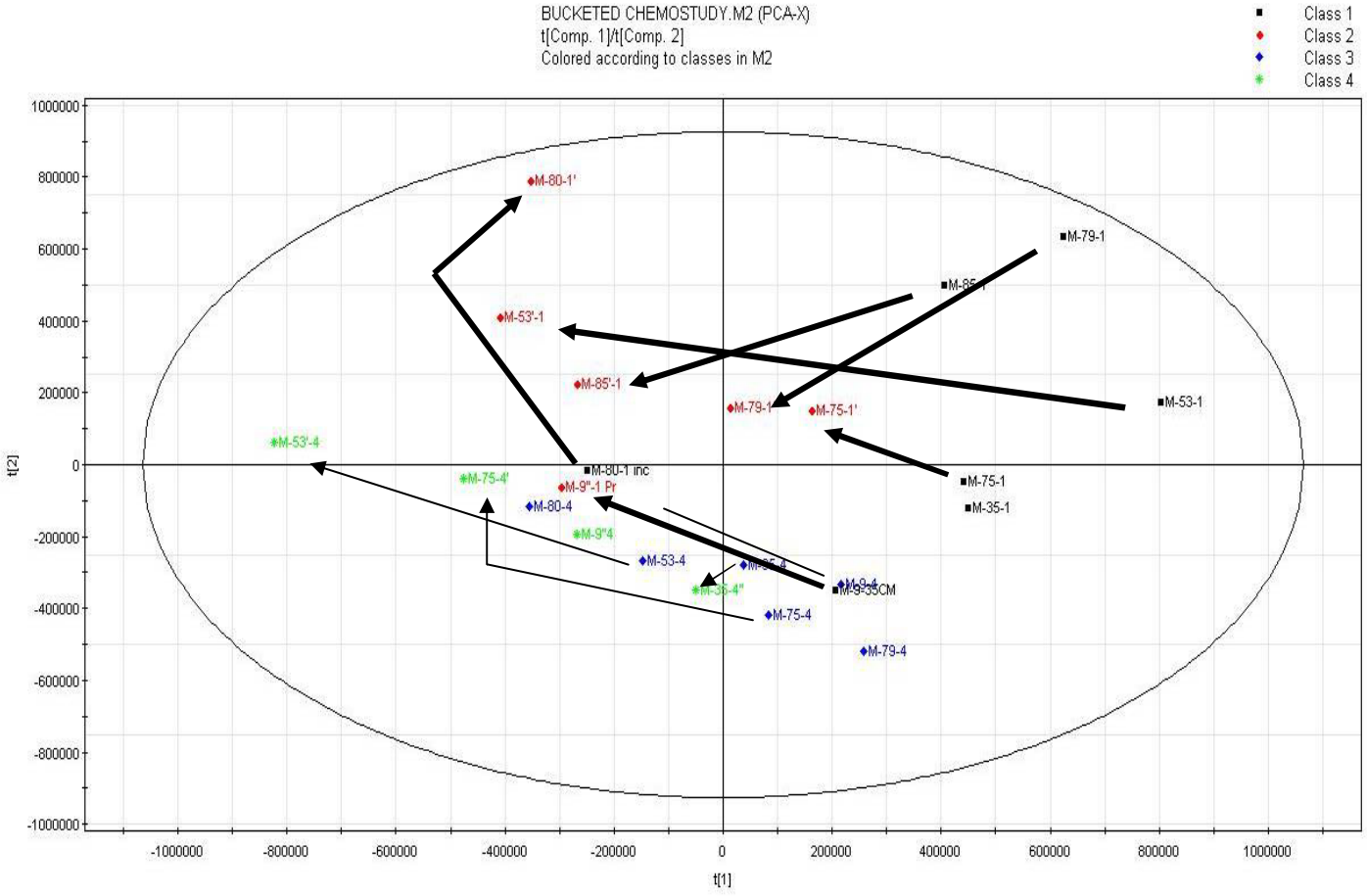


Figure 49. PCA plot showing both tumour (thick lines) and normal (thin lines) tissues from the same patients, pre and post chemotherapy, move towards a common metabolic phenotype

4.3.6 Metabolic profile components of differential response to chemotherapy

Response to chemotherapy has been histologically examined by reporting of *Mandard's* grade for 18 tumour tissue samples, all were oesophageal adenocarcinomas. Pathological properties and metabolites content of analyzed samples are shown in Table 13. Image analysis was also conducted to assess the extent of fibrosis in these samples via calculation of areas stained specifically for proliferative indices, apoptosis and fibrosis. Image analysis was positively correlated to the histological Mandard grade assessed by two independent histopathologists (*Spearman's* correlation coefficient 0.91). On the other hand, intra and inter observer reliability of pathologist grading was tested and found to have fair reproducibility among the same an different pathologists, this was assessed by *Kappa* statistics (data shown in appendix 7); therefore, the image analysis data were deemed reliable to be used for our correlation analysis. Samples were subclassified according to their Mandard grade, and various metabolites were compared to determine whether particular metabolite(s) content differed proportionally to the extent of response to chemotherapy.

Patient number	Mandard class	% Fibrosis	Lactate (1.315 - 1.4)	Lysine (1.64 - 1.78)	Glutamine (2.33-2.38)	Glutathione (2.54-2.58)	Creatine (3.025 - 3.045)	Total cholines (3.18 - 3.24)	Taurine (3.245-3.285)	Scylloinositol (3.34-3.36)	Uracil (5.88 - 5.93)	Tyrosine (6.87-6.93)	Adenines (8.255 - 8.275)
P1	4	22	3329100	324140	193040	26115	113860	1181500	415250	50171	12018	22024	2929.1
P2	1	84	1662500	368260	211220	37381	222750	820090	413440	36097	14223	27197	5269
P3	5	12	1261600	333960	226350	34590	129730	736470	351190	38579	11708	27368	2705.1
P4	5	11	1697000	266420	373890	35368	93947	1153400	529410	61422	24607	25578	2911.4
P5	4	27	1673600	295760	354690	34943	140610	600410	452420	52407	23294	30153	4251
P6	4	12	2119100	331510	274180	14659	78833	539750	371150	12524	20228	32341	5541.6
P7	4	21	1827400	391100	187140	18665	139030	1203300	535130	41033	23099	40042	4518.6
P8	3	33	3146800	243700	203400	53072	85647	636630	382380	43252	3892.3	17462	1239
P9	5	11	1664800	315900	170240	11620	207300	1151300	474760	58428	25491	29372	3743.1
P10	5	19	1146400	355130	198910	27066	136500	866170	383660	41288	33293	37623	3627.4
P11	3	38	1725300	167760	256260	45926	270230	747450	814470	104710	9397.4	12850	2984.6
P12	3	42	3016000	241970	196520	90478	231210	1136000	647580	66576	19562	20095	3199
P13	3	34	2718100	223590	216180	58092	136710	935890	518350	47998	3045.2	17162	2658.3
P14	4	21	2545700	307210	209810	67687	148150	923730	459020	45502	2729.8	25467	2685.9
P15	2	67	3035000	232900	262370	50988	128980	1896200	643510	44311	2352.2	13076	2228.9
P16	3	35	1727900	255170	226170	57995	162960	1049100	526390	50879	7709.6	14256	2848.7
P17	2	49	1506700	247930	233240	61731	188710	1205200	477670	33741	4509.1	17165	2280.1
P18	3	49	2802800	219620	294470	95362	293890	822430	597870	60614	10815	20718	1563.6

Table 13. Pathological properties (Mandard's grade of response and %fibrosis) and metabolites content (measured in average of relative integral values) of analyzed samples

It is to be noted that in the original study by *Mandard et al*, the multivariate analysis done, showed that only TRG (TRG1–3 vs. TRG4–5) remained a significant (p=0.001) predictor of disease-free survival (PMID: 8194005). This was taken as a guide to group our samples as the small number limits better informative results if the samples are to be divided to 5 Mandard groups. When patients were subdivided to Mandard grades 1-3 Vs 4 and 5, and the metabolite contents were plotted, evident changes show seven metabolites (Lysine, Glutathione, Creatine, Taurine, Uracil, Tyrosine and to some extent Adenine containing compounds) suggested to be related to quality of response of tumour tissue to chemotherapy Table 14 and Figure 50.

Metabolite / Mandard	Lactate (1.315 - 1.4)	Lysine (1.64 - 1.78)	Glutamine (2.33-2.38)	Glutathione (2.54-2.58)	Creatine (3.025 - 3.045)	Total cholines (3.18 - 3.24)	Taurine (3.245-3.285)	Scyllo - inositol (3.34-3.36)	Uracil (5.88 - 5.93)	Tyrosine (6.87-6.93)	Adenines (8.255 - 8.275)
1,2,3 Vs 4,5	0.179	0.002	0.724	0.002	0.041	0.524	0.037	0.28	0.008	0.0001	0.076

Table 14. Spearman's correlation coefficients (p-values are displayed) demonstrating metabolites that show significant change in relation to tissue responsiveness to chemotherapy

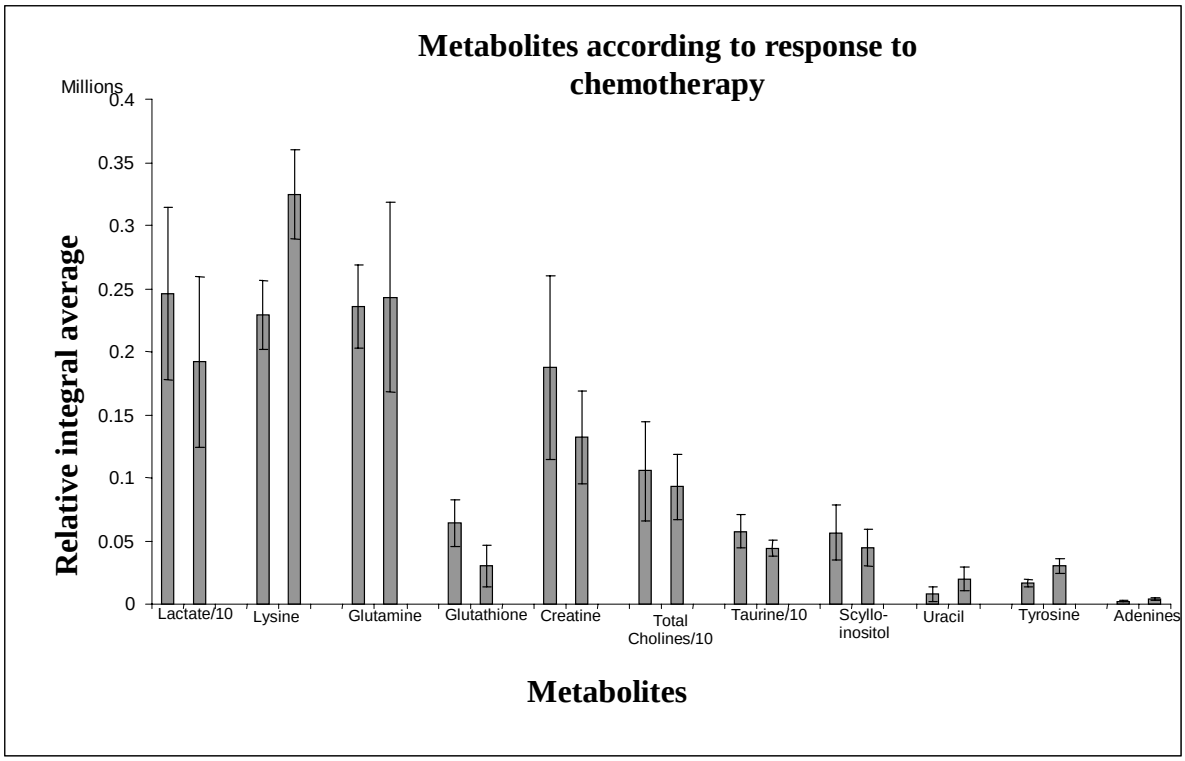


Figure 50. Metabolite differences according to response to chemotherapy when patients were divided into two groups Mandard 1-3 (left column for each metabolite) vs. Mandard 4, 5 (right column for each metabolite)

4.3.7 Summary of findings

This study showed that metabolic profiling can reliably discriminate chemotherapy treated tissue whether tumour or normal mucosa. Both generic and differential effects of chemotherapy were demonstrated in normal and cancer tissues. It could also display the correlation between variable metabolite content of malignant tissue and respective response to chemotherapy. Metabolites that were found to be significantly altered in correlation to response to chemotherapy are lysine, glutathione, creatine, taurine, uracil and tyrosine. Adenine containing compounds had the same trend but did not reach

statistical significance (p=0.07). These metabolites have been described in the literature as being closely related to malignant cell metabolism, proliferation and invasiveness, as previously discussed in the literature review section.

5. CHAPTER 5. FINAL DISCUSSION

The overall results of the study have demonstrated evidence of specific metabolic profile differences between three distinct groups of tissues: malignant, PHINOM and normal controls. It also showed characteristics of selective effect of chemotherapy on different tissues and correlated metabolic profile differences to chemotherapy response. This has been largely demonstrated in tissue analysis, and briefly cross examined in serum analysis.

5.1 Study I: Global metabonomic phenotyping of oesophageal and gastric cancer

The most significant global finding was that metabolic profiles of different tissues (oesophageal and gastric) tended to cluster closer with their new pathological designation (adenocarcinoma). This could be explained by the fact that malignant transformation of the tissue may have led to a new metabolic phenotype more or less non-specific to tissue, yet specific to the cancer process hypothetically transforming its phyico-chemical structure and mechanics. This has been clearly visualised in the PCA plots, where normal oesophageal and normal gastric samples appeared considerably apart, while malignant oesophageal and gastric samples were closer and even overlapping together.

5.1.1 Component differences between cancer and normal tissues

Glycolytic pathway compounds differentiating between benign and malignant samples seem to be closely related to a long known finding, originally described by *Warburg* in the 1920s, 'aerobic glycolysis'. This the greater tendency of tumour cells to convert glucose to lactate in the presence of normal oxygen conditions. Evidence suggests that how tumour cells glycolyse gives them selective growth advantage [23].

Recent research showed an increase in the GLUT-1 and GLUT-3 and GLUT-5 mRNA in cancers of the oesophagus, colon [218], pancreas [219], GLUT-1 and GLUT-3 mRNA were over expressed in the brain [220] and lung carcinomas [221], GLUT-1 protein expression in head and neck tumours [222], renal cell carcinoma [223], insulinomas [224] and thyroid cancers [225]; GLUT-1 and GLUT-5 over expression in breast tumours [226,227]. The over expression of GLUT-1 and GLUT-3 is only localised in the pen-necrotic zones of the tumour, where the environment of the tumour cells is hypoxic. An abundance of glucose transporters could be an adaptation that helps the tumour cell to survive and gives it an advantage over normal cells under such circumstances [222]. Of clinical importance is the question whether these changes in expression of facilitative transporters are strictly related to the malignant phenotype or occur at an early stage in carcinogenesis [22]. *Reisser et al.* [228], found that preneoplastic lesions already showed an increased expression of GLUT-1, so increases in GLUT-1 expression might be used as a diagnostic tool for detection of preneoplastic lesions.

Most of the tissue and plasma samples could show increase in lactate as the outcome product of the glycolytic pathway. This may point out to potentially, new therapeutic strategies in the future based on GLUT antagonization. Inhibition of GLUT-1 with chemicals such as phloretin, a known inhibitor of glucose membrane transport could be useful [229]. 3-O-methylglucose could also be effective as it works via competitive inhibition of glucose uptake by glucose analogues [230].

In addition, a metabolic feature of cancer that has been characterised in probably the greatest detail by NMR studies is the presence of elevated choline metabolites in tumour cells. This, together with a change in the phosphocholine/glycerophosphocholine ratio

has been shown to be a general marker for cell proliferation; and in conjunction with other metabolite measurements it could be predictive of the invasiveness of a tumour and useful in the clinical staging of disease. It is suggested that this may be in part due to increased choline transport into the cell and up regulated choline kinase activity in response to the demand for phosphatidylcholine and membrane synthesis [50,51]. Choline kinase inhibition as a therapeutic strategy has been shown to be successful in animal models [53]. This phenomenon has been observed in tissue and bio-fluid analysis of our samples.

5.1.2 Metabolic profiling of oesophageal tissue

The main focus of the larger part of the study was on oesophageal tissues. The analysis of gastric samples showed less ability of differentiation between benign and malignant than oesophageal samples. This may be either due to the fact that gastric sample numbers were relatively small to attain homogenous subgroups, or that gastric tissue has a lot more functional and anatomical variables than oesophageal tissue. These include the presence of different types of cells in gastric wall, different hormonal and nervous controls and the common presence of *Helicobacter Pylori* infection the possible metabolic effects of which is yet to be adequately examined. Therefore, given the novelty of application of this methodology and the need for initial core/baseline qualification of upper gastro intestinal tissue metabolic profiling, oesophageal tissue was the appropriate candidate for various analyses carried out throughout the course of the work; gastric tissue was used initially as a for of positive control to compare and contrast with oesophageal tissue.

5.1.2.1 Junctional Tumours

Analysis of junctional tissue proved very subtle differences from oesophageal tissues. During initial analysis and database construction, they have all has been classified as *Seiwert* type I by pathological examination; semi-quantitative comparison of metabolites on NMR spectral analysis showed no significant differences between junctional and oesophageal tissues, tumour or respective PHINOM. Thus, *Seiwert* type I junctional tumours were reclassified as oesophageal tumours. Nevertheless, junctional tumour samples were shown on PCA plots to be distributed in the region between both oesophageal and gastric cancer groups reflecting the reported clinical and pathological dilemma whether these tumours really arise from lowermost oesophageal or uppermost gastric mucosa.

5.1.2.2 Oesophageal adenocarcinoma vs. squamous carcinoma

Cancer of the oesophagus could be clustered on principal component analysis to adenocarcinoma and squamous carcinoma. The differences on examining the spectra were minimal yet obvious, mostly in lysine and adjoining lipid resonances that were more prominent in adenocarcinoma. This clustering could be seen when oesophageal samples were plotted separately (Figure 27), different types of tumour subclass i.e. adenocarcinoma and squamous carcinoma could be demonstrated on separate PCA plotting of oesophageal tissues alone. Squamous cancer could be seen relatively separate from adenocarcinoma in an area in between the fully normal epithelium and the adenocarcinoma, having the same vector of change from normal epithelium to adenocarcinoma. Nevertheless, on specific semi-quantitative comparison of the metabolites contributing to separation, subtle differences were found not mounting to

statistical significance. This could have been due to the fact that only a few squamous carcinoma samples were available for comparison, owing to the natural higher incidence of adenocarcinoma in the United Kingdom, which subsequently disproportionate the numbers affecting statistical analysis and also undermines the veracity of representability of these few samples to the actual general characteristics of this tumour. Nonetheless, the observations of analysis of these few samples could highlight the metabolic difference phenomenon and promotes the need for subsequent larger scale studies to confirm and further explain what was observed during the course of this study.

5.1.2.3 Barrett's oesophagus

The sample numbers used were not enough to sub-classify *Barrett's* samples according to grade of dysplasia or test qualitative differences in their metabolic profiles. The *Barrett's* tissue used, all originated from cancer bearing patients, and so the apparent similarity to the adenocarcinoma samples may be due to the effect of the nearby cancer and not just the local dysplasia. Barrett's samples appeared within the adenocarcinoma cluster. This may to be due to inherent similarity between metabolism of high grade dysplasia and cancer in these patients who all had cancer arising on a background of *Barrett's* mucosa. Yet again, the few number of samples analyzed was not enough for metabolite content comparison with either adenocarcinoma or normal mucosa. The collection of *Barrett's* sample collection was initially planned for; the findings of cancer tissue analysis dictated the need of collection of large number of samples where three times as much cancer and samples was collected before the final census was analyzed. This was due to different processing and analytic sample losses. The course of the study did not allow ample time and patient resources for that; new ethical approval was granted for that with recruitment

from a renowned *Barrett's* surveillance and follow up centre in London was planned, yet it has been deemed beyond the time scope of this study and has been incorporated in a future work body.

5.1.2.4 Failure of staging correlation

Few studies in the literature have attempted correlation of NMR data with clinical variables. A rather unsuccessful trial for correlation of NMR data with clinical variables was done in this study. The mathematical models developed could classify samples according to tissue of origin, oesophagus/stomach, pathological nature i.e. normal, and cancer. TNM stage and grade of differentiation may have been expected to affect the metabolic pattern as it depends on extent of genetic similarity to original cells. Nevertheless, correlation of tissue data with those factors could not be attained. This may be either due to insensitivity of the technique to these subtle differences or due to inaccuracy of the visual microscopic pathological grading, which is a rather subjective judgement of the pathologist. Other clinical variables as age, sex, BMI, co-morbidity had no apparent effect on the samples' classification at this stage. This is either due to lack of actual differences between them or due to small number of patients.

5.1.3 Pattern recognition validity

Consistent clustering of samples of different origin upon pattern recognition techniques was done in a non-supervised learning statistical model. This validates the reliability of the MAS technique starting from sample collection through data analysis. It is to be noted that the samples were obtained both surgically and endoscopically, collected from different centres and NMR run on different occasions. Of interest, two of the malignant samples that were collected endsocopically from a visible tumour mass were

unexpectedly deemed 'normal epithelium' by pathological examination. On our models they were seen among the malignant group. Further analysis of repeat samples obtained after surgical resection of this tumour confirmed its malignant nature as supported by pathology reports. An argument can be made whether metabolic profiles were actually more sensitive in classifying the two samples than pathological examination. This can be further studied by NMR analysis of future disputed samples and comparing that with results of currently used confirmatory tests as immuno-histochemical staining. The sample numbers used were not enough to sub-classify *Barrett's* samples according to grade of dysplasia or test qualitative differences in their metabolic profiles.

5.2 Study II: Field effects in non-dysplastic tissue in oesophageal cancer patients

5.2.1 Concept of 'field cancerization'

This concept was introduced by *Slaughter* in 1953 to describe the existence of generalized carcinogen induced early genetic changes in the epithelium from which multiple independent lesions occur, leading to the development of multifocal tumours [76-78]. This formed a belief that the lateral spread of tumours was due to progressive transformation of cells adjacent to a tumour, rather than the spread and destruction of the adjacent epithelium by pre-existing cancer cells [77]. Ever since, many studies were conducted to test this hypothesis in various cancers as referenced in the text; also, by investigating the genetic and epigenetic mutations, transcriptional effects and proteomic profiling aspects of tumours. With present technological advancement, including laser capture micro-dissection and high-throughput genomic technologies, carefully designed

studies using appropriate control tissue will enable identification of important molecular signatures in these genetically transformed but histologically normal cells [75].

5.2.2 Metabonomic evidence of field cancerization

By comparing histologically normal mucosa proximal to a tumour (PHINOM) with normal mucosa from non-diseased controls and tumour tissue, this study provides new evidence that field cancerization in oesophageal cancer manifests a metabolic phenotype and that metabolic profiling via ^{1}H MAS-NMR is sensitive to this phenomenon. Moreover, metabolites were identified that show a progression in detectable levels from normal to PHINOM to tumour tissue. Some of these metabolites, such as phosphocholine (PC), are well established metabolic biomarkers for malignant potential. Alterations to choline metabolism and specifically the increase in PC have been shown to differentiate malignant from normal tissue in most tumours. Also, choline kinase expression which forms PC is increased in several cancers [50]. Normal epithelial cells transformed by oncoproteins or loss of tumour suppressors, also show increases in PC and conversely reintroduction of p53 into p53-/- HCT116 cells has been shown to decrease intracellular PC levels [231]. Given that loss of heterozygosity (LOH) at loci for the tumour suppressors p16 (9p21) and p53 (17p13) have been used to map fields in the oesophagus [232], and that PC levels are affected by p53 status, our observation that PC levels were elevated in PHINOM is consistent with the hypothesis that tumours arise within a widespread genetically predisposed field. Furthermore, it has recently been shown that loss of p53 function could directly contribute to other well established aspects of the tumour metabolic phenotype, such as the *Warburg* effect (increased glucose uptake and metabolism to lactate), via regulation of mitochondrial metabolism and glycolysis [23].

While a progressive change in lactate or glucose levels was not seen, lactate levels were higher in tissue from cancer patients compared to controls. The observation that glutamate was progressively decreased in PHINOM and tumour may also reflect alterations to mitochondrial function since the increase in glutaminolysis in tumour cells is in part due to the consumption of glutamate via a truncated TCA cycle [233].

The presence of field cancerization in upper gastrointestinal cancer is widely accepted, with well documented clonal expansion in *Barrett's* dysplasia, the major pre-malignant lesion [80]. The results present in this report are of particular significance because the tissue used to define the metabolic field effect was not dysplastic nor did any of the patients have cancer that arose on a *Barrett's* background. This implies that metabolic analysis is sensitive to molecular changes that are relevant to oesophageal cancer in general and may relate to field related phenomena such as the well documented association between oesophageal and head and neck cancers; and satellite metastasis [234].

In addition to being an alternative route to genetic measurements to assess the state of the cancer field, metabolic profiling has several advantageous features. MAS-NMR profiles can be measured within 30 minutes of obtaining tissue from surgery or endoscopy so it has the potential to inform early decisions. Although histological assessment of frozen section can be carried out within the same time scale, MAS-NMR has the advantage of being able to detect changes in histologically normal tissue. Metabolic biomarkers in general have other advantages: as a phenotypic endpoint, these can reflect a number of genetic lesions that produce the same loss of function; also, a metabolite has a defined chemical structure and hence analytical protocol for analysis can translate across species and sample type. More generally, the ability to characterize the state of the field might

improve accuracy of diagnosis and staging. As noted in the first study, two of the samples which were collected endoscopically from a visible tumour mass were unexpectedly deemed 'normal epithelium' by pathological examination. In our model, they were classified as metabolically malignant, and analysis of samples obtained from the patient after surgical resection of those lesions confirmed its malignant nature. In an MAS-NMR profiling study of post-surgical prostate tissue, metabolic profiles of histologically-normal tissue were shown to systematically vary with stage [235].

5.2.3 Clinical implication of field cancerization findings

The most effective strategy to improve the outcome of oesophageal cancer was proven to be early detection [236]. Effectiveness of surveillance programmes has been disadvantaged by the low positive yield of endoscopic biopsies and lack of other biomarkers [237-239].In spite that conventional white-light endoscopy remains the gold standard surveillance procedure for pre-malignant conditions of the upper gastro-intestinal tract, its cost-effectiveness is debated [238,239]. The surveillance endoscopy, as mandated by the *American College of Gastroenterology* guidelines, yields about 20 biopsies, most of which are normal on histological assessment. Even with stepwise endoscopic biopsy in patients with confirmed high grade dysplasia, 41-66% of resected specimens had missed cancer lesions [237].

The demonstration of metabolic field changes adjoining to oesophageal cancer in this study has significant clinical implications as metabonomic profiling of histologically normal tissue of cancer patients has the potential to predict the presence of malignancy within the sampled field. This would reduce the incidence of missed cancer because of

sampling errors with significant impact on increasing the pick up rate in diagnostic endoscopy. In this way, biomarkers of field effects in oesophageal and other more prevalent gastrointestinal malignancies, such as colorectal cancer, are important for improving strategies for surveillance and disease prevention and could have enormous benefits to health and healthcare expenditure. Further studies are required to elucidate the molecular mechanisms that produce the phenomenon.

Another surgical application to this finding would be for patients who are candidates for surgical resection. If it is hypothesized that this metabolic field change is partly related to or causative of local tumour recurrence; then metabonomic mapping of the oesophagus could be done preoperatively to determine the topographic extent and severity of this field and subsequently inform the surgical decision as to the extent of surgical resection. Also, metabonomic mapping of what could be considered a sentinel lymph node i.e. the first tier of lymph nodes draining the tumour area could be useful intra-operatively to inform the surgeons plan of the radicality of lymphadenectomy, an issue that has long been a debate among upper gastro intestinal cancer surgeons.

5.3 Study III: Profiling metabonomic response of oesophageal adenocarcinoma to chemotherapy

5.3.1 Metabonomic response to chemotherapy

This study showed that metabolic profiling can reliably discriminate chemotherapy treated tissue whether tumour or normal mucosa. Both generic and differential effects of chemotherapy were demonstrated in normal and cancer tissues. It could also display the correlation between variable metabolite content of malignant tissue and respective

response to chemotherapy. Metabolites found to be significantly altered in correlation to response to chemotherapy are lysine, glutathione, creatine, taurine, uracil, tyrosine and to some extent, adenine containing compounds. These metabolites have been described in the literature as being closely related to malignant cell metabolism, proliferation and invasiveness, as previously discussed in the literature review section[1, 4, 17, 23, 44, 56, 63].

In 6 patients where pre and post chemotherapy samples were collected, a principal component analysis plot based on the previously described metabolite observations showed that both malignant and normal tissues move towards a middle metabolic phenotype after chemotherapy. This may even represent formation of fibrous tissue, the amount of which reflects the quality of response to chemotherapy. The extent of movement of the tissues towards that phenotype needs to be investigated as a surrogate marker of response to chemotherapeutics.

5.3.2 Clinical implications of metabonomic biomarkers to chemotherapy effect

The specific metabolite alterations, which were only seen in tumour tissue and not in normal mucosa, suggest the differential response of cancer tissue to chemotherapy than the normal one. This could be a product of the deranged metabolic pathways caused by perturbations inflicted by the mutated and damaged genetic structure of tumour cells. The question is: can this change be fixed whereas the response of the malignant cell metabolome to chemotherapy can be consistently qualified, in a way that can be examined to actually predict extent of response to chemotherapy. A factor that will prevent that is the genetic heterogeneity of cancer cell genomes across patients and even in the same tumour. On the other hand, one could argue that different tumours have well

described clinical behaviour and pathological features that the intercellular heterogeneity might be a subtle effecter in the process as compared to the generic, more or less expected genomic and functional genomic structure of that tumour. The literature has scant proof of biomarkers that can be used to predict response to chemotherapy[133, 136]; this leads many patients to be managed according to current treatment strategies with subsequent harm to a group of patients who are resistant to chemotherapy, where by the time they finish their planned protocol of treatment, their tumours would have even grown bigger and spread further, leading to exclusion of other approaches e.g. surgery, which might have been feasible in the beginning of these treatment protocols[145, 146].

Whether the changes imposed by carcinogenesis were normalised by the administration of chemotherapy is a material for a subsequent prospective study where appropriate numbered samples would collected and analyzed pre-chemotherapy and followed up post chemotherapy administration in a temporal fashion at distinct time points to actually monitor the levels and ratios of metabolites measured to determine the selective effect of each chemotherapy regimen on cellular metabolism and the progression of this effect with respect to time, incidence of recurrence and distant metastasis. This could give an insight as to the active components of metabolic pathways in carcinogenesis, progression, regression and invasiveness.

Predictive markers of response would therefore be invaluable in individualising patient treatment as it would enable discrimination of those patients likely to respond to combination therapy from those likely to be non-responsive, thus saving invaluable human and financial resources that is wasted otherwise. Most published studies have focussed on a single marker or a set of markers targeting specific pathways that may be

involved in cellular response to chemotherapeutics. However, it is clear that the cancer phenotype is a product of genetic and epigenetic alterations and, therefore, the ultimate response to cytotoxic therapy in cancer is also likely to be dictated by these genetic and epigenetic changes within the cancer genome and leading to alteration of the metabonomic phenotype. Thus, use of advanced metabonomic analysis exploring these possibilities has been demonstrated by this study [141].

5.3.3 Limitations of the study

Of the general limitations observed in this study is the relatively small sample numbers, where more numbers are needed to allow homogenous subgroups to study the myriad of variables as tumour subtypes, different schemes of chemotherapy and site specific subgroups of gastric cancer. Spectra of excluded outliers were examined; most of them had an abnormality in the form of broad peaks in some, non straight base line in another and poor peak expression in many. Causes of such abnormalities could be attributed to inadequacies in sample collection, storage, analysis or processing of data. It is to be noted that such exclusion decreased in the subsequent studies probably due to advancement of the learning curve of the author during the course of the studies.

5.4 Conclusions

The results of tissue analysis demonstrated differences between normal gastric and oesophageal tissue samples and their malignant counterpart. Normal oesophageal and normal gastric samples appeared considerably apart, while malignant oesophageal and gastric samples were closer and even overlapping together. There is distinct difference

between normal and cancer oesophageal tissue and between squamous and adenocarcinoma. Variable metabolites contributing to the separation between normal and cancer oesophageal tissues were identified. Choline, phosphocholine and glycerophosphocholine, taurine, tyrosine, lactate, phenylalanine, uracil, scylloinositol and myoinositol metabolites were found to be significantly higher in cancer tissue samples whereas normal tissue controls, had significantly higher content of glucose, glutamine, glutathione and adenine containing compounds.

By comparing histologically normal mucosa proximal to a tumour (PHINOM) with normal mucosa from non-diseased controls and tumour tissue, this study provides new evidence that field cancerization in oesophageal cancer manifests a metabolic phenotype and that metabolic profiling via ^{1}H MAS-NMR is sensitive to this phenomenon. Moreover, metabolites were identified that show a progression in detectable levels from normal to PHINOM to tumour tissue. Some of these metabolites, such as phosphocholine (PC), are well established metabolic biomarkers for malignant potential.

Both generic and differential effects of chemotherapy were demonstrated in normal and cancer tissues. Metabolites found to be significantly altered in correlation to response to chemotherapy are lysine, glutathione, creatine, taurine, uracil, tyrosine and to some extent adenine containing compounds. These metabolites have been described in the literature as being closely related to malignant cell metabolism, proliferation and invasiveness, as previously discussed in the literature review section.

6. CHAPTER 6. FUTURE STUDIES

6.1 Relationship between metabolic profiles and stage of cancer

Correlation with other means of investigation will be attempted by trying to correlate NMR profile changes to visual enhancements on PET imaging scans and examine relation to cancer stage. It may be possible to correlate metabolic profile changes and PET scan findings e.g. standard uptake volume, mass / volume assessment by PET scan.

Recent groups developed a prototype of endoscope mounted NMR probe which can provide realtime metabonomic profile for biliary ducts, this can be used for screening of oesophageal mucosa, this pioneering progress directs future research to translation of data acquired into a standard bedside screening test for oesophageal cancer [240].

6.2 Characterization of pre-malignant tissues:

The next step is to target premalignant conditions i.e. Barrett disease. The aim is to characterize Barrett epithelium in light of its pathological grading and determine whether there is a metabolic continuum on a scale starting at normal epithelium, passing through Barrett and finally cancer transformation. The following questions need to be answered:

- Does the metabonomic profile change corresponding to degree of dysplasia in Barrett's epithelium?
- Is Barrett's epithelium in cancer bearing oesophagus metabolically different than Barrett in otherwise normal oesophagus?
- Can the potential for malignant transformation be predicted?
- Can gene expression profiling explain metabonomic findings or direct further research on other metabolic pathways?

6.3 Effect of therapeutic modalities on body fluids metabolic profiles:

Parallel to tissue findings, differences between malignant and benign, pre and post chemo serum samples were seen. The plan for the team is to address the following questions:

- Would Radical surgery with curative intent reverse metabolic changes seen in cancer patients?, subsequently, can recurrence be detected and with what certainty?
- Can the response to chemotherapy be predicted from serum metabolic profile changes? Can changes be seen in urine?

7. REFERENCES

1. Lupulescu, A. *Cancer Cell Metabolism and Cancer Treatment*. Harwood Academic Publishers, The Netherlands (2001).

2. Dave, U., Taylor-Robinson, S. D., Walker, M. M., Mahon, M., Puri, B. K., Thursz, M. R., deSouza, N. M., Cox, I. J. In vitro ^{1}H-magnetic resonance spectroscopy of Barrett's esophageal mucosa using magic angle spinning techniques. *Eur J Gastroenterol Hepatol.* **16**,1199-1205 (2004).

3. Jones, G. R. Cancer destruction *in vivo* through disrupted energy metabolism. Part I. The endogenous mechanism of self-destruction within the malignant cell, and the roles of endotoxin, certain hormones and drugs, and active oxygen in causing cellular injury and death. *Physiol Chem. Phys. Med NMR* **24**, 169-179 (1992).

4. Kaplan, O. & Cohen, J. S. Metabolism of breast cancer cells as revealed by non-invasive magnetic resonance spectroscopy studies. *Breast Cancer Res. Treat.* **31**, 285-299 (1994).

5. Lamond, A. I. & Earnshaw, W. C. Structure and function in the nucleus. *Science* **280**, 547-553 (1998).

6. Lindon, J. C., Nicholson, J. K., Sidelmann, U. G. & Wilson, I. D. Directly coupled HPLC-NMR and its application to drug metabolism. *Drug Metab Rev.* **29**, 705-746 (1997).

7. Lupulescu, A. P. Hormones, vitamins, and growth factors in cancer treatment and prevention. A critical appraisal. *Cancer* **78**, 2264-2280 (1996).

8. Penman, S. Rethinking cell structure. *Proc. Natl. Acad. Sci. U. S. A* **92**, 5251-5257 (1995).

9. WARBURG, O. On respiratory impairment in cancer cells. *Science* **124**, 269-270 (1956).

10. Nicholson, J. K., Lindon, J. C. & Holmes, E. 'Metabonomics': understanding the metabolic responses of living systems to pathophysiological stimuli via multivariate statistical analysis of biological NMR spectroscopic data. *Xenobiotica* **29**, 1181-1189 (1999).

11. Lindon, J. C., Nicholson, J. K. & Holmes, E. *The Handbook of Metabonomics and Metabolomics*. Elsevier, The Netherlands (2007).

12. Denkert, C. *et al.* Mass spectrometry-based metabolic profiling reveals different metabolite patterns in invasive ovarian carcinomas and ovarian borderline tumors. *Cancer Res.* **66**, 10795-10804 (2006).

13. Petrik, V., Loosemore, A., Howe, F. A., Bell, B. A. & Papadopoulos, M. C. OMICS and brain tumour biomarkers. *Br J Neurosurg.* **20**, 275-280 (2006).

14. Yang, J. *et al.* Diagnosis of liver cancer using HPLC-based metabonomics avoiding false-positive result from hepatitis and hepatocirrhosis diseases. *J Chromatogr. B Analyt. Technol. Biomed. Life Sci.* **813**, 59-65 (2004).

15. Behl, C. *et al.* Neuroprotection against oxidative stress by estrogens: structure-activity relationship. *Mol. Pharmacol.* **51**, 535-541 (1997).

16. Nguyen, T., Chin, W. C. & Verdugo, P. Role of Ca2+/K+ ion exchange in intracellular storage and release of Ca2+. *Nature* **395**, 908-912 (1998).

17. Bi, X. *et al.* Proteomic analysis of colorectal cancer reveals alterations in metabolic pathways: mechanism of tumorigenesis. *Mol. Cell Proteomics.* **5**, 1119-1130 (2006).

18. Moreno, A., Rey, M., Montane, J. M., Alonso, J. & Arus, C. 1H NMR spectroscopy of colon tumors and normal mucosal biopsies; elevated taurine levels and reduced polyethyleneglycol absorption in tumors may have diagnostic significance. *NMR Biomed.* **6**, 111-118 (1993).

19. Longley, D. B., Allen, W. L. & Johnston, P. G. Drug resistance, predictive markers and pharmacogenomics in colorectal cancer. *Biochim. Biophys. Acta* **1766**, 184-196 (2006).

20. Wallace, D. C. Mitochondria as chi. *Genetics* **179**, 727-735 (2008).

21. Selig, M., Xavier, K. B., Santos, H. & Schonheit, P. Comparative analysis of Embden-Meyerhof and Entner-Doudoroff glycolytic pathways in hyperthermophilic archaea and the bacterium Thermotoga. *Arch. Microbiol.* **167**, 217-232 (1997).

22. Pauwels, E. K., Sturm, E. J., Bombardieri, E., Cleton, F. J. & Stokkel, M. P. Positron-emission tomography with [18F]fluorodeoxyglucose. Part I. Biochemical uptake mechanism and its implication for clinical studies. *J Cancer Res. Clin Oncol* **126**, 549-559 (2000).

23. Gatenby, R. A. & Gillies, R. J. Why do cancers have high aerobic glycolysis? *Nat. Rev. Cancer* **4**, 891-899 (2004).

24. Warburg, O., Wind, F. & Negelein, E. Uber den Stoffwechsel von Tumourenim Korper. *Klin Woch* **5**, 829-832 (1926).

25. Gullino, P. M., Grantham, F. H. & Courtney, A. H. Utilization of oxygen by transplanted tumors *in vivo*. *Cancer Res.* **27**, 1020-1030 (1967).

26. Weinhouse, S. On respiratory impairment in cancer cells. *Science* **124**, 267-269 (1956).

27. Semenza, G. L. *et al.* 'The metabolism of tumours': 70 years later. *Novartis. Found. Symp.* **240**, 251-260 (2001).

28. Nakashima, R. A., Paggi, M. G. & Pedersen, P. L. Contributions of glycolysis and oxidative phosphorylation to adenosine 5'-triphosphate production in AS-30D hepatoma cells. *Cancer Res.* **44**, 5702-5706 (1984).

29. Birnbaum, M. J., Haspel, H. C. & Rosen, O. M. Transformation of rat fibroblasts by FSV rapidly increases glucose transporter gene transcription. *Science* **235**, 1495-1498 (1987).

30. Flier, J. S., Mueckler, M. M., Usher, P. & Lodish, H. F. Elevated levels of glucose transport and transporter messenger RNA are induced by ras or src oncogenes. *Science* **235**, 1492-1495 (1987).

31. Singh, M., Singh, V. N., August, J. T. & Horecker, B. L. Alterations in glucose metabolism in chick embryo cells transformed by Rous sarcoma virus. Transformation-specific changes in the activities of key enzymes of the glycolytic and hexose monophosphate shunt pathways. *Arch. Biochem. Biophys.* **165**, 240-246 (1974).

32. Arora, K. K. & Pedersen, P. L. Functional significance of mitochondrial bound hexokinase in tumor cell metabolism. Evidence for preferential phosphorylation of glucose by intramitochondrially generated ATP. *J Biol. Chem.* **263**, 17422-17428 (1988).

33. Rempel, A., Bannasch, P. & Mayer, D. Differences in expression and intracellular distribution of hexokinase isoenzymes in rat liver cells of different transformation stages. *Biochim. Biophys. Acta* **1219**, 660-668 (1994).

34. Mathupala, S. P., Heese, C. & Pedersen, P. L. Glucose catabolism in cancer cells. The type II hexokinase promoter contains functionally active response elements for the tumor suppressor p53. *J Biol. Chem.* **272**, 22776-22780 (1997).

35. Mukhopadhyay, T., Maxwell, A. S. & Roth, J. A. *p53 supppressor gene*. Landes, Austin, Texas (1995).

36. Bartrons, R. & Caro, J. Hypoxia, glucose metabolism and the Warburg's effect. *J Bioenerg. Biomembr.* **39**, 223-229 (2007).

37. Strauss, L. G. & Conti, P. S. The applications of PET in clinical oncology. *J Nucl Med* **32**, 623-648 (1991).

38. Okazumi, S. *et al.* Evaluation of liver tumors using fluorine-18-fluorodeoxyglucose PET: characterization of tumor and assessment of effect of treatment. *J Nucl Med* **33**, 333-339 (1992).

39. Slosman, D. O., Pittet, N., Donath, A. & Polla, B. S. Fluorodeoxyglucose cell incorporation as an index of cell proliferation: evaluation of accuracy in cell culture. *Eur. J Nucl Med* **20**, 1084-1088 (1993).

40. Crippa, F. *et al.* Association between [18F]fluorodeoxyglucose uptake and postoperative histopathology, hormone receptor status, thymidine labelling index and p53 in primary breast cancer: a preliminary observation. *Eur. J Nucl Med* **25**, 1429-1434 (1998).

41. Brock, C. S., Meikle, S. R. & Price, P. Does fluorine-18 fluorodeoxyglucose metabolic imaging of tumours benefit oncology? *Eur. J Nucl Med* **24**, 691-705 (1997).

42. Kubota, R. *et al.* Intratumoral distribution of fluorine-18-fluorodeoxyglucose *in vivo*: high accumulation in macrophages and granulation tissues studied by microautoradiography. *J Nucl Med* **33**, 1972-1980 (1992).

43. Kubota, R. *et al.* Microautoradiographic study for the differentiation of intratumoral macrophages, granulation tissues and cancer cells by the dynamics of fluorine-18-fluorodeoxyglucose uptake. *J Nucl Med* **35**, 104-112 (1994).

44. Coles, N. W. & Johnstone, R. M. Glutamine metabolism in Ehrlich ascites-carcinoma cells. *Biochem. J* **83**, 284-291 (1962).

45. Reitzer, L. J., Wice, B. M. & Kennell, D. Evidence that glutamine, not sugar, is the major energy source for cultured HeLa cells. *J Biol. Chem.* **254**, 2669-2676 (1979).

46. van Acker, B. A. *et al.* Glutamine: the pivot of our nitrogen economy? *JPEN J Parenter. Enteral Nutr.* **23**, S45-S48 (1999).

47. Medina, M. A., Sanchez-Jimenez, F., Marquez, J., Rodriguez, Q. A. & Nunez, d. C., I Relevance of glutamine metabolism to tumor cell growth. *Mol. Cell Biochem.* **113**, 1-15 (1992).

48. Kuhajda, F. P. Fatty acid synthase and cancer: new application of an old pathway. *Cancer Res.* **66**, 5977-5980 (2006).

49. Plathow, C. & Weber, W. A. Tumor cell metabolism imaging. *J Nucl Med* **49 Suppl 2**, 43S-63S (2008).

50. Glunde, K. & Bhujwalla, Z. M. Choline kinase alpha in cancer prognosis and treatment. *Lancet Oncol* **8**, 855-857 (2007).

51. Gillies, R. J. & Morse, D. L. *In vivo* magnetic resonance spectroscopy in cancer. *Annu. Rev. Biomed. Eng* **7**, 287-326 (2005).

52. Utriainen, M. *et al.* Evaluation of brain tumor metabolism with [11C]choline PET and 1H-MRS. *J Neurooncol.* **62**, 329-338 (2003).

53. Aoyama, C., Liao, H. & Ishidate, K. Structure and function of choline kinase isoforms in mammalian cells. *Prog. Lipid Res.* **43**, 266-281 (2004).

54. Aoyama, C., Ishidate, K., Sugimoto, H. & Vance, D. E. Induction of choline kinase alpha by carbon tetrachloride (CCl4) occurs via increased binding of c-jun to an AP-1 element. *Biochim. Biophys. Acta* **1771**, 1148-1155 (2007).

55. Cuadrado, A., Carnero, A., Dolfi, F., Jimenez, B. & Lacal, J. C. Phosphorylcholine: a novel second messenger essential for mitogenic activity of growth factors. *Oncogene* **8**, 2959-2968 (1993).

56. Aboagye, E. O. & Bhujwalla, Z. M. Malignant transformation alters membrane choline phospholipid metabolism of human mammary epithelial cells. *Cancer Res.* **59**, 80-84 (1999).

57. Ramirez de, M. A. *et al.* Choline kinase activation is a critical requirement for the proliferation of primary human mammary epithelial cells and breast tumor progression. *Cancer Res.* **64**, 6732-6739 (2004).

58. Bhakoo, K. K., Williams, S. R., Florian, C. L., Land, H. & Noble, M. D. Immortalization and transformation are associated with specific alterations in choline metabolism. *Cancer Res.* **56**, 4630-4635 (1996).

59. Costello, L. C. & Franklin, R. B. 'Why do tumour cells glycolyse?': from glycolysis through citrate to lipogenesis. *Mol. Cell Biochem.* **280**, 1-8 (2005).

60. Podo, F. Tumour phospholipid metabolism. *NMR Biomed.* **12**, 413-439 (1999).

61. Kwock, L. *et al.* Clinical role of proton magnetic resonance spectroscopy in oncology: brain, breast, and prostate cancer. *Lancet Oncol* **7**, 859-868 (2006).

62. Dowling, C. *et al.* Preoperative proton MR spectroscopic imaging of brain tumors: correlation with histopathologic analysis of resection specimens. *AJNR Am. J Neuroradiol.* **22**, 604-612 (2001).

63. Howe, F. A. *et al.* Metabolic profiles of human brain tumors using quantitative *in vivo* ^{1}H magnetic resonance spectroscopy. *Magn Reson. Med* **49**, 223-232 (2003).

64. Chen, J., Huang, S. L., Li, T. & Chen, X. L. *In vivo* research in astrocytoma cell proliferation with 1H-magnetic resonance spectroscopy: correlation with histopathology and immunohistochemistry. *Neuroradiology* **48**, 312-318 (2006).

65. Jeun, S. S. *et al.* Assessment of malignancy in gliomas by 3T 1H MR spectroscopy. *Clin Imaging* **29**, 10-15 (2005).

66. Costello, L. C. & Franklin, R. B. Citrate metabolism of normal and malignant prostate epithelial cells. *Urology* **50**, 3-12 (1997).

67. Kurhanewicz, J., Vigneron, D., Carroll, P. & Coakley, F. Multiparametric magnetic resonance imaging in prostate cancer: present and future. *Curr. Opin. Urol.* **18**, 71-77 (2008).

68. Hricak, H. MR imaging and MR spectroscopic imaging in the pre-treatment evaluation of prostate cancer. *Br J Radiol.* **78 Spec No 2**, S103-S111 (2005).

69. Schoder, H. *et al.* 2-[18F]fluoro-2-deoxyglucose positron emission tomography for the detection of disease in patients with prostate-specific antigen relapse after radical prostatectomy. *Clin Cancer Res.* **11**, 4761-4769 (2005).

70. Hara, T., Kosaka, N. & Kishi, H. PET imaging of prostate cancer using carbon-11-choline. *J Nucl Med* **39**, 990-995 (1998).

71. Sutinen, E. *et al.* Kinetics of [(11)C]choline uptake in prostate cancer: a PET study. *Eur. J Nucl Med Mol. Imaging* **31**, 317-324 (2004).

72. Breeuwsma, A. J. *et al. In vivo* uptake of [11C]choline does not correlate with cell proliferation in human prostate cancer. *Eur. J Nucl Med Mol. Imaging* **32**, 668-673 (2005).

73. Giovacchini, G. *et al.* [(11)C]choline uptake with PET/CT for the initial diagnosis of prostate cancer: relation to PSA levels, tumour stage and anti-androgenic therapy. *Eur. J Nucl Med Mol. Imaging* **35**, 1065-1073 (2008).

74. Scheidler, J. *et al.* Prostate cancer: localization with three-dimensional proton MR spectroscopic imaging--clinicopathologic study. *Radiology* **213**, 473-480 (1999).

75. Dakubo, G. D., Jakupciak, J. P., Birch-Machin, M. A. & Parr, R. L. Clinical implications and utility of field cancerization. *Cancer Cell Int.* **7**, 2 (2007).

76. Slaughter, D. P. The multiplicity of origin of malignant tumours: collective review. *Internat Abstr Surg* **79**, 89-98 (1944).

77. Slaughter, D. P. Multicentric origin of intraoral carcinoma. *Surgery* **20**, 133-146 (1946).

78. Slaughter, D. P., SOUTHWICK, H. W. & SMEJKAL, W. Field cancerization in oral stratified squamous epithelium; clinical implications of multicentric origin. *Cancer* **6**, 963-968 (1953).

79. Braakhuis, B. J., Tabor, M. P., Kummer, J. A., Leemans, C. R. & Brakenhoff, R. H. A genetic explanation of Slaughter's concept of field cancerization: evidence and clinical implications. *Cancer Res.* **63**, 1727-1730 (2003).

80. Prevo, L. J., Sanchez, C. A., Galipeau, P. C. & Reid, B. J. p53-mutant clones and field effects in Barrett's esophagus. *Cancer Res.* **59**, 4784-4787 (1999).

81. Simon, R. *et al.* Cytogenetic analysis of multifocal bladder cancer supports a monoclonal origin and intraepithelial spread of tumor cells. *Cancer Res.* **61**, 355-362 (2001).

82. Tabor, M. P. *et al.* Multiple head and neck tumors frequently originate from a single preneoplastic lesion. *Am. J Pathol.* **161**, 1051-1060 (2002).

83. Tabor, M. P. *et al.* Genetically altered fields as origin of locally recurrent head and neck cancer: a retrospective study. *Clin Cancer Res.* **10**, 3607-3613 (2004).

84. Sui, G. *et al.* Mitochondrial DNA mutations in preneoplastic lesions of the gastrointestinal tract: a biomarker for the early detection of cancer. *Mol. Cancer* **5**, 73 (2006).

85. Shen, L. *et al.* MGMT promoter methylation and field defect in sporadic colorectal cancer. *J Natl. Cancer Inst.* **97**, 1330-1338 (2005).

86. Deng, G., Lu, Y., Zlotnikov, G., Thor, A. D. & Smith, H. S. Loss of heterozygosity in normal tissue adjacent to breast carcinomas. *Science* **274**, 2057-2059 (1996).

87. Heaphy, C. M. *et al.* Telomere DNA content and allelic imbalance demonstrate field cancerization in histologically normal tissue adjacent to breast tumors. *Int. J Cancer* **119**, 108-116 (2006).

88. Ha, P. K. *et al.* Mitochondrial C-tract alteration in premalignant lesions of the head and neck: a marker for progression and clonal proliferation. *Clin Cancer Res.* **8**, 2260-2265 (2002).

89. Chandran, U. R. *et al.* Differences in gene expression in prostate cancer, normal appearing prostate tissue adjacent to cancer and prostate tissue from cancer free organ donors. *BMC. Cancer* **5**, 45 (2005).

90. Birch-Machin, M. A. The role of mitochondria in ageing and carcinogenesis. *Clin Exp. Dermatol.* **31**, 548-552 (2006).

91. Roesch-Ely, M. *et al.* Proteomic analysis reveals successive aberrations in protein expression from healthy mucosa to invasive head and neck cancer. *Oncogene* **26**, 54-64 (2007).

92. Wong, D. J. *et al.* p16(INK4a) lesions are common, early abnormalities that undergo clonal expansion in Barrett's metaplastic epithelium. *Cancer Res.* **61**, 8284-8289 (2001).

93. Kim, S. K. *et al.* The epigenetic silencing of LIMS2 in gastric cancer and its inhibitory effect on cell migration. *Biochem. Biophys. Res. Commun.* **349**, 1032-1040 (2006).

94. Grepmeier, U. *et al.* Deletions at chromosome 2q and 12p are early and frequent molecular alterations in bronchial epithelium and NSCLC of long-term smokers. *Int. J Oncol* **27**, 481-488 (2005).

95. Jonason, A. S. *et al.* Frequent clones of p53-mutated keratinocytes in normal human skin. *Proc. Natl. Acad. Sci. U. S. A* **93**, 14025-14029 (1996).

96. Chu, T. Y., Shen, C. Y., Lee, H. S. & Liu, H. S. Monoclonality and surface lesion-specific microsatellite alterations in premalignant and malignant neoplasia of uterine cervix: a local field effect of genomic instability and clonal evolution. *Genes Chromosomes. Cancer* **24**, 127-134 (1999).

97. Rosenthal, A. N., Ryan, A., Hopster, D. & Jacobs, I. J. Molecular evidence of a common clonal origin and subsequent divergent clonal evolution in vulval intraepithelial neoplasia, vulval squamous cell carcinoma and lymph node metastases. *Int. J Cancer* **99**, 549-554 (2002).

98. Kakizoe, T. Development and progression of urothelial carcinoma. *Cancer Sci.* **97**, 821-828 (2006).

99. Furlan, D. *et al.* The high frequency of *de novo* promoter methylation in synchronous primary endometrial and ovarian carcinomas. *Clin Cancer Res.* **12**, 3329-3336 (2006).

100. Kitago, M. *et al.* Comparison of K-ras point mutation distributions in intraductal papillary-mucinous tumors and ductal adenocarcinoma of the pancreas. *Int. J Cancer* **110**, 177-182 (2004).

101. Hanson, J. A. *et al.* Gene promoter methylation in prostate tumor-associated stromal cells. *J Natl. Cancer Inst.* **98**, 255-261 (2006).

102. Brodsky, R. A. & Jones, R. J. Riddle: what do aplastic anemia, acute promyelocytic leukemia, and chronic myeloid leukemia have in common? *Leukemia* **18**, 1740-1742 (2004).

103. Kros, J. M., Zheng, P., Dinjens, W. N. & Alers, J. C. Genetic aberrations in gliomatosis cerebri support monoclonal tumorigenesis. *J Neuropathol. Exp. Neurol.* **61**, 806-814 (2002).

104. Barrett, M. T. *et al.* Evolution of neoplastic cell lineages in Barrett oesophagus. *Nat. Genet.* **22**, 106-109 (1999).

105. Eads, C. A. *et al.* Fields of aberrant CpG island hypermethylation in Barrett's esophagus and associated adenocarcinoma. *Cancer Res.* **60**, 5021-5026 (2000).

106. Maley, C. C. *et al.* The combination of genetic instability and clonal expansion predicts progression to esophageal adenocarcinoma. *Cancer Res.* **64**, 7629-7633 (2004).

107. Maley, C. C. *et al.* Genetic clonal diversity predicts progression to esophageal adenocarcinoma. *Nat. Genet.* **38**, 468-473 (2006).

108. Merlo, L. M., Pepper, J. W., Reid, B. J. & Maley, C. C. Cancer as an evolutionary and ecological process. *Nat. Rev. Cancer* **6**, 924-935 (2006).

109. Kang, G. H. *et al.* Genetic evidence for the multicentric origin of synchronous multiple gastric carcinoma. *Lab Invest* **76**, 407-417 (1997).

110. Kim, J. S. *et al.* Amplification of c-erbB-2 proto-oncogene in cancer foci, adjacent normal, metastatic and normal tissues of human primary gastric adenocarcinomas. *J Korean Med Sci.* **12**, 311-315 (1997).

111. Kim, J. Y. & Cho, H. J. DNA ploidy patterns in gastric adenocarcinoma. *J Korean Med Sci.* **15**, 159-166 (2000).

112. Crew, K. D. & Neugut, A. I. Epidemiology of upper gastrointestinal malignancies. *Semin. Oncol.* **31**, 450-464 (2004).

113. Bouche, O. & Lagarde, S. [Stomach cancer]. *Rev. Prat.* **55**, 123-130 (2005).

114. Cunningham, D. *et al.* Perioperative chemotherapy versus surgery alone for resectable gastroesophageal cancer. *N. Engl. J Med* **355**, 11-20 (2006).

115. Fareed, K. R. *et al.* Biomarkers of response to therapy in oesophago-gastric cancer. *Gut* **58**, 127-143 (2009).

116. Medical Research Council Oesophageal Cancer Working Group Surgical resection with or without preoperative chemotherapy in oesophageal cancer: a randomised controlled trial. *Lancet* **359**, 1727-1733 (2002).

117. Mandard, A. M. *et al.* Pathologic assessment of tumor regression after preoperative chemoradiotherapy of esophageal carcinoma. Clinicopathologic correlations. *Cancer* **73**, 2680-2686 (1994).

118. Becker, K. *et al.* Histomorphology and grading of regression in gastric carcinoma treated with neoadjuvant chemotherapy. *Cancer* **98**, 1521-1530 (2003).

119. Pinedo, H. M. & Peters, G. F. Fluorouracil: biochemistry and pharmacology. *J Clin Oncol* **6**, 1653-1664 (1988).

120. Longley, D. B., Harkin, D. P. & Johnston, P. G. 5-fluorouracil: mechanisms of action and clinical strategies. *Nat. Rev. Cancer* **3**, 330-338 (2003).

121. An, Q., Robins, P., Lindahl, T. & Barnes, D. E. 5-Fluorouracil incorporated into DNA is excised by the Smug1 DNA glycosylase to reduce drug cytotoxicity. *Cancer Res.* **67**, 940-945 (2007).

122. Venturini, M. Rational development of capecitabine. *Eur. J Cancer* **38 Suppl 2**, 3-9 (2002).

123. Schoffski, P. The modulated oral fluoropyrimidine prodrug S-1, and its use in gastrointestinal cancer and other solid tumors. *Anticancer Drugs* **15**, 85-106 (2004).

124. Deeks, E. D. & Scott, L. J. Docetaxel: in gastric cancer. *Drugs* **67**, 1893-1901 (2007).

125. Farhat, F. S. A general review of the role of irinotecan (CPT11) in the treatment of gastric cancer. *Med Oncol* **24**, 137-146 (2007).

126. Shin, S. *et al.* An anti-apoptotic protein human survivin is a direct inhibitor of caspase-3 and -7. *Biochemistry* **40**, 1117-1123 (2001).

127. Nakamura, M. *et al.* Survivin as a predictor of cis-diamminedichloroplatinum sensitivity in gastric cancer patients. *Cancer Sci.* **95**, 44-51 (2004).

128. Kato, J. *et al.* Expression of survivin in esophageal cancer: correlation with the prognosis and response to chemotherapy. *Int. J Cancer* **95**, 92-95 (2001).

129. Kang, S. Y. *et al.* Low expression of Bax predicts poor prognosis in patients with locally advanced esophageal cancer treated with definitive chemoradiotherapy. *Clin Cancer Res.* **13**, 4146-4153 (2007).

130. Zimmermann, K. C. *et al.* Cyclooxygenase-2 expression in human esophageal carcinoma. *Cancer Res.* **59**, 198-204 (1999).

131. Mao, X. Y., Wang, X. G., Lv, X. J., Xu, L. & Han, C. B. COX-2 expression in gastric cancer and its relationship with angiogenesis using tissue microarray. *World J Gastroenterol.* **13**, 3466-3471 (2007).

132. Xi, H. *et al.* High cyclooxygenase-2 expression following neoadjuvant radiochemotherapy is associated with minor histopathologic response and poor prognosis in esophageal cancer. *Clin Cancer Res.* **11**, 8341-8347 (2005).

133. Boku, N. *et al.* Biological markers as a predictor for response and prognosis of unresectable gastric cancer patients treated with 5-fluorouracil and cis-platinum. *Clin Cancer Res.* **4**, 1469-1474 (1998).

134. Okumura, H. *et al.* The predictive value of p53, p53R2, and p21 for the effect of chemoradiation therapy on oesophageal squamous cell carcinoma. *Br J Cancer* **92**, 284-289 (2005).

135. Akamatsu, M. *et al.* c-erbB-2 oncoprotein expression related to chemoradioresistance in esophageal squamous cell carcinoma. *Int. J Radiat. Oncol Biol. Phys.* **57**, 1323-1327 (2003).

136. Sarbia, M., Ott, N., Puhringer-Oppermann, F. & Brucher, B. L. The predictive value of molecular markers (p53, EGFR, ATM, CHK2) in multimodally treated squamous cell carcinoma of the oesophagus. *Br J Cancer* **97**, 1404-1408 (2007).

137. Gibson, M. K. *et al.* Epidermal growth factor receptor, p53 mutation, and pathological response predict survival in patients with locally advanced esophageal cancer treated with preoperative chemoradiotherapy. *Clin Cancer Res.* **9**, 6461-6468 (2003).

138. Izzo, J. G. *et al.* Association of activated transcription factor nuclear factor kappab with chemoradiation resistance and poor outcome in esophageal carcinoma. *J Clin Oncol* **24**, 748-754 (2006).

139. Harris, A. L. Hypoxia--a key regulatory factor in tumour growth. *Nat. Rev. Cancer* **2**, 38-47 (2002).

140. Boku, N., Ohtsu, A., Nagashima, F., Shirao, K. & Koizumi, W. Relationship between expression of vascular endothelial growth factor in tumor tissue from gastric cancers and chemotherapy effects: comparison between S-1 alone and the combination of S-1 plus CDDP. *Jpn J Clin Oncol* **37**, 509-514 (2007).

141. Chin, L. & Gray, J. W. Translating insights from the cancer genome into clinical practice. *Nature* **452**, 553-563 (2008).

142. van't Veer, L. J. & Bernards, R. Enabling personalized cancer medicine through analysis of gene-expression patterns. *Nature* **452**, 564-570 (2008).

143. Luthra, R. *et al.* Gene expression profiling of localized esophageal carcinomas: association with pathologic response to preoperative chemoradiation. *J Clin Oncol* **24**, 259-267 (2006).

144. Luthra, M. G. *et al.* Decreased expression of gene cluster at chromosome 1q21 defines molecular subgroups of chemoradiotherapy response in esophageal cancers. *Clin Cancer Res.* **13**, 912-919 (2007).

145. Ashida, A. *et al.* Expression profiling of esophageal squamous cell carcinoma patients treated with definitive chemoradiotherapy: clinical implications. *Int. J Oncol* **28**, 1345-1352 (2006).

146. Duong, C. *et al.* Pretreatment gene expression profiles can be used to predict response to neoadjuvant chemoradiotherapy in esophageal cancer. *Ann. Surg Oncol* **14**, 3602-3609 (2007).

147. Union Internationale Contre le Cancer. TNM classification if malignant tumours. 6th ed. New York: Wiley-Liss. 2002.

148. Moehler, M., Lyros, O., Gockel, I., Galle, P. R. & Lang, H. Multidisciplinary management of gastric and gastroesophageal cancers. *World J Gastroenterol.* **14**, 3773-3780 (2008).

149. Denzer, U. *et al.* Minilaparoscopy in the diagnosis of peritoneal tumor spread: prospective controlled comparison with computed tomography. *Surg Endosc.* **18**, 1067-1070 (2004).

150. Dehdashti, F. & Siegel, B. A. Neoplasms of the esophagus and stomach. *Semin Nucl Med* **34**, 198-208 (2004).

151. Fitzgerald, R. C. Review article: Barrett's oesophagus and associated adenocarcinoma--a UK perspective. *Aliment. Pharmacol. Ther.* **20 Suppl 8**, 45-49 (2004).

152. Weber, W. A. & Ott, K. Imaging of esophageal and gastric cancer. *Semin. Oncol.* **31**, 530-541 (2004).

153. Hambraeus, G. M. *et al.* Prognostic factors influencing survival in combined radiotherapy and surgery of squamous cell carcinoma of the esophagus with special reference to a histopathologic grading system. *Cancer* **62**, 895-904 (1988).

154. Lewinski, T., Morysinski, T., Pietrow, D. & Sikora, K. Preoperative radiotherapy combined with resection of squamous cell carcinoma of the mid-thoracic oesophagus. Does a histopathological malignancy grading system assess actual survival? *Eur. J Surg Oncol* **17**, 571-574 (1991).

155. Siewert, J. R. *et al.* Gastric Cancer. *Curr. Probl. Surg* **34**, 835-939 (1997).

156. Schuhmacher, C. P. *et al.* Neoadjuvant therapy for patients with locally advanced gastric carcinoma with etoposide, doxorubicin, and cisplatinum. Closing results after 5 years of follow-up. *Cancer* **91**, 918-927 (2001).

157. Tytgat, G. N. *et al.* Cancer of the esophagus and gastric cardia: recent advances. *Dis. Esophagus.* **17**, 10-26 (2004).

158. Sato, T. & Lizuka, T. *Color Atlas of Surgical Anatomy for Esophageal Cancer*. Springer-Verlag, Tokyo (1992).

159. Akiyama, H., Tsurumaru, M., Udagawa, H. & Kajiyama, Y. Radical lymph node dissection for cancer of the thoracic esophagus. *Ann. Surg* **220**, 364-372 (1994).

160. Millikan, K. W. *et al.* A 15-year review of esophagectomy for carcinoma of the esophagus and cardia. *Arch. Surg.* **130**, 617-624 (1995).

161. Hulscher, J. B. *et al.* Extended transthoracic resection compared with limited transhiatal resection for adenocarcinoma of the esophagus. *N. Engl. J. Med.* **347**, 1662-1669 (2002).

162. Lerut, T. *et al.* Extended surgery for cancer of the esophagus and gastroesophageal junction. *Journal of Surgical Research* **117**, 58-63 (2004).

163. Doran, S. T. *et al.* Pathology of Barrett's esophagus by proton magnetic resonance spectroscopy and a statistical classification strategy. *Am. J. Surg.* **185**, 232-238 (2003).

164. Spechler, S. J. Barrett's Oesophagus. *Semin Gastroeintest Dis* **7**, 51-60 (1996).

165. Waters, M. D., Selkirk, J. K. & Olden, K. The impact of new technologies on human population studies. *Mutat. Res.* **544**, 349-360 (2003).

166. Lenz, E. M., Bright, J., Wilson, I. D., Morgan, S. R. & Nash, A. F. A 1H NMR-based metabonomic study of urine and plasma samples obtained from healthy human subjects. *J. Pharm. Biomed. Anal.* **33**, 1103-1115 (2003).

167. Bell, J. D., Bhakoo, K. K. Metabolic changes underlying 31P MR spectral alterations in human hepatic tumours. *NMR Biomed.* **11(7)**, 354-9 (1998).

168. Odunsi, K. *et al.* Detection of epithelial ovarian cancer using 1H-NMR-based metabonomics. *Int. J. Cancer* **113**, 782-788 (2005).

169. de Certaines, J. D. Is biomedical nuclear magnetic resonance limited by a revisitable paradigm in physics? *Cell Mol. Biol. (Noisy. -le-grand)* **51**, 655-661 (2005).

170. Claridge, T. D. W. *High-Resolution NMR Techniques in Organic Chemistry*. Elsevier Ltd., Oxford (1999).

171. Martino, R., Bernadou, J., Malet-Martino, M. C., Roche, H. & Armand, J. P. Excretion of doxifluridine catabolites in human bile assessed by 19F NMR spectrometry. *Biomed. Pharmacother.* **41**, 104-106 (1987).

172. Nicholson, J. K., Higham, D. P., Timbrell, J. A. & Sadler, P. J. Quantitative high resolution 1H NMR urinalysis studies on the biochemical effects of cadmium in the rat. *Mol. Pharmacol.* **36**, 398-404 (1989).

173. Ellul, J. P., Murphy, G. M., Parkes, H. G., Slapa, R. Z. & Dowling, R. H. Nuclear magnetic resonance spectroscopy to determine the micellar cholesterol in human bile. *FEBS Lett.* **300**, 30-32 (1992).

174. Anthony, M. L., Gartland, K. P., Beddell, C. R., Lindon, J. C. & Nicholson, J. K. Cephaloridine-induced nephrotoxicity in the Fischer 344 rat: proton NMR spectroscopic studies of urine and plasma in relation to conventional clinical

chemical and histopathological assessments of nephronal damage. *Arch. Toxicol.* **66**, 525-537 (1992).

175. Koschorek, F. *et al.* High-resolution 1H NMR spectroscopy of cerebrospinal fluid in spinal diseases. *Neurosurg. Rev.* **16**, 307-315 (1993).

176. Husted, C., Montez, B., Le, C., Moscarello, M. A. & Oldfield, E. Carbon-13 "magic-angle" sample-spinning nuclear magnetic resonance studies of human myelin, and model membrane systems. *Magn Reson. Med.* **29**, 168-178 (1993).

177. Nicholson, J. K., Foxall, P. J., Spraul, M., Farrant, R. D. & Lindon, J. C. 750 MHz 1H and 1H-13C NMR spectroscopy of human blood plasma. *Anal. Chem.* **67**, 793-811 (1995).

178. Cheng, L. L. *et al.* Enhanced resolution of proton NMR spectra of malignant lymph nodes using magic-angle spinning. *Magn Reson. Med.* **36**, 653-658 (1996).

179. Holmes, E. *et al.* 750 MHz 1H NMR spectroscopy characterisation of the complex metabolic pattern of urine from patients with inborn errors of metabolism: 2-hydroxyglutaric aciduria and maple syrup urine disease. *J. Pharm. Biomed. Anal.* **15**, 1647-1659 (1997).

180. Liu, M., Nicholson, J. K., Parkinson, J. A. & Lindon, J. C. Measurement of biomolecular diffusion coefficients in blood plasma using two-dimensional 1H-1H diffusion-edited total-correlation NMR spectroscopy. *Anal. Chem.* **69**, 1504-1509 (1997).

181. Nicholls, A. W. *et al.* NMR spectroscopic studies on the metabolism and futile deacetylation of phenacetin in the rat. *Xenobiotica* **27**, 1175-1186 (1997).

182. Traikia, M., Langlais, D. B., Cannarozzi, G. M. & Devaux, P. F. High-resolution spectra of liposomes using MAS NMR. The case of intermediate-size vesicles. *J. Magn Reson.* **125**, 140-144 (1997).

183. Humpfer, E., Spraul, M., Nicholls, A. W., Nicholson, J. K. & Lindon, J. C. Direct observation of resolved intracellular and extracellular water signals in intact human red blood cells using 1H MAS NMR spectroscopy. *Magn Reson. Med.* **38**, 334-336 (1997).

184. Moka, D. *et al.* Biochemical classification of kidney carcinoma biopsy samples using magic-angle-spinning 1H nuclear magnetic resonance spectroscopy. *J. Pharm. Biomed. Anal.* **17**, 125-132 (1998).

185. Cheng, L. L. *et al.* Quantitative neuropathology by high resolution magic angle spinning proton magnetic resonance spectroscopy. *Proc. Natl. Acad. Sci. U. S. A* **94**, 6408-6413 (1997).

186. Beckwith-Hall, B. M. *et al.* Nuclear magnetic resonance spectroscopic and principal components analysis investigations into biochemical effects of three model hepatotoxins. *Chem. Res. Toxicol.* **11**, 260-272 (1998).

187. Tomlins, A. M. *et al.* High resolution 1H NMR spectroscopic studies on dynamic biochemical processes in incubated human seminal fluid samples. *Biochim. Biophys. Acta* **1379**, 367-380 (1998).

188. Guo, W., Morrisett, J. D., Lawrie, G. M., DeBakey, M. E. & Hamilton, J. A. Identification of different lipid phases and calcium phosphate deposits in human carotid artery plaques by MAS NMR spectroscopy. *Magn Reson. Med.* **39**, 184-189 (1998).

189. Tomlins, A. M. *et al.* High-resolution magic-angle spinning ^{1}H nuclear magnetic resonance analysis of intact prostatic hyperplastic and tumour tissues. *Analytical Communications* **35**, 113-115 (1998).

190. Cheng, L. L., Chang, I. W., Smith, B. L. & Gonzalez, R. G. Evaluating human breast ductal carcinomas with high-resolution magic-angle spinning proton magnetic resonance spectroscopy. *J. Magn Reson.* **135**, 194-202 (1998).

191. Meshitsuka, S. *et al.* Nuclear magnetic resonance studies of synovial fluids from patients with rheumatoid arthritis and osteoarthritis. *Clin. Chim. Acta* **281**, 163-167 (1999).

192. Tkadlecova, M., Havelcek, J., Volka, K., Soucek, P. & Karel, I. Study of aqueous humour by ^{1}H NMR spectroscopy. *Journal of Molecular Structure* **480**, 601-605 (1999).

193. Millis, K. *et al.* Classification of human liposarcoma and lipoma using ex vivo proton NMR spectroscopy. *Magn Reson. Med.* **41**, 257-267 (1999).

194. Garrod, S. *et al.* High-resolution magic angle spinning 1H NMR spectroscopic studies on intact rat renal cortex and medulla. *Magn Reson. Med.* **41**, 1108-1118 (1999).

195. Griffin, J. L. *et al.* The initial pathogenesis of cadmium induced renal toxicity. *FEBS Lett.* **478**, 147-150 (2000).

196. Sitter, B. *et al.* Cervical cancer tissue characterized by high-resolution magic angle spinning MR spectroscopy. *MAGMA.* **16**, 174-181 (2004).

197. Mun, C. W. *et al.* Ex vivo proton MR spectroscopy (1H-MRS) for evaluation of human gastric carcinoma. *Magn Reson. Imaging* **22**, 861-870 (2004).

198. Bourne, R. M. *et al. In vivo* and *ex vivo* proton MR spectroscopy of primary and secondary melanoma. *Eur. J. Radiol.* **53**, 506-513 (2005).

199. Holmes, E. *et al.* Metabolic Profiling of CSF: Evidence That Early Intervention May Impact on Disease Progression and Outcome in Schizophrenia. *PLoS. Med.* **3**, (2006).

200. Bala, L. *et al.* Malabsorption syndrome with and without small intestinal bacterial overgrowth: a study on upper-gut aspirate using 1H NMR spectroscopy. *Magn Reson. Med.* **56**, 738-744 (2006).

201. Fang, F. *et al.* Discrimination of metabolic profiles of pancreatic cancer from chronic pancreatitis by high-resolution magic angle spinning 1H nuclear magnetic resonance and principal components analysis. *Cancer Sci.* **98**, 1678-1682 (2007).

202. Tessem, M. B. *et al.* Evaluation of lactate and alanine as metabolic biomarkers of prostate cancer using 1H HR-MAS spectroscopy of biopsy tissues. *Magn Reson. Med* **60**, 510-516 (2008).

203. Jordan, K. W. *et al.* Metabolomic characterization of human rectal adenocarcinoma with intact tissue magnetic resonance spectroscopy. *Dis. Colon Rectum* **52**, 520-525 (2009).

204. Bollard, M. E. *et al.* NMR-based metabolic profiling identifies biomarkers of liver regeneration following partial hepatectomy in the rat. *J Proteome. Res.* (2009).

205. Smith, L. M. *et al.* Large-scale human metabolic phenotyping and molecular epidemiological studies via 1H NMR spectroscopy of urine: investigation of borate preservation. *Anal. Chem.* **81**, 4847-4856 (2009).

206. Delikatny, E. J. *et al.* Proton MR and human cervical neoplasia: ex vivo spectroscopy allows distinction of invasive carcinoma of the cervix from carcinoma *in situ* and other preinvasive lesions. *Radiology* **188**, 791-796 (1993).

207. Russell, P. *et al.* Proton magnetic resonance and human thyroid neoplasia. I: Discrimination between benign and malignant neoplasms. *Am. J. Med.* **96**, 383-388 (1994).

208. Lean, C. L. *et al.* Diagnosis of follicular thyroid lesions by proton magnetic resonance on fine needle biopsy. *J. Clin. Endocrinol. Metab* **80**, 1306-1311 (1995).

209. Sharaf, M. A., Illman, D. L. & Kowalski, B. R. *Chemometrics*. (Chichester:J. Wiley and Sons), (1986).

210. Lindon, J. C., Holmes, E. & Nicholson, J. K. Pattern recognition methods and applications in biomedical magnetic resonance. *Progress in NMR Spectroscopy* **39**, 1-40 (2001).

211. Holmes, E. *et al.* Development of a model for classification of toxin-induced lesions using 1H NMR spectroscopy of urine combined with pattern recognition. *NMR Biomed.* **11**, 235-244 (1998).

212. Brown, T. R. & Stoyanova, R. NMR spectral quantitation by principal-component analysis. II. Determination of frequency and phase shifts. *J. Magn Reson. B* **112**, 32-43 (1996).

213. Pearson, K. On lines and planes of closest fit to systems of points in space. *Philosophical Magazine* **2**, 559-572 (1901).

214. Hotelling, H. Analysis of a complex of statistical variables into principal components. *Journal of Educational Psychology* **24**, 417-441 (1933).

215. Lindon, J. C., Holmes, E. & Nicholson, J. K. So what's the deal with metabonomics? *Anal. Chem.* **75**, 384A-391A (2003).

216. Dieterle, F., Ross, A., Schlotterbeck, G. & Senn, H. Probabilistic quotient normalization as robust method to account for dilution of complex biological mixtures. Application in 1H NMR metabonomics. *Anal. Chem.* **78**, 4281-4290 (2006).

217. Kelsen, D. P. *et al.* Chemotherapy followed by surgery compared with surgery alone for localized esophageal cancer. *N. Engl. J Med* **339**, 1979-1984 (1998).

218. Mesonero, J., Matosin, M., Cambier, D., Rodriguez-Yoldi, M. J. & Brot-Laroche, E. Sugar-dependent expression of the fructose transporter GLUT5 in Caco-2 cells. *Biochem. J* **312 (Pt 3)**, 757-762 (1995).

219. Yamamoto, T. *et al.* Over-expression of facilitative glucose transporter genes in human cancer. *Biochem. Biophys. Res. Commun.* **170**, 223-230 (1990).

220. Nishioka, T. *et al.* Distribution of the glucose transporters in human brain tumors. *Cancer Res.* **52**, 3972-3979 (1992).

221. Younes, M., Brown, R. W., Stephenson, M., Gondo, M. & Cagle, P. T. Overexpression of Glut1 and Glut3 in stage I nonsmall cell lung carcinoma is associated with poor survival. *Cancer* **80**, 1046-1051 (1997).

222. Mellanen, P., Minn, H., Grenman, R. & Harkonen, P. Expression of glucose transporters in head-and-neck tumors. *Int. J Cancer* **56**, 622-629 (1994).

223. Nagase, Y. *et al.* Immunohistochemical localization of glucose transporters in human renal cell carcinoma. *J Urol.* **153**, 798-801 (1995).

224. Boden, G., Murer, E. & Mozzoli, M. Glucose transporter proteins in human insulinoma. *Ann. Intern. Med* **121**, 109-112 (1994).

225. Haber, R. S., Weiser, K. R., Pritsker, A., Reder, I. & Burstein, D. E. GLUT1 glucose transporter expression in benign and malignant thyroid nodules. *Thyroid* **7**, 363-367 (1997).

226. Brown, R. S. & Wahl, R. L. Overexpression of Glut-1 glucose transporter in human breast cancer. An immunohistochemical study. *Cancer* **72**, 2979-2985 (1993).

227. Zamora-Leon, S. P. *et al.* Expression of the fructose transporter GLUT5 in human breast cancer. *Proc. Natl. Acad. Sci. U. S. A* **93**, 1847-1852 (1996).

228. Reisser, C., Eichhorn, K., Herold-Mende, C., Born, A. I. & Bannasch, P. Expression of facilitative glucose transport proteins during development of squamous cell carcinomas of the head and neck. *Int. J Cancer* **80**, 194-198 (1999).

229. Miller, J. H., Mullin, J. M., McAvoy, E. & Kleinzeller, A. Polarity of transport of 2-deoxy-D-glucose and D-glucose by cultured renal epithelia (LLC-PK1). *Biochim. Biophys. Acta* **1110**, 209-217 (1992).

230. Hwang, Y. Y., Kim, S. G., Evelhoch, J. L. & Ackerman, J. J. Nonglycolytic acidification of murine radiation-induced fibrosarcoma 1 tumor via 3-O-methyl-D-glucose monitored by 1H, 2H, 13C, and 31P nuclear magnetic resonance spectroscopy. *Cancer Res.* **52**, 1259-1266 (1992).

231. Glunde, K., Jie, C. & Bhujwalla, Z. M. Molecular causes of the aberrant choline phospholipid metabolism in breast cancer. *Cancer Res.* **64**, 4270-4276 (2004).

232. Galipeau, P. C., Prevo, L. J., Sanchez, C. A., Longton, G. M. & Reid, B. J. Clonal expansion and loss of heterozygosity at chromosomes 9p and 17p in premalignant esophageal (Barrett's) tissue. *J Natl. Cancer Inst.* **91**, 2087-2095 (1999).

233. Mazurek, S. & Eigenbrodt, E. The tumor metabolome. *Anticancer Res.* **23**, 1149-1154 (2003).

234. Ferlito, A. *et al.* "Skip metastases" from head and neck cancers. *Acta Otolaryngol.* **122**, 788-791 (2002).

235. Cheng, L. L. *et al.* Metabolic characterization of human prostate cancer with tissue magnetic resonance spectroscopy. *Cancer Res.* **65**, 3030-3034 (2005).

236. Lerut, T. *et al.* Three-field lymphadenectomy for carcinoma of the esophagus and gastroesophageal junction in 174 R0 resections: impact on staging, disease-free survival, and outcome: a plea for adaptation of TNM classification in upper-half esophageal carcinoma. *Ann. Surg* **240**, 962-972 (2004).

237. Falk, G. W., Rice, T. W., Goldblum, J. R. & Richter, J. E. Jumbo biopsy forceps protocol still misses unsuspected cancer in Barrett's esophagus with high-grade dysplasia. *Gastrointest. Endosc.* **49**, 170-176 (1999).

238. Sampliner, R. E. Updated guidelines for the diagnosis, surveillance, and therapy of Barrett's esophagus. *Am. J Gastroenterol.* **97**, 1888-1895 (2002).

239. Lovat, L. B. *et al.* Elastic scattering spectroscopy accurately detects high grade dysplasia and cancer in Barrett's oesophagus. *Gut* **55**, 1078-1083 (2006).

240. Cox, I. J., Sharif, A., Cobbold, J. F., Thomas, H. C., Taylor-Robinson, S. D. Current and future applications of in vitro magnetic resonance spectroscopy in hepatobiliary disease. *World J Gastroenterol.* **12(30)**, 4773-83 (2006).

8. APPENDIX 1.

Appendix 1. Letters and forms relevant to establishment of tissue bank

1. Establishment of tissue bank ethics approval letter

NHS

St Mary's Research Ethics Committee
Internal Mail Box 121
St Marys Hospital
Paddington
London
W2 1NY

Telephone: 020 7886 6514
Facsimile: 020 7886 1529

05 December 2005

Mr George B Hanna
Senior Lecturer & Honorary Upper GI Consultant Surgeon
Imperial College London
Department of Surgical Oncology & Technology
10th Floor, QEQM Wing, St Mary's Hospital
South Wharf Road, London
W2 1NY

Dear Mr Hanna

Full title of study: **Establishment of a Tissue Bank for Oesophageal and Gastric Cancer**
REC reference number: **04/Q0403/119**

The REC gave a favourable ethical opinion to this study on 31 March 2005.

Further notification(s) have been received from local site assessor(s) following site-specific assessment. On behalf of the Committee, I am pleased to confirm the extension of the favourable opinion to the new site(s). I attach an updated version of the site approval form, listing all sites with a favourable ethical opinion to conduct the research.

Research governance approval

The Chief Investigator or sponsor should inform the local Principal Investigator at each site of the favourable opinion by sending a copy of this letter and the attached form. The research should not commence at any NHS site until research governance approval from the relevant NHS care organisation has been confirmed.

Statement of compliance

The Committee is constituted in accordance with the Governance Arrangements for Research Ethics Committees (July 2001) and complies fully with the Standard Operating Procedures for Research Ethics Committees in the UK.

04/Q0403/119	Please quote this number on all correspondence

Yours sincerely

Mrs Rosalind Cooke
Committee Co-ordinator

An advisory committee to North West London Strategic Health Authority

2. Research and Development approval letter

St Mary's NHS
NHS Trust

St Mary's NHS Trust
Research & Development Office
Mailbox 121
St Mary's Hospital
Praed St
London
W2 1NY
Tel: 020 7886 7952/1330
Fax: 020 7886 1529

03 August 2005

Dear Mr Hanna

Project Title:

Establishment of Imperial College – St Mary's Hospital Upper Gastrointestinal Tissue Bank.

Project R&D Number: **04/BH/0014E** Project Ethics Number: **04/Q0403/119E**

Project Investigators: Mr G Hanna, Dr Marjorie Walker

I confirm that this project has now been approved by the Research & Development Department. The project may now start at St Mary's site.

Before you commence your research, please note that you must be aware of your obligations to comply with the minimum requirements for compliance with the Research Governance Indicators 17 (Data Protection); 25 (Health & Safety) and 22 (Financial Probity). Details of the requirements to be met can be found at the Trust Research Governance Implementation Plan Annex J1/J2 in the R&D Annual Report 2002–2003, R&D Management Office (ext 7952), or on the Trust Intranet under Research & Development.

Under Research Governance regulations patient consent forms for all recruited patients on the study and Serious Adverse event reports must be forwarded to the Research & Development Office.

I wish you well in your research, and look forward to seeing regular annual progress reports, and funding details, as well as information about any publications resulting from the study.

Yours sincerely

Professor Sebastian Johnston
Director of Research & Development
St Mary's NHS Trust

3. Patient information sheet

Division of Surgery, Anaesthetics & Intensive care
Department of Surgical Oncology and Technology
Imperial College London
10th Floor, QEQM Building
St Mary's Hospital
Praed Street, London W2 1NY
Tel: +44(0)20 7886 2125
Fax: +44(0)20 7413 0470

Mr George Hanna PhD, FRCS
Senior Lecturer and Consultant Surgeon
g.hanna@imperial.ac.uk
www.imperial.ac.uk

TISSUE BANK PATIENT INFORMATION LEAFLET

Academic Surgical Unit - St Mary's Hospital
Upper Gastro-Intestinal Tissue Bank
REC Ref. no. 04/Q0403/119

Department of Surgical Oncology and Technology
Mr George Hanna PhD, FRCS
Senior Lecturer/Consultant Upper GI Surgeon and named custodian of the tissue bank

Date: / /

Dear Sir/Madam

You are being invited to take part in the tissue bank project. Before you decide it is important for you to understand why the tissue bank is being established and what it will involve. Please take time to read the following information carefully and discuss it with others if you wish. Ask us if there is anything that is not clear or if you would like more information. Take time to decide whether or not you wish to take part. Thank you for reading this information sheet.

What is a tissue bank?

A tissue bank is a collection of tissue samples being stored long term that will be used to assist in future research into a specific disease or group of diseases or investigate disease processes and their treatment. Tissue banks are a valuable research resource and are increasingly being established at local, regional and national level.

What will the tissues in the tissue bank be used for?

The tissues will be used to help our understanding of Oesophageal and Gastric cancer. We will be looking at how tumours grow, why some tumours spread and trying to find new treatments for these types of cancer.

Tissue and blood samples might be used for DNA and/or protein analysis or other molecular biology studies in a way to identify mechanisms of development of this disease as well as effect of different treatments on the course of these tumours.

Tissues may also be used in unforeseen research projects in the future. None of these will allow linking of the specimens for identification of patients they were taken from.

Why have I been chosen?

You have been chosen because you are undergoing treatment of oesophageal or gastric cancer.

Do I have to take part?

Taking part in the research is entirely voluntary. It is up to you to decide whether or not to take part. If you do decide to take part you will be given this information sheet to keep and be asked to sign a consent form. If you decide to take part you are still free to withdraw at any time and without giving a reason. A decision to withdraw at any time, or a decision not to take part, will not affect the standard of care you receive.

What do I have to do?

Nothing, except to approve of giving your tissues to be stored in the tissue bank, and to keep a copy of your hospital records containing details of your blood tests results, radiography reports and other documents explaining your condition.

How much of my tissues will be taken?

Before your operation a blood sample among the samples taken for your routine assessment will be taken. Also any tissue biopsies taken in the course of diagnosis of your disease will be taken. During the course of your operation the

tumour and tumour related tissue removed, will be conserved in the tissue bank. No additional tissue will be taken beyond that clinically needed. These tissues are to be used in future research.

After your operation another blood sample will be taken again among the samples taken for your routine assessment will be taken.

What will happen to the tissues?

Tissues will be preserved in the tissue bank for an indefinite period of time. The specimens will remain the property of the Academic Surgical Unit - St Mary's Hospital Upper Gastro-Intestinal Tissue Bank. The principal investigator Mr GB Hanna is the named custodian of all tissue specimens. Sections of the specimens may be used for future research purposes.

Will I be contacted again in the future?

You need to indicate in the consent form whether or not you would like to be contacted should the result of any research carried out on your tissue yield new findings that may have an impact on your care; This information can be discussed with you either by your hospital Consultant or General Practitioner. The, information about your tissues will be available for you at any time through contacting the Tissue Bank Custodian, Mr Hanna.

What if something goes wrong?

We do not believe you will be harmed by donating tissue to the Academic Surgical Unit – St Mary's Hospital Upper Gastro-Intestinal Tissue Bank. There is no additional intervention or change in your treatment plan implemented if you choose to participate.

If you wish to complain, or have any concerns about any aspect of the way you have been approached or treated during the course of this study, the normal National Health Service complaints mechanisms should be available to you.

Who will have access to my tissue and how will confidentiality be maintained?

Access to your tissue samples will be only available through the *Academic Surgical Unit – St Mary's Hospital Upper Gastro-Intestinal Tissue Bank*, controlled by *Imperial College London*. The named custodian is Mr George Hanna will hold responsibility of storage and management of your tissue samples as well as your records.

Researchers under Mr George Hanna's direct supervision or after his approval may also have access to the tissue samples.

The handling of your tissue samples will be treated with the usual degree of confidentiality under the data protection act. All samples will be coded and pseudonomised before transfer to other research partners - you will not be identified in any way from your tissue sample.

He will be responsible for keeping proper records of all uses that have been made of the material, whether by himself or by others. Users of pseudonomised samples will be required undertake not to attempt to identify individual research participants. Where linked pseudonomised samples are provided to a third party, the custodian. The stored data will not be linked with you. It will be coded. Nevertheless, you or your legal representative can gain access to these information through writing to Mr Hanna, the named custodian of the Tissue Bank and guardian of the codes, who will break the code and present the information, if so required.

The custodian will be formally responsible for the safe keeping, control of use and disposal of tissue samples in accordance with the consent you give. He will be officially responsible to ensure that procedures and security arrangements are sufficient to prevent breaches of confidentiality. Data that has not been pseudonomised will not be transferred without informed consent from you or from your next of kin or legal representative in case you cannot consent.

All future research projects which wish to use tissue from the tissue bank will need the approval of an NHS Research Ethics Committee. Copies of such approvals will be kept and archived for reference.

All research that involves NHS patients or staff, information from NHS medical records or uses NHS patients or staff, information from NHS medical records or uses NHS premises or facilities must be approved by an NHS Research Ethics Committee before it goes ahead. Approval does not guarantee that you will not come to any harm if you take part. However, approval means that the Committee is satisfied that your rights will be respected, that any risks have been reduced to a minimum and balanced against possible benefits and that you have been given sufficient information on which to make an informed decision to take part or not.

Will I receive payment for the tissue that I donate to the tissue bank?

You will not receive any payment for the tissue. The tissue is a gift - neither you nor your relatives will benefit from any inventions that result from the use of the tissue.

What happens if I wish to have my tissue removed from the tissue bank?

If you no longer wish your tissues to be held in the tissue bank you may withdraw them at any time, without justifying your decision and your future treatment will not be affected in any way.

If you wish to have your tissue removed from the tissue bank please contact Mr George Hanna for suitable arrangements.

Who is organising and funding body of the tissue bank?

The Academic Surgical Unit, St Mary's hospital, Praed street, London W2 1NY

Who has reviewed the establishment of the bank?

The St Mary's Hospital Local Research Ethics Committee.

Thank you for reading this information leaflet.

Correspondence for further information:

Mr George B Hanna

Senior Lecturer/Consultant Upper GI Surgeon
Academic Surgical Unit
10th Floor, QEQM Building
St Mary's Hospital
Praed street,
London W2 1NY
Tel: 0207 886 2124
Fax: 0207 886 1810
E-mail: g.hanna@imperial.ac.uk

4. Consent form

Imperial College London

Division of Surgery, Anaesthetics & Intensive care
Department of Surgical Oncology and Technology
Imperial College London
10th Floor, QEQM Building
St Mary's Hospital
Praed Street, London W2 1NY
Tel: +44(0)20 7886 2125
Fax: +44(0)20 7413 0470

Mr George Hanna PhD, FRCS
Senior Lecturer and Consultant Surgeon
g.hanna@imperial.ac.uk
www.imperial.ac.uk

TISSUE BANK CONSENT FORM

Patient name, address, DOB *(or ID label)*

Title of Tissue Bank:
Academic Surgical Unit – St Mary's Hospital Upper Gastro-Intestinal Tissue Bank
REC Ref. no. 04/Q0403/119

Principal Investigator and named Custodian of Tissue Bank:
Mr George Hanna PhD, FRCS
Senior Lecturer/Consultant Upper GI Surgeon

Please initial boxes as applicable

I confirm that I have read and understand the information leaflet sheet dated ...../...../..... for the above Tissue Bank and have had the opportunity to ask questions. ☐

I understand that I may withdraw my consent to my tissue being included in the tissue bank at any time without justifying my decision and without affecting my normal care and medical management. ☐

I agree to donate the tissue samples as detailed below and allow their use in medical research as described in the Patient Information Leaflet. ☐

I understand that sections of any of my medical notes may be looked at by responsible individuals from the research team, or from regulatory authorities where it is relevant to my taking part in research. I give permission for these individuals to have access to my records. ☐

I do /do not give consent to the use of my tissue in future research projects if an unanticipated use emerges in the future, which is not described in this information leaflet *(delete as applicable)* ☐

I understand that tissue samples will not be used to undertake any genetic tests whose results may have adverse consequences on my or my families insurance or employment. ☐

I agree / do not agree to my tissue samples being used to undertake genetic research *(delete as applicable)* ☐

I understand that if research using my tissues produces information, which has immediate clinical relevance to me, I would/ would not like to be informed by my hospital consultant or GP and be given an opportunity to discuss the results. I realise that these information will be readily available to me upon requesting it from the Tissue bank Custodian. *(delete as applicable)* ☐

I understand that the tissue is a gift and that I will not benefit from any intellectual property that results from the use of the tissue. ☐

The samples which I hereby consent to donate are: ☐

. Pre and postoperative blood samples. ☐
. Preoperative tissue biopsy samples produced along the course of my assessment and diagnosis plan. ☐
. Intra-operatively removed surgical specimen containing tumour or tumour invaded tissues e.g. lymphatics, lymph nodes and metastases…etc.which are removed as a part of the surgical operation planned for my treatment. ☐

_____	_____	_____
Name of Patient	DateSignature	
_____	_____	_____
Name of Parent/guardian/ legal representative ***(If applicable)***	DateSignature	
_____	_____	_____
Researcher	Date	Signature

Original for researcher / tissue bank, 1 copy for patient, 1 copy for hospital notes

5. Tissue information form

Imperial College London

Division of Surgery, Anaesthetics & Intensive care
Department of Surgical Oncology and Technology
Imperial College London
10th Floor, QEQM Building
St Mary's Hospital
Praed Street, London W2 1NY
Tel: +44(0)20 7886 2125
Fax: +44(0)20 7413 0470

Academic Surgical Unit – St Mary's Hospital Upper Gastro-Intestinal Tissue Bank

REC Ref. no. 04/Q0403/119

Named Custodian: Mr GB Hanna PhD FRCS

Tissue information form

Patient details:

Patient name, address, DOB *(or ID label)*

Centre name: Date:
Patient Number: Diagnosis:
Tissue bank code: Pathology request number:

Specimen details:

Serial no.	Type	Time to freezing (min)	Amount in stock
1			
2			
3			
4			
5			
6			
7			
8			

Time tissue rendered ischemic (roughly): Time of excision:
Time of start cutting up: Time freezing completed:
Method of freezing: Isopentane LN2
Method of transport to tissue bank:
Time of transport to tissue bank after freezing:

---------- - ---------- ----------
Researcher name Date Signature

9. APPENDIX 2.

Appendix 2. Letters and forms relevant to conduct of metabonomic analysis

1. Ethical approval letter

Brompton, Harefield & NHLI Ethics Committee NHS
Royal Brompton Hospital
Sydney Street
LONDON SW3 6NP

Telephone: 020 7351 8437
Facsimile:

18 October 2005

Mr George Hanna
Reader/Consultant Upper GI Surgeon
Imperial College London
Department of Biosurgery and Surgical Technology,10th Floor,QEQM Wing
St Mary's Hospital
Praed Street
W2 1NY

Dear Mr Hanna

Full title of study: **Metabonomic profiling of Gastric and Oesophageal Cancer, potentials in diagnosis and follow up**
REC reference number: **05/Q0404/73**

The REC gave a favourable ethical opinion to this study on 17 August 2005.

Further notification has been received from local site assessors following site-specific assessment. On behalf of the Committee, I am pleased to confirm the extension of the favourable opinion to the new site. I attach an updated version of the site approval form, listing all sites with a favourable ethical opinion to conduct the research.

Research governance approval

The Chief Investigator or sponsor should inform the local Principal Investigator at each site of the favourable opinion by sending a copy of this letter and the attached form. The research should not commence at any NHS site until research governance approval from the relevant NHS care organisation has been confirmed.

Statement of compliance

The Committee is constituted in accordance with the Governance Arrangements for Research Ethics Committees (July 2001) and complies fully with the Standard Operating Procedures for Research Ethics Committees in the UK.

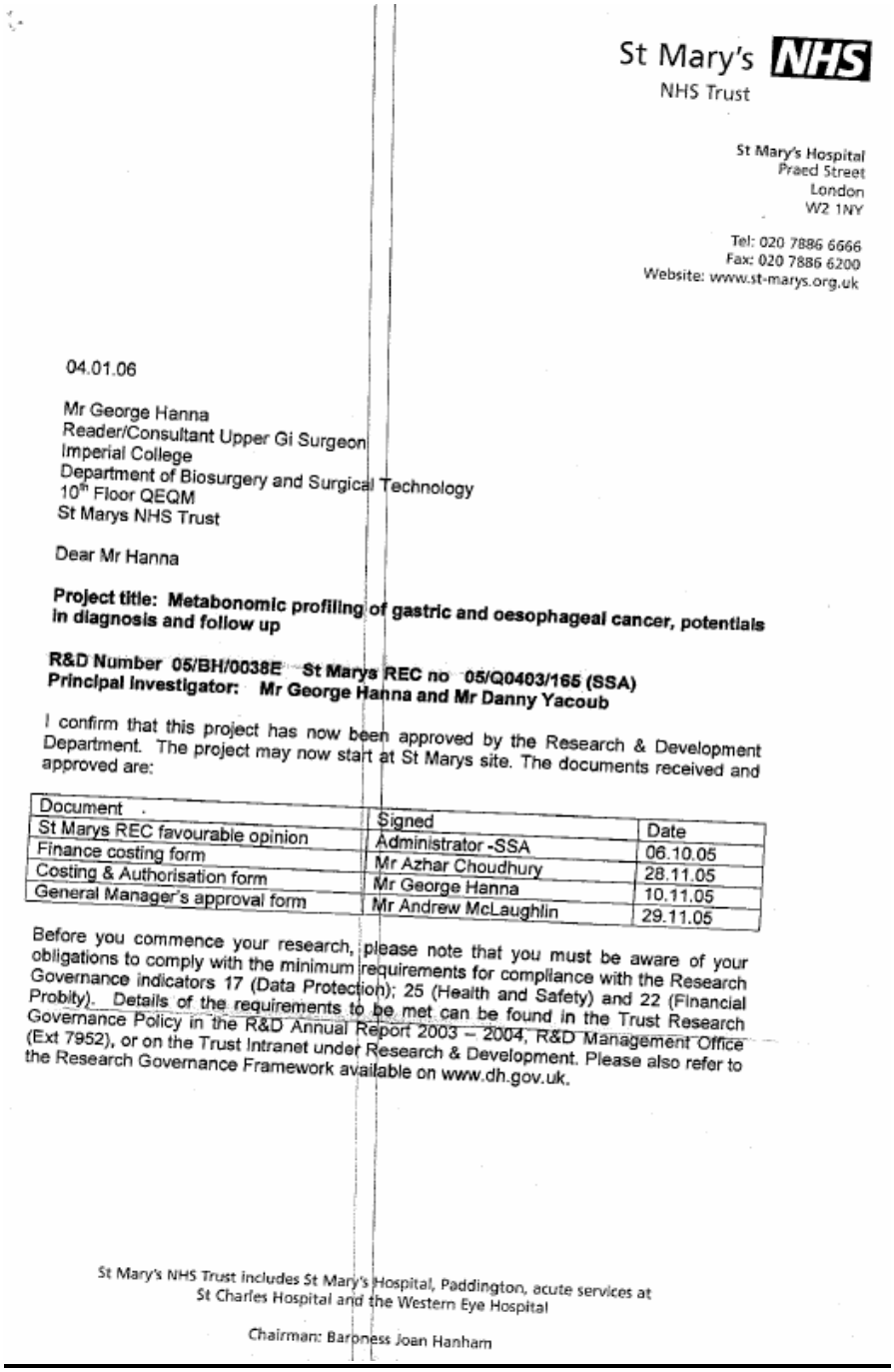
05/Q0404/73	**Please quote this number on all correspondence**

Yours sincerely

Irene Gordon

Irene Gordon
Assistant Committee Co-ordinator

2. Research and Development approval letter



St Mary's NHS
NHS Trust

St Mary's Hospital
Praed Street
London
W2 1NY

Tel: 020 7886 6666
Fax: 020 7886 6200
Website: www.st-marys.org.uk

04.01.06

Mr George Hanna
Reader/Consultant Upper Gi Surgeon
Imperial College
Department of Biosurgery and Surgical Technology
10th Floor QEQM
St Marys NHS Trust

Dear Mr Hanna

Project title: Metabonomic profiling of gastric and oesophageal cancer, potentials in diagnosis and follow up

R&D Number 05/BH/0038E St Marys REC no 05/Q0403/165 (SSA)
Principal Investigator: Mr George Hanna and Mr Danny Yacoub

I confirm that this project has now been approved by the Research & Development Department. The project may now start at St Marys site. The documents received and approved are:

Document	Signed	Date
St Marys REC favourable opinion	Administrator -SSA	06.10.05
Finance costing form	Mr Azhar Choudhury	28.11.05
Costing & Authorisation form	Mr George Hanna	10.11.05
General Manager's approval form	Mr Andrew McLaughlin	29.11.05

Before you commence your research, please note that you must be aware of your obligations to comply with the minimum requirements for compliance with the Research Governance indicators 17 (Data Protection); 25 (Health and Safety) and 22 (Financial Probity). Details of the requirements to be met can be found in the Trust Research Governance Policy in the R&D Annual Report 2003 – 2004, R&D Management Office (Ext 7952), or on the Trust Intranet under Research & Development. Please also refer to the Research Governance Framework available on www.dh.gov.uk.

St Mary's NHS Trust includes St Mary's Hospital, Paddington, acute services at St Charles Hospital and the Western Eye Hospital

Chairman: Baroness Joan Hanham

3. Patient information sheet

Imperial College London

Division of Surgery, Anaesthetics & Intensive care
Department of Biosurgery and Surgical Technology
Imperial College London
10th Floor, QEQM Building
St Mary's Hospital
Praed Street, London W2 1NY
Tel: +44(0)20 7886 2125
Fax: +44(0)20 7413 0470

Mr George Hanna PhD, FRCS
Reader and Consultant Surgeon
g.hanna@imperial.ac.uk
www.imperial.ac.uk

PATIENT INFORMATION LEAFLET

Title of Project:
Metabonomic Profiling of Gastric and Oesophageal Cancer
REC Ref. 05/Q0404/73
Version: 2

Principal investigator:
Mr GB Hanna PhD FRCS MErgS
Reader and Consultant Upper GI Surgeon
Imperial College London, St Mary's Hospital, London.
Co-investigator:
Mr Danny Yakoub MSc MRCSEd
Clinical Research Fellow, Imperial College London

Date: / /
Dear Sir/Madam

You are being invited to take part in the Metabonomic Profiling of Gastric and Oesophageal Cancer project. Please take time to read the following information carefully and discuss it with others if you wish. Ask us if there is anything that is not clear or if you would like more information. Take time to decide whether or not you wish to take part. Thank you for reading this information sheet.

What are the details of the project?

The study involves collecting tissue, blood and urine samples to be analysed using special imaging techniques, in order to detect compounds specific to gastric and oesophageal cancer.

What will the tissues be used for?

The tissues will be used to help our understanding of oesophageal and gastric cancer. We will be looking at compounds released by tumours in order to understand how these tumours grow, why some tumours spread and trying to find new treatments for these types of cancer.

Why have I been chosen?
You have been chosen because you are undergoing treatment for oesophageal or gastric cancer.

Do I have to take part?
Taking part in the research is entirely voluntary. It is up to you to decide whether or not to take part. If you do decide to take part you will be given this information sheet to keep and be asked to sign a consent form. If you decide to take part you are still free to withdraw at any time and without giving a reason. A decision to withdraw at any time, or a decision not to take part, will not affect the standard of care you receive, now or in the future.

What do I have to do?
Nothing, except to agree to make a gift to us of specimens of tissue removed during your operation which would otherwise be destroyed, or tissue obtained during endoscopy, in addition to blood and urine samples. We also need your permission to keep a copy of your hospital records containing details of your blood tests results, radiography reports and other documents explaining your condition.

How much of my tissues will be taken?

Before your operation, blood and urine samples (15-20 mls, about the volume of 2 table spoons) will be taken along with your routine assessment samples. No extra needle pricks or vein punctures are required. Also part of tissue biopsied during endoscopy will be taken.

We will also take tumour sample and tissue around it (40-100 mg, about the size of a pea) removed in the surgical specimen and otherwise would have been destroyed. No additional tissue will be taken beyond that needed for your treatment. After your operation, blood and urine samples will be taken again along with the samples taken for your routine assessment.

What will happen to the tissues?

Tissues will first be preserved in the tissue bank. Then they will be processed and prepared for analysis through the use of a magnetic resonance device to define types and amounts of compounds within the tissues. After the completion

of the study, we would like to retain the blood/tissue samples for possible future research at a future date, when new tests/techniques may be available. We would not contact you again for further permission before doing this. If you agree to take part in this study, you will also be giving consent for possible future use of the sample; this is why we ask you to make a gift of them. Samples will remain the property of the Academic Surgical Unit - St Mary's Hospital Upper Gastro-Intestinal Tissue Bank.

Specimens that have not been used in the study or stored in the tissue bank will be decently disposed of in light of the provisions of the Human Tissue Act 2004, and through the regulations of the Human Tissue authority established in the Act to oversee such arrangements. No genetic, HIV, Hepatitis B or other communicable disease testing will be done on the specimens collected. The principal investigator Mr GB Hanna is the named custodian of all tissue specimens. Sections of the specimens may be used for future research purposes.

Will I be contacted again in the future?

You need to indicate in the consent form whether or not you would like to be contacted should the result of any research carried out on your tissue yield new findings that may have an impact on your care; This information can be discussed with you by your hospital Consultant. The, information about your tissues will be available for you at any time through contacting the Tissue Bank Custodian, Mr Hanna.

What if something goes wrong?

We do not believe you would be harmed by donating tissue to the study. There is no additional intervention or change in your treatment plan implemented if you choose to participate.
If you wish to complain, or have any concerns about any aspect of the way you have been approached or treated during the course of this study, the normal National Health Service complaints mechanisms would be available to you.

Who will have access to my tissue and how will confidentiality be maintained?

Tissues and samples will be stored in the Academic Surgical Unit – St Mary's Hospital Upper Gastro-Intestinal Tissue Bank and access to your tissue samples will be only available through it. The named custodian is Mr George Hanna, who is also the chief investigator in this study will hold responsibility of storage and management of your tissue samples as well as your records.

Researchers under Mr George Hanna's direct supervision or after his approval may also have access to the tissue samples.

The handling of your tissue samples will be treated with strict confidentiality under the Data Protection Act. All samples will be coded and pseudonymised before transfer to other research partners, so that you cannot be identified from your tissue sample.

The custodian will be responsible for keeping proper records of all uses that have been made of the material, whether by himself or by others. Users of pseudonymised samples will not attempt to identify individual research participants. The stored data will be coded. Nevertheless, you or your legal representative can access this information by writing to Mr Hanna, the custodian of the Tissue Bank and guardian of the codes, who will break the code and present the information if so required.

For tissues that has not been used in the study, and stored in the tissue bank, future research projects will need the approval of an NHS Research Ethics Committee. Copies of such approvals will be kept and archived for reference.

All research that involves NHS patients or staff, information from NHS medical records or uses NHS patients or staff, information from NHS medical records or uses NHS premises or facilities must be approved by an NHS Research Ethics Committee before it goes ahead. Approval does not guarantee that you will not come to any harm if you take part. However, approval means that the Committee is satisfied that your rights will be respected, that any risks have been reduced to a minimum and balanced against possible benefits and that you have been given sufficient information on which to make an informed decision to take part or not.

Will I receive payment for the tissue that I donate to the tissue bank or the study?

No, we shall treat your samples as a gift to the Imperial College Upper GI Cancer Tissue Bank at St Mary's Hospital, London, and you would thus relinquish any interest in it.

What happens if I wish to have my tissue removed from the tissue bank or the study?

If you no longer wish your tissues to be held in the tissue bank you may withdraw them at any time, without justifying your decision and your future treatment will not be affected in any way. If you wish to have your tissue removed from the tissue bank please contact Mr George Hanna for suitable arrangements.

Who is organising and funding body of the tissue bank and the study?

The Academic Surgical Unit, Imperial College London, St Mary's hospital, Praed street, London W2 1NY

Who has reviewed the establishment of the bank?

The St Mary's Hospital Local Research Ethics Committee.

Who has reviewed the ethical considerations of the study?

Brompton, Harefield and NHLI Local Research Ethics Committee

Thank you for reading this information leaflet.

Correspondence for further information:

Mr George B Hanna
Reader/Consultant Upper GI Surgeon
Department of Biosurgery and Surgical Technology
10th Floor, QEQM Building
St Mary's Hospital, London
Praed Street,
London W2 1NY
Tel: 0207 886 2124
Fax: 0207 886 1810
E-mail: g.hanna@imperial.ac.uk

4. Patient consent form

Imperial College London

Division of Surgery, Anaesthetics & Intensive care
Department of Biosurgery and Surgical Technology
Imperial College London
10th Floor, QEQM Building
St Mary's Hospital
Praed Street, London W2 1NY
Tel: +44(0)20 7886 2125
Fax: +44(0)20 7413 0470

Mr George Hanna PhD, FRCS
Reader and Consultant Surgeon
g.hanna@imperial.ac.uk
www.imperial.ac.uk

PATIENT CONSENT FORM

Patient name, address, DOB *(or ID label)*

Title of Project:
Metabonomic Profiling of Gastric and Oesophageal Cancer
REC Ref. 05/Q0404/73
Version: 2
Principal investigator:
Mr GB Hanna PhD FRCS MErgS
Reader and Consultant Upper GI Surgeon
Imperial College London, St Mary's Hospital.
Assistant:
Mr Danny Yakoub MSc MRCSEd
Clinical Research Fellow, Imperial College London

I confirm that I have read and understood the information leaflet dated ...../...../..... for the above study and have had the opportunity to ask questions.	☐ YES	☐ NO
I understand that I may withdraw consent to my tissue being included in the study at any time without justifying my decision and without affecting my normal care and medical management.	☐ YES	☐ NO
I agree to donate the tissue samples as detailed below and allow their use in the medical research as described in the Patient Information Leaflet.	☐ YES	☐ NO

I understand that sections of any of my medical records may be looked at by responsible individuals from the research team, or from regulatory authorities where it is relevant to my taking part in research. I give permission for these individuals to have access to my records.	☐ YES	☐ NO
I give consent to the use of my tissues in future research projects if an unanticipated use emerges, which is not described in this information leaflet	☐ YES	☐ NO
I understand that tissue samples will not be used to undertake any genetic tests, results of which may have adverse consequences on my or my family's insurance or employment.	☐ YES	☐ NO
I agree on the use of my tissue samples in genetic research.	☐ YES	☐ NO
I understand that the tissue is a gift and that I will not benefit from any intellectual property privilege that results from the use of the tissues in research studies.	☐ YES	☐ NO
I would like to be contacted should the result of any research carried out on my tissue yield new findings that may have an impact on my care	☐ YES	☐ NO
The samples which I hereby consent to donate are: a. Pre-operative blood and urine samples	☐ YES	☐ NO
b. Pre-operative tissue biopsy samples produced along the course of my assessment and diagnosis plan including endoscopic biopsies.	☐ YES	☐ NO
c. Intra-operatively removed surgical specimen containing tumour or tumour invaded tissues, which are removed as a part of the surgical operation planned for my treatment.	☐ YES	☐ NO
d. Post operative blood and urine samples during the course of my follow up.	☐ YES	☐ NO

_____ _____ _____

Name of Patient Date Signature

_____ _____ _____

Researcher Date Signature

Original for researcher / tissue bank, 1 copy for patient, 1 copy for hospital notes

5. Control candidate information sheet

Imperial College London

Division of Surgery, Anaesthetics & Intensive care
Department of Biosurgery and Surgical Technology
Imperial College London
10th Floor, QEQM Building
St Mary's Hospital
Praed Street, London W2 1NY
Tel: +44(0)20 7886 2125
Fax: +44(0)20 7413 0470

Mr George Hanna PhD, FRCS
Reader and Consultant Surgeon
g.hanna@imperial.ac.uk
www.imperial.ac.uk

CONTROL CANDIDATE INFORMATION LEAFLET

Title of Project:
Metabonomic Profiling of Gastric and Oesophageal Tissues
REC Ref. 05/Q0403/165
Version 3

Principal investigator:
Mr GB Hanna PhD FRCS MErgS
Reader and Consultant Upper GI Surgeon
Imperial College London, St Mary's Hospital, London.
Co-Investigator:
Mr Danny Yakoub MSc MRCSEd
Clinical Research Fellow, Imperial College London

Date: / /

Dear Sir/Madam

You are being invited to take part in our study titled: "Metabonomic Profiling of Gastric and Oesophageal Tissues". Please read the following information carefully and discuss it with others if you wish. Ask us if there is anything that is not clear or if you would like more information. Take time to decide whether or not you wish to participate. Thank you for reading this information sheet.

What are the details of the project?
The study involves collecting tissue, blood and urine samples to be analysed using special devices, in order to detect compounds specific to gastric and oesophageal tissues. This is planned to be done through comparison between patients with various upper GI diseases and those who do not have it as a control group from which you are a candidate. Samples will be stored in a tissue bank and later processed in our research project.

What will be the use of the collected samples?
As a control candidate, your tissues and other samples will be compared with those of other diseases patients' samples, to detect these compounds specific to each disease. This will help our understanding of oesophageal and gastric diseases and trying to find new treatments. Also it might be used as a potential tool for diagnosis in the future.

Why have I been chosen?
You have been chosen because you are having a diagnostic upper GI endoscopy.

Do I have to take part?
Taking part in the research is entirely voluntary. It is up to you to decide whether or not to take part. If you do decide to take part you will be given this information sheet to keep and be asked to sign a consent form. If you decide to take part you are still free to withdraw at any time and without giving a reason. A decision to withdraw at any time, or a decision not to take part, will not affect the standard of care you receive, now or in the future.

What do I have to do?
Nothing, except to agree to make a gift to us of two specimens of tissue obtained during your endoscopy, in addition to blood and urine samples. And also permit us to keep a copy of your hospital records containing details of your blood tests results, radiography reports and other documents explaining your condition.

How much of my tissues will be taken?
A spoon-full of blood, ½ a cup of urine and bits of tissue in the size of a pin head.

What will happen to the tissues?
Tissues will first be preserved in the tissue bank. Then they will be processed and prepared for analysis through the use of a magnetic resonance device to define types and amounts of compounds within the tissues. After the completion of the study, we would like to retain the blood/tissue samples for possible future research at a future date, when new tests/techniques may be available. We would not contact you again for further permission before doing this. If you agree to take part in this study, you will also be giving consent for possible future use of the sample; this is why we ask you to make a gift of them. Samples will remain the property of the Academic Surgical Unit - St Mary's Hospital Upper Gastro-Intestinal Tissue Bank.
No genetic, HIV, Hepatitis B or other communicable disease testing will be done on the specimens collected. The principal investigator Mr GB Hanna is the named custodian of all tissue specimens. Sections of the specimens may be used for future research purposes.

Will I be contacted again in the future?
You need to indicate in the consent form whether or not you would like to be contacted should the result of any research carried out on your tissue yield new findings that may have an impact on your care; This information can be discussed with you by your hospital Consultant. The, information about your tissues will be available for you at any time through contacting the Tissue Bank Custodian, Mr Hanna.

What if something goes wrong?
We do not believe you would be harmed by donating tissue to the study. There is no additional intervention or change in your treatment plan implemented if you choose to participate. If you wish to complain, or have any concerns about any aspect of the way you have been approached or treated during the course of this study, the normal National Health Service complaints mechanisms would be available to you.

Who will have access to my tissue and how will confidentiality be maintained?
Samples will be stored in the Academic Surgical Unit – St Mary's Hospital Upper Gastro-Intestinal Tissue Bank and access to your samples will be only available through it. The named custodian is Mr George Hanna, who is also the chief investigator in this study will hold responsibility of storage and management of your samples as well as your records. Researchers under Mr George Hanna's direct supervision or after his approval may also have access to the tissue samples. The handling of your tissue samples will be treated with strict confidentiality under the Data Protection Act. All samples will be coded and pseudonymised before transfer to other research partners, so that you cannot be identified from your tissue sample. The custodian will be responsible for keeping proper records of all uses that have been made of the material, whether by himself or by others. Users of pseudonymised samples will not attempt to identify individual research participants. The stored data will be coded. Nevertheless, you or your legal representative can access this information by writing to Mr Hanna, the custodian of the Tissue Bank and guardian of the codes, who will break the code and present the information, if so required.

For samples that have not been used in the study, and stored in the tissue bank, future research projects will need the approval of an NHS Research Ethics Committee. Copies of such approvals will be kept and archived for reference. All research that involves NHS patients or staff, information from NHS medical records or uses NHS patients or staff, information from NHS medical records or uses NHS premises or facilities must be approved by an NHS Research Ethics Committee before it goes ahead which means that the Committee is satisfied that your rights will be respected, that any risks have been reduced to a minimum and balanced against possible benefits and that you have been given sufficient information on which to make an informed decision to take part or not.

Will I receive payment for the tissue that I donate to the tissue bank or the study?
No, we shall treat your samples as a gift to the Imperial College Upper GI Tissue Bank at St Mary's Hospital, London, and you would thus relinquish any interest in it.

What happens if I wish to have my tissue removed from the tissue bank or the study?
If you no longer wish your tissues to be held in the tissue bank, you may withdraw them at any time, without justifying your decision and your future treatment will not be affected in any way. If you wish to have your tissues removed from the tissue bank please contact Mr George Hanna for suitable arrangements.

Who is organising and funding body of the tissue bank and the study?

The Academic Surgical Unit, Imperial College London, St Mary's hospital, Praed street, London W2 1NY

Who has reviewed the establishment of the bank?

The St Mary's Hospital Local Research Ethics Committee.

Who has reviewed the ethical considerations of this study?

Brompton, Harefield and NHLI Local Research Ethics Committee

Thank you for reading this information leaflet.

If you agree to participate, please bring the signed consent form along with you on the day of your planned endoscopy.

Correspondence for further information:

Mr George B Hanna
Reader/Consultant Upper GI Surgeon
Department of Biosurgery and Surgical Technology
10th Floor, QEQM Building
St Mary's Hospital, London
Praed street,
London W2 1NY
Tel: 0207 886 2124
Fax: 0207 886 1810
E-mail: g.hanna@imperial.ac.uk

6. Control candidate consent form

Imperial College London

Division of Surgery, Anaesthetics & Intensive care
Department of Biosurgery and Surgical Technology
Imperial College London
10th Floor, QEQM Building
St Mary's Hospital
Praed Street, London W2 1NY
Tel: +44(0)20 7886 2125
Fax: +44(0)20 7413 0470

Mr George Hanna PhD, FRCS
Reader and Consultant Surgeon
g.hanna@imperial.ac.uk
www.imperial.ac.uk

CONTROL CANDIDATE CONSENT FORM

Patient name, address, DOB *(or ID label)*

Title of Project:
Metabonomic Profiling of Gastric and Oesophageal Tissues
REC Ref. 05/Q0403/165
Version: 3

Principal investigator:
Mr GB Hanna PhD FRCS MErgS
Reader and Consultant Upper GI Surgeon
Imperial College London, St Mary's Hospital, London.
Co-investigator:
Mr Danny Yakoub MSc MRCSEd
Clinical Research Fellow, Imperial College London

Please initial boxes as applicable

I confirm that I have read and understood the information leaflet dated...../...../..... for the above study and have had the opportunity to ask questions. ☐ YES ☐ NO

I understand that I may withdraw consent to my tissue being included in the study at any time without justifying my decision and without affecting my normal care and medical management. ☐ YES ☐ NO

I agree to donate the tissue samples as detailed below and allow their use in the medical research as described in the Information Leaflet.	☐ YES	☐ NO
I understand that sections of any of my medical records may be looked at by responsible individuals from the research team or from regulatory authorities where it is relevant to my taking part in research. I give permission for these individuals to have access to my records.	☐ YES	☐ NO
I give consent to the use of my tissues in future research projects if an unanticipated use emerges, which is not described in this information leaflet	☐ YES	☐ NO
I understand that tissue samples will not be used to undertake any genetic tests, results of which may have adverse consequences on my or my family's insurance or employment.	☐ YES	☐ NO
I understand that the tissue is a gift and that I will not benefit from any intellectual property privilege that result from the use of the tissues in research studies.	☐ YES	☐ NO
I would like to be contacted should the result of any research carried out on my tissue yield new findings that may have an impact on my care	☐ YES	☐ NO

The samples which I hereby consent to donate are:

a. Pre-endoscopy blood and urine samples	☐ YES	☐ NO
b. Endoscopy tissue biopsy samples produced along the course of my assessment and diagnosis plan.	☐ YES	☐ NO

_____ _____ _____
Name of Patient Date Signature

_____ _____ _____
Researcher Date Signature

Original for researcher / tissue bank, 1 copy for patient, 1 copy for hospital notes

10. APPENDIX 3.

Appendix 3. Snap shot of the extraction table used to summarize the data before analysis

Sample number	1	2	3
Patient number	29	120	1
Sample Bank code	M-29-1	H1-9-1	M-1-1
MatLab code	10102	20201	10201
SIMCA code	OSCRG_001	JACSG_002	OACSG_003
Sample type (tumour=1, N Prox st=2, N dis st=3, N oes=4)	1	1	1
Chemo state (0=nochemo, 1=post chemo)	0	1	1
Pathological type of ptnt(0=none, 1=Ad, 2=Sq)	2	1	1
Class in field study (MM=1, NM=2, NN=3, OTHER =4)	4	1	1
Included in field study (0=No, 1=Yes)	0	1	1
Surgical/endoscopic (endosc=0, surgical =1)	0	1	0
Anaesthetic (0=none, 1=LA, 2=GA)	2	2	2
T Stage	2	2	3
N stage	0	0	0
Grade (Well=1, Moderate=2, Poor=3, undiff=4)	2	3	2
Age	65	51	70
Sex (0=F, 1=M)	1	1	1
sample weight (mg)	18.1	18.1	29.9
Metabolites			
Lactate (1.315 - 1.4)	1.51E+06	3.33E+06	1.66E+06
Lysine (1.64 - 1.78)	2.81E+05	3.24E+05	3.68E+05
Glutamine (2.33-2.38)	2.06E+05	1.93E+05	2.11E+05
Glutathione (2.54-2.58)	1.42E+05	26115	37381
Creatine (3.025 - 3.045)	1.74E+05	1.14E+05	2.23E+05
Total cholines (3.18 - 3.24)	3.99E+05	1.18E+06	8.20E+05
Taurine (3.245-3.285)	3.81E+05	4.15E+05	4.13E+05
Scylloinositol (3.34-3.36)	23186	50171	36097
Uracil (5.88 - 5.93)	11317	12018	14223
Tyrosine (6.87-6.93)	23272	22024	27197
Adenines (8.255 - 8.275)	3663.5	2929.1	5269
Bucketed data			
0.80487	1944.2	5675.1	4880.2
0.81488	2503.5	5805.1	5779.7
0.82488	3387.2	6704.7	7342.2

11. APPENDIX 4.

Appendix 4. **Table 15.** Sample weights in sequence of analysis

Sample No.	Weight (mg)	Sample No.	Weight (mg)	Sample No.	Weight (mg)	Sample No.	Weight (mg)	Sample No.	Weight (mg)	Sample No.	Weight (mg)
1	18.1	53	36.3	105	31.2	157	27.5	209	49.1	261	53.2
2	18.1	54	40.2	106	69.3	158	35	210	38.4	262	57.5
3	29.9	55	51.7	107	30.4	159	22.2	211	27	263	43.9
4	29.9	56	44.2	108	33.7	160	39	212	34.7	264	48.4
5	31.6	57	38.7	109	11	161	16.8	213	53	265	58.5
6	23.8	58	33.2	110	48.7	162	32.2	214	37.6	266	58.5
7	30.3	59	21.7	111	39.7	163	45.7	215	44.7	267	60
8	37.8	60	17.7	112	42.7	164	49.8	216	34.1	268	54.1
9	35.7	61	54.7	113	34.2	165	28.2	217	33.2	269	40.4
10	30.5	62	24.7	114	27.7	166	59.1	218	49.8	270	25.2
11	31.2	63	38.7	115	44.6	167	37.4	219	57	271	36.4
12	37.8	64	47.3	116	32.6	168	47.2	220	22.5	272	53.2
13	31.2	65	56.7	117	22.6	169	31	221	48	273	55.8
14	49.6	66	41.2	118	30.2	170	36.2	222	53.6	274	47.8
15	57.4	67	41.2	119	39.7	171	58.4	223	49.1	275	41.8
16	29.7	68	26.7	120	33.3	172	28	224	42.7	276	45.8
17	38.4	69	27.7	121	30.5	173	41.9	225	42.9	277	42.2
18	27.7	70	47.7	122	27.7	174	38.6	226	50.5	278	48.8
19	38.6	71	58.2	123	31	175	29.2	227	31.9	279	40.3
20	48.6	72	43.2	124	66.2	176	43.6	228	35.7	280	63.1
21	21.1	73	32.2	125	31.2	177	39.2	229	56.8	281	53.5
22	38.2	74	26.3	126	42.2	178	31.2	230	42.7	282	55.4
23	26.9	75	40	127	49.7	179	45.3	231	43.8		
24	24.4	76	35.7	128	11.8	180	23	232	48.3		
25	35.6	77	23.5	129	33.2	181	23.4	233	41.9		
26	33.4	78	46	130	39.2	182	20.4	234	42.4		
27	27.7	79	38.7	131	29.2	183	22.3	235	48.8		
28	23.6	80	32.5	132	24.9	184	19.6	236	45.3		
29	28.7	81	47	133	44.4	185	18.9	237	49.4		
30	22.2	82	44.3	134	29.6	186	17.7	238	47.4		
31	29.4	83	39.7	135	31.7	187	17.2	239	68.6		
32	28.2	84	53.9	136	43.4	188	16.5	240	43.2		
33	35	85	33.1	137	32	189	17.5	241	53.2		
34	35.1	86	27	138	37.9	190	19.5	242	53.2		
35	38.3	87	24.8	139	44.7	191	20	243	58.7		
36	38.1	88	20.4	140	34.4	192	19.6	244	49.4		
37	25.6	89	24.8	141	31.4	193	18	245	48.8		
38	24.6	90	24.2	142	42.3	194	22.3	246	37.2		
39	20.8	91	20.4	143	31.7	195	26	247	53.2		
40	24.4	92	29.5	144	36.9	196	24.3	248	41.6		
41	41.2	93	43.2	145	49.9	197	24.3	249	48.4		
42	26.6	94	25.8	146	39.9	198	22.1	250	57.2		
43	35.2	95	34.8	147	38	199	23.3	251	47.1		
44	26.2	96	32.7	148	39.5	200	38	252	35.9		
45	28.7	97	30.2	149	32.8	201	33.4	253	43.7		
46	42.5	98	32.5	150	41.2	202	30.2	254	51.2		
47	36.7	99	27.9	151	28.4	203	40.3	255	49		
48	54.2	100	6.4	152	44.2	204	34.1	256	64.9		
49	36.5	101	17.6	153	52.1	205	28.2	257	57.2	**Average**	36.9
50	42.6	102	6.9	154	8	206	58.2	258	29.4	**Range**	6.4 -
51	42.6	103	8.2	155	24.9	207	33.4	259	43.8		69.3
52	44.2	104	18.7	156	32.1	208	58.1	260	50.6		

12. APPENDIX 5.

Appendix 5. Semiquantitative comparison of metabolites in oesophageal sample groups

Table 16. All carcinoma tissue versus all normal oesophageal tissues

Peak centre	PPM range	Peak shape	Compound	Trend in spectra	P-value
0.09	0.85-0.93	Multiplet (broad)	CH3 lipids	Nor = cancer	0.64
0.96, 0.91, 1.01	0.94-1.02	Triplet, 2 doublets	A Acids(Isoleu,Leu)	Cx > Nor	0.04
1.043	1.03-1.075	Doublet	Amino Acids(val,pro)	Nor = cancer	0.11
1.2	1.19-1.21	Doublet	A-hydroxy-butyrate	Nor = cancer	0.2
1.305	1.26-1.312	Singlet (broad)	Ch2 lipids	Nor = cancer	0.72
1.33	1.314-1.343	Doublet	Lactate	Cx>Nor	<0.001
1.47	1.465-1.492	Doublet	alanine	Nor = cancer	1.0
1.72	1.65-1.78	Multiplet (broad)	CH2-lipids	Nor = cancer	0.13
1.92	1.88-1.95	Singlet	acetate	Nor = cancer	0.64
2.05	2-2.09	Multiplet (broad)	lipids	Nor = cancer	0.18
2.14	2.1-2.19	Multiplet (broad)	lipids	Nor > Cx	0.04
2.353	2.3-2.39	Multiplet/quartet	glutamine	Nor > Cx	0.01
2.56	2.54-2.58	Multiplet/triplet	glutathione	Nor > Cx	0.02
2.801	2.78-2.81	Doublet	?δ-amino-levul	Cx > Nor	0.095
2.83	2.81-2.845	Multiplet	?aspartate	Cx > Nor	0.085
2.96	2.93-2.98	Multiplet	Asparatate/A-keto glutarate	Nor = cancer	0.13
3.01	2.99-3.025	Singlet	lysine	Nor = cancer	0.81
3.04	3.028-3.046	Singlet	creatine	Cx > Nor	0.07
3.204	3.19-3.21	Singlet	Free choline	Cx > Nor	0.002
3.223	3.214-2.224	Singlet	Phophocholine	Cx > Nor	0.03
3.23	3.2245-3.24	Singlet	Glycerophophocholine	Cx > Nor	0.02
3.263	3.24-3.3	Triplet	Taurine+Myoinositol	Nor = cancer	0.53
3.426	3.4-3.6	Doublet	Scylloinositol	Cx > Nor	0.03
3.525, 3.542	3.51-3.55	Double doublets	Myoinositol	Cx > Nor	0.049
3.56	3.55-3.565	Singlet	glycine	Nor = cancer	0.93
3.606	3.585-3.615	Singlet	Glyceraldehyde/β-glucose	Nor = cancer	0.24
3.779	3.73-3.8	Triplet (broad)	Glycine/ α-Glucose/α-CH	Nor = cancer	0.26
3.933	3.925-3.94	Singlet	creatine	Nor > Cx	0.06
3.986	3.965-4.005	Multiplet (broad)	Phophoryl-ethanolamine	Nor = cancer	0.26
4.06	4.045-4.08	Singlet/triplet(broad)	choline/myoinositol	Nor = cancer	0.56
4.118	4.09-4.14	Quartet	lactate	Nor > Cx	0.002
4.17	4.15-4.2	Singlet (broad)	?β-OH-butyrte	Nor = cancer	0.98
4.66	4.63-4.68	Doublet	β -glucose	Nor >cancer	0.05
5.232	5.22-5.245	Doublet	α-glucose	Nor >cancer	0.046
5.33	5.28-5.38	Multiplet broad	Fatty acids	Nor = cancer	0.93
5.42	5.395-5.44	Multiplet	α -Glu-1-X	Nor = cancer	0.15
5.797	5.785-5.81	Doublet	Uracil	Cx > Nor	0.053
5.9	5.88-5.93	2 Singlets, Doublet	Uracil	Cx > Nor	0.03

5.98	5.96-6	Multiplets	?cytosine	Nor = cancer	0.24
6.521	6.51-6.53	Singlet	Fumarate	Nor = cancer	0.4
6.891	6.87-6.91	Doublet	Tyrosine	Cx > Nor	0.02
7.187	7.15-7.2	Doublet	Tyrosine	Nor = cancer	0.31
7.376	7.355-7.395	Doublet	Phenyl alanine	Cx > Nor	0.005
7.423	7.405-7.435	Doublet/triplet	tryptophan	Cx > Nor	0.01
7.53	7.515-7.54	Doublet	Tryptophan/tryptamine	Cx > Nor	0.04
7.888	7.86-7.9	Doublet	uroconate	Nor = cancer	0.64
7.965	7.94-7.99	Multiplet	?guanosine	Nor = cancer	0.64
8.186,208,239	8.17-8.24,8.36	3 singlets	adenine	Nor > Cx	0.002

Nor=normal mucosa from cancer patients, Cx=tumour tissue

Table 17. All oesophageal versus junctional cancer tissues

Peak centre	**PPM range**	**Peak shape**	**Compound**	**Trend in spectra**	**P-value**
0.09	0.85-0.93	Multiplet (broad)	CH3 lipids	variable	0.32
0.96, 0.91, 1.01	0.94-1.02	Triplet, 2 doublets	A Acids(Isoleu,Leu)	Oes = Jun	0.66
1.043	1.03-1.075	Doublet	Amino Acids(val,pro)	Oes = Jun	0.93
1.2	1.19-1.21	Doublet	A-hydroxy-butyrate	Oes = Jun	0.12
1.305	1.26-1.312	Singlet (broad)	Ch2 lipids	variable	0.42
1.33	1.314-1.343	Doublet	lactate	variable	0.9
1.47	1.465-1.492	Doublet	alanine	Oes = Jun	0.79
1.72	1.65-1.78	Multiplet (broad)	CH2-lipids	Oes = Jun	0.66
1.92	1.88-1.95	Singlet	acetate	Oes = Jun	1.0
2.05	2-2.09	Multiplet (broad)	lipids	Jun > Oes	0.052
2.14	2.1-2.19	Multiplet (broad)	lipids	variable	0.19
2.353	2.3-2.39	Multiplet/quartet	glutamine	variable	0.25
2.56	2.54-2.58	Multiplet/triplet	glutathione	Oes = Jun	0.66
2.801	2.78-2.81	Doublet	?δ-amino-levul	variable	0.66
2.83	2.81-2.845	Multiplet	?aspartate	variable	0.66
2.96	2.93-2.98	Multiplet	Asparatate/A-keto glutarate	Jun > Oes	0.08
3.01	2.99-3.025	Singlet	lysine	variable	0.9
3.04	3.028-3.046	Singlet	creatine	variable	0.9
3.204	3.19-3.21	Singlet	Free choline	Oes = Jun	0.66
3.223	3.214-2.224	Singlet	Phophocholine	Oes = Jun	1.0
3.23	3.2245-3.24	Singlet	Glycerophophocholine	Oes = Jun	0.79
3.263	3.24-3.3	Triplet	Taurine+Myoinositol	Oes = Jun	0.54
3.426	3.4-3.6	Doublet	Scylloinositol	variable	0.12
3.525, 3.542	3.51-3.55	Double doublets	Myoinositol	Oes = Jun	0.43
3.56	3.55-3.565	Singlet	glycine	variable	0.54
3.606	3.585-3.615	Singlet	Glyceraldehyde/β-glucose	Oes = Jun	1.0

3.779	3.73-3.8	Triplet (broad)	Glycine/ α-Glucose/α-CH	variable	0.66
3.933	3.925-3.94	Singlet	creatine	Oes = Jun	0.4
3.986	3.965-4.005	Multiplet (broad)	Phophoryl-ethanolamine	Oes = Jun	0.33
4.06	4.045-4.08	Singlet/triplet(broad)	choline/myoinositol	Oes = Jun	0.33
4.118	4.09-4.14	Quartet	lactate	Oes = Jun	0.9
4.17	4.15-4.2	Singlet (broad)	?β-OH-butyrte	Oes = Jun	0.54
4.66	4.63-4.68	Doublet	β -glucose	Oes = Jun	0.66
5.232	5.22-5.245	Doublet	α-glucose	Oes = Jun	0.79
5.33	5.28-5.38	Multiplet broad	Fatty acids	variable	0.9
5.42	5.395-5.44	Multiplet	α -Glu-1-X	variable	0.66
5.797	5.785-5.81	Doublet	Uracil	variable	0.43
5.9	5.88-5.93	2 Singlets, Doublet	Uracil	variable	0.08
5.98	5.96-6	Multiplets	?cytosine	Oes = Jun	0.66
6.521	6.51-6.53	Singlet	Fumarate	Oes > Jun	0.052
6.891	6.87-6.91	Doublet	Tyrosine	Oes = Jun	1.0
7.187	7.15-7.2	Doublet	Tyrosine	Oes = Jun	1.0
7.376	7.355-7.395	Doublet	Phenyl alanine	variable	0.66
7.423	7.405-7.435	Doublet/triplet	tryptophan	Oes = Jun	0.79
7.53	7.515-7.54	Doublet	Tryptophan/tryptamine	Oes = Jun	0.54
7.888	7.86-7.9	Doublet	uroconate	Oes = Jun	0.54
7.965	7.94-7.99	Multiplet	?guanosine	Oes = Jun	0.43
8.186,208,239	8.17-8.24,8.36	3 singlets	adenine	Oes = Jun	0.66

13. APPENDIX 6.

Appendix 6. Immuno-histochemical comparison between healthy controls and normal mucosa from cancer patients

Healthy patients	% positive	% positive	% positive	% positive		Cancer patients	% positive	% positive	% positive	% positive
n = 54	ki-67	TUNEL	mucin	p53		n = 34	ki-67	TUNEL	mucin	p53
1	2.2	1.1	0	0		1	3.1	3	0	0
2	3.3	2.5	0	0		2	2.3	2.3	0	0
3	1	1.8	0	0		3	4.5	1.3	0	0
4	4.9	3.7	0	0		4	5.4	3.8	0	0
5	7.1	3.3	0	0		5	3.6	3.6	0	0
6	1.9	3.8	0	0		6	3.5	5	0	0
7	2.2	5.8	0	0		7	2.4	1.1	0	0
8	3.8	4.6	0	0		8	1.1	0.5	0	0
9	4.9	4.4	0	0		9	5.2	4.3	0	0
10	2.9	2.8	0	0		10	5.3	3.7	0	0
11	6.7	2.2	0	0		11	6.2	5.2	0	0
12	4.4	0	0	0		12	3.4	1.9	0	0
13	3.3	0.9	0	0		13	4.8	1.1	0	0
14	3.2	1.3	0	0		14	4.9	1.5	0	0
15	4.9	3.3	0	0		15	3.7	1.8	0	0
16	1.1	5.1	0	0		16	5.1	2.5	0	0
17	3.5	0.8	0	0		17	5	3.6	0	0
18	3.9	1.5	0	0		18	3.4	4.6	0	0
19	4.8	3.1	0	0		19	2.3	2.1	0	0
20	5.1	2	0	0		20	8.1	1.9	0	0
21	4.1	4.1	0	0		21	5.3	2.1	0	0
22	3.2	1.6	0	0		22	4.5	4.2	0	0
23	3.3	6.1	0	0		23	6.7	3.8	0	0
24	4.6	3.6	0	0		24	5.9	1.8	0	0
25	5.1	3.6	0	0		25	6.1	1.6	0	0
26	4.4	1.9	0	0		26	4.9	2.6	0	0
27	1.4	1.1	0	0		27	0.6	2.2	0	0
28	2.6	0	0	0		28	4.1	2.8	0	0
29	4.9	2.6	0	0		29	3.6	5.1	0	0
30	7.1	3.3	0	0		30	3.4	3.8	0	0
31	5.5	0.8	0	0		31	4.4	3.3	0	0
32	1.8	3.3	0	0		32	3.1	1.1	0	0
33	4.2	2.6	0	0		33	5.3	3.7	0	0
34	3.9	0.2	0	0		34	4.7	0	0	0
35	4.4	4.4	0	0		**Average**	**4.29**	**2.73**	0	0
36	4.9	3	0	0						
37	5.1	0.5	0	0						
38	3.9	0.7	0	0						
39	4.4	4.4	0	0						
40	4.8	2.7	0	0						
41	4.4	4.1	0	0						
42	4.9	3.9	0	0			**Marker**	**Ki67**	**TUNEL**	
43	6.2	1.8	0	0			**p-value**	0.33	0.82	
44	2.8	0	0	0						
45	7.5	2.6	0	0						

46	4.4	3.8	0	0						
47	4	2.2	0	0						
48	2.8	3.3	0	0						
49	1.9	4.6	0	0						
50	2.5	4.4	0	0						
51	1.8	1.8	0	0						
52	2.6	3.2	0	0						
53	4.6	3.6	0	0						
54	4.9	0	0	0						
Average	**3.96**	**2.66**	0	0						

14. APPENDIX 7.

Appendix 7. Intra and inter observer reliability testing among pathologists for determination of Mandard grading of tissue response to chemotherapy

Pathologist	Kappa	Standard error
Pathologist 1	0.45	0.066
Pathologist 2	0.48	0.064
Pathologist 3	0.49	0.062
Pathologist 4	0.47	0.065

Table 18. Intraobserver agreement on Mandard regression grading (MRG) after neoadjuvant therapy

As shown from Table 16 the level of reproducibility as for the intraobserver variation, ranged between 0.45 – 0.49, which indicated only a fair agreement according to the Kappa classification, with the standard error between 0.062 – 0.065.

	Test 1		Test 2	
Pathologists	**Kappa**	**Standard error**	**Kappa**	**Standard error**
Pathologist 1 vs. 2	0.33	0.069	0.38	0.066
Pathologist 1 vs. 3	0.32	0.066	0.27	0.066
Pathologist 1 vs. 4	0.31	0.066	0.33	0.066
Pathologist 2 vs. 3	0.44	0.064	0.31	0.065
Pathologist 2 vs. 4	0.36	0.067	0.32	0.067
Pathologist 3 vs. 4	0.37	0.064	0.27	0.064

Table 19. Interobserver reproducibility Mandard regression grading (MRG) after neoadjuvant therapy

As for the level of agreement when the results were compared again among the 4 pathologists using Weighted Kappa statistics, the range of agreement went from a minimum of 0.27, which is considered a weak agreement, up to 0.44, which is again considered fair agreement, with the range of standard error between 0.064 – 0.069.